

CHEMICAL SYNTHESIS OF HEPARIN LIKE HEAD TO TAIL MULTIMERS

By

Jicheng Zhang

A DISSERTATION

Submitted to
Michigan State University
in partial fulfillment of the requirements
for the degree of

Chemistry—Doctor of Philosophy

2020

ABSTRACT

CHEMICAL SYNTHESIS OF HEPARIN LIKE HEAD TO TAIL MULTIMERS

By

Jicheng Zhang

Heparin, a heterogeneously sulfated glycosaminoglycan (GAG), consists of α -1,4-linked glucosamine (GlcN) and uronic acid [either D-glucuronic acid (GlcA) or L-iduronic acid (IdoA)] disaccharide repeating units. It has been used as an anticoagulant drug for over 80 years. In addition, it plays significant roles in various biological processes such as inflammation, growth factor regulation, bacterial and viral infection, cell adhesion, cell growth, tumor metastasis, lipid metabolism and diseases of the nervous system. However, the complex heterogeneity of natural heparin polysaccharides has hindered efforts to understand the relationship between their diverse structures and biological functions. While chemical and enzymatic syntheses of heparin oligosaccharides have seen tremendous advances in recent years, it is still challenging to prepare heparin analogs approaching the length of polysaccharides with distinct backbone structures and sulfation patterns. In this project, we have developed a new strategy, where (GlcN-IdoA) disaccharide modules with defined sulfation pattern are synthesized and conjugated through amide bond formation. Novel “head-to-tail” multimers are accessed to mimic the linear connections in natural GAG polysaccharides. The ligand requirements of fibroblast growth factor 2 (FGF-2) are studied using bio-layer interferometry (BLI) and surface plasmon resonance (SPR), and the results show the synthetic multimers could mimic the natural heparin mimetics. Heparanase inhibitory activities have also been examined through the colorimetric assay.

Copyright by
JICHENG ZHANG
2020

ACKNOWLEDGEMENTS

First and foremost, I would like to show my deepest gratitude to my supervisor, Professor Xuefei Huang, who has provided me with consistent and outstanding support through every aspect of my graduate career. Aside from Prof. Huang, many faculty members at the chemistry department have been paragons of aid. Professor Wulff graciously agreed to be my second reader and write letters of recommendation for my post-doc application. I would like to thank Prof. Frost and Prof. Hong for reviewing this thesis and serving on my graduate committee.

I would also like to thank all my coworkers who have helped me to develop the fundamental and essential academic competence. Postdocs Weizhun, Kedar, Sherif, Xuanjun, and Tianlu are knowledgeable and generous with their time and talents. Graduate students in the Huang group have also been extremely helpful for solving both synthetic and biological problems. Support staff has also played important roles in my research. Professor Dan Jones, Lijun Chen, and Tony Schillmiller in the Mass Spectrometry facility assisted me to figure out the optimized conditions for my sugar. Tom Dexheimer in drug discovery spent tremendous time and effort on SPR binding assays.

My parents, Weiguo and Yun, and my wife, Jiexi, have supported me all the time. I would like to thank them for their loving considerations and great confidence in me all through these years.

TABLE OF CONTENTS

LIST OF FIGURES	vii
LIST OF SCHEMES.....	xv
KEY TO ABBREVIATIONS.....	xvi
Chapter 1. A Review of Heparin Mimetics as Therapeutic Agents.....	1
1.1. Introduction	1
1.2. Heparin Mimetics as Anticoagulants.....	3
1.3 Heparin Mimetics as Growth Factor Binders.....	13
1.4. Heparin Mimetics as Heparanase Inhibitors	20
1.5. Conclusions	27
Chapter 2. Chemical Synthesis of Heparin Like Head to Tail Multimers	30
2.1. Introduction	30
2.2. Synthetic Challenges in Preparation of Disaccharide Modules	32
2.3. Monosaccharide Building Block Preparation	41
2.4. Synthesis of Disaccharide modules with Various Sulfation Patterns	43
2.5. Synthesis of a Library of 27 Pseudo-hexasaccharide Heparin Mimetics.....	46
2.6. Conclusions	48
2.7. Experimental Section	49
2.7.1. General synthetic procedures.....	49
2.7.2. General procedure for pre-activation Based Single-step Glycosylation.	49
2.7.3. General procedure for deprotection of PMB.	50
2.7.4. General procedure for protection of 6-OH with Lev.	50
2.7.5. General procedure for O-Acetylation.	51
2.7.6. General procedure for N-Acetylation.	51
2.7.7. General procedure for protection of OH with Fmoc.	51
2.7.8. General procedure for protection of NH ₂ with Fmoc.	52
2.7.9. General procedure for preparation of methyl ester.....	52
2.7.10. General procedure for NH-Fmoc Deprotection.....	52
2.7.11. General procedure for preparation of pseudo-tetrasaccharides/hexasaccharides.	53
2.7.12. General procedure for hydrogenolysis.	53
2.7.13. General procedure for saponification of methyl esters.....	53
APPENDIX	106
Chapter 3. Biological Studies of Pseudo-hexasaccharide Heparin Mimetics.....	182
3.1. Bio-Layer Interferometry (BLI) Competition Assay on FGF-2-heparin interaction	182
3.2. Binding Studies of Pseudo-hexasaccharides and FGF-2 Using Surface Plasmon Resonance (SPR).....	184
3.3. Heparanase Inhibitory Activity Tests Through the Colorimetric Assay	187
3.4. Experimental Section	189
3.4.1. Bio-Layer Interferometry (BLI).	189

3.4.2. Surface Plasmon Resonance (SPR)	190
3.4.3. Heparanase Colorimetric Assays.....	190
REFERENCES.....	193

LIST OF FIGURES

Figure 1.1. Structure of the disaccharide repeating unit of heparin and HS.	1
Figure 1.2. “Non-glycosamino” glycan analogs	5
Figure 1.3. Idrabiotaparinux.....	6
Figure 1.4. A series of “non-glycosamino” glycan heparin mimetics.	8
Figure 1.5. Maltotrioside 21 , antithrombin binding domain 22 , sulfo-SIAB 23 , and glycoconjugates 24 , 25 and 26	11
Figure 1.6. Structures of poly(GEMA) 27 and poly(GEMA) sulfate 28	12
Figure 1.7. Heparin-based glycopolymers 29 and 30 prepared through ROMP.....	13
Figure 1.8. Cyclitol-based heparin mimetics 31 and 32	14
Figure 1.9. Compound 33 synthesized <i>via</i> the click reaction.	15
Figure 1.10. Representative heparin mimetic compounds synthesized <i>via</i> the Ugi reaction for growth factor binding.....	15
Figure 1.11. Structures of heparin oligosaccharides and heparin glycodendrimers.	17
Figure 1.12. A library of neoPGs 45 - 50	19
Figure 1.13. Linear heparin mimetics with glyco-amino acid oligomers 51-57	20
Figure 1.14. PI-88, a heparin mimetic with heparanase inhibitory activities.	21
Figure 1.15. Structure of PG545.	22
Figure 1.16. Structure of JG3.....	23
Figure 1.17. Structure of suramin.	24
Figure 1.18. Diantennary and monoantennary monomers 62 , 63 and 64	25
Figure 1.19. Disaccharide motifs 65-70 with various sulfation patterns used for glycopolymer construction.....	26
Figure 1.20. Dendrimer glycomimetics 71-76 for heparanase inhibition.	27

Figure 2.1. Target tetrasaccharide modules.	33
Figure 2.2. ^1H -NMR of 30 (500 MHz CDCl_3).....	107
Figure 2.3. ^{13}C -NMR of 30 (125 MHz CDCl_3).....	107
Figure 2.4. ^1H - ^1H gCOSY of 30 (500 MHz CDCl_3).....	108
Figure 2.5. ^1H -NMR of 31 (500 MHz CDCl_3).....	108
Figure 2.6. ^{13}C -NMR of 31 (125 MHz CDCl_3).....	109
Figure 2.7. ^1H - ^1H gCOSY of 31 (500 MHz CDCl_3).....	109
Figure 2.8. ^1H -NMR of 33 (500 MHz CDCl_3).....	110
Figure 2.9. ^{13}C -NMR of 33 (125 MHz CDCl_3).....	110
Figure 2.10. ^1H - ^1H gCOSY of 33 (500 MHz CDCl_3).....	111
Figure 2.11. ^1H - ^{13}C gHSQCAD of 33 (500 MHz CDCl_3).....	111
Figure 2.12. ^1H -NMR of 34 (500 MHz CDCl_3).....	112
Figure 2.13. ^{13}C -NMR of 34 (125 MHz CDCl_3).....	112
Figure 2.14. ^1H - ^1H gCOSY of 34 (500 MHz CDCl_3).....	113
Figure 2.15. ^1H - ^{13}C gHSQCAD of 34 (500 MHz CDCl_3).....	113
Figure 2.16. ^1H -NMR of 35 (500 MHz CDCl_3).....	114
Figure 2.17. ^{13}C -NMR of 35 (125 MHz CDCl_3).....	114
Figure 2.18. ^1H - ^1H gCOSY of 35 (500 MHz CDCl_3).....	115
Figure 2.19. ^1H - ^{13}C gHSQCAD of 35 (500 MHz CDCl_3).....	115
Figure 2.20. ^1H - ^{13}C gHMBCAD of 35 (500 MHz CDCl_3).....	116
Figure 2.21. ^1H -NMR of 36 (500 MHz CDCl_3).....	116
Figure 2.22. ^{13}C -NMR of 36 (125 MHz CDCl_3).....	117
Figure 2.23. ^1H -NMR of 37 (500 MHz CD_3OD).....	117
Figure 2.24. ^{13}C -NMR of 37 (125 MHz CD_3OD).....	118

Figure 2.25. ^1H - ^1H gCOSY of 37 (500 MHz CD_3OD).....	118
Figure 2.26. ^1H -NMR of 38 (500 MHz CD_3OD).....	119
Figure 2.27. ^1H -NMR of 39 (500 MHz CD_3OD).....	119
Figure 2.28. ^{13}C -NMR of 39 (125 MHz CD_3OD).....	120
Figure 2.29. ^1H - ^1H gCOSY of 39 (500 MHz CD_3OD).....	120
Figure 2.30. ^1H -NMR of 40 (500 MHz CD_3OD).....	121
Figure 2.31. ^{13}C -NMR of 40 (125 MHz CD_3OD).....	121
Figure 2.32. ^1H -NMR of 41 (500 MHz D_2O)	122
Figure 2.33. ^{13}C -NMR of 41 (125 MHz D_2O)	122
Figure 2.34. ^1H -NMR of 42 (500 MHz D_2O)	123
Figure 2.35. ^{13}C -NMR of 42 (125 MHz D_2O)	123
Figure 2.36. ^1H - ^{13}C gHSQCAD of 42 (500 MHz D_2O).....	124
Figure 2.37. ^1H -NMR of 43 (500 MHz CD_3OD).....	124
Figure 2.38. ^{13}C -NMR of 43 (125 MHz CD_3OD).....	125
Figure 2.39. ^1H -NMR of 44 (500 MHz CD_3OD).....	125
Figure 2.40. ^{13}C -NMR of 44 (125 MHz CD_3OD).....	126
Figure 2.41. ^1H -NMR of 45 (500 MHz CD_3OD).....	126
Figure 2.42. ^{13}C -NMR of 45 (125 MHz CD_3OD).....	127
Figure 2.43. ^1H -NMR of 46 (500 MHz CD_3OD).....	127
Figure 2.44. ^{13}C -NMR of 46 (125 MHz CD_3OD).....	128
Figure 2.45. ^1H - ^{13}C gHSQCAD of 46 (500 MHz CD_3OD).....	128
Figure 2.46. ^1H -NMR of 47 (500 MHz D_2O)	129
Figure 2.47. ^{13}C -NMR of 47 (125 MHz D_2O).....	129

Figure 2.48. ^1H -NMR of 48 (500 MHz CD_3OD).....	130
Figure 2.49. ^{13}C -NMR of 48 (125 MHz CD_3OD).....	130
Figure 2.50. ^1H - ^1H gCOSY of 48 (500 MHz CD_3OD).....	131
Figure 2.51. ^1H - ^{13}C gHSQCAD of 48 (500 MHz CD_3OD).....	131
Figure 2.52. ^1H -NMR of 49a (500 MHz D_2O)	132
Figure 2.53. ^{13}C -NMR of 49a (125 MHz D_2O)	132
Figure 2.54. ^1H -NMR of 49b (500 MHz D_2O)	133
Figure 2.55. ^{13}C -NMR of 49b (125 MHz D_2O).....	133
Figure 2.56. ^1H - ^1H gCOSY of 49b (500 MHz D_2O)	134
Figure 2.57. ^1H -NMR of 49c (500 MHz CD_3OD).....	134
Figure 2.58. ^{13}C -NMR of 49c (125 MHz CD_3OD).....	135
Figure 2.59. ^1H -NMR of 49d (500 MHz CD_3OD)	135
Figure 2.60. ^{13}C -NMR of 49d (125 MHz CD_3OD)	136
Figure 2.61. ^1H -NMR of 49e (500 MHz CD_3OD).....	136
Figure 2.62. ^{13}C -NMR of 49e (125 MHz CD_3OD).....	137
Figure 2.63. ^1H -NMR of 49f (500 MHz CD_3OD)	137
Figure 2.64. ^{13}C -NMR of 49f (125 MHz CD_3OD)	138
Figure 2.65. ^1H - ^1H gCOSY of 49f (500 MHz CD_3OD).....	138
Figure 2.66. ^1H - ^{13}C gHSQCAD of 49f (500 MHz CD_3OD).....	139
Figure 2.67. ^1H - ^{13}C gHMBCAD of 49f (500 MHz CD_3OD)	139
Figure 2.68. ^1H -NMR of 49g (500 MHz CD_3OD).....	140
Figure 2.69. ^{13}C -NMR of 49g (125 MHz CD_3OD).....	140
Figure 2.70. ^1H -NMR of 49h (500 MHz CD_3OD)	141

Figure 2.71. ^{13}C -NMR of 49h (125 MHz CD_3OD)	141
Figure 2.72. ^1H - ^1H gCOSY of 49h (500 MHz CD_3OD).....	142
Figure 2.73. ^1H - ^{13}C gHSQCAD of 49h (500 MHz CD_3OD).....	142
Figure 2.74. ^1H - ^{13}C gHMBCAD of 49h (500 MHz CD_3OD).....	143
Figure 2.75. ^1H -NMR of 49i (500 MHz CD_3OD).....	143
Figure 2.76. ^{13}C -NMR of 49i (125 MHz CD_3OD)	144
Figure 2.77. ^1H - ^1H gCOSY of 49i (500 MHz CD_3OD).....	144
Figure 2.78. ^1H - ^{13}C gHSQCAD of 49i (500 MHz CD_3OD).....	145
Figure 2.79. ^1H - ^{13}C gHSQCAD of 49i (500 MHz CD_3OD).....	145
Figure 2.80. ^1H - ^{13}C gHMBCAD of 49i (500 MHz CD_3OD).....	146
Figure 2.81. ^1H -NMR of 50 (500 MHz D_2O)	146
Figure 2.82. ^{13}C -NMR of 50 (125 MHz D_2O)	147
Figure 2.83. ^1H - ^1H gCOSY of 50 (500 MHz D_2O)	147
Figure 2.84. ^1H -NMR of 50a (500 MHz D_2O)	148
Figure 2.85. ^{13}C -NMR of 50a (125 MHz D_2O)	148
Figure 2.86. ^1H - ^{13}C gHSQCAD of 50a (500 MHz D_2O).....	149
Figure 2.87. ^1H -NMR of 50b (500 MHz D_2O).....	149
Figure 2.88. ^{13}C -NMR of 50b (125 MHz D_2O).....	150
Figure 2.89. ^1H - ^1H gCOSY of 50b (500 MHz D_2O)	150
Figure 2.90. ^1H -NMR of 50c (500 MHz D_2O)	151
Figure 2.91. ^{13}C -NMR of 50c (125 MHz D_2O)	151
Figure 2.92. ^1H - ^{13}C gHSQCAD of 50c (500 MHz D_2O).....	152
Figure 2.93. ^1H -NMR of 50d (500 MHz D_2O).....	152

Figure 2.94. ^{13}C -NMR of 50d (125 MHz D_2O).....	153
Figure 2.95. ^1H - ^{13}C gHSQCAD of 50d (500 MHz D_2O)	153
Figure 2.96. ^1H -NMR of 50e (500 MHz D_2O)	154
Figure 2.97. ^{13}C -NMR of 50e (125 MHz D_2O)	154
Figure 2.98. ^1H -NMR of 50f (500 MHz D_2O).....	155
Figure 2.99. ^{13}C -NMR of 50f (125 MHz D_2O).....	155
Figure 2.100. ^1H - ^{13}C gHSQCAD of 50f (500 MHz D_2O)	156
Figure 2.101. ^1H -NMR of 50g (500 MHz D_2O)	156
Figure 2.102. ^{13}C -NMR of 50g (125 MHz D_2O).....	157
Figure 2.103. ^1H - ^{13}C gHSQCAD of 50g (500 MHz D_2O).....	157
Figure 2.104. ^1H -NMR of 50h (500 MHz D_2O).....	158
Figure 2.105. ^{13}C -NMR of 50h (125 MHz D_2O).....	158
Figure 2.106. ^1H - ^{13}C gHSQCAD of 50h (500 MHz D_2O)	159
Figure 2.107. ^1H -NMR of 50i (500 MHz D_2O).....	159
Figure 2.108. ^1H -NMR of 50j (500 MHz D_2O).....	160
Figure 2.109. ^{13}C -NMR of 50j (125 MHz D_2O).....	160
Figure 2.110. ^1H - ^{13}C gHSQCAD of 50j (500 MHz D_2O)	161
Figure 2.111. ^1H -NMR of 50k (500 MHz D_2O).....	161
Figure 2.112. ^{13}C -NMR of 50k (125 MHz D_2O).....	162
Figure 2.113. ^1H - ^{13}C gHSQCAD of 50k (500 MHz D_2O)	162
Figure 2.114. ^1H -NMR of 50l (500 MHz D_2O)	163
Figure 2.115. ^1H - ^1H gCOSY of 50l (500 MHz D_2O)	163
Figure 2.116. ^1H -NMR of 50m (500 MHz D_2O).....	164

Figure 2.117. ^1H -NMR of 50n (500 MHz D_2O)	164
Figure 2.118. ^{13}C -NMR of 50n (125 MHz D_2O)	165
Figure 2.119. ^1H - ^{13}C gHSQCAD of 50n (500 MHz D_2O)	165
Figure 2.120. ^1H -NMR of 50o (500 MHz D_2O)	166
Figure 2.121. ^1H - ^{13}C gHSQCAD of 50o (500 MHz D_2O)	166
Figure 2.122. ^1H -NMR of 50p (500 MHz D_2O)	167
Figure 2.123. ^{13}C -NMR of 50p (125 MHz D_2O)	167
Figure 2.124. ^1H - ^{13}C gHSQCAD of 50p (500 MHz D_2O)	168
Figure 2.125. ^1H -NMR of 50q (500 MHz D_2O)	168
Figure 2.126. ^{13}C -NMR of 50q (125 MHz D_2O)	169
Figure 2.127. ^1H -NMR of 50r (500 MHz D_2O)	169
Figure 2.128. ^{13}C -NMR of 50r (125 MHz D_2O)	170
Figure 2.129. ^1H - ^{13}C gHSQCAD of 50r (500 MHz D_2O)	170
Figure 2.130. ^1H -NMR of 50s (500 MHz D_2O)	171
Figure 2.131. ^{13}C -NMR of 50s (125 MHz D_2O)	171
Figure 2.132. ^1H - ^{13}C gHSQCAD of 50s (500 MHz D_2O)	172
Figure 2.133. ^1H -NMR of 50t (500 MHz D_2O)	172
Figure 2.134. ^{13}C -NMR of 50t (125 MHz D_2O)	173
Figure 2.135. ^1H - ^{13}C gHSQCAD of 50t (500 MHz D_2O)	173
Figure 2.136. ^1H -NMR of 50u (500 MHz D_2O)	174
Figure 2.137. ^{13}C -NMR of 50u (125 MHz D_2O)	174
Figure 2.138. ^1H - ^{13}C gHSQCAD of 50u (500 MHz D_2O)	175
Figure 2.139. ^1H -NMR of 50v (500 MHz D_2O)	175

Figure 2.140. ^{13}C -NMR of 50v (125 MHz D_2O)	176
Figure 2.141. ^1H - ^{13}C gHSQCAD of 50v (500 MHz D_2O).....	176
Figure 2.142. ^1H -NMR of 50w (500 MHz D_2O)	177
Figure 2.143. ^{13}C -NMR of 50w (125 MHz D_2O)	177
Figure 2.144. ^1H - ^{13}C gHSQCAD of 50w (500 MHz D_2O).....	178
Figure 2.145. ^1H -NMR of 50x (500 MHz D_2O)	178
Figure 2.146. ^1H -NMR of 50y (500 MHz D_2O)	179
Figure 2.147. ^{13}C -NMR of 50y (125 MHz D_2O)	179
Figure 2.148. ^1H - ^{13}C gHSQCAD of 50y (500 MHz D_2O).....	180
Figure 2.149. ^1H -NMR of 50z (500 MHz D_2O)	180
Figure 2.150. ^{13}C -NMR of 50z (125 MHz D_2O)	181
Figure 3.1. The sensorgram of heparin-FGF-2 interaction.	183
Figure 3.2. The sensorgrams of competition BLI. A: heparin as the inhibitor. Concentrations from top to bottom: 0, 3.2, 6.5, 13.1, 26.1, 51.7, 77.8 nM. B: compound 50k . Concentrations from top to bottom: 0, 12.5, 25, 50, 100, 500, 1000 μM . C: fondaparinux. Concentrations from top to bottom: 0, 1.0, 10.0, 25, 50, 1000, 2000 μM	183
Figure 3.3. The SPR sensorgram of FGF-2 and compound 50 interaction at different concentrations	184
Figure 3.4. Heparin hexa-, tetra- and disaccharides.....	185
Figure 3.5. Measurement of inhibition of 27 pseudo-hexasaccharides on FGF-2-heparin interaction using competition SPR.....	186
Figure 3.6. Competition SPR for IC_{50} measurements for pseudo-hexasaccharides 50 (A), 50a (B), 50b (C), and 50r (D).....	187
Figure 3.7. Inhibition of heparanase by heparin	189
Figure 3.8. Inhibition of heparanase by A: compound 50a (10, 50, 100, 1000, and 1000 nM). B: compound 50f (0.1, and 10 μM).	189

LIST OF SCHEMES

Scheme 2.1. “Head-to-tail” strategy <i>via</i> chemoselective oxime ligation.	34
Scheme 2.2. Failed glycosylation with idose acceptor 2	35
Scheme 2.3. Glycosylation with various donors.	35
Scheme 2.4. Preparation of disaccharide 9	36
Scheme 2.5. Hydroxylamine bond cleavage under hydrogenation conditions	37
Scheme 2.6. Disaccharide module deprotection sequence.	37
Scheme 2.7. Hydroxylamine group installation.	38
Scheme 2.8. Synthesis of Fmoc protected hydroxylamine disaccharide 17	38
Scheme 2.9. Hydrolysis of ketoxime under pseudo-hexasaccharide formation condition.	39
Scheme 2.10. Failure of reductive amination reaction to link the amine bearing disaccharide module and a ketone bearing disaccharide.	40
Scheme 2.11. Lactone formation from carboxylic acid 26 during HTAU mediated amide formation reaction.	41
Scheme 2.12. Glucosamine donor synthesis.	42
Scheme 2.13. Idopyranosyluronate acceptor 34 preparation.	43
Scheme 2.14. Disaccharide synthesis and modification.	44
Scheme 2.15. Preparation of disaccharides bearing various sulfation patterns.	45
Scheme 2.16. Reducing end sequence disaccharides 46-48	46
Scheme 2.17. Pseudo tetrasaccharide formation.	47
Scheme 2.18. A library of 27 pseudo-hexasaccharides.	48
Scheme. 3.1. Heparanase colorimetric assay.	188

KEY TO ABBREVIATIONS

Ac ₂ O	acetic anhydride
AcOH	acetic acid
AF488	Alex Fluor 488
AgOTf	silver trifluoromethanesulfonate
APS	ammonium peroxodisulfate
ATM	Ataxia-telangiectasia-mutated kinase
AT-III	antithrombin III
BAIB	bis(acetoxy)iodobenzene
BF ₃ ·Et ₂ O	boron trifluoride etherate
BLI	bio-layer interferometry
Bn	benzyl
BnBr	benzyl bromide
BSA	bovine serum albumin
Bz	benzoyl
Cbz	benzyloxycarbonyl
CH ₃ CN	acetonitrile
CSA	camphorsulfonic acid
CVDs	cardiovascular diseases
DBU	1, 8-diazabicyclo[5.4.0]undec-7-ene
DCM	dichloromethane
DDQ	2, 3-dichloro-5, 6-dicyanobenzoquinone
DIPEA	diisopropylethylamine
DMAP	4-dimethylaminopyridine

DMF	dimethylformamide
DMSO	dimethyl sulfoxide
DTT	dithiothreitol
ECM	extracellular matrix
EDC·HCl	1-ethyl-3-(3-dimethylaminopropyl)carbodiimide hydrochloride
ELISA	enzyme-linked immunosorbent assay
ESI-MS	electrospray-ionization mass spectrometry
EtOAc	ethyl acetate
Et ₃ N	trimethylamine
FDA	Food and Drug Administration
FGFs	fibroblast growth factors
FGFRs	FGF receptors
Fmoc	9-fluorenylmethoxycarbonyl
FmocCl	Fmoc chloride
Fmoc-Osu	Fmoc <i>N</i> -hydroxysuccinimide ester
FXa	activated factor X
GAGs	glycosaminoglycans
GEMA	glucosyloxyethyl methacrylate
GlcA	glucuronic acid
GlcN	glucosamine
GlcNAc	2-acetamido-2-deoxy-glucose
GlcNS	<i>N</i> -sulfated glucosamine
HCl	hydrochloric acid

HIT	heparin-induced thrombocytopenia
H ₂ O	water
H ₂ O ₂	hydrogen peroxide
HMBC	heteronuclear multiple bond correlation
HOBT	hydroxybenzotriazole
HPLC	high performance liquid chromatography
HRMS	high resolution mass spectrometry
HS	heparan sulfate
HSPGs	heparan sulfate proteoglycans
HSQC	heteronuclear single quantum correlation
IdoA	iduronic acid
IV	intravenous
K ₂ CO ₃	potassium carbonate
kDa	kilo-dalton
KPB	potassium phosphate buffer
LevOH	levulinic acid
LiAlH ₄	lithium aluminum hydride
LiOH	lithium hydroxide
LMWH	low-molecular-weight heparin
MALDI-TOF	matrix assisted laser desorption ionization-time of flight
MeI	methyl iodide
MeOH	methanol
mESCs	mouse embryonic stem cells
MS	mass spectrometry

NaBH ₄	sodium borohydride
NaCNBH ₃	sodium cyanoborohydride
NaH	sodium hydride
NaHCO ₃	sodium bicarbonate
NaN ₃	sodium azide
Na ₂ SO ₄	sodium sulfate
neoPGs	neoproteoglycans
NF- κ B	nuclear factor kappa B
NH ₄ OH	ammonium hydroxide
NHS	<i>N</i> -hydroxysuccinimide
NIS	<i>N</i> -iodosuccinimide
NMO	4-methylmorpholine <i>N</i> -oxide
NMR	nuclear magnetic resonance spectroscopy
OD	Optical density
OsO ₄	osmium tetroxide
PBS	phosphate buffered saline
PBST	PBS/0.5% Tween-20
Pd(OH) ₂	palladium hydroxide
PF4	platelet factor 4
Ph	phenyl
PMB	<i>p</i> -methoxybenzyl
<i>p</i> -TolSCl	<i>p</i> -toluenesulfonyl chloride
<i>p</i> -TolSH	<i>p</i> -toluenethiol
Py/Pyr	pyridine

ROMP	ring-opening metathesis polymerization
SA	streptavidin
sat.	saturated
SC	subcutaneous
SEC	size exclusion chromatography
SPR	surface plasmon resonance
TAMRA	tetramethylrhodamine
TBAI	tetrabutylammonium iodide
TBDPS	<i>t</i> -butyldiphenylsilyl
TBS	<i>t</i> -butyldimethylsilyl
<i>t</i> -Bu	<i>t</i> -butyl
TCT	tracheal cytotoxin
TEMPO	2, 2, 6, 6-tetramethyl-1-piperidinyloxy
TFA	trifluoroacetic acid
Tf ₂ O	trifluoromethanesulfonic anhydride
THF	tetrahydrofuran
TLC	thin layer chromatography
TR-FRET	Time-resolved fluorescence energy transfer
TrocCl	trichloroethyl chloroformate
TTBP	2,4,6-tri- <i>t</i> -butylpyrimidine
UFH	unfractionated heparin
ULMW	ultralow molecular weight
VEGF	vascular endothelial growth factor
WHO	World Health Organization

Chapter 1. A Review of Heparin Mimetics as Therapeutic Agents

1.1. Introduction

Glycosaminoglycans (GAGs) are highly negatively charged, linear polysaccharides. As members of the GAG family, heparin and heparan sulfate (HS) have highest densities of negative charges among all biological macromolecules. The structures of heparin and HS are remarkably heterogeneous, which contain complex linear disaccharide repeating units of D -glucosamine (GlcN) α -(1-4)-linked to a uronic acid (90% L -iduronic acid (IdoA) and 10% D -glucuronic acid (GlcA)). 2-OH of GlcA and IdoA residues can be sulfated. The GlcN monosaccharide can be either N -acetylated (GlcNAc) or N -sulfated (GlcNS), while O -sulfation could be at 6-OH and 3-OH (**Figure 1.1**).¹

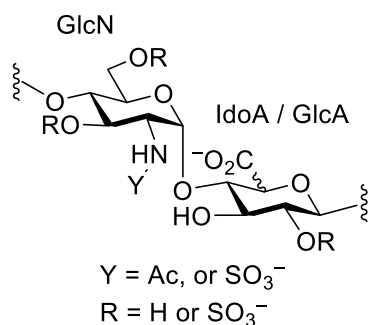


Figure 1.1. Structure of the disaccharide repeating unit of heparin and HS.

Heparin has been used as an anticoagulant drug for over 80 years. Doyon firstly recorded heparin as an anticoagulant in 1912, and the discovery of heparin was also reported by the physiologist William Howell when he investigated the purification of tissue thromboplastin. In 1918-1920, Howell improved the isolation method and named the polysaccharide anticoagulant “heparin”. It was not until the 1930s that preparations of heparin were ready for clinical trials. One of the most famous landmarks in heparin analysis was the identification of L -

iduronic acid in an acid hydrolysate of heparin by Cifonelli and Dorfman in 1962, as early on, it was mistakenly considered that D-glucuronic acid was the only uronic acid in the heparin structure. The configuration of glucosaminidic and uronidic linkages was established by Roden in 1989.²⁻⁵ The sulfation positions, especially 3-O sulfation, were discussed in his report as well. The description of the minimal binding requirement for antithrombin is another important landmark for heparin structure research. Lindahl's group was able to identify a unique pentasaccharide sequence from an isolated octasaccharide, which was thought to be the smallest fragment required for antithrombin binding.⁶

There are three forms of heparin approved by US Food and Drug Administration (FDA) as anti-coagulant drugs: unfractionated heparin (UFH, average molecular weight (MW) 14,000 Da), low-molecular-weight heparin (LMWH, MW 3500–6500 Da) (12-20 saccharide units) and the synthetic pentasaccharide, fondaparinux (MW 1508.3 Da).¹ As a well-known anticoagulant drug, UFH is a mixture of polysaccharides in different lengths with various sulfation patterns.^{7, 8} As it is sourced from animals (primarily from porcine intestinal mucosa with some from bovine), with the heterogeneity of compounds from nature, the reliability and safety of heparin preparations have received increasing attention. This is especially the case after the incident caused by the worldwide distribution of oversulfated chondroitin sulfate contaminated heparin in 2007-2008, with adverse reactions identified in over 100 patients in 13 states alone in less than three months.^{9, 10} As a result, less heterogeneous or even homogenous heparin derivatives are highly desired. Bemiparin and M-Enoxaparin are currently marketed in Europe and the U.S. as LMWH anticoagulant drugs.¹¹⁻¹³ Ultralow molecular weight (ULMW) heparin pentasaccharide fondaparinux as a chemically pure anticoagulant is the most expensive drug among heparins as results of its challenging chemical synthesis (~50 steps) with an overall low yield (~0.1%).^{14, 15}

Besides the anticoagulant activities, heparin can mediate many other protein functions. It is involved in tumor growth and metastasis in part as a result of its inhibition of heparanase, a β -endoglycosidase capable of cleaving HS side chains of heparan sulfate proteoglycans (HSPGs) on the cell surface and in the extracellular matrix (ECM). Furthermore, it can interact with angiogenesis mediators such as fibroblast growth factors (FGFs) and vascular endothelial growth factor (VEGF) in the ECM to promote cell proliferation.¹⁶⁻¹⁹

Synthesis of homogeneous heparin polysaccharides is a formidable challenge due to their length and structural complexity. Heparin's polypharmacy and anticoagulant properties suggest that they need to be tailored for clinical use in applications other than anticoagulation. Synthetic or semi-synthetic heparin mimetics could be designed to address these challenges associated with heparin. In this review, we focus on compounds that can mimic the structural characters and activities of heparin in three common functions, i.e., anti-coagulant, growth factor binding, and heparanase inhibition. Due to space limitation, more native-like heparin oligo and longer saccharide sequences prepared through innovative chemical²⁰⁻²⁵ as well as chemoenzymatic syntheses,²⁶⁻³³ are not included. Interested readers are referred to several excellent reviews covering those compounds.^{32, 34-36}

1.2. Heparin Mimetics as Anticoagulants

According to the World Health Organization (WHO) 2017 fact sheets, cardiovascular diseases (CVDs) are the number one cause of death (31%) globally, accounting for 17.9 million deaths in 2016. Thrombosis and inflammation are strongly related to different types of CVDs, including heart attack, stroke, arterial thrombosis, and venous thromboembolism.³⁷⁻³⁹ UFH, as a commonly used anticoagulant with low costs, is rapid-onset, and its effects can be reversed with

the administration of protamine.⁴⁰ However, heparin-induced thrombocytopenia (HIT) is a significant and life-threatening side effect caused by the interaction of UFH with platelet factor 4 (PF4), a positively charged chemokine.⁴¹⁻⁴⁴ Besides the side effects, short half-life (< 1 h) and low dose-response relationships encourage scientists to discover improved anticoagulants.⁴⁵ LMWH and ULMH are currently approved anticoagulant drugs. LMWH was introduced in the 1940s with its subcutaneous administration route, improved bioavailability, and longer half-life.¹⁴⁶ With those advantages, LMWH has been the most prescribed heparin in the US.⁴⁷ However, LMWH preparation still depends on the source of UFH, and incomplete neutralization with protamine occurs with risks of bleeding.³¹ On the other hand, fondaparinux, the chemically synthesized pentasaccharide, reduces the risk of contamination and limits the interactions with other plasma proteins. Nevertheless, the laborious chemical synthesis and high cost impede it being widely prescribed. Thus, heparin mimetics are developed in recent years to overcome these limitations of heparin and heparin derivatives.

“Non-glycosamino” glycan analogs of heparins were reported in 1992 to reduce the synthetic steps of antithrombin III binding pentasaccharide.⁴⁸ Glucose was used to substitute the glucosamine unit (Compounds **1-6**, **Figure 1.2**), which simplified building block preparations, and avoided the need for selective *N*-sulfation. Furthermore, only acyl and benzyl esters were applied as temporary protecting groups for building blocks used in synthesis, which reduced the number of deprotection steps needed. Overall, the synthetic route was shortened to approximate 25 steps in comparison to ~50 steps for fondaparinux preparation. Idraparinux **4** was found as a potent pentasaccharide derivative, which showed inhibition of thrombin generation *via* both the extrinsic and intrinsic pathways. 1611 anti-Xa units/mg and a long *in vivo* half-life (9.2 hours in rats and 61.9 hours in baboons) were observed after intravenous (IV) and subcutaneous (SC)

administration with a linear pharmacokinetic profile. Idraparinux had been tested to prevent stroke in atrial fibrillation and venous thromboembolism (VTE). However, its antithrombotic activity cannot be reversed due to a lack of neutralizing agents. Idrabiotaparinux **7** (Figure 1.3) is a biotinylated Idraparinux derivative to bestow the reversibility with avidin, which has no reported toxicity and a very short pharmacokinetic half-life.⁴⁹⁻⁵² The pharmacodynamic results from the Phase I study confirmed that by forming an avidin-idrabiotaparinux complex, avidin effectively reversed the anti-FXa activity of idrabiotaparinux.^{53, 54} Phase III clinical trial study of idrabiotaparinux for arterial fibrillation was halted because it did not show better results than standard long-term warfarin treatment for VTE.⁵⁵

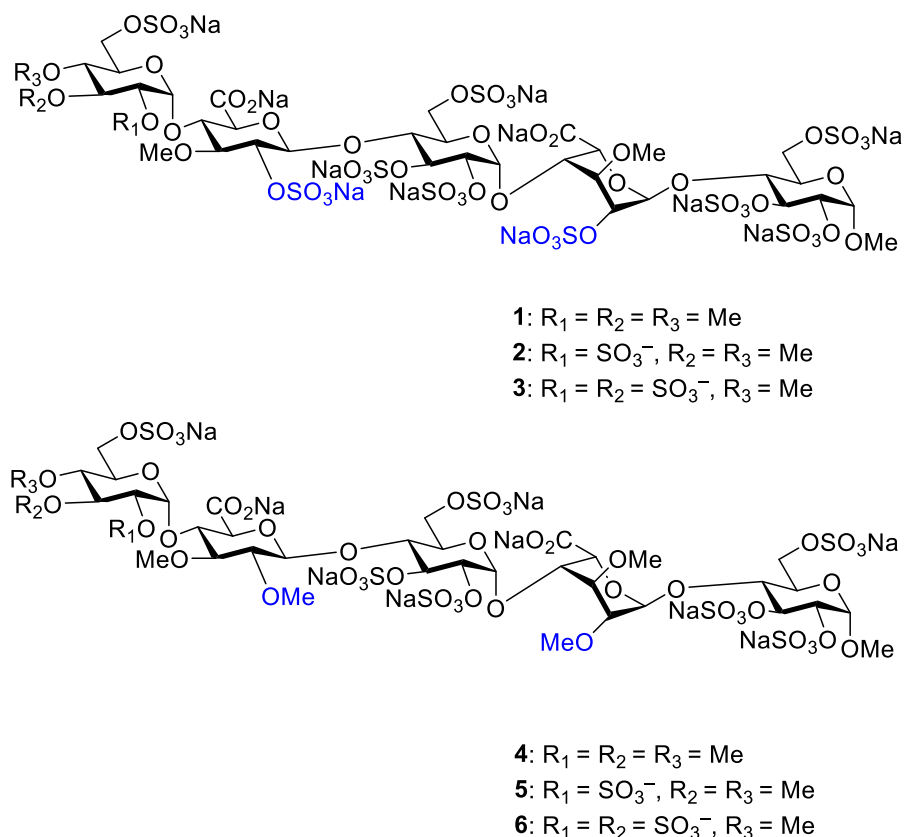


Figure 1.2. “Non-glycosamino” glycan analogs.

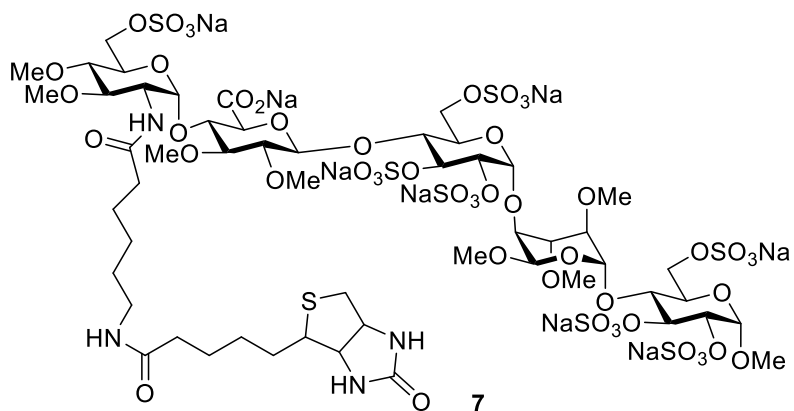
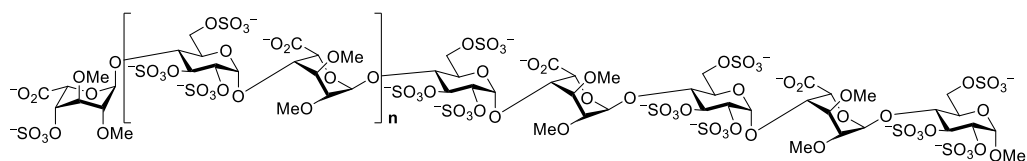


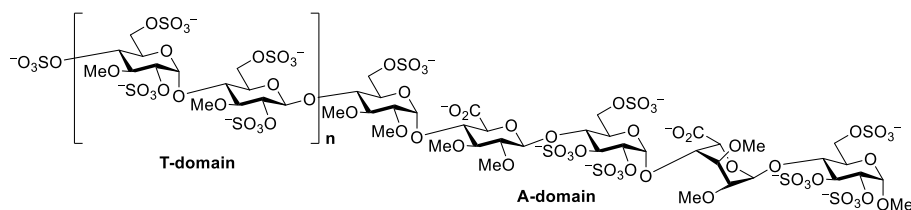
Figure 1.3. Idrabiotaparinux.

To obtain more potent antithrombic drugs, Petitou et al. synthesized a series of “non-glycosamino” glycan heparin mimetics to reach full anticoagulant activity, including thrombin inhibitory properties.⁵⁶ As discussed above, UFH binds with many plasma proteins causing significant side effects, particularly PF4. In this study, various lengths of oligosaccharides were designed to discriminate between thrombin and PF4. 6-mer to 14-mer **8-11** (**Figure 1.4**) did not display high antithrombin activities. The size-dependent increases in activities were observed for 16-mer (**12**) to 20-mer (**14**), with the 20-mer (**14**) being half as potent as UFH. To mimic the full anticoagulant activity of heparin, the structure of an oligosaccharide or even longer saccharide sequence would include an antithrombin-binding domain (A-domain) coupled to a thrombin-binding domain (T-domain). Another important issue is how to link these two domains. Repeating α and β -linked 3-*O*-methyl-2,6-di-*O*-sulfo-D-glucose units were attached to both the reducing and non-reducing ends as a thrombin-binding domain. Compounds **15-17** with T-domain at the non-reducing end were inhibitors of both factor Xa and thrombin. Thrombin inhibition was also size-dependent, and compound **17** was about twice more potent than heparin according to their IC_{50} values. With the A-domain at the non-reducing end and T-domain at the reducing end, 18-mer (**18**) showed 30 to 100 times weaker activities for thrombin inhibition than

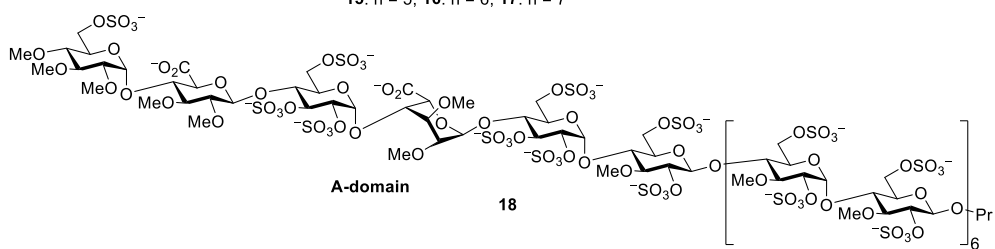
the corresponding 17/19-mer saccharides **16** and **17** bearing the T-domain at the non-reducing end instead. All compounds **8-18** showed effective *in vivo* anti-FXa activities, and dose-dependent thrombin inhibition activities were observed for compounds **12-17**. Even though compounds **15-17** inhibited both factor Xa and thrombin, the cross-reactivity with PF4 was hardly overcome, with the compounds failing to abolish the interactions with PF4.



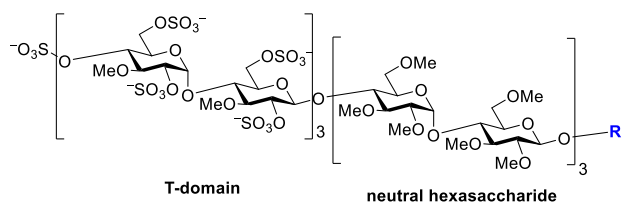
8: n = 0, 9: n = 2, 10: n = 3, 11: n = 4, 12: n = 5, 13: n = 6, 14: n = 7



15: n = 5, 16: n = 6, 17: n = 7



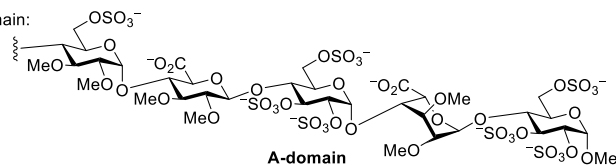
18



T-domain

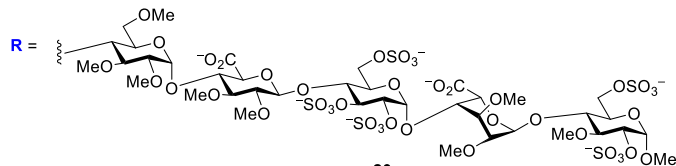
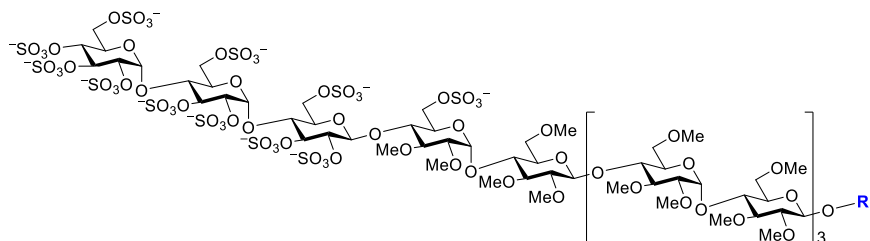
neutral hexasaccharide

R = A-domain:



A-domain

19



20

Figure 1.4. A series of “non-glycosamino” glycan heparin mimetics.

To reduce PF4 binding, the charge of a molecule is an essential parameter for consideration to avoid the nonspecific binding. Compound **19** was designed with a pentasaccharide as A-binding domain and a hexasaccharide at the non-reducing end as the T domain, which was connected by a neutral methylated hexasaccharide. Both domains contain oligosaccharides that are shorter than 8-mer, the minimum unit required for PF4 binding.⁵⁷ Compound **19** showed no significant interactions with PF4 even at high concentrations (100 ug/ml) and exhibited higher antithrombotic activity compared to heparin.⁵⁶ SA123781A, compound **20**, is another “non-glycosaminoglycan” synthetic heparin mimetics based on the strategy of charge reduction for polyanionic compounds, which is a structural variant of compound **19**.⁵⁸ SR123781A exhibited high affinity for human antithrombin and potent factor Xa and thrombin inhibition in multiple animal models for arterial-venous thrombosis. However, its development was halted during phase IIb clinical study due to the success of the LMWH.⁵⁹

To display full anticoagulant activities, both antithrombin and thrombin binding domains are required to be present on the same polysaccharide chain. Glycoconjugate was designed to link both domains to facilitate the anticoagulant activity of the compound. Glycoconjugate **24** (**Figure 1.5**) comprises the antithrombin binding pentasaccharide, a linear spacer, and a persulfated maltotrioside thrombin binding region.⁶⁰ Polysulfated maltotrisaccharide 1-amino-hexaethylene glycol derivative (**21**) was prepared for thrombin binding, and a thioacetyl-substituted spacer was linked to a pentasaccharide as the antithrombin binding domain **22**. Sulfosuccinimidyl (4-iodoacetylamino) benzoate (sulfo-SIAB) (**23**) was applied to connect **21** with **22** to form glycoconjugate **24**, which has the similar length as a heparin 18-mer oligosaccharide. In order to study the binding requirement for thrombin, cellobiose heptasulfate and multipennate hexadecasulfate were attached to synthesize

antithrombin binding pentasaccharide (**25**, **26**). Symmetric pentasaccharide glycoconjugates were also prepared with various sulfation patterns. All the compounds showed good to potent *in vitro* anti-FXa and antithrombin inhibitory activity, and higher antithrombin activities were observed with the glycoconjugate **26** bearing higher charges. However, the binding with PF4 was not completely avoided.

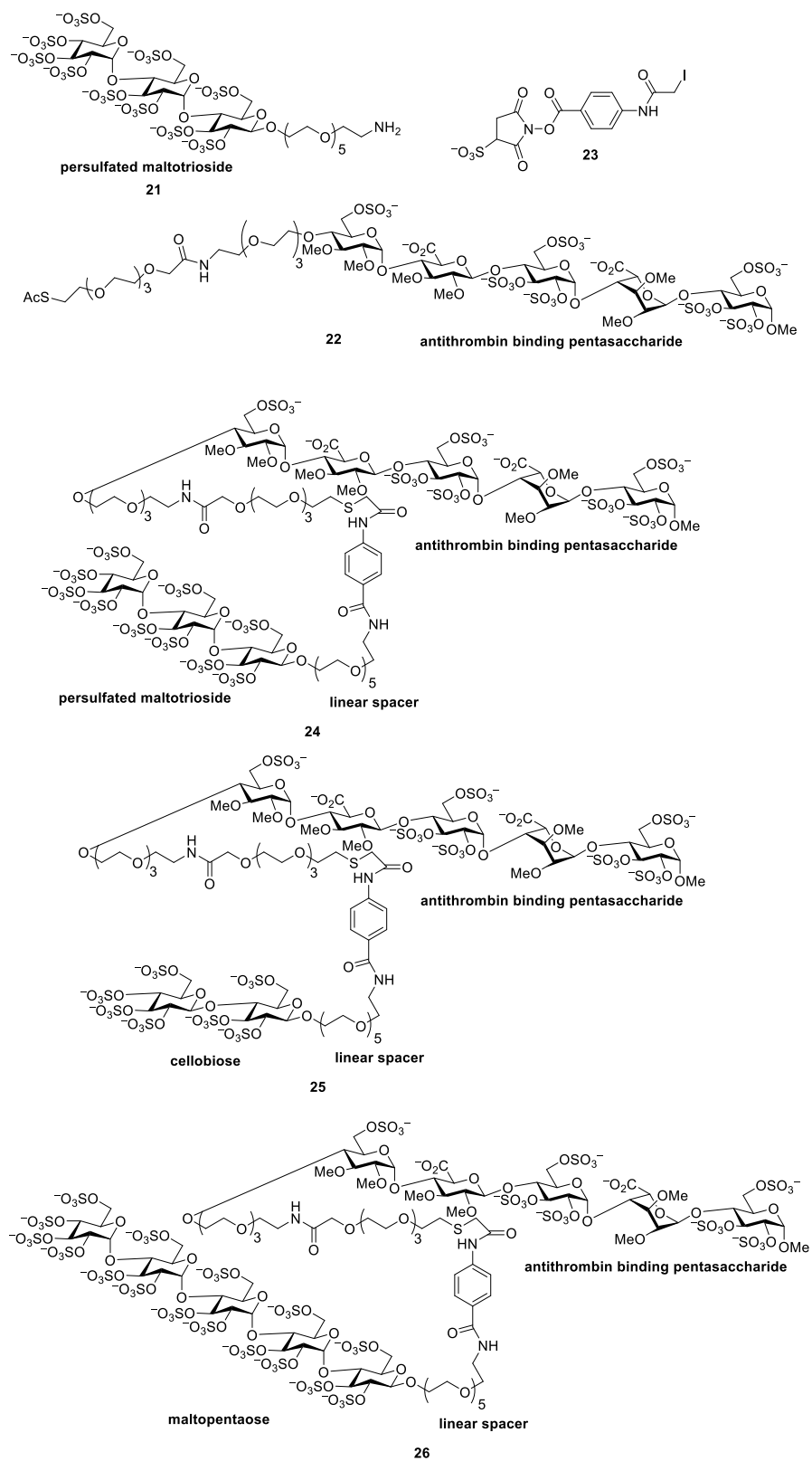


Figure 1.5. Maltotriose **21**, antithrombin binding domain **22**, sulfo-SIAB **23**, and glycoconjugates **24**, **25** and **26**.

Glycopolymers with well-defined pendants have been developed in recent years. Free radical polymerization and copolymerization of glucosyloxyethyl methacrylate (GEMA) were reported for the preparation of highly water-soluble polymers.^{61, 62} Akashi and colleagues utilized the poly(GEMA) **27** with pendant glucoside residue to synthesize poly(GEMA) sulfate **28** (Figure 1.6). The degree of sulfation in **28** varied from 1.91 to 3.75 per sugar according to the amount of DMF/sulfur trioxide complex added and the reaction time.⁶³ The anticoagulant activity of poly(GEMA) sulfate polymer **28** was tested, which showed anticoagulant activity with prolonged coagulation time. However, the anticoagulant effect was about 180 times weaker than that of heparin.⁶⁴ The Hsieh-Wilson group utilized ring-opening metathesis polymerization (ROMP) to generate heparin glycopolymers **29** and **30** carrying disaccharide units (Figure 1.7).⁶⁵ Anti-FXa and anti-FIIa activities of these glycopolymers were measured via chromogenic substrate assays.⁶⁶ Impressively, glycopolymer **29-45** (45-mer) showed high potency against FIIa and FXa, with activities 100 fold higher than those of UFH or LMWH. The lack of 3-*O*-sulfation on **30-155** (155-mer) led to significantly attenuated FXa and FIIa inhibition reaffirming the importance of 3-*O*-sulfation. However, the anticoagulant activity of **29-45** was neutralized by the addition of PF4.⁶⁵ Interestingly, the anti-FIIa activity of glycopolymer **29-30** (polymer with an average length of 30 monomers) was only partially neutralized by PF4, suggesting that the PF4 reactivity can be reduced by modulating the length of the glycopolymer.

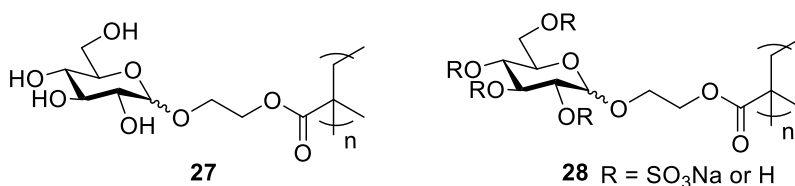


Figure 1.6. Structures of poly(GEMA) **27** and poly(GEMA) sulfate **28**.

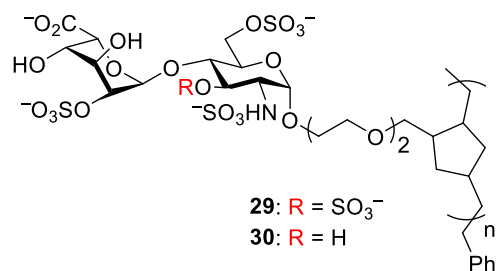


Figure 1.7. Heparin-based glycopolymers **29** and **30** prepared through ROMP.

1.3 Heparin Mimetics as Growth Factor Binders

FGFs and vascular endothelial growth factor (VEGF) initiate cell signaling pathways, and regulate cell proliferation and angiogenesis by forming ternary complexes with heparin/HS and cell surface receptors.⁶⁷ These growth factors were also found sequestered by HS in the ECM. Therefore, reducing heparin and HS binding with these growth factors by heparin mimetics has been investigated in recent years as a novel approach to block cell proliferation.

Parish and coworkers reported structurally well-defined cyclitol-based heparin mimetics with a wide variety of linker chain lengths and extent of sulfation.⁶⁸ The sulfated tetrameric cyclitols mimicked heparin disaccharide units linked through a 2 to 8 carbon atom spacer (**Figure 1.8**). Growth factors exhibited distinct binding patterns with various spacer lengths. Cyclitols with a short spacer of 2 carbon atoms (**31**) effectively bound with FGF-1 but poorly inhibited FGF-2 and VEGF. Compound **32** with a longer linker possessed highest inhibitory activity for the latter two growth factors. This study indicated subtle changes in the spacer could affect the binding ability toward proteins and supported the idea that different domains of heparin account for the binding of various proteins.

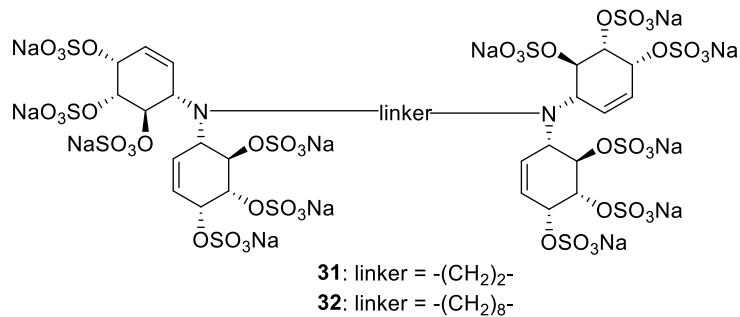


Figure 1.8. Cyclitol-based heparin mimetics **31** and **32**.

A 6-azido-6-deoxy- α -D-mannopyranoside was employed as a heparin mimetic core structure template to investigate the binding affinity and selectivity against growth factors FGF-1, FGF-2, and VEGF. Preliminary binding studies showed 2,3-disulfated mannoside has a similar binding ability with FGF-1 and VEGF as a trisulfated monosaccharide.⁶⁹ Therefore, [3+2] copper-catalyzed alkyne azide cycloaddition and Swern oxidation-Wittig reactions were applied to further decorate the 2,3-disulfate template by selected hydrophobic or polar groups. An 18-membered library, including the lead compound **33**, was successfully prepared (**Figure 1.9**).⁷⁰ All the mimetics had good binding affinity towards FGF-1 and VEGF and selectivity over FGF-2. The attachment of phenyl groups improved the binding to FGF-1 and VEGF, and an extra anionic group such as carboxylate could enhance binding. Compound **33** with a trifluoromethyl substituted aromatic linker exhibited the best binding affinity with FGF-1 and VEGF ($K_D = 84$ and 49 μM , respectively) and good selectivity over FGF-2 (29- and 51-fold, respectively). Ugi four-component condensation reaction was used for a monosaccharide library preparation to introduce additional hydrophobic groups (**Figure 1.10**).⁷¹ The library was used to examine the effect of the hydrophobic groups on binding with growth factors (FGF-1, FGF-2, and VEGF). Surface plasmon resonance (SPR) binding assay showed the compounds with either an aromatic group or an extra negative charge is preferred over an aliphatic group for increased affinity with

growth factors, especially FGF-2 and VEGF.

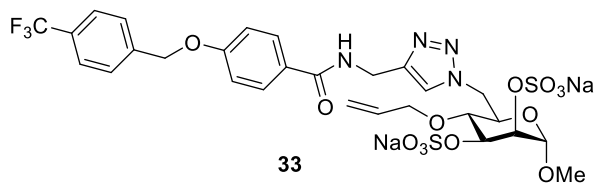


Figure 1.9. Compound **33** synthesized *via* the click reaction.

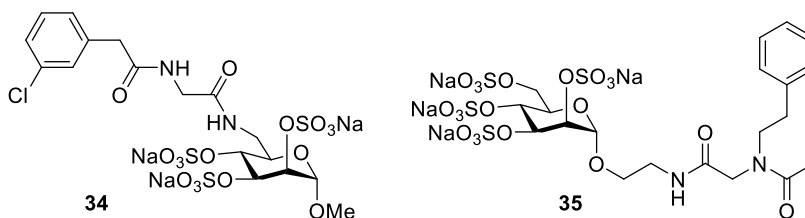


Figure 1.10. Representative heparin mimetic compounds synthesized *via* the Ugi reaction for growth factor binding.

Nontoxic polyanionic compounds were developed to inhibit FGF-2 induced biological activities.⁷² RG-13577 is a synthetic poly-4-hydroxyphenyl acetic acid aromatic compound with an average of 5,000 molecular weight. Effect of RG-13577 on FGF-2 binding was tested in competition with the binding of heparin to FGF-2, and 50% competition was observed at 3 ug/ml. Heparin-induced FGF receptor dimerization and formation of a ternary FGF-2-FGFR-heparin complex are essential steps in FGF-2 signaling.⁷³ Compound RG-13577 alone did not promote the binding between FGF-2 and soluble or cell-surface FGFR1 and abrogated heparin-mediated dimerization of FGF-2 and FGFR1 at 10 ug/ml. In the presence of 5–10 ug/ml compound RG-13577, vascular endothelial cell proliferation was dramatically inhibited.

Sulfated peptide combinatorial libraries are another novel polyanionic structures that mimic heparin, and its biologic activity toward FGFs.⁷⁴ Peptides were chosen as templates for heparin mimetics due to the ease in accessing a range of peptide structures *via* automated solid-

phase peptide synthesis. The structures can be readily modified by split–pool synthesis to create combinatorial peptide libraries. *O*-Sulfation of heparin was mimicked by sulfated serine, threonine, and hydroxyproline residues, and *N*-sulfated amino acid resembled *N*-sulfation of heparin. The sulfated peptide library (240,000 members) was screened with fluorescence-labeled FGF-1 to pinpoint heparin mimetic candidates. Eight peptides were identified and further investigated by SPR. However, only 2 out of 8 peptides showed low micromolar IC₅₀ value of FGF-1 binding in competition assays against heparin immobilized on the sensor chip.

To improve binding with growth factors, multivalent constructs of heparin oligosaccharide such as dendrimers have been investigated. Hexasaccharide **36** could bind strongly with FGF-2, as demonstrated by microarray analysis (**Figure 1.11**).²⁵ Disaccharide **37** and monosaccharide **38** also exhibited binding with FGF-2. The Seeberger group synthesized glycodendrimers incorporating synthetic heparin analogs (**36-39**) to improve the interactions with FGFs. FGF-2 was incubated with heparin glycodendrimers for competitive microarray assay against immobilized heparin. Dendrimers **41** and **42** (IC₅₀ = 43 and 165 μM respectively) showed weaker inhibitory activities than **40** (IC₅₀ = 1.4 μM), but remarkably better than the monovalent counterpart **37** and **38**, indicating the increased avidity associated with the multivalent dendrimers. The binding results were confirmed by SPR experiments. In order to validate the performance of heparin dendrimers in the heparin-mediated biological process, dendrimer **40** was tested for the ability to mediate FGF-FGFR complex formation, which successfully activated FGF-2-mediated signaling in L6 myoblasts.⁷⁵

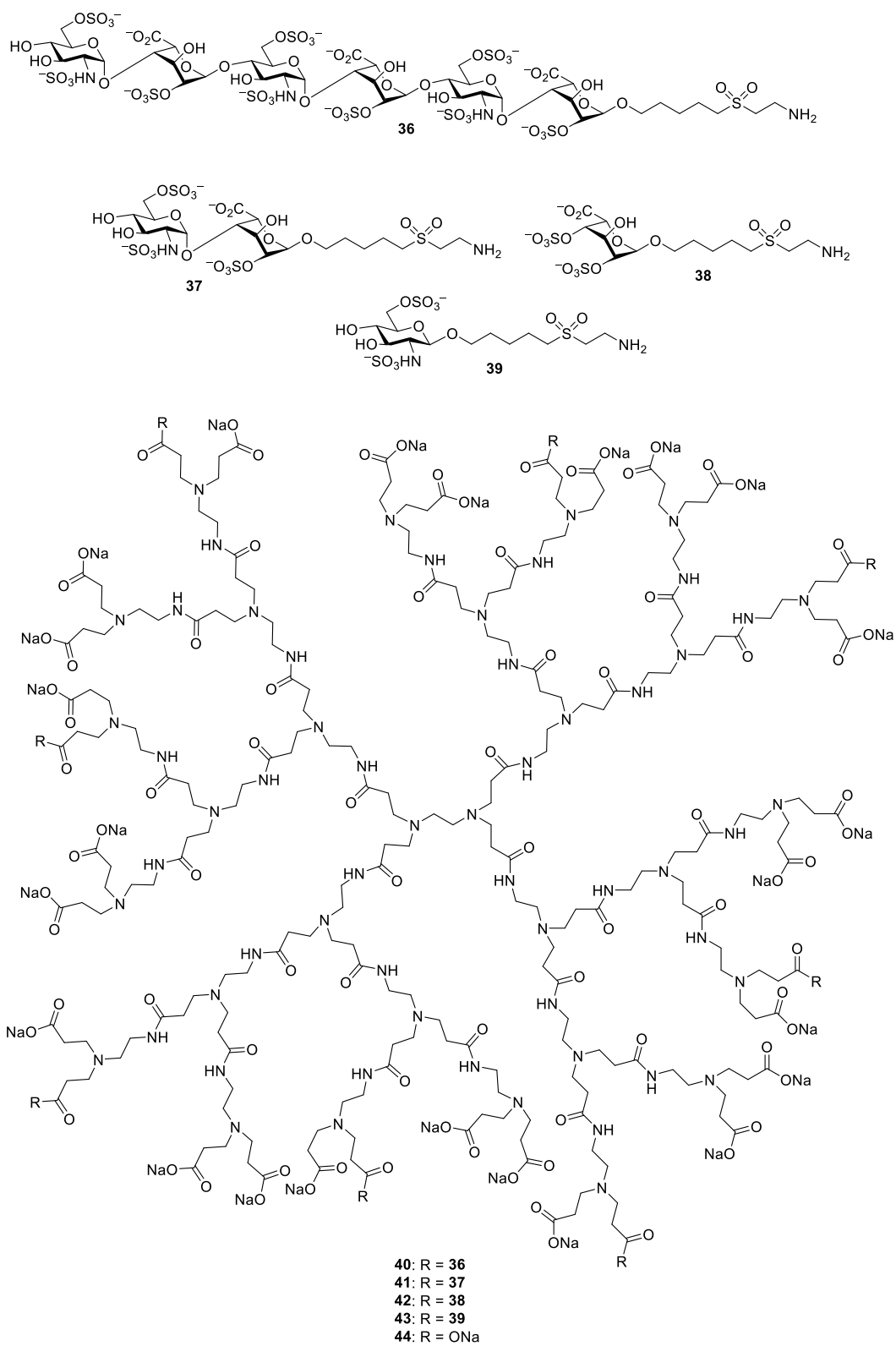


Figure 1.11. Structures of heparin oligosaccharides and heparin glycodendrimers.

Besides dendrimers, glycopolymers have been used to enhance FGF binding. The Godula group reported synthetic neoproteoglycans (neoPGs) utilizing the poly(acrylamide) scaffold and disaccharides prepared by HS depolymerization.⁷⁶ A library of tetramethylrhodamine (TAMRA)-labeled 12 disaccharides and 5 monosaccharide glycopolymers were successfully generated. The trends of structure dependence of FGF-2 binding obtained from microarray screening were consistent with those previously reported for HS.²⁴ 2-*O*-sulfations on disaccharide motifs were required for FGF-2 binding, and neoPGs **46** was the best FGF-2 binder within mimetics **45-50** (**Figure 1.12**). In order to introduce neoPGs to the mouse embryonic stem cells (mESCs), phospholipid tail and Alex Fluor 488 (AF488) tag were installed for membrane insertion and imaging. With neoPGs inserted on cell membrane, increased FGF-2 binding was observed with mESCs remodeled with **49**, while NeoPGs **48** and **50** failed to bind FGF-2 on the cell surface. To confirm FGF-2 binding, a growth factor stimulation assay was performed. The cells remodeled with **47** successfully formed neural rosettes in neural monolayer differentiation experiments.⁷⁷ Furthermore, several kinases isolated from these mESCs showed significantly increased degree of phosphorylation by Western blot suggesting FGF-2 indeed facilitated signaling in cells.

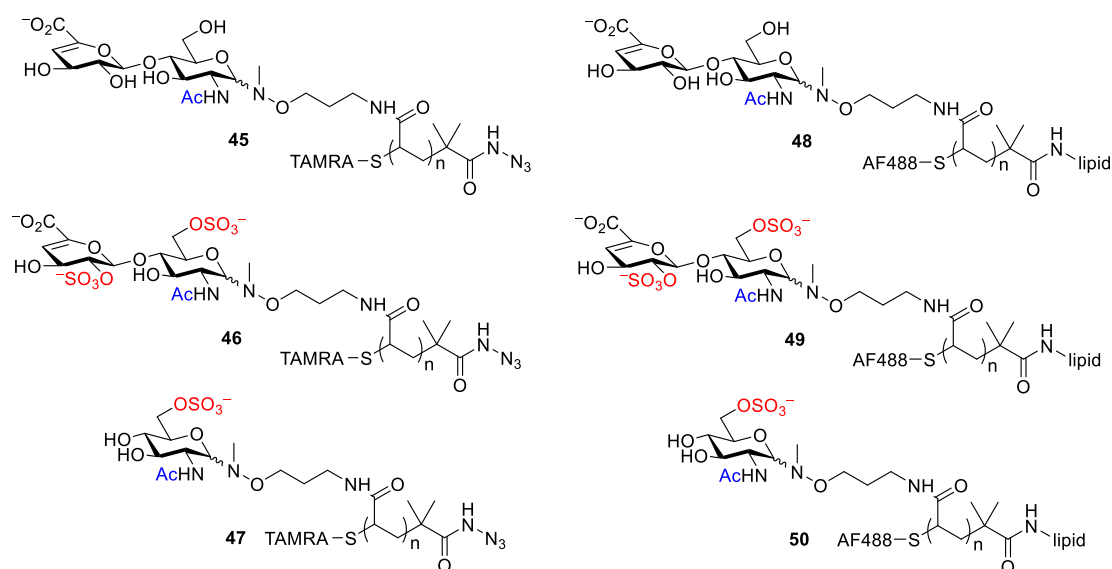


Figure 1.12. A library of neoPGs **45** - **50**.

While current glycopolymers with well-defined saccharide moieties and glycomimetic clusters of heparin provided multivalency in receptor binding, these compounds do not mimic the natural linear connection in heparin. A new generation of linear mimetics was designed using modified GlcN monosaccharide (compounds **51** – **57**) (**Figure 1.13**).^{78, 79} A serine was added to GlcN to mimic the uronic acid residue. The oligomers without sulfate groups and those with 6-*O* and 3-*O* sulfate groups on the GlcN moiety were synthesized through amide bond coupling. The interactions of these compounds with FGF-2 were performed by SPR, and results showed higher binding affinity with increased chain length and 3-*O*-sulfation. Compounds without sulfate groups and short 6-*O*-sulfated oligomer exhibited little interactions with FGF-2, and stronger binding was observed with 3-*O*-sulfation and longer chain length. Overall, the binding affinities were still modest with the most potent compound **57** having a K_D value of 448 μM .

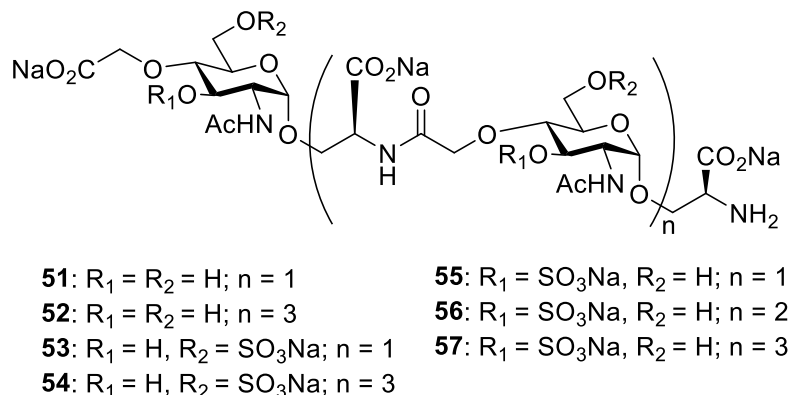


Figure 1.13. Linear heparin mimetics with glyco-amino acid oligomers **51-57**.

1.4. Heparin Mimetics as Heparanase Inhibitors

With their presence on cell surface and in the ECM, heparin and HS can function as a reservoir of growth factors, chemokines, receptors and lipoproteins.^{16, 80} Moreover, by binding with ECM components such as laminin, fibronectin, and collagens I and IV, heparan sulfate linked to proteins, also known as heparan sulfate proteoglycans, contribute to the structural integrity of the ECM and basement membrane, and are involved in cell survival, proliferation, and migration.⁸¹ Heparanase is the sole endoglycosidase degrading HS side chains of heparan sulfate proteoglycans. Due to its impact on cancer, inflammation, and other disease processes, heparanase has been a potential target for anti-cancer therapeutics. Heparin shares the same polysaccharide backbone structure as HS, which makes it the potential heparanase inhibitor candidate. While heparin exhibited potent anti-heparanase activity, its anticoagulant property restrains its clinical use as heparanase inhibitors. Heparin mimetics without any anticoagulant activities are considered as potential therapeutic drugs for cancers.

PI-88 (**58**), a mixture of highly sulfated phosphosulfomannan, was isolated from the

yeast *Pichia holstii* NRRL Y-2448 (**Figure 1.14**). PI-88 contains heterogeneous oligosaccharides ranging from di- to hexa-saccharides, with major components being tetra- (~30%) and penta-saccharides (~60%).⁸² PI-88 showed 2 ug/ml heparanase inhibitory IC₅₀ value, which is comparable to that of heparin (1 ug/ml). Besides its inhibition of heparanase, PI-88 inhibited angiogenesis by abolishing the interactions between growth factors and their receptors.⁸³⁻⁸⁵ *In vivo* study of PI-88 showed that it was effective in inhibiting tumor growth, metastasis, and angiogenesis.⁸³ PI-88 also minimized the malignant cell load in rodent models of human myeloid leukemia.⁸⁶ In addition to heparanase, Hsulf-1 and Hsulf-2, two human extracellular endoglucosamine 6-sulfatases, which are upregulated in several types of cancers, are inhibited by PI-88 in a concentration-dependent manner.⁸⁷ However, a phase III study for hepatocellular carcinoma has been terminated in 2015 due to a lack of significant improvements in disease-free survival compared to other treatment methods suggesting further development of PI-88 like mimetics is needed.

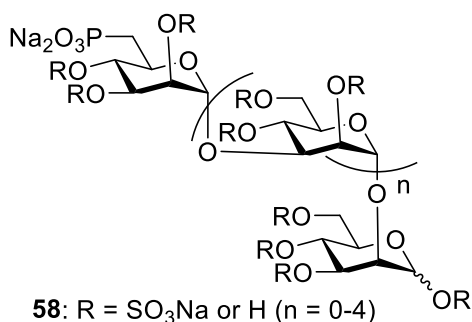


Figure 1.14. PI-88, a heparin mimetic with heparanase inhibitory activities.

PG 500 is a library of synthetic, fully sulfated, and anomerically pure oligosaccharides with the reducing ends modified by various lipophilic aglycones.⁸⁸ PG500 compound series were reported as dual inhibitors of heparanase and angiogenesis *via* inhibition of the enzyme and growth factors. They exhibited low nanomolar binding with FGF-1, FGF-2, and VEGH through

the BIAcore binding assay. Both tube formation and rat aortic *in vivo* assays indicated the antiangiogenic activity of PG500 compounds. B16 solid tumor and metastatic model studies also showed the inhibition of tumor development by PG500. Based on the biological results and accessibility of the compounds, a member of the PG500 series, PG545 (**59**) (**Figure 1.15**), had been selected as the lead clinical candidate for further research.⁸⁸ The Hammond group reported the inhibition of tumor growth and metastasis in the orthotopic 4T1 breast cancer model by PG545.⁸⁹ Recently, PG545 was reported to attenuate the growth of patient-derived lung cancer xenografts from fifteen patients.⁹⁰ Phase I clinical trial (NCT02042781) demonstrated the safety and tolerability of PG545 in patients with advanced solid tumors.⁹¹

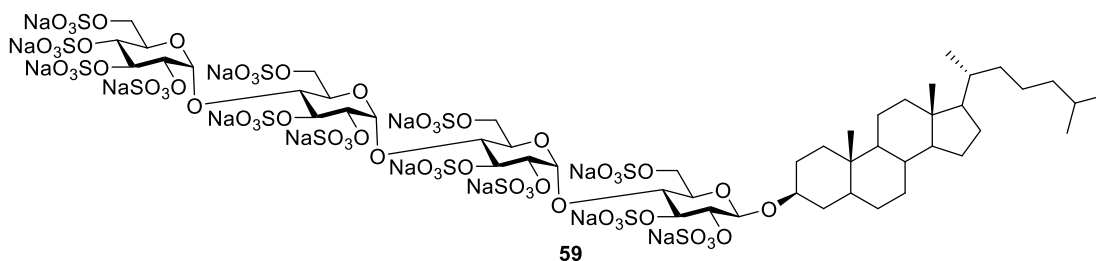


Figure 1.15. Structure of PG545.

Oligomannurinate sulfate (JG3) (**60**) are derived from sodium alginate, ranging from tetra- to deca-saccharides (**Figure 1.16**).⁹² JG3 inhibited heparanase activity by binding to the KKDC and QPLK domains of the heparanase molecule. *In vitro* studies showed the inhibition of heparanase derived from NIH 3T3 and MDA-MB-435 human breast cancer cells by JG3. In an *ex vivo* aorta sprout outgrowth assay, 100 ug/ml JG3 inhibited 77% microvessel growth, and the antiangiogenic property of JG3 was confirmed in an *in vivo* chorioallantoic membrane model and the direct binding with FGF-2. JG3 modulated tumor angiogenesis and metastasis.⁹² Moreover, it inhibited nuclear factor kappa B (NF- κ B) transcription factor activation, which is aberrantly

regulated in cancer development and involved in chemotherapy resistance. The inhibition mechanism is attributed to antagonizing the doxorubicin triggered Ataxia-telangiectasia-mutated kinase (ATM) and the successive MEK/ERK/p90Rsk/IKK signaling pathway. Thus, JG3 could be a potential chemotherapy sensitizer and NF- κ B inhibitor.⁹³

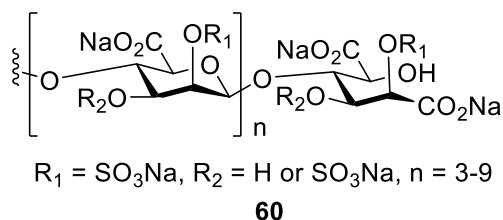


Figure 1.16. Structure of JG3.

Suramin (**61**), a polysulfated naphthylurea, has been tested to treat acquired immunodeficiency syndrome (**Figure 1.17**). Suramin was investigated as a heparanase inhibitor due to its potential inhibitive activity of glycosaminoglycan catabolism. Melanoma-derived heparanase was completely inhibited by suramin at ~ 100 μM ($\text{IC}_{50} = 46$ μM), which was more potent than similar-sized oversulfated heparin tetrasaccharide. B16 melanoma cell invasion was effectively inhibited by suramin as well.⁹⁴ Suramin inhibited the human ovarian and cervical cancer cell growth with modest potencies (IC_{50} values around 350 $\mu\text{g/ml}$) and significantly downregulated heparanase expression.⁹⁵ However, suramin had been associated with multotoxicity at the therapeutic concentration in patients,⁹⁶⁻⁹⁸ which led to the disapproval of its use by the FDA. Several suramin analogs have been reported to address the toxicity issue.^{99, 100}

investigated with a variety of other potential targets for heparin interactions through biolayer interferometry (BLI). The glycopolymers showed very low binding affinity to growth factors (FGF-1, FGF-2, and VEGF) and PF4, suggesting the high selectivity of the glycopolymer as heparanase inhibitors. The glycopolymer was effective in reducing cancer metastasis when evaluated in a mouse 4T1 breast cancer model, demonstrating its high translational potential.

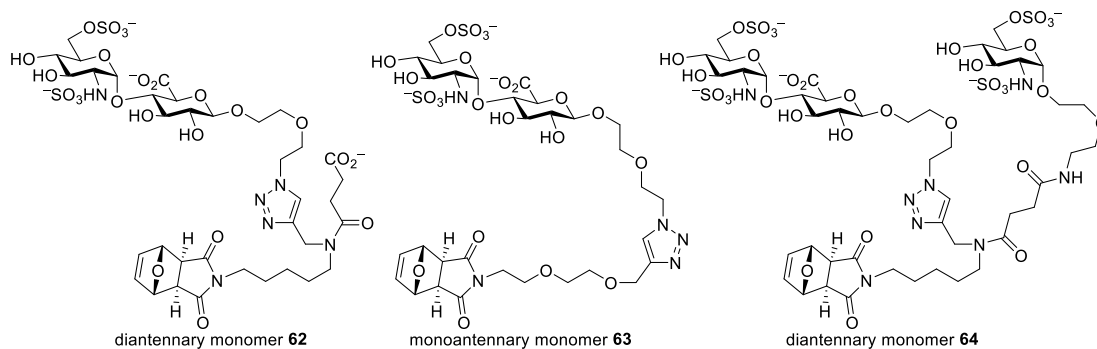


Figure 1.18. Diantennary and monoantennary monomers **62**, **63** and **64**.

In order to investigate the relationship between the sulfation pattern on the pendant disaccharides and their biological functions, a systematic study on sulfation patterns of glycopolymers was reported.¹⁰⁴ Structurally, the GlcN unit in the disaccharide module may be the key for heparanase recognition. Disaccharide motifs bearing different sulfation patterns on GlcN were designed (**65-70**) (**Figure 1.19**). The correlation between sulfation patterns of the GlcN and heparanase inhibition had been investigated. 6-*O*-sulfation was found crucial for heparanase inhibition, as removal of 6-*O* sulfate (**65** vs **66**) drastically reduced the inhibition. The addition of 3-*O*-sulfate was detrimental to heparanase inhibition. Replacement of *N*-sulfate with acetamide or ammonium (compounds **68** and **69**) did not significantly affect the inhibitory activities.

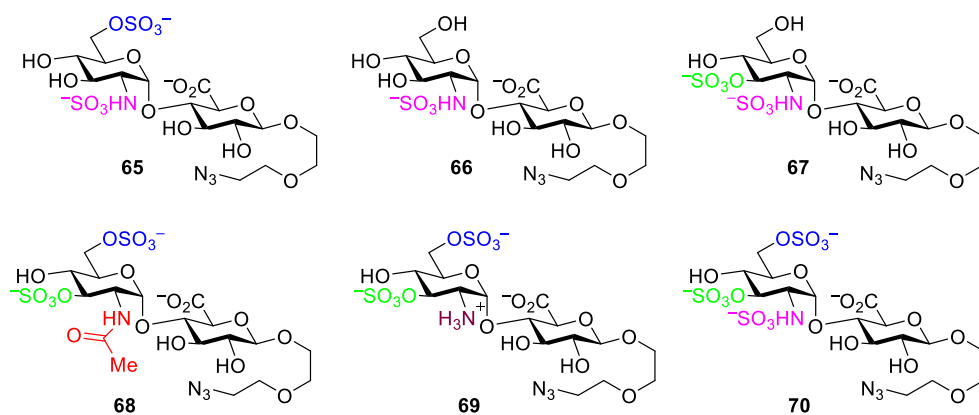


Figure 1.19. Disaccharide motifs **65-70** with various sulfation patterns used for glycopolymer construction.

Recently, Turnbull and coworkers employed multivalent single-entity heparin sulfate dendrimers to enhance their heparanase inhibitory activities (**Figure 1.20**).¹⁰⁵ Since *N*-sulfated heparin oligosaccharide dendrimer did not exhibit high potency in heparanase inhibition ($IC_{50} \sim 1 \mu\text{M}$), glucose and maltose with higher sulfation levels were chosen as dendritic pendants with various dendritic core length. Glucose tetramers moderately inhibited heparanase with IC_{50} values over $1 \mu\text{M}$. In comparison, maltose tetramers, especially “short-armed” ones such as **74** and **75**, showed similar potencies ($IC_{50} = 11$ and 23 nM respectively) as PG 545 ($IC_{50} = 8 \text{ nM}$) as the positive control. The glycodendrimer **75** significantly reduced tumor growth in a xenograft mouse model with human myeloma cells (88.5% inhibition at 4 weeks). The dendrimers **74** and **75** also showed potential inhibitory activity against angiogenesis. Importantly, unlike PG 545, the glycodendrimers exhibited little anticoagulant capabilities, reducing the potential concerns of anti-coagulation side effects, a hurdle for clinical applications as heparanase inhibitors.

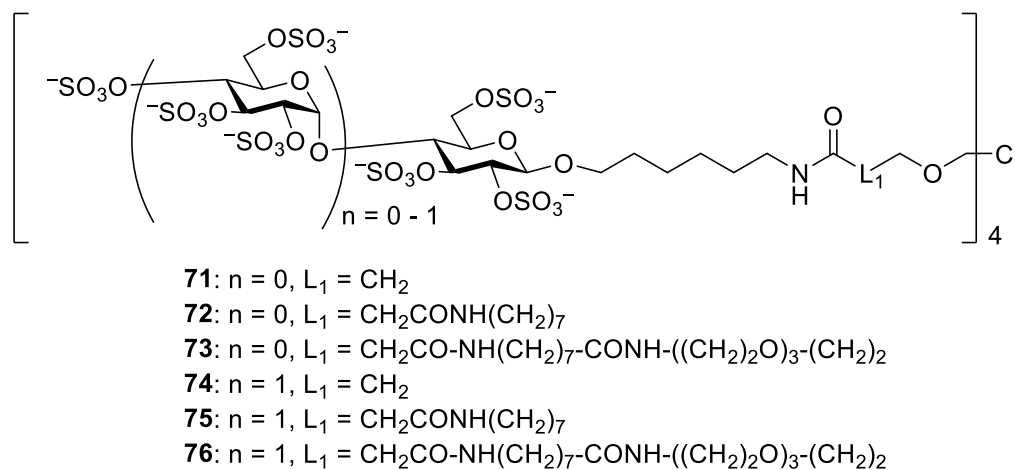


Figure 1.20. Dendrimer glycomimetics **71-76** for heparanase inhibition.

1.5. Conclusions

Heparin, a well-known anticoagulant drug, has been widely prescribed. However, in some patients, heparin can induce life-threatening side effects such as HIT. The heparin contamination crisis in 2007 and 2008 has further stimulated the interests in discovery of more structurally defined heparin compounds for biomedical applications. LMWH has improved pharmacokinetic profiles, but its heterogeneity and the reliance on animal source for heparin are still concerns for wide applications. Fondaparinux, a synthetic heparin oligosaccharide of defined structures, demonstrated the feasibility of obtaining pure heparin structures through organic synthesis. However, the long synthesis needed (around 50 steps) to prepare fondaparinux hinders its wide applications.

To expedite biomedical applications, heparin mimetics have been investigated as attractive substitutes of native heparin, with some of the innovative design and applications of heparin mimetics summarized in this chapter. Three major types of biological functions have been discussed, which include anti-coagulants, growth factor binding, and heparanase inhibition.

For anti-coagulation applications, “non-glycosamino” glycan analogs exemplified by idraparinux **4** have been designed, which contains glucose moiety in lieu of the glucosamine unit. As a result, the synthesis was significantly shortened with idraparinux taking about 25 steps to prepare, half of those required for fondaparinux. At the same time, these synthetic analogs can maintain potent anti-coagulant activities. Furthermore, structural features can be built into these mimetics to recruit further factors involved in anti-coagulation and to modulate neutralization of the compounds if necessary.

Growth factors play important roles in regulating cell proliferation and angiogenesis. A variety of sulfated glycans and cyclitols have been investigated for growth factor binding. To expand structural diversity, multicomponent Ugi reaction has been utilized to introduce additional structural features such as hydrophobic groups and anions into the mimetics, which can help enhance growth factor binding. Furthermore, with the ease in automated solid-phase synthesis, sulfated peptide libraries were screened for growth factor binding leading to binders with modest affinity to FGF-1. To enhance the avidity towards growth factors, glycopolymers and glycodendrimers bearing sulfated mono- or oligo-saccharides have been prepared. These mimetics can present sugar moieties in a multivalent manner, which can be used to modulate heparin-protein interactions, including the regulation of embryonic stem cell differentiation.

Heparanase plays important roles in cell survival, proliferation and migration. Heparin is a potent heparanase inhibitor, which can potentially inhibit tumor growth and metastasis. Nevertheless, the anticoagulant activities of heparin impede its clinical use as heparanase inhibitors. A variety of sulfated glycans including phosphosulfomannan PI-88, hydrophobic aglycon bearing PG500 series, oligomannururate sulfate JG3, as well as polysulfated naphthylurea suramin have been investigated. However, they have relatively modest efficacy

and/or potential toxicities, which need to be improved to enable further clinical evaluations.

Glycodendrimers and glycopolymers bearing sulfated mono- and di-saccharides have shown promising heparanase inhibitory activities with potency ($IC_{50} < 1$ nM) of some compounds higher than that by native heparin. Furthermore, the structures of these mimetics can be tuned to avoid the interactions with other heparin-binding proteins including growth factors, and blood coagulating factors. When evaluated in mouse tumor models, these novel mimetics could significantly reduce tumor development, thus providing promising leads for further development.

Compared to native heparin, heparin mimetics can be synthesized with more homogeneous structures. While the field has witnessed great progress, there are still some limitations with current heparin mimetics. Native heparin contains sulfated and non-sulfated domains connected linearly. Current mimetics have not been able to approach the structural complexity and diversity present in heparin yet. For example, glycopolymers and glycodendrimers are only constructed in a branched fashion. Linearly linking the sulfated and non-sulfated modules may more closely mimic the native heparin structures. With the great advances achieved in synthesis, especially chemoenzymatic synthesis of heparin like oligosaccharides, more sophisticated heparin mimetics will be sure to be prepared in the near future to aid in more thorough understanding of the structure-activity relationship of heparin and the development of advanced agents for biomedical applications.

Chapter 2. Chemical Synthesis of Heparin Like Head to Tail Multimers

2.1. Introduction

Heparin is a highly sulfated, complex linear polysaccharide that belongs to the family of glycosaminoglycans (GAG). It is composed of disaccharide repeating units consisting of D-glucosamine (GlcN) and α -(1-4)-linked to a uronic acid (90% L-iduronic acid (IdoA) and 10% D-glucuronic acid (GlcA)).¹⁰⁶ The most common disaccharide unit includes three sulfate groups, which makes heparin one of the biological macromolecules with the highest density of negative charges. 2-OH of GlcA and IdoA residues may be sulfated. The glucosamine monosaccharide can be either *N*-acetylated (GlcNAc) or *N*-sulfated (GlcNS), while *O*-sulfation normally occurs at 6-OH and/or 3-OH. Due to the heterogeneity and variability of its structure, heparin can interact with a wide variety of proteins.¹⁰⁷ Heparin has been the most widely used anticoagulant drug in the world since the 1930s. Heparin exerts its anticoagulant activities by binding with serine protease inhibitor antithrombin III (AT III), resulting in a conformational change and facilitating its interaction with thrombin and activated factor X (FXa). A unique pentasaccharide sequence with 3-*O*-sulfated GlcN is the minimum requirement for FXa inhibition. On the other hand, heparin fragments with at least 14-18 saccharides long can inhibit the action of thrombin.¹⁰⁸⁻¹¹¹ The heparin-AT III interaction is the most thoroughly studied among heparin-binding proteins. However, the interpretation of detailed structure-activity relationships has been stymied by the chemical complexity of heparin polysaccharide.

Heparin chains are elongated and modified in the Golgi compartment of the mast cell with alternating addition of glucuronate and *N*-acetyl-glucosamine residues to form a linear polymer, which is attached to a serine residue in a core protein. A series of modifications of

heparin backbone begin with *N*-deacetylation/*N*-sulfation of the *N*-acetylglucosamine in the presence of 3'-phosphoadenosine 5'-phosphosulfate (PAPS), followed by C5-epimerization of GlcA to IdoA and stepwise *O*-sulfations of the component sugars.¹¹² A total of 12 enzymes is involved in heparin biosynthesis. However, the sulfation and epimerization of the backbone are often incomplete, accounting for the heterogeneity of heparin. The molecular weights of commercially available heparins could range from 7,000 to 25,000 Da.

The availability of large heparin oligosaccharide libraries is an important tool in understanding the interactions of heparin and a plethora of proteins. The libraries of well-defined heparin/heparan sulfate (HS) di- and tetra-saccharides have been built through chemical synthesis by the Hung and Boons groups.^{24, 113} The structure-activity relationships between heparin and binding proteins, especially fibroblast growth factors (FGFs), have been revealed. However, disaccharide and even tetrasaccharide may not represent full binding epitopes. Extended heparin-based libraries are needed to establish more extensive structure and activity relationship.¹¹⁴ Building libraries with longer heparin oligosaccharides is hampered by tedious and challenging heparin chemical syntheses. Synthesis of the most common trisulfated heparin disaccharide takes about 20 steps from monosaccharide building blocks. Thus, efficient strategies that can quickly elongate the heparin sequence and provide a variety of sulfation patterns are required. To achieve this goal, we developed a novel "head-to-tail" mimetics design based on well-defined disaccharide modules containing various sulfation patterns. Instead of glycosidic linkage, the disaccharide modules were connected from the reducing end to the non-reducing end. The deprotection and sulfation sequences are applied to disaccharide modules instead of longer oligosaccharides, which significantly reduces the complexity of chemical synthesis. Furthermore, the disaccharide modular approach permits the easy access to different

sulfation patterns on each disaccharide module of pseudo-oligosaccharides and facile preparations of long pseudo-oligosaccharide sequences.

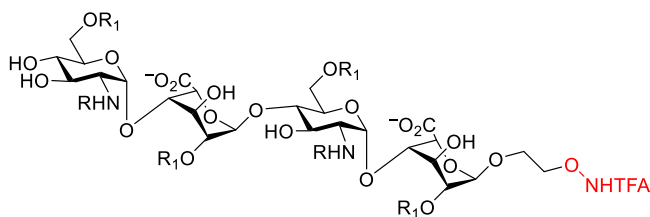
Here, we report the synthesis of a library of 27 heparin pseudo-hexasaccharides through the “head-to-tail” strategy, and binding studies with FGF-2 confirm that the pseudo-hexasaccharides can mimic the natural heparin oligosaccharides. With 23 different members, the FGF family is involved in cell proliferation, migration, differentiation, morphogenesis, and angiogenesis.^{115, 116} The most extensively investigated members of FGF family are FGF-1 and FGF-2. High-resolution X-ray crystal structure of a dimeric 2:2:2 FGF-FGFR-heparin ternary complex explained the dual role for heparin in augmenting FGF-FGFR binding and promoting FGFR dimerization.^{73, 117-119} The heparin pseudo-oligosaccharide library will provide insights into structure-function studies.

2.2. Synthetic Challenges in Preparation of Disaccharide Modules

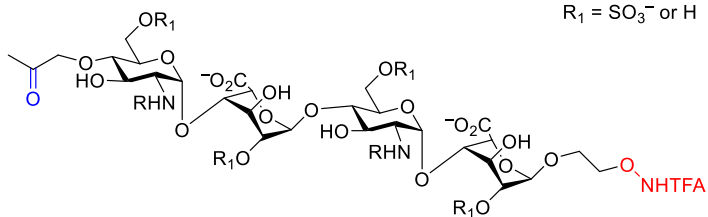
In order to build our heparin mimetics library, we first investigated a modular strategy with ketone and hydroxylamine-functionalized heparin tetrasaccharide modules (**Figure 2.1**). The tetrasaccharide modules could be linked through chemoselective oxime ligation between the hydroxylamine bearing non-reducing end module with the ketone moiety on the elongation sequence (**Scheme 2.1**).¹²⁰ The pseudo heparin oligosaccharides generated could be further elongated by repeating TFA deprotection and oxime formation sequence. The pseudo oligosaccharides mimic the natural linear connection of heparin, and the sulfation pattern could be readily modified on individual modules to achieve great diversity in structures. Moreover, the modular strategy significantly reduced the complexity of oligosaccharide synthesis. Partial

deprotection and sulfation could be performed on the short modules rather than the long final oligosaccharides, leading to higher overall yields. Furthermore, the chain length of the mimetics would be readily elongated.

Non-reducing end sequence:

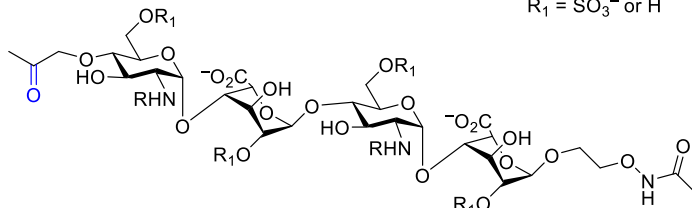


Elongation sequence:



R = Ac or H
R₁ = SO₃⁻ or H

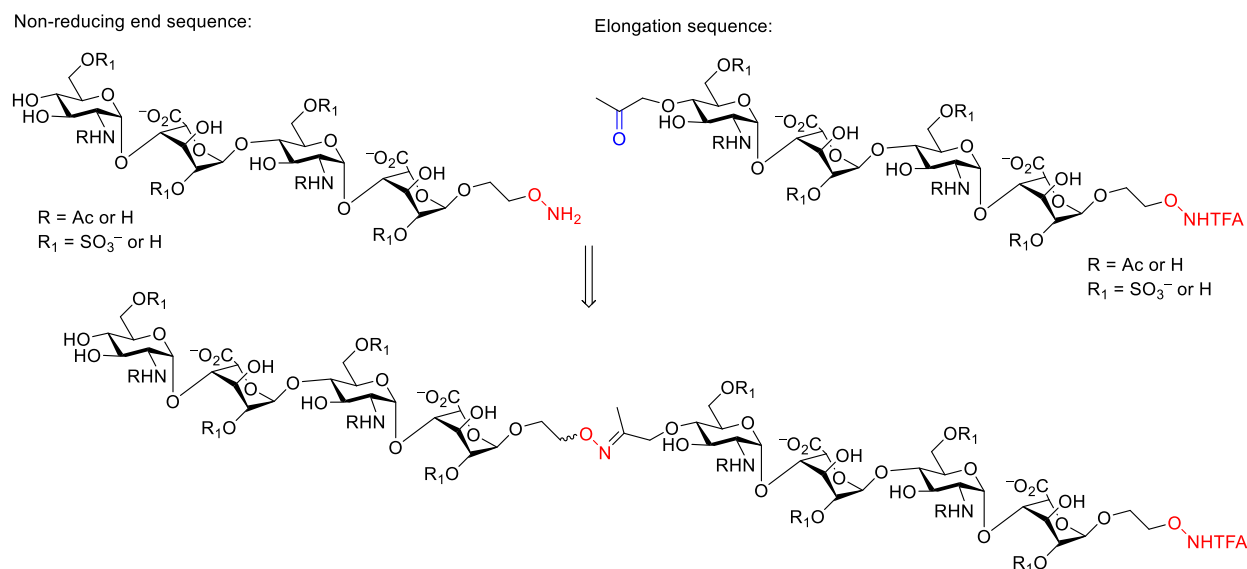
Reducing end sequence:



R = Ac or H
R₁ = SO₃⁻ or H

R = Ac or H
R₁ = SO₃⁻ or H

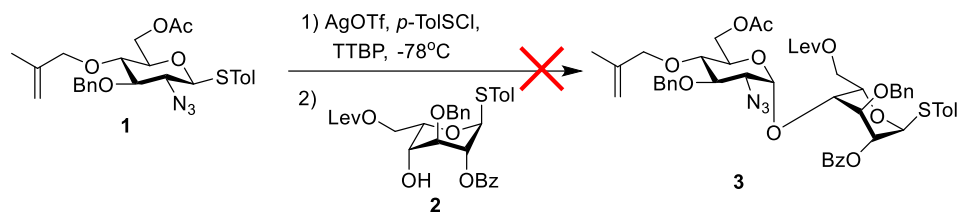
Figure 2.1. Target tetrasaccharide modules.



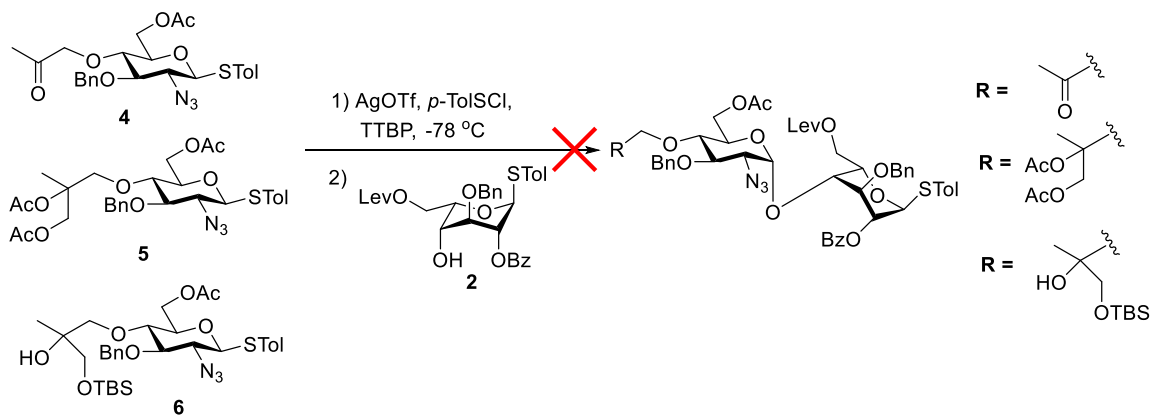
Scheme 2.1. “Head-to-tail” strategy *via* chemoselective oxime ligation.

To obtain the tetrasaccharide modules, we designed a [2 + 2] synthetic route. 2-Amino-2-deoxy-D-glucopyranose (GlcN) and L-idose were applied for disaccharide formation. Methallyl group was installed at the 4-*O* position of the GlcN **1**, which could be oxidized to ketone for oxime synthesis. 6-*O*-Levulinoyl (6-*O*-Lev) of idose **2** would be selectively removed, and the remaining primary alcohol would be oxidized to carboxylate after completion of the chain assembly. However, the preactivation-based glycosylation¹²¹⁻¹²³ failed to generate the desired disaccharide product in high yields. We observed decomposed donor **1**, and most receptor **2** was recovered (**Scheme 2.2**). Then, we investigated glucosamine donors with different protective groups at 4-OH. The methallyl group was oxidized to a vicinal diol by treatment with osmium tetroxide and 4-methylmorpholine *N*-oxide, which was subsequently protected by Ac (**5**) or *tert*-butyldimethylsilyl (TBS) group (**6**). The diol was also converted to a ketone (**4**) under sodium periodate oxidation condition. Unfortunately, all the glycosylation reactions with **4-6** yielded less than 10% of the desired disaccharides with recovered acceptor **2**

and decomposed donors (**Scheme 2.3**). Since various donors were tested, we assumed the failure was attributed to the electron-withdrawing property of the Lev group, which reduced the nucleophilicity power of acceptor **2**.



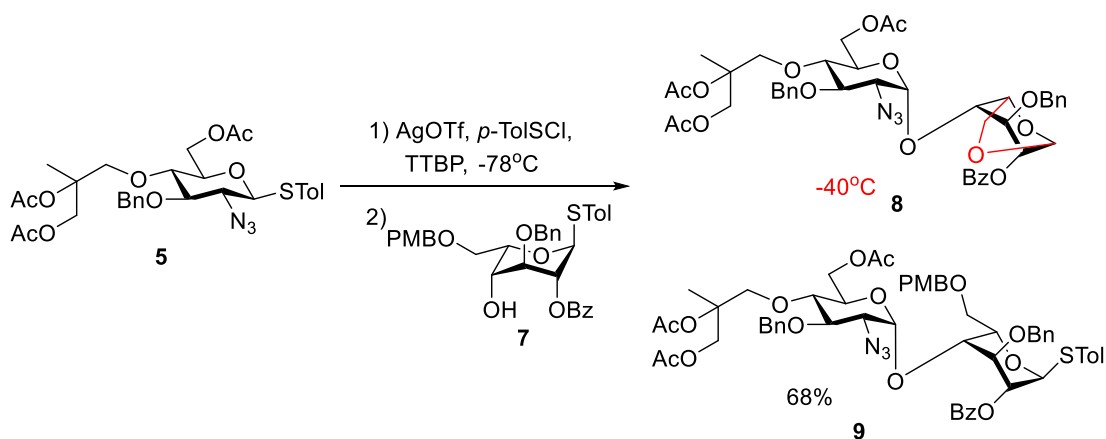
Scheme 2.2. Failed glycosylation with idose acceptor **2**.



Scheme 2.3. Glycosylation with various donors.

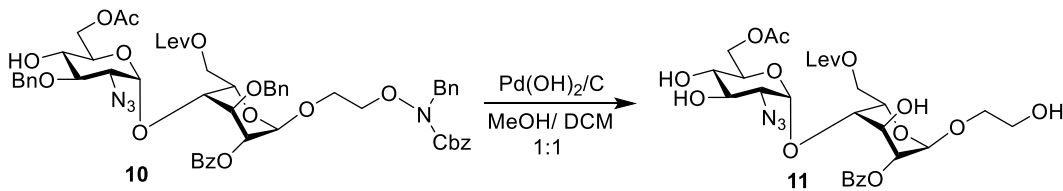
For the purpose of increasing the nucleophilicity of idose acceptor, we chose to replace the 6-*O*-Lev with an electron-donating group, such as *p*-methoxybenzyl (PMB).¹²⁴ The donor **5** was activated by *p*-TolSCl/AgOTf at -78 °C and followed by the addition of 2,4,6-tri-*tert*-butylpyrimidine (TTBP) and acceptor **7**. The consumption of acceptor **7** was indicated by TLC after the reaction was warmed up to room temperature. 1,6-anhydro disaccharide **8** was formed as the sole product. We proposed that the PMB group increased the nucleophilicity of 6-*O* on the idose. The glycosylation was carefully monitored with a steadily raised temperature. The

disaccharide **8** started to form at $-40\text{ }^{\circ}\text{C}$, and most of the desired product **9** was converted to **8** when the temperature reached $0\text{ }^{\circ}\text{C}$. Finally, the desired disaccharide **9** was successfully produced in 68% yield when the reaction temperature was kept at $-78\text{ }^{\circ}\text{C}$ with recovered acceptor **7** (~20%) (**Scheme 2.4**).



Scheme 2.4. Preparation of disaccharide **9**.

With the desired tetrasaccharide in hand, deprotection and sulfation were carried out. However, we found the hydroxylamine group might not survive under Pd/C catalyzed hydrogenation conditions, typically utilized to remove benzyl protective groups.¹²⁵ Disaccharide **10** was used as a model to test the stability of the hydroxylamine group. The O-N bond was found to be cleaved before all the *O*- and *N*-benzyl (Bn) were removed (**Scheme 2.5**). Next, disaccharide **10** was treated with H_2 in DMSO/TEA/IPA mixture, which was reported as the reduction condition for *N*-aryl hydroxylamines synthesis from nitroaromatics.¹²⁶ We observed significant O-N bond cleavage byproduct **11** along with incomplete Bn removal.



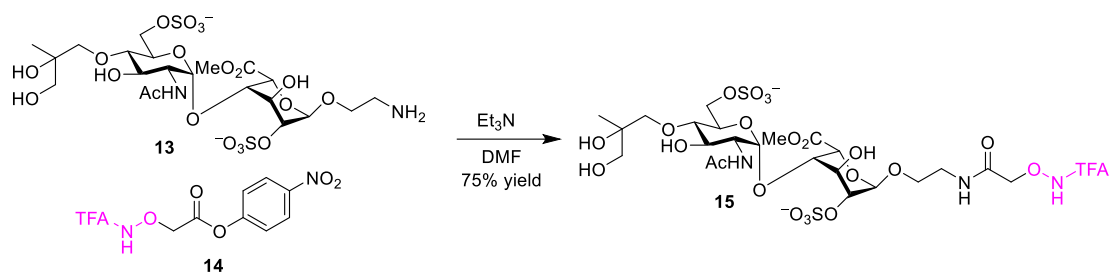
Scheme 2.5. Hydroxylamine bond cleavage under hydrogenation conditions.

With the aim of solving the hydroxylamine stability issue and reducing the complexity of synthesis, we started to prepare disaccharide modules instead of tetrasaccharides and attempted to install hydroxylamine after hydrogenolysis. After we had disaccharide **12** in hand, Ac and benzoyl (Bz) groups were removed by sodium metal in MeOH. The diol at the non-reducing end was protected by benzylidene acetal initially and followed by *O*-sulfation and hydrogenolysis to afford compound **13** (**Scheme 2.6**).



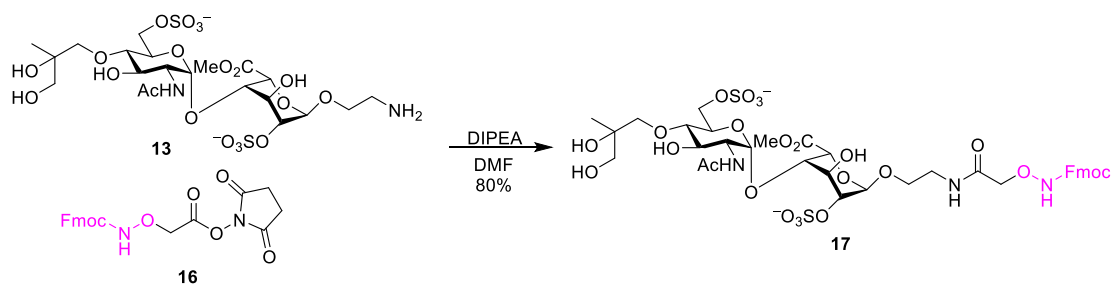
Scheme 2.6. Disaccharide module deprotection sequence.

Next, the hydroxylamine was installed by the amidation reaction. The free amine at the reducing end of disaccharide **13** coupled with *p*-nitrophenol activated ester **14** to generate disaccharide **15** successfully (**Scheme 2.7**). Unfortunately, TFA protecting group could not be removed from **15** in high yields under either saponification or NaBH₄ conditions. A major byproduct was isolated with the amide bond on the linker cleaved. We assumed the electronics of hydroxylamine stabilized the TFA protective group, rendering it challenging to selectively remove the TFA.



Scheme 2.7. Hydroxylamine group installation.

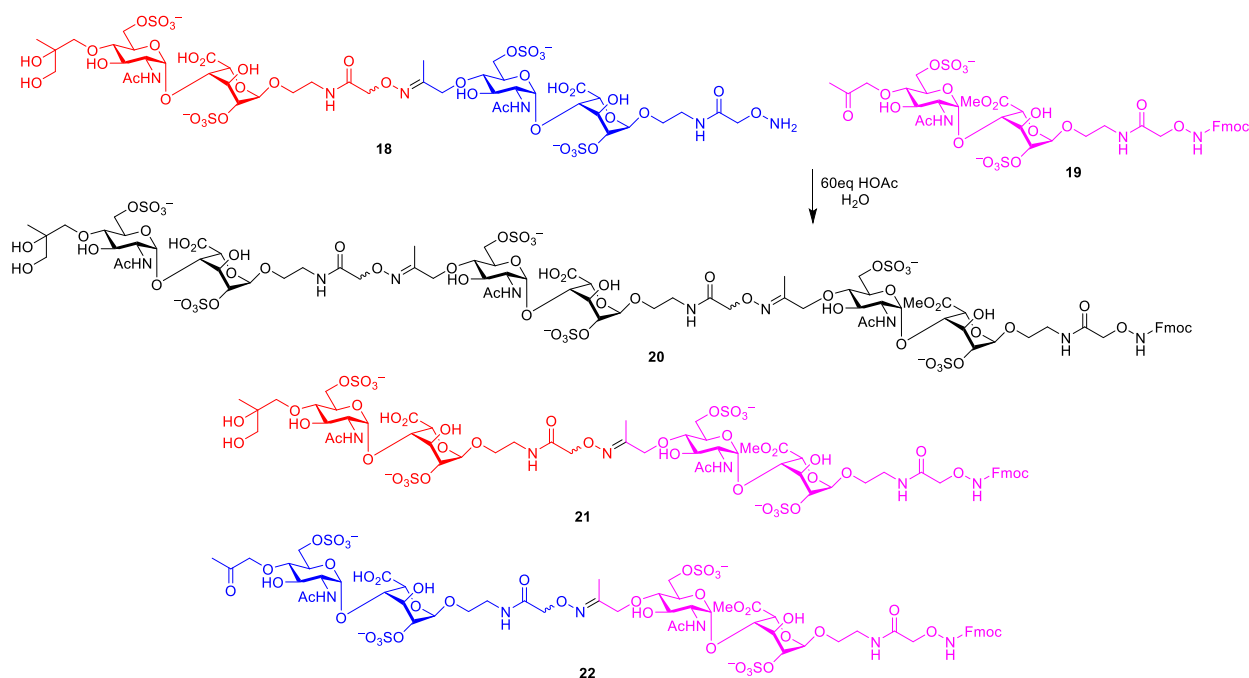
Since TFA selective deprotection was not feasible, 9-fluorenylmethoxycarbonyl (Fmoc) was explored as an alternative to TFA protective group (**Scheme 2.8**). The free amine bearing disaccharide **13** was treated with Fmoc protected hydroxylamine NHS ester **16**, which led to the desired Fmoc protected disaccharide **17**.



Scheme 2.8. Synthesis of Fmoc protected hydroxylamine disaccharide **17**.

The Fmoc protecting group was removed by piperidine, and the tetrasaccharide **18** was successfully prepared by oxime formation *via* coupling between hydroxylamine and ketone from disaccharide modules under HOAc conditions. Nevertheless, the ketoxime group was not stable under [4 + 2] hexasaccharide formation. Besides the desired hexasaccharide (**20**) (< 20% yield), a mixture of tetrasaccharides (**21**, **22**) was generated (**Scheme 2.9**). G-15 gel column failed to separate the hexa- from tetra-saccharides due to the similar molecular weight of the compounds.

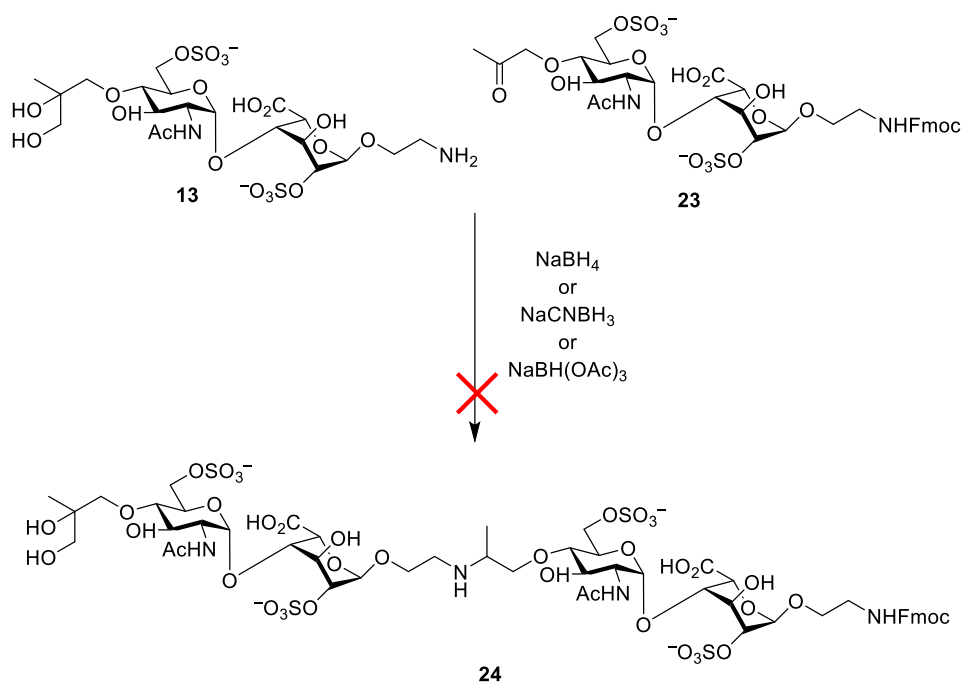
To overcome this issue, we attempted to reduce the ketoxime of pseudo tetrasaccharides. We investigated various ketoxime reduction conditions. Unfortunately, neither NaBH_4 nor NaCNBH_3 could afford the desired reduced product as the major component in the reaction mixture. The reductive reactions were sluggish under low concentrations of HOAc ($< 20\%$), but higher concentrations resulted in ketoxime bond cleavage. Furthermore, acetone adduct to hydroxylamine was a persistent byproduct of oxime formation reactions presumably due to trace contamination of acetone in the reaction mixture.



Scheme 2.9. Hydrolysis of ketoxime under pseudo-hexasaccharide formation condition.

Since the ketoxime formation has become a difficult hurdle for pseudo hexasaccharide synthesis, we next tried reductive amination reaction between ketone **13** and amine **23** to connect disaccharide modules.¹²⁷ Unfortunately, the desired tetrasaccharide was not produced as the major product. Under both NaBH_4 and NaCNBH_3 conditions, ketone was mostly reduced to an

alcohol. $\text{NaBH}(\text{OAc})_3$ was reported for ketone reductive amination reaction in DCE or THF.¹²⁸ Nevertheless, the disaccharides (**13**, **23**) could dissolve in neither of the solvents with, no desired products generated. The solubility issue was resolved by using DMF. Unfortunately, no reactions occurred and the disaccharides were recovered (**Scheme 2.10**).

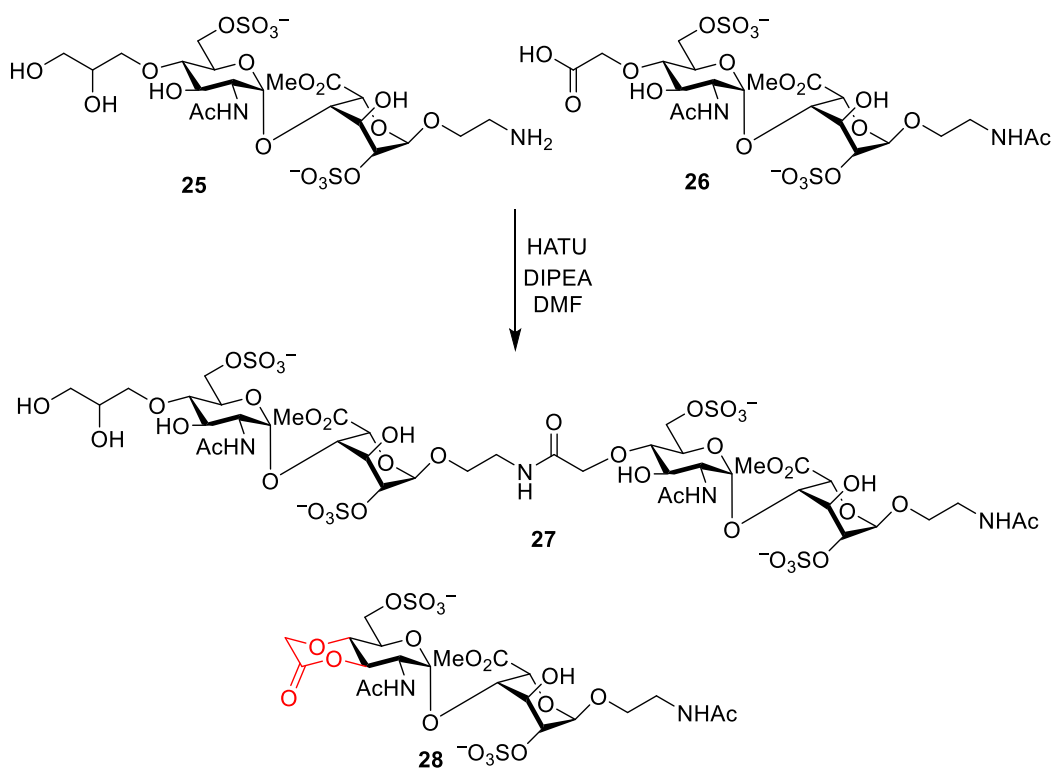


Scheme 2.10. Failure of reductive amination reaction to link the amine bearing disaccharide module and a ketone bearing disaccharide.

Since the ketoxime formation has become a difficult hurdle for pseudo hexasaccharide synthesis, we switched to reductive amination reactions with an aldehyde at the reducing end of disaccharide modules. However, similar to the results for ketone reactions, the aldehyde was partially reduced under acidic conditions. Oxime formation and reductive amination failed to give us our target pseudo hexasaccharides.

These difficulties prompted us to shift our focus to amide bond formation. The

carboxylate group was introduced at the non-reducing end of disaccharide **26** for HATU mediated coupling with amine **25**. In addition to the desired pseudo tetrasaccharide **27** (<10%), the six-membered lactone **28** was also formed as the major byproduct during the HATU coupling reaction (**Scheme 2.11**).

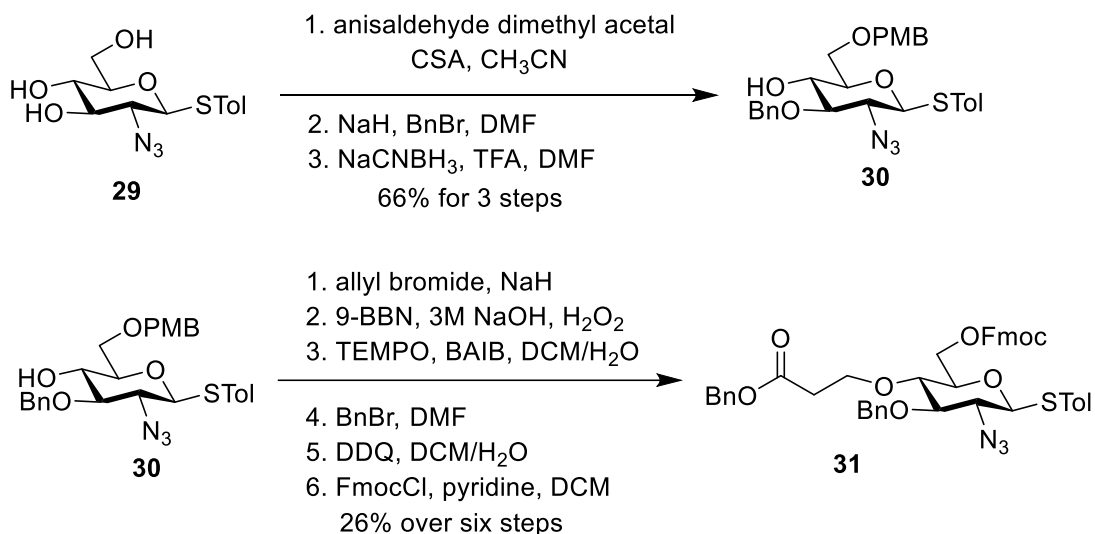


Scheme 2.11. Lactone formation from carboxylic acid **26** during HATU mediated amide formation reaction.

2.3. Monosaccharide Building Block Preparation

To overcome the lactone formation, we envisioned that if we can extend the carboxylic acid linker by one more carbon, the seven-membered ring would be more difficult to form than the six-membered lactone, thus favoring the desired amide product formation. To fulfill this idea, we started with GlcN donor modification. 4-Methoxybenzylidene acetal was utilized to protect

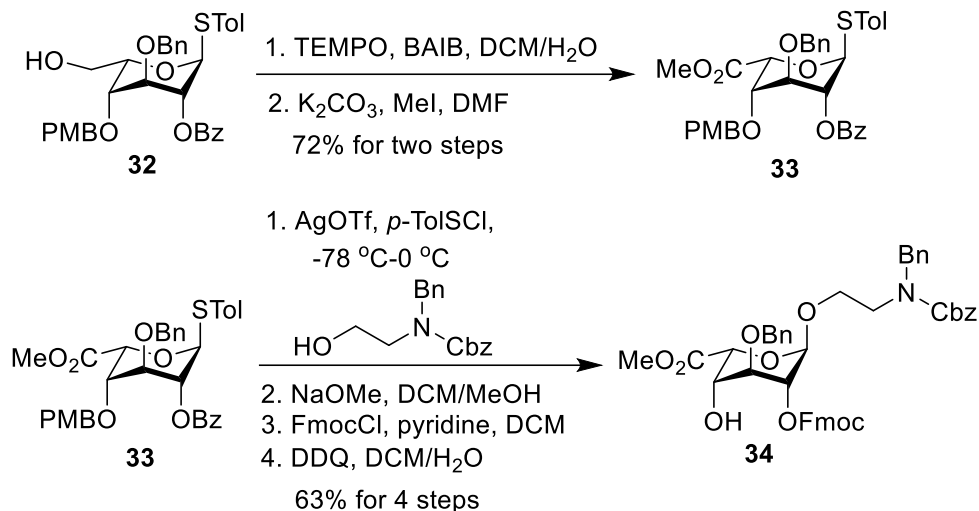
the 4-*O* and 6-*O* positions of compound **29**, and the 3-*O* was protected by the Bn group. NaCNBH₃-mediated reductive 4-methoxybenzylidene 4-*O*-ring opening afforded compound **30**. Allyl group was installed at 4-*O* position of **30** followed by a hydroboration-oxidation reaction to obtain the primary alcohol linker. The alcohol was then oxidized to a carboxylate group, which was subsequently protected as a benzyl ester. The 6-*O*-PMB protecting group was replaced with Fmoc as a potential *O*-sulfation site to form the GlcN donor **31** (**Scheme 2.12**).



Scheme 2.12. Glucosamine donor synthesis.

6-OH on idopyranosyluronate **32** was oxidized by a catalytic amount of 2,2,6,6-tetramethyl-1-piperidinyloxy (TEMPO) with bis(acetoxy)iodobenzene (BAIB), followed by methyl ester formation to afford idopyranosyluronate **33**. Glycosylation of **33** with *N*-Cbz and *N*-Bn protected ethanolamine linker provided α product in 87% yield. The stereochemistry was confirmed by one-bond coupling constants between the anomeric carbon and hydrogen atoms ($^1J_{\text{CH}} = 172$ Hz). 2-*O*-Bz conferred better neighboring group assistance than 2-*O*-Fmoc, which only afforded α/β stereoselectivity in 3:1 ratio. 2-*O*-Bz was removed by NaOMe in DCM and

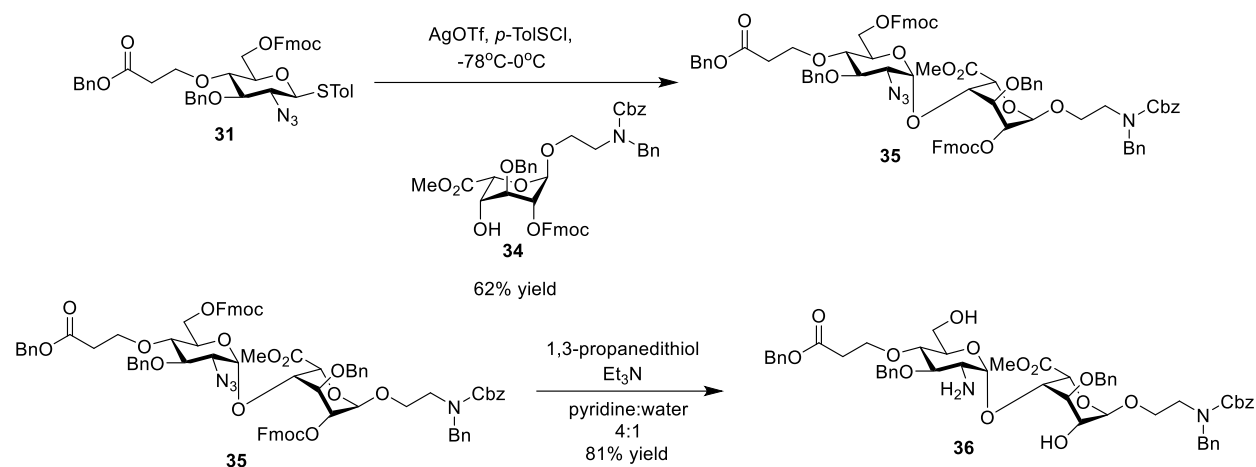
MeOH cosolvent system followed by 2-*O*-Fmoc protection and 4-*O*-PMB deprotection to provide idopyranosyluronate acceptor **34** (**Scheme 2.13**).



Scheme 2.13. Idopyranosyluronate acceptor **34** preparation.

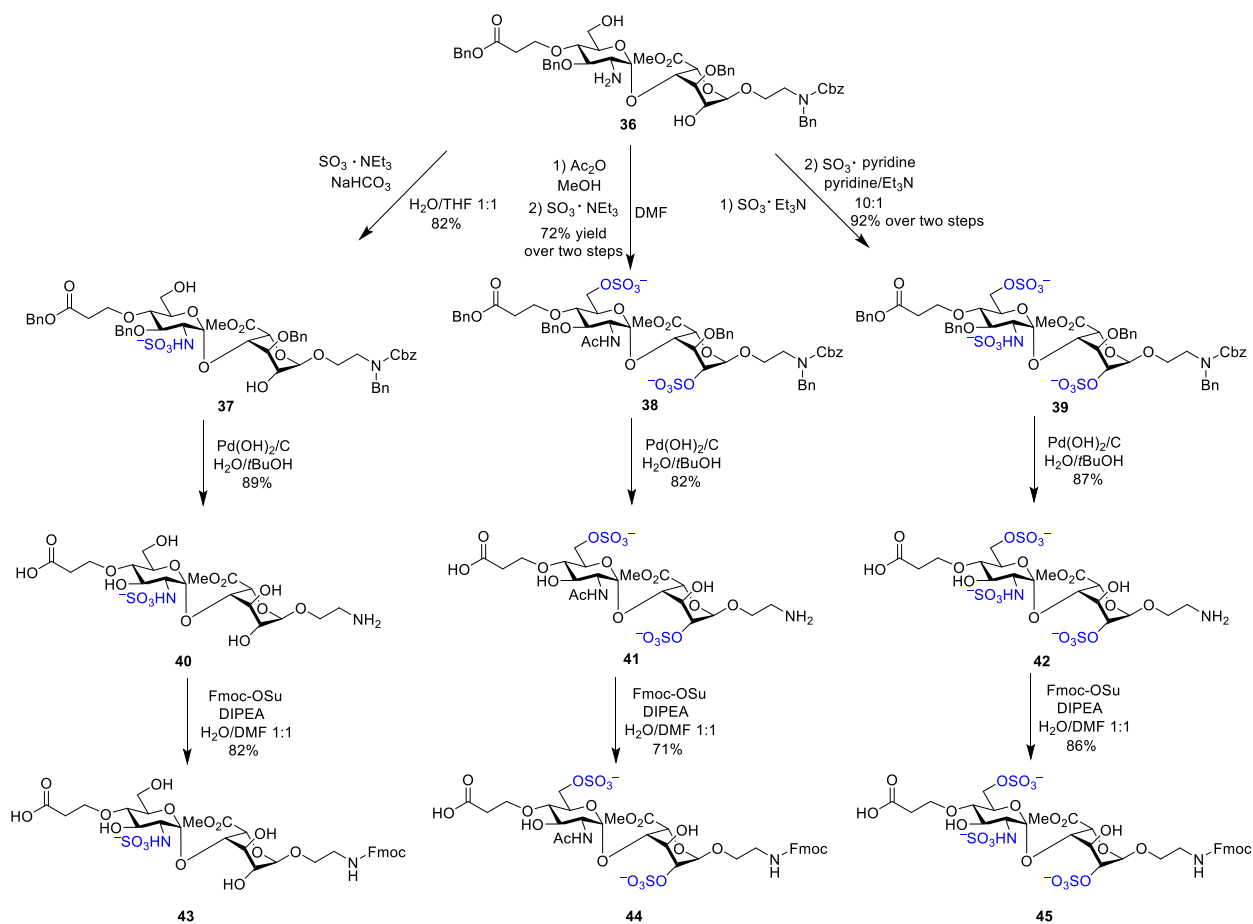
2.4. Synthesis of Disaccharide modules with Various Sulfation Patterns

The presence of non-participating azide group at C2 of glucosamine donor **31** assisted the formation of the desired 1,2-*cis* disaccharide **35** ($^1J_{\text{CH}} = 173$ Hz) *via* promotion by *p*-TolSCl/AgOTf (**Scheme 2.14**). Disaccharide **36** was originally obtained by a two-step procedure of azide reduction with Zn/HOAc followed by Fmoc deprotection. Instead, treatment of **36** with 1,3-propanedithiol in Et₃N furnished **36** in one step with an 81% yield (**Scheme 2.14**).¹²⁹



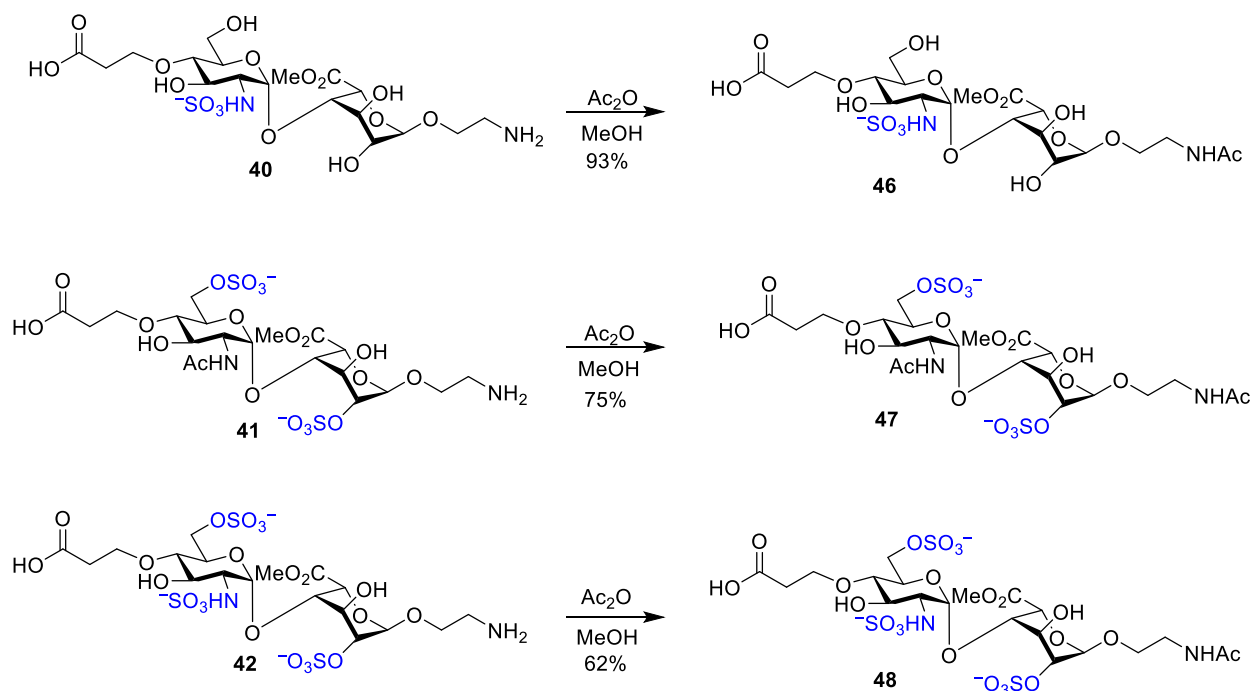
Scheme 2.14. Disaccharide synthesis and modification.

Next, we explored whether different sulfation pattern disaccharides could be generated from **36** under various sulfation conditions. *N*-sulfation of **37** was achieved by treatment with $\text{SO}_3 \cdot \text{Et}_3\text{N}$ in a H_2O and THF cosolvent system. The amine of **36** was converted to acetamide followed by *O*-sulfation *via* $\text{SO}_3 \cdot \text{Et}_3\text{N}$ at 55°C in DMF to obtain *O*-sulfated disaccharide **38**. $\text{SO}_3 \cdot \text{pyridine}$ complex in pyridine solution was implemented for fully sulfated compound **39** preparation. However, incomplete sulfation byproduct was observed even with extended reaction time and an increased amount of sulfation reagents. Two-step sulfation was performed next with *O*-sulfation followed by *N*-sulfation to furnish **39** in 92% yield over two steps. The Bn and Cbz protecting groups were removed by hydrogenation with Pd/C to afford compounds **40-42**. The elongation sequence disaccharides **43-45** were prepared by *N*-Fmoc protection of amines. FmocCl gave the Fmoc protected carboxylate byproduct, and Fmoc-OSu was used to afford selectively *N*-Fmoc protected **43-45** (Scheme 2.15).¹³⁰



Scheme 2.15. Preparation of disaccharides bearing various sulfation patterns.

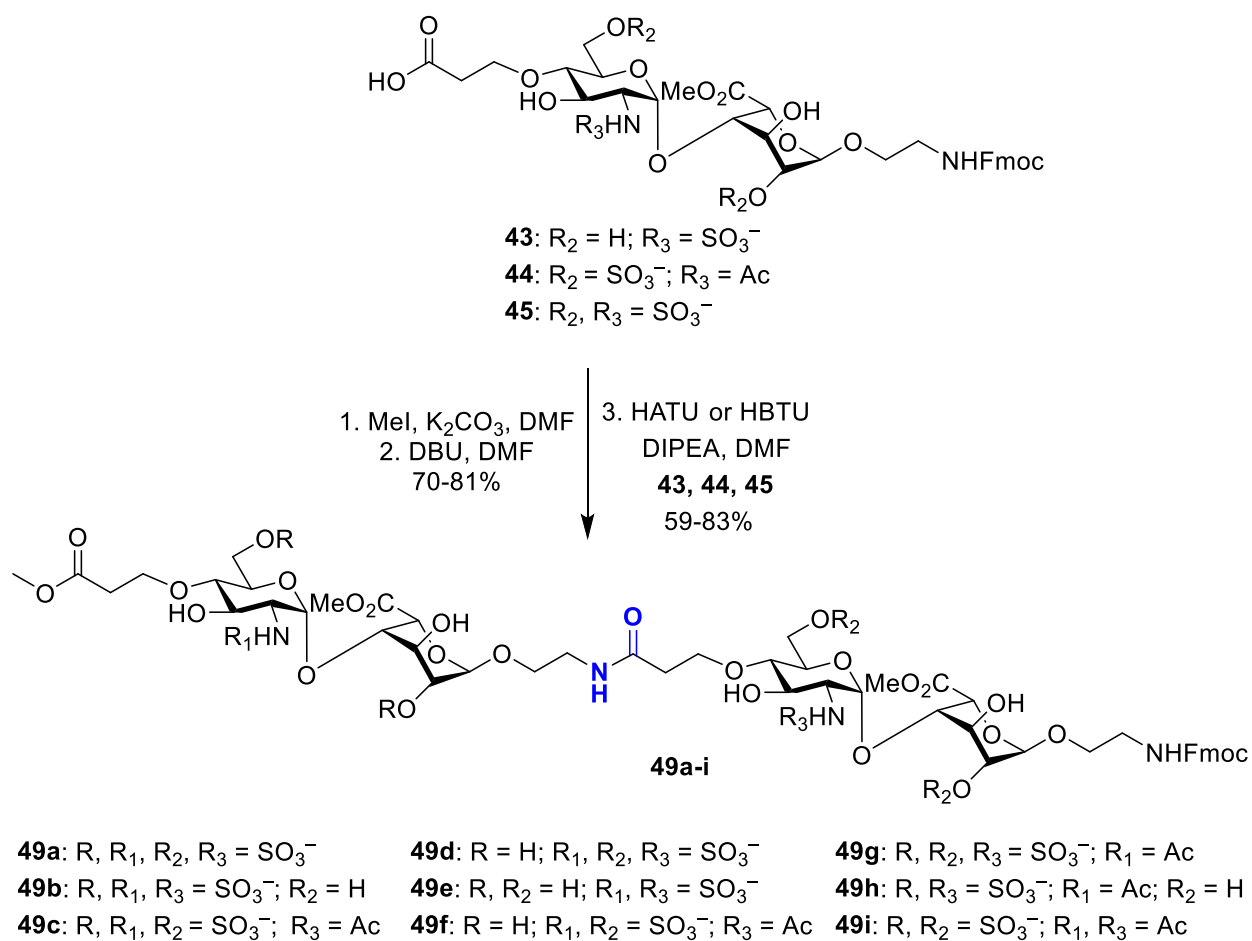
Next, the reducing end sequence disaccharides were designed with a masked amine as part of the aglycon linker. Treatment with acetic anhydride in MeOH enabled acetylation of amines to furnish desired disaccharides **46-48** (Scheme 2.16).



Scheme 2.16. Reducing end sequence disaccharides **46-48**.

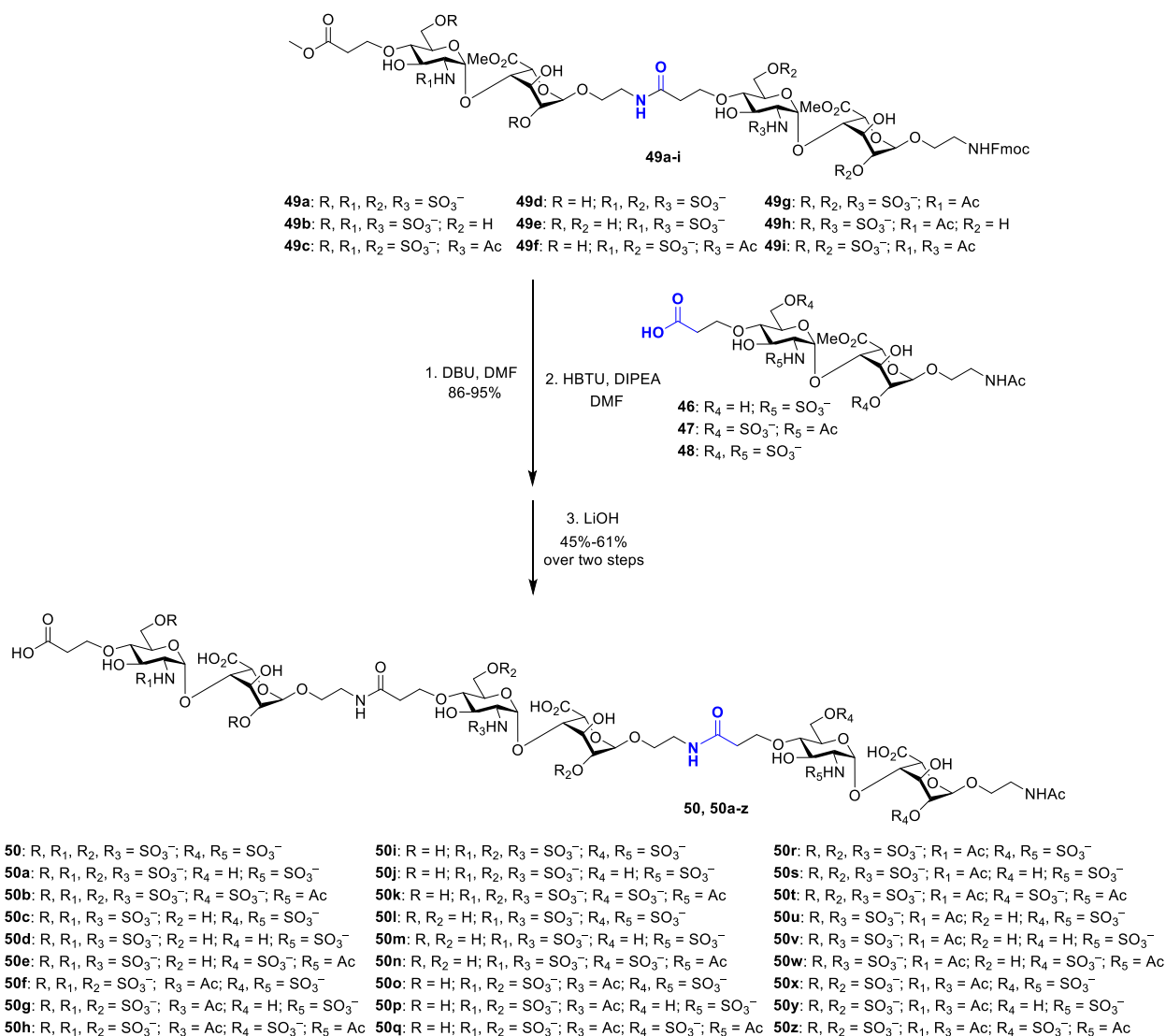
2.5. Synthesis of a Library of 27 Pseudo-hexasaccharide Heparin Mimetics

In order to build a pseudo tetrasaccharide library, the carboxylate groups of disaccharides **43-45** were blocked by methyl ester followed by *N*-Fmoc deprotection *via* DBU. Nine pseudo-tetrasaccharides with different combinations of sulfation patterns on disaccharide modules were prepared by HATU or HBTU mediated coupling reactions. We observed seven-membered lactone byproduct (10-20%) produced with fully sulfated disaccharide **45**. In this case, HBTU was used for amidation reactions (**Scheme 2.17**).



Scheme 2.17. Pseudo tetrasaccharide formation.

As each disaccharide module possesses three different sulfation patterns, 27 various pseudo hexasaccharide mimetics could be generated. Developing such a library is regarded as a potential tool to understand the heparin structure and its biological functions. The pseudo tetrasaccharides (**49a-i**) were treated with DBU to deprotect the *N*-Fmoc group followed by HATU or HBTU coupling reaction to furnish the desired pseudo hexasaccharides. Saponification of methyl esters afforded the fully deprotected 27 pseudo hexasaccharides (**50, 50a-z**) (**Scheme 2.18**).



Scheme 2.18. A library of 27 pseudo-hexasaccharides.

2.6. Conclusions

In conclusion, a library of 27 pseudo-hexasaccharide heparin mimetics has been rapidly created through disaccharide modules. Oxime formation failed due to the instability of the O-N bond under both hydrogenation and acidic conditions. Reductive amination could not afford the desired pseudo-tetrasaccharide. Finally, the disaccharide modules were linked through amide

bonds. With our “head-to-tail” synthetic strategies, the pseudo heparin oligosaccharides could be easily extended to longer sequences, and each disaccharide unit could have distinct sulfation pattern. Next, the bioactivity of pseudo-hexasaccharides will be studied.

2.7. Experimental Section

2.7.1. General synthetic procedures.

All reactions were performed under a nitrogen atmosphere with anhydrous solvents. Solvents were dried using a solvent purification system. Glycosylation reactions were performed with 4Å molecular sieves that were flamed dried under high vacuum. Chemicals used were reagent grade unless noted. Reactions were visualized by UV light (254 nm) and by staining with either $\text{Ce}(\text{NH}_4)_2(\text{NO}_3)_6$ (0.5g) and $(\text{NH}_4)\text{Mo}_7\text{O}_{24}\cdot 4\text{H}_2\text{O}$ (24.0 g) in 6% H_2SO_4 (500 mL), 5% H_2SO_4 in EtOH. Flash chromatography was performed on silica gel 601 (230-400 Mesh). NMR spectra were referenced using residual CHCl_3 , CO_3OD , and D_2O . Peak and coupling constants assignments are based on ^1H -NMR, ^1H - ^1H gCOSY, ^1H and ^1H - ^1H TOCSY, ^1H - ^1H NOESY, ^1H - ^{13}C gHSQC, ^1H - ^{13}C gHMBC.

2.7.2. General procedure for pre-activation Based Single-step Glycosylation.

A solution of the donor (1.0 equiv) and freshly activated molecular sieve MS 4 Å in DCM was stirred for 20 minutes under room temperature and then cooled to $-78\text{ }^\circ\text{C}$. A solution of AgOTf (3.0 equiv) in anhydrous $\text{Et}_2\text{O}/\text{DCM}$ (10/1, v/v) was added to the reaction solution without touching the wall of the flask. After 5 minutes, orange-colored *p*-TolSCI (1.0 equiv) was added to the solution through a microsyringe. *p*-TolSCI should be added directly to the reaction

solution to prevent it from freezing on the flask wall and stir bar. The characteristic orange color of *p*-TolSCl should dissipate within a few seconds indicating consumption of *p*-TolSCl promoter. TLC analysis could confirm the complete activation of the donor in 5 minutes. A solution of acceptor (1.0 equiv) with TTBP (1.0 equiv) in DCM was added to reaction solution (0.3 M). The reaction mixture can be warmed up to 0 °C under stirring in 2 hours, depending on the reactivity of both donor and acceptor. The reaction mixture was quenched by Et₃N (NaHCO₃ saturated solution for Fmoc protected compounds) and filtered over Celite with DCM. DCM solution was washed by NaHCO₃ and NaCl saturated solutions. The organic layer was collected and dried over Na₂SO₄, concentrated and purified by silica gel flash chromatography.

2.7.3. General procedure for deprotection of PMB.

The PMB-protected compound (1.0 equiv) was dissolved in DCM/H₂O (0.1 M, 10:1, v/v). The mixture was cooled to 0 °C, followed by the addition of DDQ (1.5 equiv). The mixture was stirred at room temperature for 1 hour. The residue was diluted with DCM and washed with saturated solutions of NaHCO₃ and NaCl, dried (Na₂SO₄), and filtered. The filtrate was concentrated *in vacuo*, and the residue was purified by silica gel flash chromatography.

2.7.4. General procedure for protection of 6-OH with Lev.

The compound containing 6-OH (1.0 equiv) was dissolved in DCM (0.3 M), followed by the addition of EDC-HCl (3.0 equiv), levulinic acid (1.4 equiv) and DMAP (1.0 equiv). The mixture was stirred under room temperature for 1 hour. The residue was diluted with DCM and washed with 10% HCl, saturated solutions of NaHCO₃ and NaCl. The organic solution was dried

over Na₂SO₄ and concentrated *in vacuo*, then purified by silica gel flash chromatography.

2.7.5. General procedure for O-Acetylation.

The compound containing -OH (1.0 equiv) was dissolved in pyridine (1.2 M), followed by the addition of acetic anhydride (7.0 equiv for each hydroxyl group) at 0 °C. The mixture was stirred at room temperature overnight and then washed with 3 x 1.0 M HCl and saturated solutions of NaHCO₃ and NaCl. The organic solution was dried over Na₂SO₄, filtered and concentrated *in vacuo*, then purified by silica gel flash chromatography to afford the desired compounds.

2.7.6. General procedure for N-Acetylation.

The compound containing -NH₂ (1.0 equiv) was dissolved in MeOH (0.04 M), followed by the addition of acetic anhydride (3.0 equiv) and Et₃N (3.0 equiv). The mixture was stirred at room temperature for 1 h and then was passed through LH-20 gel column with MeOH to afford the desired compounds.

2.7.7. General procedure for protection of OH with Fmoc.

To a solution of starting material in DCM (0.3 M), FmocCl (3.0 equiv) and pyridine (4.0 equiv) were added. The reaction mixture was stirred at room temperature for 1 h and diluted with DCM. The organic mixture was washed with 3 x 1 M HCl, NaHCO₃ saturated solution, and brine. The organic layer was dried over anhydrous Na₂SO₄ and filtered. The filtrate was concentrated by rotary evaporation and the desired product was purified by silica gel column

chromatography.

2.7.8. General procedure for protection of NH₂ with Fmoc.

To a solution of starting material in H₂O/DMF (1/1, v/v, 0.3 M), Fmoc-OSu (3.0 equiv) and DIPEA (1.5 equiv) were added. The reaction mixture was stirred at room temperature for 2 h. The organic mixture was washed with 3 x 1 M HCl, NaHCO₃ saturated solution and brine. The organic layer was dried over anhydrous Na₂SO₄ and filtered. The filtrate was concentrated by rotary evaporation and the desired product was purified by silica gel column chromatography. For disaccharide Fmoc protection, after the reaction completed as indicated by TLC (EtOAc/MeOH/H₂O 3/1/1), the reaction mixture was passed through an LH-20 gel column with MeOH. A column of Dowex 50WX4 Na⁺ resin was used for ion exchange for giving products as sodium salts.

2.7.9. General procedure for preparation of methyl ester.

K₂CO₃ (10.0 equiv) and CH₃I (6.0 equiv) was added to a solution of starting material (1.0 equiv) in DMF (0.13M). The reaction mixture was stirred at room temperature for 4 h. After completion, the mixture was passed through an LH-20 gel column to afford pure compounds.

2.7.10. General procedure for NH-Fmoc Deprotection.

A mixture of starting material (1.0 equiv) and DBU (5.0 equiv) in DMF (0.15 M) was stirred for 1 h at room temperature. After TLC (EtOAc/MeOH/H₂O, 3/1/1, v/v/v) indicating that

the reaction was complete, the reaction mixture was passed through an LH-20 gel column to give pure compounds.

2.7.11. General procedure for preparation of pseudo-tetrasaccharides/hexasaccharides.

A solution of carboxyethyl disaccharides (1.0 equiv), HATU or HBTU (1.0 equiv) and DIPEA (2.0 equiv) in DMF was added to starting material (1.0 equiv) in DMF (0.013 M). After stirring 1 h at room temperature, TLC (EtOAc/MeOH/H₂O, 2.5/1/1, v/v/v) indicated completion of the reaction. Then the reaction mixture was passed through an LH-20 gel column, and the fractions containing product were collected and concentrated under reduced pressure. A column of Dowex 50WX4 Na⁺ resin was used for ion exchange to give products as sodium salts.

2.7.12. General procedure for hydrogenolysis.

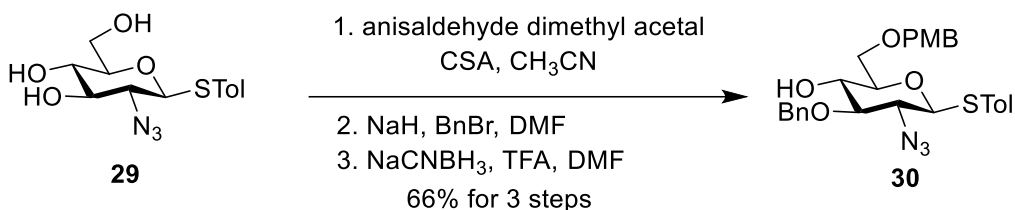
A solution of the compound in mixed *t*BuOH and water [1/1 (v/v), 3 mL] in the presence of 10% Pd(OH)₂/C (80 mg) at room temperature was exposed to H₂ gas. After overnight, the suspension was filtered through Celite, and the filtrate was concentrated *in vacuo*. The residue was passed through an LH-20 gel column using MeOH as eluent. The product fractions were concentrated under reduced pressure to give the target molecule.

2.7.13. General procedure for saponification of methyl esters.

The starting material (1.0 equiv) was added to a LiOH (10.0 equiv per CO₂Me) solution (0.006 M) at 0 °C. The reaction mixture was stirred at 0 °C for 8 h. After TLC (EtOAc/MeOH/H₂O, 1.5/1/1, v/v/v) indicated the reaction completion, Amberlite H⁺ resin was

added until pH ~ 7. The reaction mixture was passed through G-15, and Dowex 50WX4 Na⁺ gel columns to give pure products as the sodium salts.

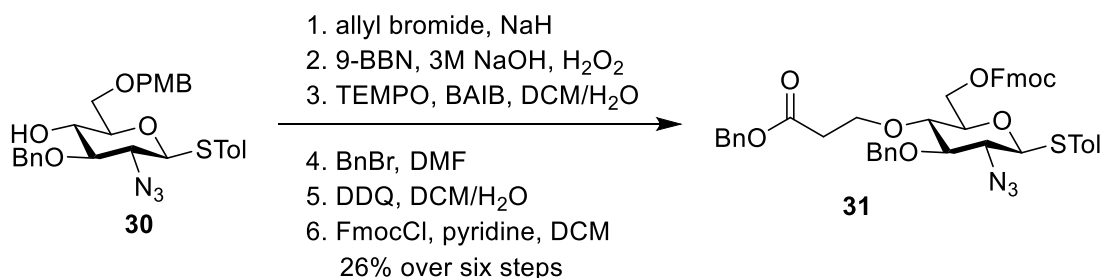
Product Preparation and Characterization Data



p-Tolyl 2-azido-3-*O*-benzyl-2-deoxy-6-*O*-*para*-methoxybenzyl-1-thio- β -D-glucopyranoside (30)

The starting material **29** (3.8 g, 12.2 mmol) was dissolved in CH₃CN (0.4 M, 32.0 ml), and anisaldehyde dimethyl acetal (4.1 ml, 24.4 mmol) and CSA (1.1 g, 4.9 mmol) were added. After stirring at room temperature overnight, the reaction mixture was neutralized with Et₃N and concentrated under reduced pressure. The residue was diluted with DCM and washed with saturated NaHCO₃ solution and brine. The organic solution was dried over Na₂SO₄ and filtered. The filtrate was concentrated under reduced pressure, and the residue was purified by silica gel column chromatography using a gradient of DCM and methanol (from 20/1 to 12/1, v/v). A solution of the above compound **30** (4.2 g, 9.9 mmol), NaH (0.6 g, 14.8 mmol) and BnBr (2.3 ml, 19.7 mmol) in DMF (15 ml, 0.7 M) was kept stirring at room temperature for 2 h. After the starting material was completely consumed, the reaction mixture was neutralized with NH₄Cl saturated solution and sequentially washed with NaHCO₃ saturated solution (3 x 70 ml) and brine (75 ml). The organic layer was dried over anhydrous Na₂SO₄ and concentrated *in vacuo*,

and the residue was purified by flash column chromatography to afford the desired product. The above compound (4.9 g, 9.5 mmol) was dissolved in DMF (30 ml, 0.3 M), followed by the addition of NaCNBH₃ (6.0 g, 95 mmol) and TFA (7.3 ml, 95 mmol) at 0 °C. The reaction mixture was warmed to room temperature and stirred overnight, and then diluted with EtOAc. The organic mixture was washed with water (3 x 70 ml) to get rid of DMF, NaHCO₃ saturated solution (3 x 70 ml) and brine (50 ml). The organic layer was concentrated under reduced pressure, and the residue was purified by silica gel column chromatography using a gradient of hexanes and EtOAc (from 3/1 to 2/1, v/v) to give the desired product (**30**) (4.2 g, 66% for 3 steps). ¹H NMR (500 MHz, CDCl₃) δ 7.51 – 7.47 (m, 2H; ArCH₂-), 7.43 – 7.31 (m, 5H; Ar-H), 7.29 – 7.25 (m, 2H; ArCH₂-), 7.11 (d, J = 8.0 Hz, 2H; ArCH₂-), 6.95 – 6.88 (m, 2H; ArCH₂-), 4.92 – 4.83 (m, 2H; BnCH₂), 4.57 – 4.48 (m, 2H; PMBCH₂), 4.39 (d, J = 9.0 Hz, 1H; 1-H), 3.84 (s, 3H; OCH₃), 3.78 (dd, J = 10.3, 4.9 Hz, 1H; 6-H), 3.73 (dd, J = 10.3, 4.9 Hz, 1H; 6'-H), 3.65 – 3.59 (m, 1H; 4-H), 3.47 – 3.41 (m, 1H; 5-H), 3.38 (t, J = 9.0 Hz, 1H; 3-H), 3.30 (t, J = 9.0 Hz, 1H; 2-H), 2.85 (d, J = 2.5 Hz, 1H; OH), 2.35 (s, 3H; STolCH₃). ¹³C NMR (125 MHz, CDCl₃) δ 159.37, 138.75, 137.88, 134.20, 129.81, 129.74, 129.44, 128.63, 128.27, 128.12, 127.07, 113.88, 86.14, 84.57, 77.86, 75.50, 73.44, 72.24, 70.11, 64.30, 55.32, 21.22. HRMS: m/z calc. for C₂₈H₃₁N₃O₅S [M+NH₄⁺]⁺: 539.2323; found: 539.2336.



***p*-Tolyl 2-azido-3-*O*-benzyl-4-*O*-benzyl propionate-2-deoxy-6-*O*-
fluorenylmethoxycarbonyl-1-thio- β -D-glucopyranoside (31)**

The starting material **30** (11 g, 21 mmol) was dissolved in DMF (30 ml, 0.7 M), then NaH (1.6 g, 63 mmol) and allyl bromide (3.8 ml, 42 mmol) were added at 0 °C. The reaction mixture was warmed up to room temperature and stirred for 1 h until TLC (Hexanes/EtOAc 3:1, v/v) indicated completion of the reaction. After neutralization with saturated NH₄Cl solution, the reaction mixture was diluted with DCM and washed with saturated NaHCO₃ solution (3 x 200 ml) and brine (200 ml), dried (Na₂SO₄). The organic layer was filtered, and the filtrate was concentrated *in vacuo*, then purified by silica gel column chromatography using a gradient of hexanes and EtOAc (from 15/1 to 12/1, v/v). The above compound (11 g, 20 mmol) was dissolved in THF (87 ml, 0.2 M) and cooled to 0 °C. A solution of 9-BBN in THF (0.5 M, 77 ml, 38 mmol) was added and the reaction mixture was warmed to room temperature and stirred overnight. After hydroboration was complete, ethanol (50 ml) was added slowly to the reaction mixture at 0 °C, followed by the addition of NaOH (1.0 M aq, 98 ml) and H₂O₂ (30 wt% aq, 98 ml). The reaction mixture was warmed to 60 °C for 3 h, then quenched with saturated NH₄Cl solution and extracted into EtOAc (3 x 100 ml). The combined organic extracts were washed with NaHCO₃ saturated solution (3 x 100 ml) and brine (100 ml), dried over Na₂SO₄ and filtered. The filtrate was concentrated by rotary evaporation, and the residue was purified by silica gel column chromatography from pure hexanes to hexanes/EtOAc (10/1, v/v). The above compound (6.7 g, 11.6 mmol), BAIB (8.2 g, 25.5 mmol) and TEMPO (0.5 g, 3.5 mmol) were dissolved in DCM/H₂O (4/1, v/v, 1.2 M). After stirring at room temperature for 2 h, the reaction mixture was diluted in DCM and washed with water (3 x 75 ml) and Na₂S₂O₃ (40 ml) solution. The organic solvent was evaporated under reduced pressure. The residue (6.8 g, 11.5 mmol) was dissolved in

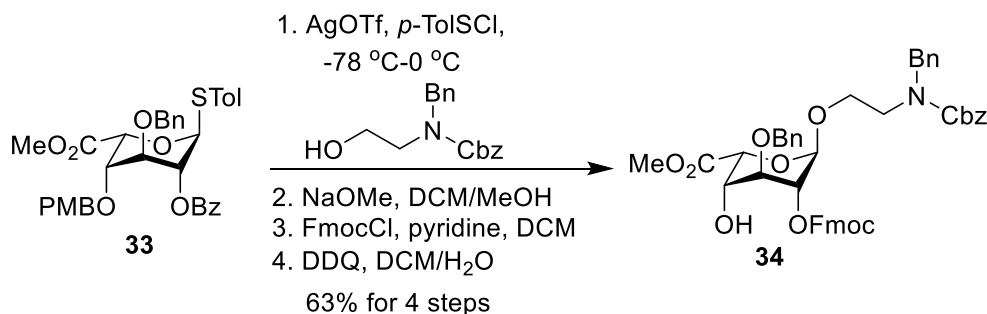
DMF (23 ml, 0.5 M), followed by the addition of K₂CO₃ (9.5 g, 69 mmol) and BnBr (8.2 ml, 69 mmol). The reaction mixture was stirred at room temperature for 4 h and diluted with EtOAc and washed with 1M HCl (3 x 75 ml), NaHCO₃ saturated solution (3 x 75 ml) and brine (75 ml). The organic solution was dried over Na₂SO₄, and the filtrate was concentrated by rotary evaporation. The residue was purified by silica gel column chromatography from pure hexanes to hexanes/EtOAc (15/1 to 12/1, v/v). The above compound (5.4 g, 8.0 mmol) was treated according to the general procedures of PMB deprotection and Fmoc protection to give compound **31** (4.3 g, 26% for six steps). ¹H NMR (500 MHz, CDCl₃) δ 7.82 – 7.76 (m, 2H; ArCH₂-), 7.65 (ddd, J = 7.6, 4.5, 1.0 Hz, 2H; ArCH₂-), 7.52 – 7.22 (m, 15H; ArCH-), 7.12 – 7.06 (m, 2H; ArCH₂-), 5.14 (s, 2H; BnCH₂-), 4.85 – 4.76 (m, 2H; BnCH₂-), 4.54 – 4.41 (m, 3H; 6-H, FmocCH₂-), 4.36 – 4.26 (m, 3H; 1-H, 6'-H, FmocCH-), 4.14 – 4.04 (m, 1H; -OCH₂-), 3.88 – 3.81 (m, 1H; -OCH₂-), 3.47 – 3.39 (m, 2H; 4-H, 5-H), 3.34 – 3.21 (m, 2H; 2-H, 3-H), 2.64 – 2.51 (m, 2H; CO₂BnCH₂-), 2.30 (s, 3H; STolCH₃). ¹³C NMR (125 MHz, CDCl₃) δ 171.02, 154.96, 143.40, 143.33, 141.29, 138.88, 137.44, 135.72, 134.31, 129.79, 128.57, 128.54, 128.37, 128.31, 128.11, 127.91, 127.23, 127.21, 125.22, 120.07, 85.85, 84.74, 77.62, 76.93, 75.79, 70.04, 68.22, 66.50, 66.27, 64.70, 46.77, 35.36, 21.19. HRMS: m/z calc. for C₄₅H₄₃N₃O₈S [M+NH₄⁺]⁺: 803.3109; found: 803.3099.



***p*-Tolyl methyl-2-*O*-benzoyl-3-*O*-benzyl-4-*O*-para-methoxybenzyl-1-thio- α -L-idopyranosiduronate (**33**)**

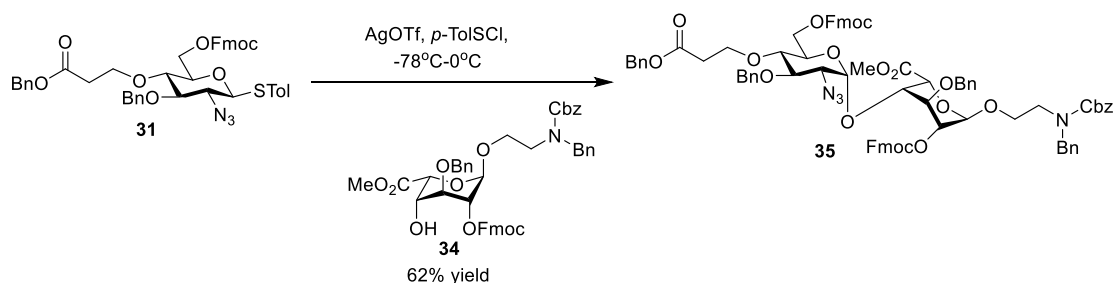
A mixture of starting material **32** (9.6 g, 16.0 mmol), BAIB (11.3 g, 35.2 mmol) and

TEMPO (0.74 g, 4.8 mmol) was dissolved in DCM/H₂O (4/1, 0.64 M). After stirring at room temperature for 4 h, the reaction mixture was diluted in DCM and washed with water (3 x 100 ml) and Na₂S₂O₃ (50 ml) solution. The organic solvent was evaporated under reduced pressure. The residue (9.8 g, 15.9 mmol) was dissolved in DMF (40 ml, 0.4 M), followed by the addition of K₂CO₃ (13.2 g, 95.4 mmol) and CH₃I (6.0 ml, 95.4 mmol). The reaction mixture was stirred at room temperature for 4 h and diluted with EtOAc and washed with 1M HCl (3 x 100 ml), NaHCO₃ saturated solution (3 x 100 ml) and brine (100 ml). The organic solution was dried over Na₂SO₄, and the filtrate was concentrated by rotary evaporation. The residue was purified by silica gel column chromatography from pure hexanes to hexanes/EtOAc (9/1 to 8/1) to yield pure compound **33** (7.2 g, 72% yield for two steps). ¹H NMR (500 MHz, CDCl₃) δ 7.99 (dd, J = 8.2, 1.5 Hz, 2H; ArCH₂-), 7.55 – 7.19 (m, 9H; ArCH-), 7.11 (d, J = 7.9 Hz, 2H; ArCH₂-), 7.07 – 7.00 (m, 2H; ArCH₂-), 6.83 – 6.66 (m, 2H; ArCH₂-), 5.77 – 5.65 (m, 1H; 1-H), 5.45 – 5.43 (m, 1H; 2-H), 5.34 – 5.25 (m, 1H; 5-H), 4.90 (d, J = 11.9 Hz, 1H; BnCH₂-), 4.66 (d, J = 11.9 Hz, 1H; BnCH₂-), 4.48 – 4.30 (m, 2H; PMBCH₂-), 3.99 – 3.92 (m, 3H; 3-H, 4-H, 5-H), 3.84 – 3.76 (m, 6H), 2.32 (s, 3H; SPhCH₃).



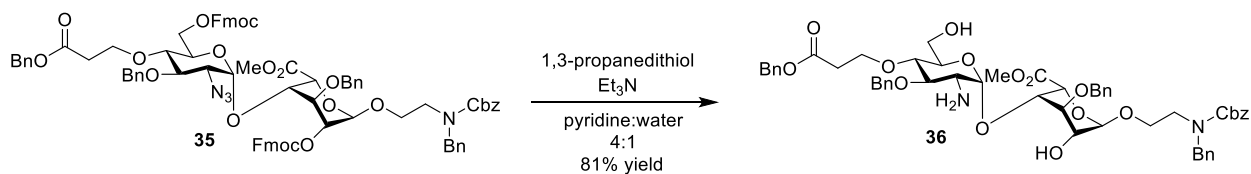
***N*-(Benzyl)-benzyloxycarbonyl-2-aminoethyl methyl-2-*O*-fluorenylmethyloxycarbonyl-3-*O*-benzyl-4-*O*-*para*-methoxybenzyl-1-thio- α -L-idopyranosiduronate (**34**)**

Compound **33** (2.4 g, 3.7 mmol) was treated according to the general procedures of pre-activation based single-step glycosylation with the acceptor (1.5 equiv) to give the desired compound. A mixture of the above compound (2.66 g, 3.37 mmol) and NaOMe (25% in MeOH) (0.31 ml, 1.7 mmol) in DCM/MeOH (1/2, v/v, 0.2M) was stirred at room temperature for 1 h. Then the reaction mixture was neutralized with Amberlite-H⁺ resin and filtered. The crude was evaporated under reduced pressure and subjected to 2-OH Fmoc protection and 4-OH PMB deprotection according to the general procedures to give compound **34** (1.9 g, 72% yield for 3 steps). ¹H NMR (500 MHz, CDCl₃) δ 7.77 (dt, J = 7.6, 1.0 Hz, 2H; ArCH₂-), 7.57 (ddd, J = 7.7, 4.2, 1.0 Hz, 2H; ArCH₂-), 7.41 (tt, J = 7.6, 1.4 Hz, 2H; ArCH₂-), 7.38 – 7.19 (m, 13H; ArCH-), 7.16 – 6.99 (m, 2H; ArCH-2-), 5.22 – 5.11 (m, 2H; 2-H, CbzCH₂-), 5.03 – 4.95 (m, 1H; 1-H), 4.83 – 4.76 (m, 2H; 5-H, CbzCH₂-), 4.75 – 4.70 (m, 1H; OBnCH₂-), 4.66 – 4.59 (m, 1H; OBnCH₂-), 4.57 – 4.37 (m, 4H; FmocCH-, NBnCH₂-), 4.24 (t, J = 7.4 Hz, 1H; FmocCH-), 4.07 (br, 1H; 3-H), 3.99 – 3.87 (m, 1H; -OCH₂-), 3.86 – 3.81 (m, 3H), 3.74 – 3.51 (m, 2H; -CH₂NBnCbz, -OCH₂-), 3.46 – 3.35 (m, 2H; 4-H, -CH₂NBnCbz), 2.78 (s, 1H). ¹³C NMR (125 MHz, CDCl₃) δ 169.68, 156.34, 153.75, 143.04, 141.33, 137.82, 137.23, 136.62, 129.06, 128.55, 128.53, 128.25, 128.08, 127.98, 127.87, 127.76, 127.32, 127.23, 125.33, 125.17, 125.13, 120.16, 98.49, 74.39, 72.32, 70.77, 70.60, 68.02, 67.74, 67.45, 52.46, 51.61, 46.69, 45.67. HRMS: m/z calc. for C₄₆H₄₅NO₁₁ [M+NH₄⁺]⁺: 805.3331; found: 805.3311.



***N*-(Benzyl)-benzyloxycarbonyl-2-aminoethyl 3-*O*-benzyl-4-*O*-benzylpropionate-2-azido-2-deoxy-6-*O*-fluorenylmethyloxycarbonyl-1-thio- α -D-glucopyranoside-(1 \rightarrow 4)-methyl-3-*O*-benzyl-2-*O*-fluorenylmethyloxycarbonyl-1-thio- α -L-idopyranosiduronate (35).**

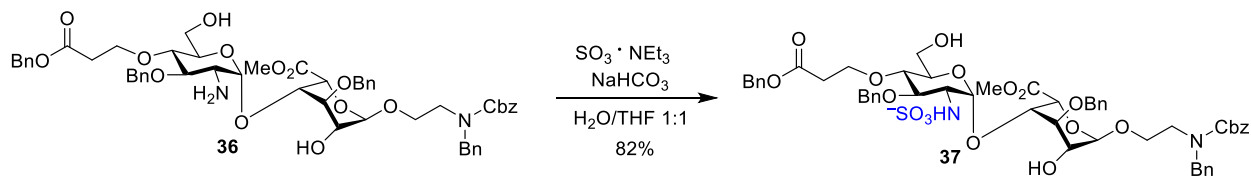
Compound **31** (1.8 g, 2.3 mmol) and **34** (1.8 g, 2.3 mmol) were treated according to the general procedures of pre-activation based single-step glycosylation to give compound **35** (2.05 g, 62%, α/β , 3/1). ^1H NMR (500 MHz, CDCl_3) δ 7.81 – 7.66 (m, 3H; Ar-H), 7.66 – 7.50 (m, 4H; Ar-H), 7.46 – 7.18 (m, 25H; Ar-H), 7.18 – 7.01 (m, 4H; Ar-H), 5.24 – 5.04 (m, 5H, 1-H, 5-H, CbzCH₂-), 4.93 – 4.86 (m, 1H, 1'-H), 4.86 – 4.69 (m, 5H), 4.63 – 4.44 (m, 4H; 2-H), 4.43 – 4.29 (m, 4H), 4.27 – 4.01 (m, 5H), 4.01 – 3.81 (m, 4H; anomeric linker-OCH₂-), 3.78 – 3.71 (m, 3H; -CO₂CH₃), 3.68 – 3.59 (m, 1H), 3.57 – 3.35 (m, 4H; 2'-H, 3'-H, 4-H, 5'-H), 3.34 – 3.21 (m, 1H), 2.60 – 2.49 (m, 2H; BnCO₂CH₂-), ^{13}C NMR (125 MHz, CDCl_3) δ 171.00, 169.39, 156.18, 154.99, 154.58, 144.24, 143.35, 143.26, 141.27, 140.22, 137.75, 137.67, 137.34, 135.46, 131.39, 130.39, 130.20, 130.08, 128.77, 128.58, 128.47, 128.45, 128.35, 128.25, 128.00, 127.97, 127.91, 127.84, 127.80, 127.40, 127.29, 127.23, 127.19, 127.15, 125.36, 125.26, 125.15, 120.60, 120.09, 120.04, 98.50, 79.62, 76.78, 75.09, 73.89, 73.24, 70.42, 70.00, 69.61, 68.07, 67.70, 67.32, 66.44, 65.81, 63.30, 52.36, 51.59, 46.72, 46.56, 35.34.



***N*-(Benzyl)-benzyloxycarbonyl-2-aminoethyl 2-amino-3-*O*-benzyl-4-*O*-benzylpropionate-2-deoxy-1-thio- α -D-glucopyranoside-(1 \rightarrow 4)-methyl-3-*O*-benzyl-1-thio- α -L-**

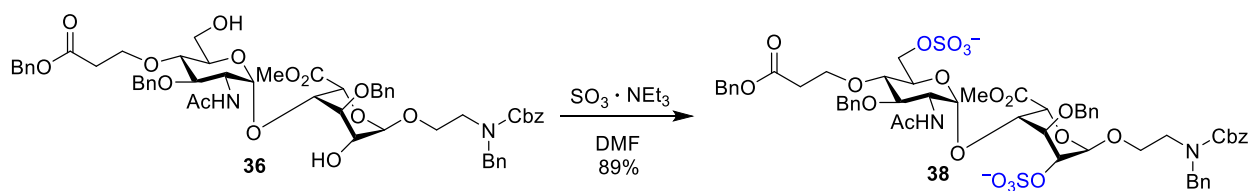
idopyranosiduronate (36).

At 50 °C under N₂ atmosphere, 1,3-propanedithiol (2.8 ml, 27.0 mmol) and Et₃N (3.7 ml, 27.0 mmol) were added to a solution of starting material **35** (0.7 g, 0.48 mmol) in pyridine/H₂O (4/1, 0.04 M) and the reaction mixture was stirred for 2 h. The reaction mixture was concentrated by rotary evaporation and purified by silica gel column chromatography using a gradient of DCM and MeOH (from 50/1 to 40/1 to 20/1, v/v) to give the desired product **36** (0.38 g, 81%). ¹H NMR (500 MHz, CDCl₃) δ 7.45 – 6.95 (m, 19H; Ar-H), 7.12 – 7.04 (m, 2H; ArCH₂-), 5.21 – 5.06 (m, 4H; 1-H, 1'-H), 5.00 – 4.90 (m, 2H), 4.88 – 4.80 (m, 2H; BnCH-), 4.70 (d, J = 11.9 Hz, 1H; BnCH-), 4.62 – 4.43 (m, 4H), 4.15 (s, 1H), 4.05 – 3.98 (m, 1H), 3.96-3.84 (m, 3H), 3.78 – 3.64 (m, 6H; -CO₂CH₃, -NCH₂-), 3.64 – 3.51 (m, 1H), 3.46 – 3.32 (m, 4H), 2.83 (dd, J = 10.1, 3.7 Hz, 1H), 2.63 – 2.52 (m, 2H; BnCO₂CH₂-). ¹³C NMR (125 MHz, CDCl₃) δ 171.56, 138.09, 135.60, 128.60, 128.53, 128.49, 128.46, 128.42, 128.36, 128.32, 127.94, 127.82, 127.74, 127.66, 127.18, 101.88, 96.50, 82.19, 78.58, 76.77, 75.57, 72.23, 72.03, 7.87, 67.80, 67.36, 67.22, 66.54, 66.43, 61.22, 55.04, 52.37, 51.61, 46.68, 45.70, 35.41. HRMS: m/z calc. for C₅₄H₆₂N₂O₁₅ [M+H]⁺: 978.4150; found: 978.4205.



***N*-(Benzyl)-benzyloxycarbonyl-2-aminoethyl 3-*O*-benzyl-4-*O*-benzylpropionate-2-deoxy-2-sulfoamino-1-thio- α -D-glucopyranoside-(1 \rightarrow 4)-methyl-3-*O*-benzyl-1-thio- α -L-idopyranosiduronate (37).**

The starting material **36** (90 mg, 0.09 mmol) was dissolved in H₂O/THF (1/1, v/v, 0.05 M) mixture, followed by addition of NaHCO₃ (115 mg, 1.37 mmol) and sulfur trioxide triethylamine complex (142 mg, 0.9 mmol). The reaction mixture was stirred at room temperature for 2 h and diluted with DCM. The organic mixture was washed with water and brine, and then filtered. The filtrate was concentrated under reduced pressure and the residue was purified by silica gel column chromatography using a mixture of DCM and methanol to give desired product **37** (20/1, v/v). ¹H NMR (500 MHz, CD₃OD) δ 7.45 (d, J = 7.4 Hz, 2H; ArCH₂-), 7.40 – 7.10 (m, 16H; Ar-H), 7.01-6.91 (m, 2H; ArCH₂-), 5.41 (d, J = 3.4 Hz, 1H; 1'-H), 5.16 – 5.06 (m, 3H; CO₂BnCH₂-, CbzCH-), 4.99 (d, J = 10.8 Hz, 1H; CbzCH-), 4.88 (s, 2H; 1-H, 5-H), 4.81 (d, J = 9.5 Hz, 1H; OBnCH-), 4.75 – 4.59 (m, 3H; OBnCH₂-), 4.58 – 4.33 (m, 2H; NBnCH₂-), 4.18 (s, 2H; 2-H, 4-H), 4.05 – 3.97 (m, 1H; 4'-linker-OCH-), 3.95 – 3.80 (m, 3H; 4'-linker-OCH-, 6'-H), 3.78 – 3.51 (m, 5H; 5'-H, 3-H, 4'-H, anomeric linker-OCH₂-), 3.49 – 3.25 (m, 5H; NCH₂-, 2'-H, 3'-H), 2.54 – 2.48 (m, 2H; BnCO₂CH₂-). ¹³C NMR (125 MHz, CD₃OD) δ 171.81, 170.46, 156.65, 139.00, 138.10, 137.68, 128.24, 128.13, 128.10, 128.06, 128.01, 127.86, 127.84, 127.79, 127.77, 127.56, 127.52, 127.47, 127.38, 127.34, 127.26, 127.02, 126.90, 126.87, 101.38, 96.25, 79.92, 77.36, 74.71, 73.59, 72.15, 71.56, 67.64, 67.42, 66.47, 65.88, 60.36, 58.11, 51.55, 51.28, 46.67, 45.78, 35.15. HRMS: m/z calc. for C₅₄H₆₁N₂O₁₈S⁻ [M]⁻: 1057.3646; found: 1057.3646.

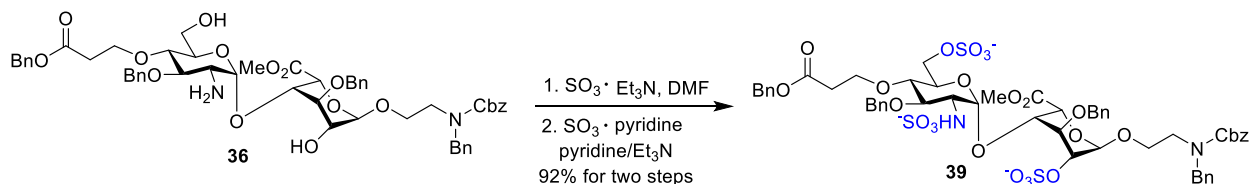


***N*-(Benzyl)-benzyloxycarbonyl-2-aminoethyl**

2-acetamido-3-*O*-benzyl-4-*O*-

benzylpropionate-2-deoxy-6-O-sulfonato-1-thio- α -D-glucopyranoside-(1 \rightarrow 4)-methyl-3-O-benzyl-2-O-sulfonato-1-thio- α -L-idopyranosiduronate (38).

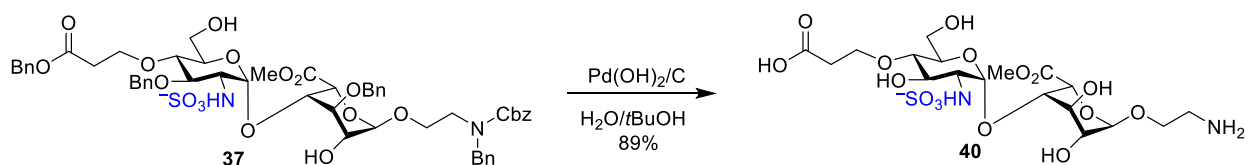
To a solution of starting material **36** (225 mg, 0.22 mmol) in DMF (0.08 M) was added sulfur trioxide triethylamine complex (800mg, 4.4 mmol) and the resulting reaction mixture was stirred at 55 °C for 2 h. The reaction mixture was purified by a LH-20 gel column with CH₃OH. Fractions containing the product were collected under reduced pressure and the residue was passed through a column of Dowex 50WX4 Na⁺ resin using H₂O as the eluent to give sodium form product **38** (223 mg, 89%). ¹H NMR (500 MHz, CD₃OD) δ 7.49 – 7.60 (m, 1H; Ar-H), 7.41 – 7.14 (m, 16H; Ar-H), 7.12-6.96 (m, 2H; ArCH₂-), 5.22 – 5.09 (m, 4H; CO₂BnCH₂-, 1-H, 1'-H), 4.83 – 4.73 (m, 3H; 5-H, CbzCH₂-), 4.73 – 4.57 (m, 4H; OBnCH₂-, OBnCH₂-), 4.56 – 4.41 (m, 2H; NBnCH₂-), 4.29 – 4.13 (m, 3H; 2-H, 6'-H), 4.12 – 4.03 (m, 3H; 4-H, 7-H), 4.00 – 3.85 (m, 2H; NCH₂-), 3.80-3.74 (m, 3H, CO₂CH₃), 3.70 – 3.61 (m, 3H; 5'-H, 3-H, 4'-H), 3.45 – 3.36 (m, 2H; 2'-H, 3'-H), 2.64 – 2.52 (m, 2H; BnCO₂CH₂-). HRMS: m/z calc. for C₅₆H₆₂N₂O₂₂S₂²⁻ [M]²⁻: 589.1623; found: 589.1611.



N-(Benzyl)-benzyloxycarbonyl-2-aminoethyl 3-O-benzyl-4-O-benzylpropionate- 2-deoxy-2-sulfoamino-6-O-sulfonato- α -D-glucopyranoside-(1 \rightarrow 4)-methyl-3-O-benzyl-2-O-sulfonato-1-thio- α -L-idopyranosiduronate (39).

To a solution of starting material **36** (0.3 g, 0.3 mmol) in DMF (2.0 ml, 0.15 M) was

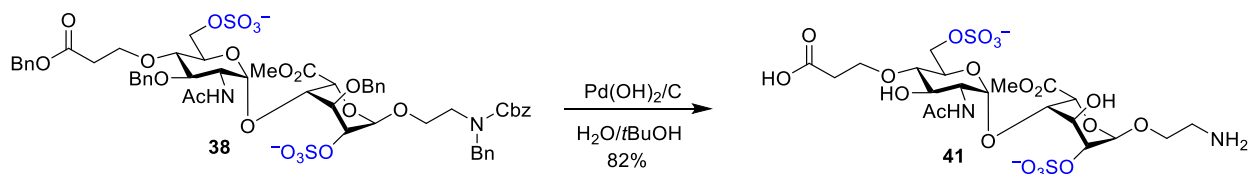
added sulfur trioxide triethylamine complex (1.12 g, 6.0 mmol) and the resulting reaction mixture was stirred at 55 °C for 2 h. The reaction mixture was purified by a LH-20 gel column with CH₃OH. Fractions containing product were collected under reduced pressure and the crude was dissolved in pyridine/Et₃N (10/1, v/v, 0.15M). Sulfur trioxide pyridine complex (0.45 g, 3 mmol) was added to the reaction mixture at 55 °C and stirred for 2 h. After reaction completion as indicated by TLC (EtOAc/MeOH/H₂O 6/1/1), the reaction mixture was passed through LH-20 gel column with CH₃OH. A column of Dowex 50WX4 Na⁺ resin was used for ion exchange to give sodium form product **39** (0.34 g, 92% for two steps). ¹H NMR (500 MHz, CD₃OD) δ 7.42 – 7.48 (d, J = 7.5 Hz, 2H; ArCH₂-), 7.41 – 7.27 (m, 8H; Ar-H), 7.25 – 7.07 (m, 8H; Ar-H), 6.98 – 6.85 (m, 2H; ArCH₂-), 5.40 (d, J = 3.4 Hz, 1H; 1'-H), 5.21 – 5.16 (m, 1H), 5.13 – 5.07 (m, 4H; 1-H), 5.05 – 5.01 (m, 1H), 4.81 – 4.71 (m, 3H; 5-H), 4.66 (d, J = 11.4, 1H), 4.50 – 4.37 (m, 1H; 6'-H), 4.34 – 4.19 (m, 4H; 2-H, 6'-H), 4.07-4.01 (m, 1H), 3.95–3.85 (m, 2H), 3.82 – 3.71 (m, 4H; 4'-linker-OCH₂-), 3.70 – 3.56 (m, 2H), 3.46 – 3.38 (m, 3H; 2'-H), 2.51 (t, J = 6.4 Hz, 2H). ¹³C NMR (125 MHz, CD₃OD) δ 172.29, 170.58, 156.68, 138.91, 137.97, 137.64, 137.43, 136.15, 128.34, 128.32, 128.24, 128.18, 128.11, 128.07, 128.00, 127.97, 127.89, 127.87, 127.61, 127.54, 127.46, 127.43, 127.32, 126.97, 99.33, 98.72, 79.70, 77.42, 75.01, 73.47, 73.06, 72.41, 70.87, 70.03, 67.90, 67.25, 66.75, 66.37, 66.13, 65.90, 58.15, 58.07, 52.18, 51.45, 51.38, 46.69, 45.72, 35.26. HRMS: m/z calc. for C₅₄H₅₉N₂O₂₄S₃³⁻ [M+H⁺]²⁻: 608.1355; found: 608.1370.



Aminoethyl 4-O-carboxyethyl-2-deoxy-2-sulfoamino-1-thio- α -D-glucopyranoside-(1 \rightarrow 4)-

methyl-1-thio- α -L-idopyranosiduronate (40).

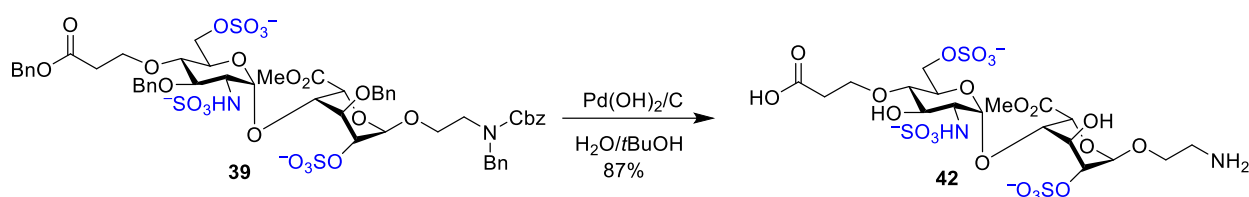
Compound **37** (170 mg, 0.16 mmol) was treated according to the general procedures of hydrogenolysis to give compound **40** (80.5 mg, 87%). ^1H NMR (500 MHz, CD_3OD) δ 5.36 (d, J = 3.7 Hz, 1H; 1'-H), 4.95 (d, J = 3.0 Hz, 1H; 1-H), 4.80 (d, J = 3.2 Hz, 1H; 5-H), 4.18 (t, J = 4.3 Hz, 1H; 3-H), 4.06 – 3.97 (m, 2H; 2-H, 4-H), 3.92 – 3.84 (m, 2H; 6'- CH_2 -), 3.75 (s, 3H; - CO_2CH_3), 3.73 – 3.68 (m, 2H; 5'-H, 4'-linker- OCH_2 -), 3.67 – 3.58 (m, 3H; 4'-linker- OCH_2 -, anomeric linker- OCH_2 -), 3.57 – 3.53 (m, 1H; 4'-H), 3.44 – 3.38 (m, 1H, 3'-H), 3.27 – 3.22 (m, 1H; 2'-H), 3.07-2.99 (m, 2H; NH_2CH_2 -), 2.39 (t, J = 5.9 Hz, 2H; CO_2HCH_2 -). ^{13}C NMR (125 MHz, CD_3OD) δ 170.39, 101.45, 96.63, 78.53, 74.10, 71.71, 69.08, 68.65, 68.01, 67.12, 64.71, 60.57, 58.06, 51.62, 46.32, 42.68, 39.26, 36.85. HRMS: m/z calc. for $\text{C}_{18}\text{H}_{31}\text{N}_2\text{O}_{16}\text{S}^-$ [M] $^-$: 563.1400; found: 563.1401.



Aminoethyl 2-acetamido-4-*O*-carboxyethyl-2-deoxy-6-*O*-sulfonato- α -D-glucopyranoside-(1 \rightarrow 4)-methyl-2-*O*-sulfonato- α -L-idopyranosiduronate (41).

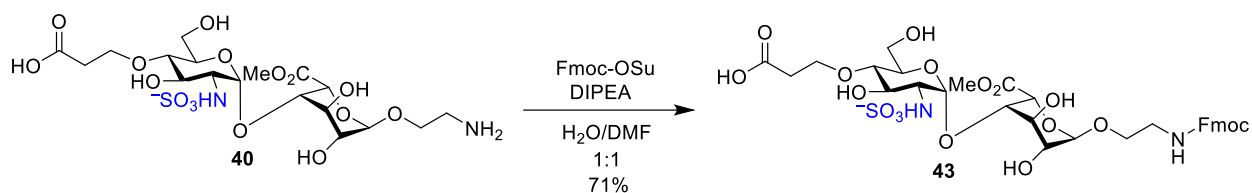
Compound **38** (290 mg, 0.25 mmol) was treated according to the general procedures of hydrogenolysis to give compound **41** (138 mg, 82%). ^1H NMR (500 MHz, D_2O) δ 7.72 (d, J = 9.6 Hz, 1H; NHAc), 5.02 (s, 1H; 1'-H), 4.95 (d, J = 3.4 Hz, 1H, 1-H), 4.83 (d, J = 1.9 Hz, 1H; 5-H), 4.20 (d, J = 3.0 Hz, 1H; 3-H), 4.15 – 4.06 (m, 3H; 2-H, 6'- CH_2 -), 3.99 – 3.94 (m, 1H; 4-H), 3.92 – 3.82 (m, 3H; 5'-H, 4'-linker- OCH_2 -), 3.80 – 3.74 (m, 1H; anomeric linker- OCH_2 -), 3.66

(s, 3H; -CO₂CH₃), 3.64 – 3.59 (m, 1H; anomeric linker-OCH₂-), 3.50 – 3.41 (m, 2H; 3'-H, 4'-H), 3.25 – 3.16 (m, 1H; 2'-H), 3.25 – 3.00 (m, 2H; NH₂CH₂-), 2.47 (t, J = 5.9 Hz, 2H; CO₂HCH₂-), 1.88 (s, 3H; -NHCOCH₃). ¹³C NMR (125 MHz, D₂O) δ 171.11, 98.96, 94.39, 77.66, 72.93, 71.10, 70.95, 69.64, 68.33, 66.58, 66.42, 64.67, 62.93, 52.96, 52.85, 38.83, 22.03. HRMS: m/z calc. for C₂₀H₃₂N₂O₂₀S₂²⁻ [M+H⁺]: 685.1074; found: 685.1086.



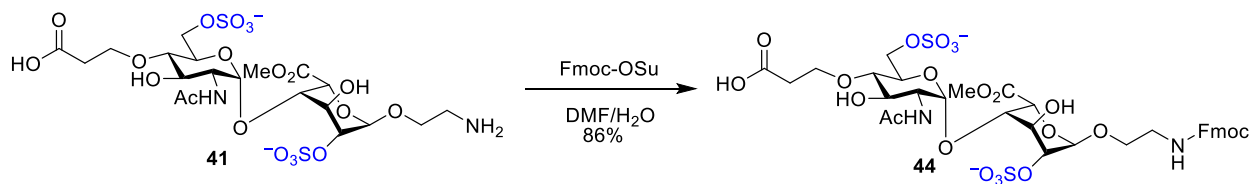
Aminoethyl 2-acetamido-4-*O*-carboxyethyl-2-deoxy-6-*O*-sulfonato-1-thio- α -D-glucopyranoside-(1 \rightarrow 4)-methyl-2-*O*-sulfonato-1-thio- α -L-idopyranosiduronate (42).

Compound **39** (350 mg, 0.29 mmol) was treated according to the general procedures of Hydrogenolysis to give compound **42** (180 mg, 87%). ¹H NMR (500 MHz, D₂O) δ 5.19 (d, J = 3.4 Hz, 1H, 1'-H), 5.02 (d, J = 2.0 Hz, 1H, 1-H), 4.77 (d, J = 2.1 Hz, 1H; 5-H), 4.26 (t, J = 4.0 Hz, 1H; 3-H), 4.19 – 4.05 (m, 3H; 2-H, 6'-CH₂-), 4.04 – 4.00 (m, 1H, 4-H), 3.90 – 3.83 (m, 2H; 5'-H, 4'-linker-OCH₂-), 3.81 – 3.75 (m, 1H; 4'-linker-OCH₂-), 3.69 (s, 3H; -CO₂CH₃), 3.65 – 3.56 (m, 2H; anomeric linker-OCH₂-), 3.48 (t, J = 9.8 Hz, 1H, 4'-H), 3.25 (t, J = 9.8 Hz, 1H, 3'-H), 3.16 – 3.05 (m, 3H; 2'-H, NH₂CH₂-), 2.43 – 2.29 (m, 2H; CO₂HCH₂-). ¹³C NMR (125 MHz, D₂O) δ 170.99, 99.30, 98.96, 77.76, 76.90, 74.53, 70.46, 69.25, 69.07, 67.26, 67.11, 66.16, 64.60, 57.61, 53.01, 38.89. HRMS: m/z calc. for C₁₈H₂₉N₂O₂₂S₃³⁻ [M+H⁺]²⁻: 361.0232; found: 361.0238.



***N*-Fluorenylmethyloxycarbonyl-2-aminoethyl 4-*O*-carboxyethyl-2-deoxy-2-sulfoamino-1-thio- α -D-glucopyranoside-(1 \rightarrow 4)-methyl-1-thio- α -L-idopyranosiduronate (43).**

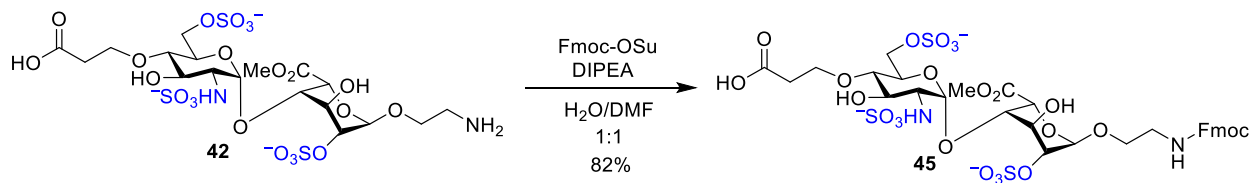
Compound **40** (80 mg, 0.14 mmol) was treated according to the general procedures of protection of NH₂ with Fmoc to give compound **43** (79 mg, 71%). ¹H NMR (500 MHz, CD₃OD) δ 7.79 (d, *J* = 7.5 Hz, 2H, Ar-H), 7.64 (d, *J* = 7.5 Hz, 2H, Ar-H), 7.39 (dt, *J* = 7.5 Hz, 1.2 Hz, 2H, Ar-H), 7.31 (td, *J* = 7.5, 1.2 Hz, 2H, Ar-H), 5.35 (d, *J* = 3.7 Hz, 1H; 1'-H), 4.91 – 4.89 (m, 1H; 1-H), 4.79 (d, *J* = 2.9 Hz, 1H; 5-H), 4.37 – 4.28 (m, 2H; FmocCH₂-), 4.22 – 4.13 (m, 2H; FmocCH-, 3-H), 4.04 – 3.95 (m, 2H; 2-H, 6'-CH₂-), 3.90 – 3.82 (m, 1H; 6'-CH₂-), 3.78 – 3.70 (m, 3H; 5'-H, 4'-linker-OCH₂-), 3.68 (s, 3H; -CO₂CH₃), 3.61 – 3.47 (m, 3H; 4'-H, anomeric linker-OCH₂-), 3.43 – 3.35 (m, 1H; 3'-H), 3.35 – 3.32 (m, 1H; -CH₂NHFmoc), 3.28 – 3.21 (m, 2H; 2'-H, -CH₂NHFmoc), 2.40 (t, *J* = 5.9 Hz, 2H; CO₂HCH₂-). ¹³C NMR (125 MHz, CD₃OD) δ 178.87, 170.39, 157.50, 143.88, 141.15, 127.36, 126.77, 124.76, 119.48, 101.33, 96.54, 78.64, 74.02, 71.71, 71.48, 69.30, 69.10, 67.67, 67.59, 67.00, 66.37, 60.46, 57.79, 51.53, 51.51, 40.21, 37.97. HRMS: *m/z* calc. for C₃₃H₄₁N₂O₁₈S⁻ [M]⁻: 785.2081; found: 785.2103.



***N*-Fluorenylmethyloxycarbonyl-2-aminoethyl 2-acetamido-4-*O*-carboxyethyl-2-deoxy-6-*O*-**

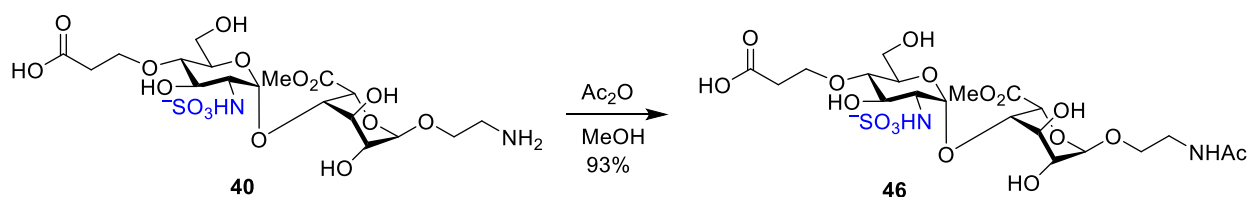
sulfonato-1-thio- α -D-glucopyranoside-(1 \rightarrow 4)-methyl-2-O-sulfonato-1-thio- α -L-idopyranosiduronate (44).

Compound **41** (167 mg, 0.24 mmol) was treated according to the general procedures of protection of NH₂ with Fmoc to give compound **44** (190 mg, 86%). ¹H NMR (500 MHz, CD₃OD) δ 7.80 (d, J = 7.5 Hz, 2H; Ar-CH), 7.67 (d, J = 7.5 Hz, 2H; Ar-CH), 7.50 (d, J = 9.2 Hz, 1H; NHAc), 7.40 (dt, J = 7.5, 1.7 Hz, 2H; Ar-CH), 7.33 (dt, J = 7.5, 1.7 Hz, 2H; Ar-CH), 5.16 (s, 1H; 1'-H), 5.03 (d, J = 3.4 Hz, 1H; 1-H), 4.86 (d, J = 2.1 Hz, 1H; 5-H), 4.34 – 4.28 (m, 4H; 3-H, 2-H, FmocCH₂-), 4.25 – 4.17 (m, 3H; 6'-CH₂-, FmocCH-), 4.07 – 3.91 (m, 5H; 4-H, 5'-H, 4'-linker-OCH₂-, anomeric linker-OCH₂-), 3.84-3.75 (m, 2H; anomeric linker-OCH₂-, -CH₂NHFmoc), 3.73 (s, 3H; CO₂CH₃), 3.69-3.65 (m, 1H; 3'-H), 3.64-3.55 (m, 2H; 4'-H, -CH₂NHFmoc), 3.28-3.24 (m, 1H, 2'-H), 2.44 (dd, J = 6.8, 5.1 Hz, 2H; CO₂HCH₂-), 2.07 (s, 3H, NHCOCH₃). ¹³C NMR (125 MHz, CD₃OD) δ 178.30, 172.95, 170.30, 157.48, 143.88, 141.14, 127.37, 126.80, 124.86, 119.46, 99.57, 95.93, 78.75, 73.28, 72.93, 71.48, 69.91, 69.14, 67.55, 66.48, 66.36, 66.03, 64.34, 52.95, 51.75, 40.18, 37.44, 21.75. HRMS: m/z calc. for C₃₅H₄₂N₂O₂₂S₂²⁻ [M]²⁻: 453.0841; found: 453.0840.



N-Fluorenylmethyloxycarbonyl-2-aminoethyl 2-acetamido-4-O-carboxyethyl-2-deoxy-6-O-sulfonato-1-thio- α -D-glucopyranoside-(1 \rightarrow 4)-methyl-2-O-sulfonato-1-thio- α -L-idopyranosiduronate (45).

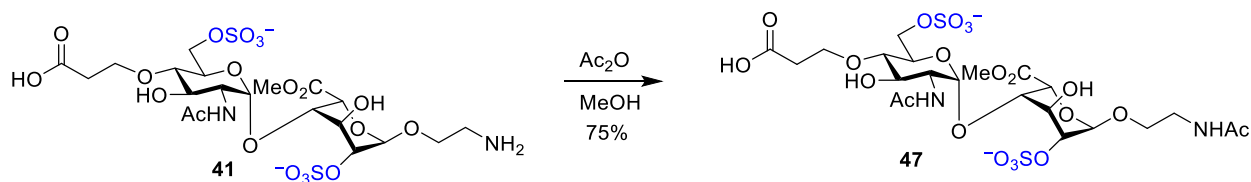
Compound **42** (220 mg, 0.31 mmol) was treated according to the general procedures of protection of NH₂ with Fmoc to give compound **45** (235 mg, 82%). ¹H NMR (500 MHz, CD₃OD) δ 7.80 (d, J = 7.8 Hz, 2H; ArCH-), 7.67 (d, J = 7.5 Hz, 2H; ArCH-), 7.40 (dt, J = 7.8, 2.6 Hz, 2H; ArCH-), 7.33 (td, J = 7.5 Hz, 2.6 Hz, 2H; ArCH-), 5.26 (d, J = 3.4 Hz, 1H, 1'-H), 5.21 (s, 1H, 1-H), 4.84 (d, J = 2.2 Hz, 1H; 5-H), 4.43 – 4.39 (m, 1H; 3-H), 4.34 – 4.28 (m, 3H; 2-H, FmocCH₂-), 4.25 – 4.17 (m, 3H; 6'-CH₂-, FmocCH-), 4.10 – 4.04 (m, 1H, 4-H), 4.01 – 3.94 (m, 2H, 5'-H, 4'-linker-OCH₂-), 3.82 – 3.76 (m, 1H, 4'-linker-OCH₂-), 3.74 (s, 3H, -CO₂CH₃), 3.68 – 3.61 (m, 2H; anomeric linker-OCH₂-), 3.60 – 3.53 (m, 1H; 4'-H), 3.37-3.34 (m, 2H; -CH₂NHFmoc), 3.30-3.25 (m, 1H; 2'-H), 2.61 – 2.50 (m, 2H; CO₂HCH₂-). ¹³C NMR (125 MHz, CD₃OD) δ 170.51, 143.88, 141.13, 127.39, 126.80, 124.88, 124.85, 119.48, 99.31, 98.68, 78.87, 75.80, 73.53, 71.03, 69.75, 67.70, 66.60, 66.54, 66.14, 65.95, 57.62, 51.88, 40.12, 37.32. HRMS: m/z calc. for C₃₃H₃₉N₂O₂₄S₃³⁻ [M]³⁻: 314.3690; found: 314.3696.



Acetamidoethyl 4-O-carboxyethyl-2-deoxy-2-sulfoamino-1-thio- α -D-glucopyranoside-(1 \rightarrow 4)-methyl-1-thio- α -L-idopyranosiduronate (46**).**

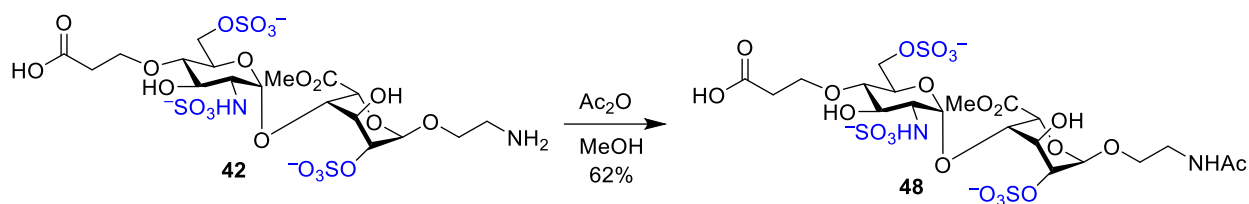
Compound **40** (40 mg, 0.07 mmol) was treated according to the general procedures of hydrogenolysis to give compound **46** (40 mg, 93%). ¹H NMR (500 MHz, CD₃OD) δ 5.36 (d, J = 3.6 Hz, 1H, 1'-H), 4.89 (s, 1H, 1-H), 4.80 (d, J = 3.0 Hz, 1H; 5-H), 4.16 (t, J = 4.3 Hz, 1H; 3-H), 4.08 – 3.97 (m, 2H; 2-H, 4-H), 3.93 – 3.85 (m, 1H; 6'-CH₂-), 3.80 – 3.69 (m, 6H; -CO₂CH₃, 5'-H,

6'-CH₂-, 4'-linker-OCH₂-), 3.62 – 3.50 (m, 3H; 4'-linker-OCH₂-, 4'-H, anomeric linker-OCH₂-), 3.45 – 3.34 (m, 3H; anomeric linker-OCH₂-, 3'-H, -CH₂NHAc), 3.30 – 3.22 (m, 2H; 2'-H, -CH₂NHAc), 2.49 – 2.42 (m, 2H; CO₂HCH₂-), 1.94 (s, 3H; -NHCOCH₃). ¹³C NMR (125 MHz, CD₃OD) δ 177.09, 171.96, 170.45, 101.41, 96.58, 78.48, 74.12, 71.67, 71.62, 69.30, 68.55, 67.89, 67.27, 67.22, 60.53, 57.92, 51.55, 38.94, 36.65, 21.13. HRMS: m/z calc. for C₂₀H₃₃N₂O₁₇S⁻ [M]⁻: 605.1505; found: 605.1513.



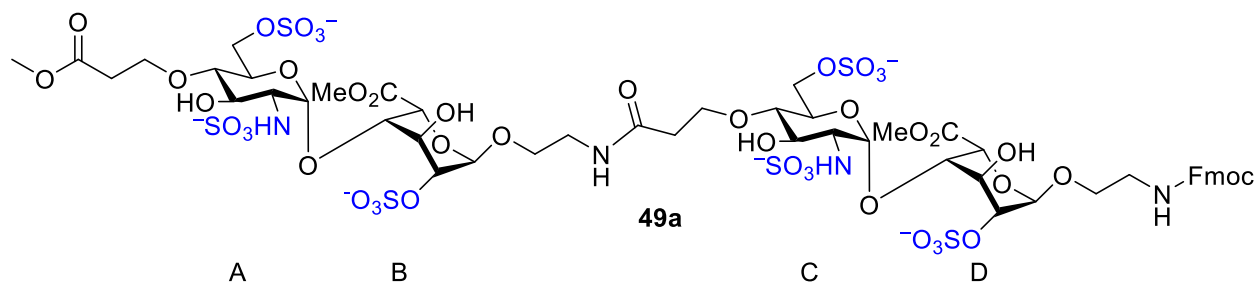
Acetmidoethyl 2-acetamido-4-O-carboxyethyl-2-deoxy-6-O-sulfonato-1-thio- α -D-glucopyranoside-(1 \rightarrow 4)-methyl-2-O-sulfonato-1-thio- α -L-idopyranosiduronate (47).

Compound **41** (19 mg, 0.03 mmol) was treated according to the general procedures of Hydrogenolysis to give compound **47** (15 mg, 75%). ¹H NMR (500 MHz, D₂O) δ 4.98 (s, 1H, 1'-H), 4.96 (d, J = 3.5 Hz, 1H, 1-H), 4.81 (d, J = 2.2 Hz, 1H; 5-H), 4.18 (d, J = 3.0 Hz, 1H, 3-H), 4.14 – 4.10 (m, 3H; 2-H, 6'-CH₂-), 3.93 (m, 1H; 4-H), 3.91 – 3.82 (m, 2H; 4'-linker-OCH₂-), 3.79 – 3.72 (m, 1H; anomeric linker-OCH₂-), 3.71 – 3.63 (m, 4H; -CO₂CH₃, 5'-H), 3.58 – 3.46 (m, 3H; 3'-H, 4'-H, anomeric linker-OCH₂-), 3.26 – 3.19 (m, 3H; 2'-H, -CH₂NHAc), 2.37 – 2.31 (m, 2H; CO₂HCH₂-), 1.89 (s, 3H; NHAc on linker), 1.82 (s, 3H; NHAc). ¹³C NMR (125 MHz, D₂O) δ 174.64, 174.16, 171.21, 99.07, 94.35, 77.88, 73.08, 71.02, 69.63, 69.41, 67.33, 66.56, 66.32, 63.00, 53.07, 52.71, 48.75, 39.00, 37.35, 22.07, 21.68. HRMS: m/z calc. for C₂₂H₃₄N₂O₂₁S₂²⁻ [M]²⁻: 363.0553; found: 363.0555.



Acetmidoethyl **2-acetamido-4-O-carboxyethyl-2-deoxy-6-O-sulfonato-1-thio- α -D-glucopyranoside-(1 \rightarrow 4)-methyl-2-O-sulfonato-1-thio- α -L-idopyranosiduronate (48).**

Compound **42** (20 mg, 0.03 mmol) was treated according to the general procedures of *N*-acetylation to give compound **48** (13 mg, 62%). ^1H NMR (500 MHz, CD_3OD) δ 5.32 (d, $J = 3.5$ Hz, 1H, 1'-H), 5.15 (d, $J = 2.7$ Hz, 1H, 1-H), 4.80 (d, $J = 2.9$ Hz, 1H; 5-H), 4.36 – 4.32 (m, 1H; 3-H), 4.30 – 4.26 (m, 1H; 2-H), 4.21 (d, $J = 2.8$ Hz, 2H; 6'- CH_2 -), 4.14 – 3.92 (m, 3H; 4-H, 4'-linker- OCH_2 -), 3.81 (s, 4H; CO_2CH_3 , anomeric linker- OCH_2 -), 3.72 – 3.67 (m, 1H; 5'-H), 3.64 – 3.59 (m, 1H; 4'-H), 3.58 – 3.56 – 3.49 (m, 1H; anomeric linker- OCH_2 -), 3.47 – 3.38 (m, 1H; 3'-H), 3.37-3.30 (m, 2H; $-\text{CH}_2\text{NHAc}$), 3.28-3.23 (m, 1H, 2'-H) 2.64 – 2.47 (m, 2H, CO_2HCH_2 -), 1.95 (s, 3H; $-\text{NHCOCH}_3$). ^{13}C NMR (125 MHz, CD_3OD) δ 175.49, 171.98, 170.26, 99.76, 98.97, 78.53, 76.58, 75.02, 71.53, 69.71, 67.96, 67.85, 67.54, 67.41, 66.03, 58.04, 51.76, 38.81, 35.41, 21.13. HRMS: m/z calc. for $\text{C}_{20}\text{H}_{31}\text{N}_2\text{O}_{23}\text{S}_3^{3-}$ $[\text{M}+\text{Na}^+]^{2-}$: 393.0194; found: 393.0200.

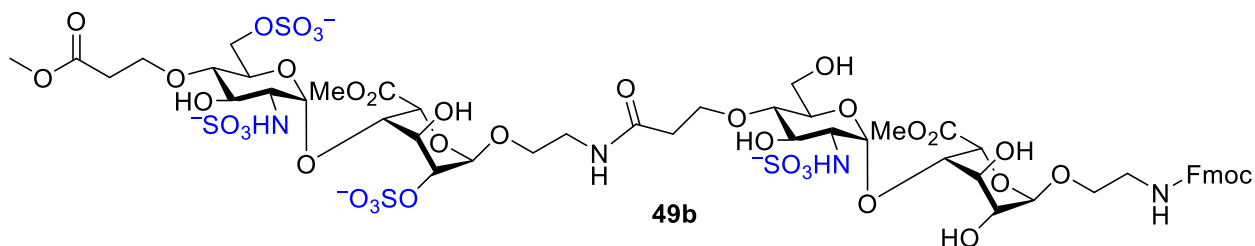


***N*-Fluorenylmethyloxycarbonyl-2-aminoethyl**

***O*-(4-*O*-methylpropionate-2-deoxy-2-**

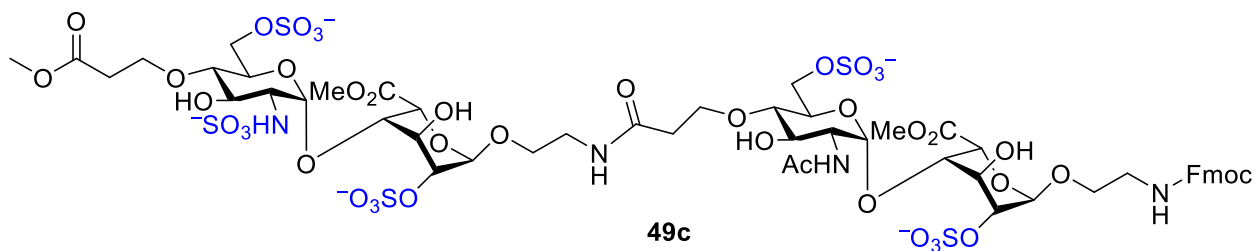
sulfoamino-6-*O*-sulfoamino-1-thio- α -D-glucopyranoside)-(1 \rightarrow 4)-*O*-(methyl-2-*O*-sulfonato-1-thio- α -L-idopyranosiduronate)-(1 \rightarrow 4)-*O*-(4-*O*-carboxyethyl-2-deoxy-2-sulfoamino-6-*O*-sulfonato-1-thio- α -D-glucopyranoside)-(1 \rightarrow 4)-*O*-methyl-2-*O*-sulfonato-1-thio- α -L-idopyranosiduronate (49a).

Starting material (9 mg, 0.012 mmol) was treated according to the general procedures of pseudo-tetrasaccharide preparation with HBTU to give compound **49a** (15 mg, 76%). ^1H NMR (500 MHz, D_2O) δ 7.79 (d, $J = 7.5$ Hz, 2H), 7.56 (t, $J = 7.5$ Hz, 2H), 7.40 – 7.33 (m, 2H), 7.32 – 7.23 (m, 2H), 5.17 – 5.08 (m, 2H; A-1, C-1), 4.94 (s, 1H; B-1), 4.89 (s, 1H; D-1), 4.54 (s, 1H), 4.42 – 4.34 (m, 1H), 4.31 – 4.24 (m, 2H), 4.22 – 4.00 (m, 7H), 3.95 – 3.79 (m, 5H), 3.75 (s, 1H), 3.67 – 3.61 (m, 3H), 3.55 (s, 3H), 3.52 – 3.38 (m, 6H), 3.28 – 3.22 (m, 2H), 3.19 (s, 3H), 3.12 – 3.03 (m, 3H), 2.55 – 2.47 (m, 2H), 2.39 – 2.29 (m, 2H). ^{13}C NMR (125 MHz, D_2O) δ 174.62, 173.99, 171.17, 148.60, 143.64, 140.89, 128.16, 128.02, 127.44, 125.17, 124.96, 120.70, 120.10, 99.61, 99.20, 77.44, 77.36, 77.18, 73.69, 70.62, 70.27, 69.13, 69.05, 68.27, 67.48, 67.31, 67.03, 66.40, 66.26, 66.05, 65.86, 57.91, 52.90, 52.67, 52.18, 46.91, 40.09, 38.89, 36.46, 34.74.



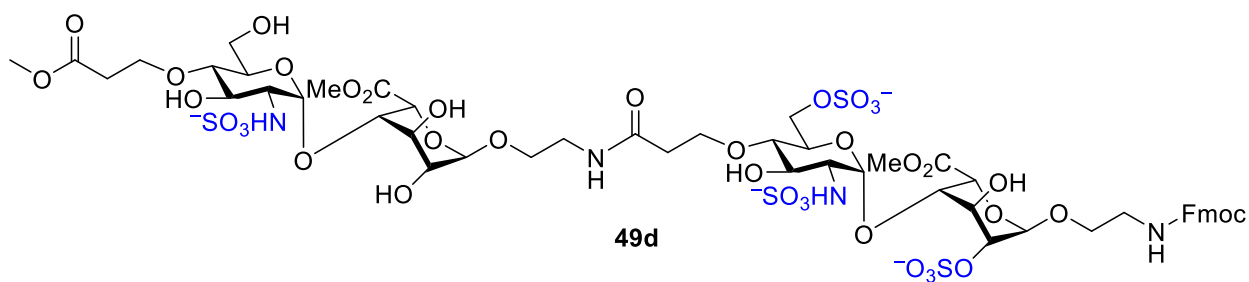
***N*-Fluorenylmethyloxycarbonyl-2-aminoethyl *O*-(2-deoxy-4-*O*-methylpropionate-2-sulfoamino-6-*O*-sulfoamino-1-thio- α -D-glucopyranoside)-(1 \rightarrow 4)-*O*-(methyl-2-*O*-sulfonato-1-thio- α -L-idopyranosiduronate)-(1 \rightarrow 4)-*O*-(4-*O*-carboxyethyl-2-deoxy-2-sulfoamino-1-thio- α -D-glucopyranoside)-(1 \rightarrow 4)-*O*-methyl-1-thio- α -L-idopyranosiduronate (49b).**

Starting material (13.5 mg, 0.018 mmol) was treated according to the general procedures of pseudo-tetrasaccharide preparation with HBTU to give compound **49b** (17 mg, 65%). ¹H NMR (500 MHz, D₂O) δ 7.77 (d, J = 7.5 Hz, 2H), 7.55 (t, J = 6.9 Hz, 2H), 7.36 (t, J = 7.5 Hz, 2H), 7.29 – 7.22 (m, 2H), 5.18 (d, J = 3.5 Hz, 1H; A-1), 5.13 (d, J = 3.5 Hz, 1H; C-1), 4.95 (s, 1H; B-1), 4.74 – 4.71 (m, 1H; D-1), 4.68 – 4.67 (m, 1H), 4.58 (d, J = 2.6 Hz, 1H), 4.42 – 4.35 (m, 1H), 4.31 – 4.23 (m, 2H), 4.16 – 4.00 (m, 5H), 3.95 (t, J = 2.6 Hz, 2H), 3.92 – 3.78 (m, 5H), 3.76 – 3.65 (m, 3H), 3.64 (s, 3H), 3.61 – 3.51 (m, 9H), 3.51 – 3.45 (m, 3H), 3.31 – 3.22 (m, 3H), 3.21 – 3.15 (m, 3H), 3.13 – 3.00 (m, 5H), 2.53 – 2.45 (m, 2H), 2.37 – 2.26 (m, 2H). ¹³C NMR (125 MHz, CD₃OD) δ 173.05, 170.54, 170.44, 157.55, 143.90, 141.15, 127.38, 126.79, 124.84, 124.81, 119.50, 101.24, 99.58, 98.79, 96.69, 78.29, 78.16, 76.10, 74.19, 71.60, 71.30, 69.65, 69.00, 67.88, 67.66, 67.44, 67.08, 66.86, 66.42, 65.95, 60.37, 58.12, 51.84, 51.70, 50.85, 40.21, 38.75, 36.47, 34.77. HRMS: m/z calc. for C₃₇H₆₀N₄O₃₇S₄⁴⁻ [M+H⁺]³⁻: 427.0638; found: 427.0630.



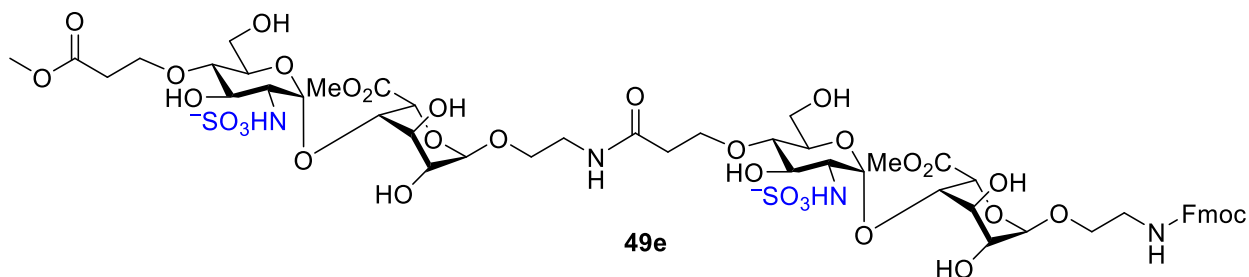
***N*-Fluorenylmethyloxycarbonyl-2-aminoethyl *O*-(4-*O*-methylpropionate-2-deoxy-2-sulfoamino-6-*O*-sulfonato-1-thio- α -D-glucopyranoside)-(1 \rightarrow 4)-*O*-(methyl-2-*O*-sulfonato-1-thio- α -L-idopyranosiduronate)-(1 \rightarrow 4)-*O*-(4-*O*-carboxyethyl-2-deoxy-2-acetamido-6-*O*-sulfonato-1-thio- α -D-glucopyranoside)-(1 \rightarrow 4)-*O*-methyl-2-*O*-sulfonato-1-thio- α -L-idopyranosiduronate (**49c**).**

Starting material (18 mg, 0.024 mmol) was treated according to the general procedures of pseudo-tetrasaccharide preparation with HBTU to give compound **49c** (25 mg, 63%). ¹H NMR (500 MHz, CD₃OD) δ 7.80 (d, J = 7.5 Hz, 2H), 7.67 (d, J = 7.5 Hz, 2H), 7.44 – 7.37 (m, 2H), 7.35 – 7.29 (m, 2H), 5.28 (d, J = 3.6 Hz, 1H; A-1), 5.18 (d, J = 4.4 Hz, 2H; C-1, B-1), 5.00 (d, J = 3.4 Hz, 1H; D-1), 4.86 (d, J = 1.9 Hz, 1H), 4.84 (d, J = 2.4 Hz, 1H), 4.40 (t, J = 3.7 Hz, 1H), 4.35 – 4.27 (m, 5H), 4.25 – 4.15 (m, 5H), 4.13 – 4.05 (m, 2H), 4.03 – 3.94 (m, 5H), 3.84 – 3.76 (m, 5H), 3.74 – 3.71 (m, 2H), 3.69 (s, 3H), 3.66 – 3.54 (m, 5H), 3.48 – 3.34 (m, 5H), 3.26 (dd, J = 10.6, 3.4 Hz, 1H), 2.66 – 2.56 (m, 2H), 2.48 (t, J = 5.9 Hz, 2H), 2.08 (s, 3H). ¹³C NMR (125 MHz, CD₃OD) δ 173.02, 170.48, 157.50, 143.89, 141.14, 127.39, 126.81, 124.89, 119.48, 99.55, 98.86, 96.42, 78.29, 76.15, 73.75, 73.44, 73.08, 71.53, 69.95, 69.64, 68.35, 67.56, 67.42, 67.37, 66.49, 66.21, 65.93, 64.31, 58.15, 53.35, 51.85, 50.84, 40.15, 38.62, 36.53, 34.76, 21.79. HRMS: m/z calc. for C₃₉H₆₁N₄O₄₁S₅⁵⁻ [M+H⁺]⁴⁻: 350.5379; found: 350.5379.



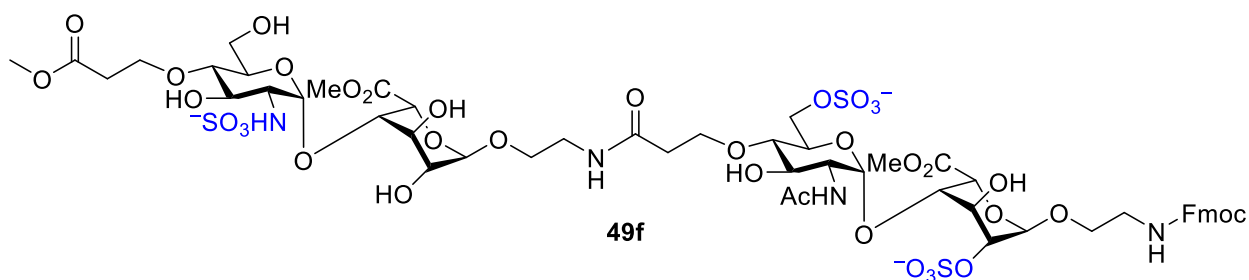
***N*-Fluorenylmethyloxycarbonyl-2-aminoethyl-*O*-(2-deoxy-4-*O*-methylpropionate-2-sulfoamino-1-thio- α -D-glucopyranoside)-(1 \rightarrow 4)-*O*-(methyl-1-thio- α -L-idopyranosiduronate)-(1 \rightarrow 4)-*O*-(4-*O*-carboxyethyl-2-deoxy-2-sulfoamino-6-*O*-sulfonato-1-thio- α -D-glucopyranoside)-(1 \rightarrow 4)-*O*-methyl-2-*O*-sulfonato-1-thio- α -L-idopyranosiduronate (**49d**).**

Starting material (21 mg, 0.036 mmol) was treated according to the general procedures of pseudo-tetrasaccharide preparation with HATU to give compound **49d** (32 mg, 59%). ¹H NMR (500 MHz, CD₃OD) δ 7.80 (d, J = 7.5 Hz, 2H), 7.67 (d, J = 7.4 Hz, 2H), 7.43 – 7.38 (m, 2H), 7.33 (td, J = 7.5, 1.2 Hz, 2H), 5.41 (d, J = 3.6 Hz, 1H; A-1), 5.28 – 5.19 (m, 2H; C-1, B-1), 4.97 (d, J = 2.8 Hz, 1H; D-1), 4.84 (t, J = 2.9 Hz, 2H), 4.43 (d, J = 3.2 Hz, 1H), 4.35 – 4.28 (m, 3H), 4.23 – 4.15 (m, 4H), 4.10 – 4.03 (m, 2H), 4.02 – 3.96 (m, 3H), 3.93 – 3.86 (m, 2H), 3.81 – 3.77 (m, 3H), 3.76 – 3.73 (m, 6H), 3.73 – 3.70 (m, 2H), 3.68 (s, 3H), 3.66 – 3.55 (m, 6H), 3.50 – 3.45 (m, 1H), 3.43 – 3.34 (m, 5H), 3.30 – 3.21 (m, 3H), 2.65 – 2.50 (m, 4H), 2.46 – 2.36 (m, 2H). ¹³C NMR (125 MHz, CD₃OD) δ 173.21, 172.85, 170.56, 157.50, 143.90, 141.13, 127.38, 126.82, 124.91, 124.87, 119.47, 101.44, 99.36, 99.17, 96.17, 78.16, 77.94, 76.57, 73.61, 73.43, 71.74, 71.48, 71.35, 69.59, 68.99, 67.99, 67.92, 67.57, 67.33, 66.75, 66.50, 66.36, 66.10, 65.65, 60.51, 58.27, 58.03, 51.83, 51.52, 50.72, 40.17, 38.86, 36.63, 34.74. HRMS: m/z calc. for C₃₇H₆₀N₄O₃₇S₄⁴⁻ [M]⁴⁻: 320.0460; found: 320.0446.



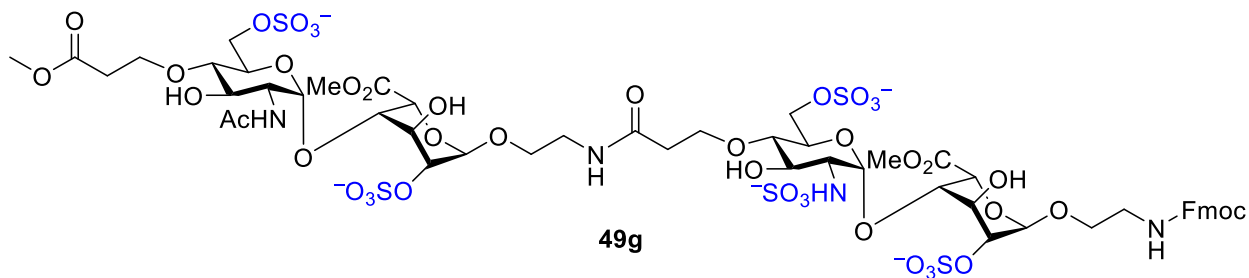
***N*-Fluorenylmethyloxycarbonyl-2-aminoethyl 4-*O*-methylpropionate-2-deoxy-2-sulfoamino-1-thio- α -D-glucopyranoside)-(1 \rightarrow 4)-(methyl-1-thio- α -L-idopyranosiduronate-(1 \rightarrow 4)-4-*O*-carboxyethyl-2-deoxy-2-sulfoamino-1-thio- α -D-glucopyranoside)-(1 \rightarrow 4)-methyl-1-thio- α -L-idopyranosiduronate (**49e**).**

Starting material (12 mg, 0.020 mmol) was treated according to the general procedures of pseudo-tetrasaccharide preparation with HATU to give compound **49e** (20 mg, 70%). ¹H NMR (500 MHz, CD₃OD) δ 7.81 (d, J = 7.5 Hz, 2H), 7.66 (d, J = 7.5 Hz, 2H), 7.40 (t, J = 7.5 Hz, 2H), 7.33 (t, J = 7.5 Hz, 2H), 5.35 (d, J = 3.5 Hz, 1H; A-1), 5.32 (d, J = 3.5 Hz, 1H; C-1), 4.97 (d, J = 2.6 Hz, 1H; B-1), 4.82 – 4.77 (m, 2H; D-1), 4.37 – 4.27 (m, 2H), 4.22 – 4.16 (m, 3H), 4.10 – 3.95 (m, 5H), 3.92 – 3.85 (m, 3H), 3.76 – 3.72 (m, 5H), 3.73 – 3.68 (m, 8H), 3.67 (s, 3H), 3.63 – 3.59 (m, 4H), 3.58 – 3.53 (m, 4H), 3.43 – 3.48 (m, 3H), 3.32 – 3.29 (m, 6H), 2.62 – 2.47 (m, 5H), 2.41 – 2.32 (m, 2H). ¹³C NMR (125 MHz, CD₃OD) δ 173.03, 172.75, 170.43, 143.93, 141.17, 127.38, 126.80, 124.84, 119.50, 101.54, 101.37, 96.93, 96.39, 78.14, 78.08, 74.57, 74.04, 72.13, 71.63, 71.44, 69.30, 69.01, 67.92, 67.88, 67.46, 67.27, 67.21, 66.40, 60.62, 60.46, 58.45, 58.30, 54.42, 53.98, 51.50, 51.41, 50.66, 46.48, 42.39, 40.27, 38.88, 37.97, 36.57, 34.78. HRMS: m/z calc. for C₃₇H₆₂N₄O₃₁S₂²⁻ [M]²⁻: 561.1425; found: 561.1426.



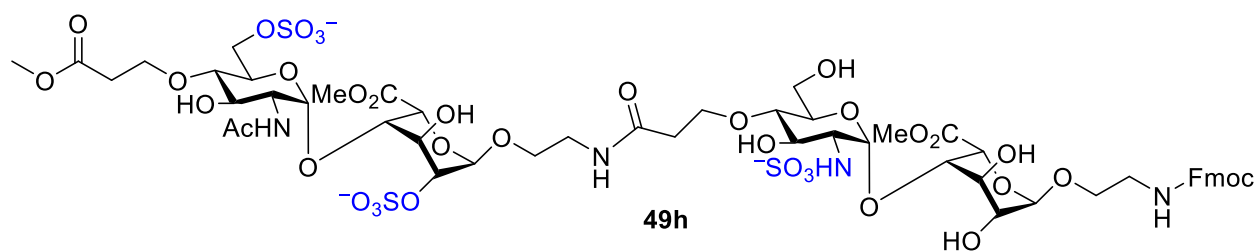
***N*-Fluorenylmethyloxycarbonyl-2-aminoethyl** ***O*-(4-*O*-methylpropionate-2-deoxy-2-sulfoamino-1-thio- α -D-glucopyranoside)-(1 \rightarrow 4)-*O*-(methyl-1-thio- α -L-idopyranosiduronate)-(1 \rightarrow 4)-*O*-(2-acetamido-4-*O*-carboxyethyl-2-deoxy-6-*O*-sulfonato-1-thio- α -D-glucopyranoside)-(1 \rightarrow 4)-*O*-methyl-2-*O*-sulfonato-1-thio- α -L-idopyranosiduronate (49f).**

Starting material (8 mg, 0.013 mmol) was treated according to the general procedures of pseudo-tetrasaccharide preparation with HATU to give compound **49f** (20 mg, 61%). ¹H NMR (500 MHz, CD₃OD) δ 7.81 (d, J = 7.5 Hz, 2H), 7.67 (d, J = 7.6 Hz, 2H), 7.40 (tt, J = 7.6, 1.6 Hz, 2H), 7.33 (tt, J = 7.5, 1.4 Hz, 2H), 5.37 (d, J = 3.6 Hz, 1H; A-1), 5.18 (s, 1H; C-1), 4.96 (d, J = 3.4 Hz, 1H; B-1), 4.92 (d, J = 2.9 Hz, 1H; D-1), 4.85 (d, J = 2.0 Hz, 1H), 4.83 (d, J = 3.0 Hz, 1H), 4.35 – 4.27 (m, 4H), 4.24 – 4.15 (m, 4H), 4.11 – 4.04 (m, 2H), 4.03 – 3.94 (m, 4H), 3.82 – 3.85 (m, 2H), 3.81 – 3.74 (m, 5H), 3.73 – 3.66 (m, 8H), 3.64 – 3.52 (m, 5H), 3.43 – 3.37 (m, 2H), 3.29 – 3.19 (m, 2H), 2.64 – 2.52 (m, 3H), 2.49 – 2.39 (m, 3H), 2.09 (s, 3H). ¹³C NMR (125 MHz, CD₃OD) δ 173.03, 172.97, 172.79, 170.47, 170.40, 143.90, 141.14, 127.37, 126.81, 124.90, 124.87, 119.47, 101.36, 99.53, 97.08, 96.29, 77.28, 78.12, 74.22, 73.87, 73.06, 71.87, 71.48, 71.42, 69.92, 69.17, 68.31, 67.87, 67.50, 67.29, 67.16, 66.48, 66.10, 65.84, 64.69, 60.55, 58.16, 53.60, 51.76, 51.51, 50.69, 40.18, 38.75, 36.62, 34.74, 21.75. HRMS: m/z calc. for C₃₉H₆₃N₄O₃₅S₃³⁻ [M+H]⁺²⁻: 622.1262; found: 622.1260.



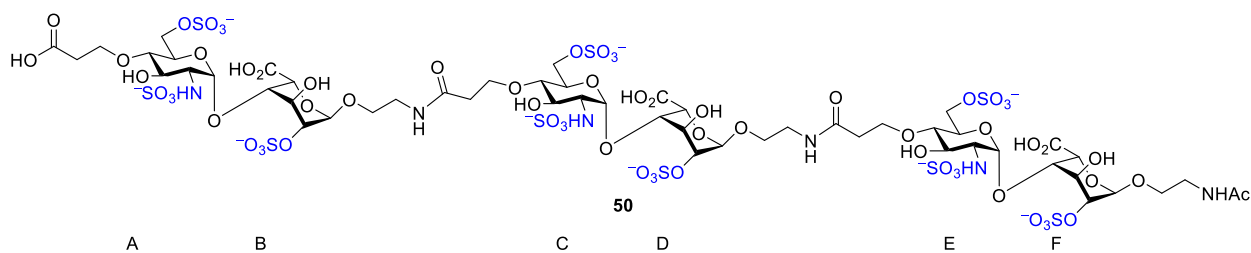
***N*-Fluorenylmethyloxycarbonyl-2-aminoethyl** ***O*-(2-acetamido-2-deoxy-4-*O*-methylpropionate-6-*O*-sulfonato-1-thio- α -D-glucopyranoside)-(1 \rightarrow 4)-*O*-(methyl-2-*O*-sulfonato-1-thio- α -L-idopyranosiduronate)-(1 \rightarrow 4)-*O*-(4-*O*-carboxyethyl-2-deoxy-2-sulfoamino-6-*O*-sulfonato-1-thio- α -D-glucopyranoside)-(1 \rightarrow 4)-*O*-methyl-2-*O*-sulfonato-1-thio- α -L-idopyranosiduronate (49g).**

Starting material (22 mg, 0.03 mmol) was treated according to the general procedures of pseudo-tetrasaccharide preparation with HATU to give compound **49g** (26 mg, 62%). ¹H NMR (500 MHz, CD₃OD) δ 8.00 (d, J = 7.6 Hz, 2H), 7.78 (t, J = 7.0 Hz, 2H), 7.58 (td, J = 7.6, 3.6 Hz, 2H), 7.52 – 7.46 (m, 2H), 5.37 (d, J = 3.6 Hz, 1H; A-1), 5.19 (s, 1H; C-1), 5.15 – 5.07 (m, 2H; B-1, D-1), 4.98 (s, 1H), 4.76 (d, J = 2.2 Hz, 1H), 4.64 – 4.59 (m, 1H), 4.52 – 4.47 (m, 1H), 4.45 – 4.20 (m, 9H), 4.18 – 3.94 (m, 8H), 3.89 – 4.81 (m, 5H), 3.76 (s, 4H), 3.72 – 3.55 (m, 7H), 3.51 – 3.41 (m, 4H), 3.33 – 3.22 (m, 3H), 2.77 – 2.66 (m, 2H), 2.56 (t, J = 5.9 Hz, 2H), 2.10 (s, 3H). ¹³C NMR (125 MHz, CD₃OD) δ 173.39, 173.31, 172.68, 169.77, 169.41, 142.34, 139.55, 126.65, 126.07, 123.81, 123.58, 118.73, 98.01, 97.65, 97.22, 93.48, 76.05, 75.93, 75.20, 73.28, 71.48, 70.13, 69.61, 69.24, 68.15, 67.75, 66.88, 66.52, 65.98, 65.82, 65.42, 64.86, 64.74, 64.66, 61.61, 56.36, 51.32, 51.62, 51.49, 50.81, 47.38, 45.57, 38.71, 37.54, 35.12, 33.52, 20.69. HRMS: m/z calc. for C₃₉H₆₁N₄O₄₁S₅⁵⁻ [M]⁵⁻: 280.2288; found: 280.2278.



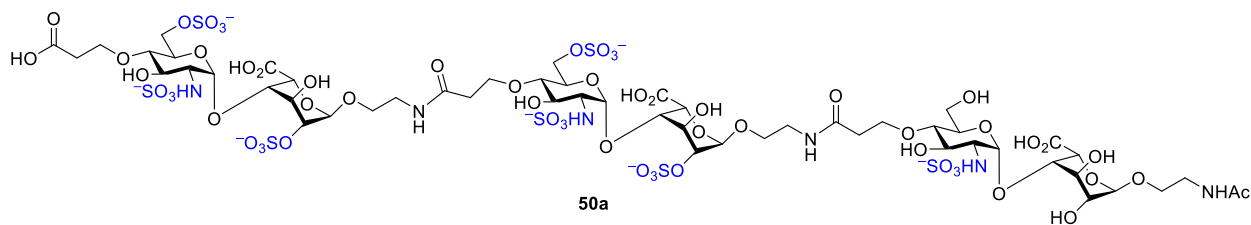
***N*-Fluorenylmethyloxycarbonyl-2-aminoethyl** ***O*-(2-acetamido-2-deoxy-4-*O*-methylpropionate-6-*O*-sulfonato-1-thio- α -D-glucopyranoside)-(1 \rightarrow 4)-*O*-(methyl-2-*O*-sulfonato-1-thio- α -L-idopyranosiduronate)-(1 \rightarrow 4)-*O*-(4-*O*-carboxyethyl-2-deoxy-2-sulfoamino-1-thio- α -D-glucopyranoside)-(1 \rightarrow 4)-*O*-methyl-1-thio- α -L-idopyranosiduronate (49h).**

Starting material (8.0 mg, 0.01 mmol) was treated according to the general procedures of pseudo-tetrasaccharide preparation with HATU to give compound **49i** (12.7 mg, 80%). ¹H NMR (500 MHz, CD₃OD) δ 7.81 (d, J = 7.5 Hz, 2H), 7.67 (d, J = 7.5 Hz, 2H), 7.40 (tt, J = 7.5, 1.5 Hz, 2H), 7.33 (tt, J = 7.5, 1.5 Hz, 2H), 5.16 (d, J = 4.8 Hz, 2H; A-1, C-1), 4.99 (d, J = 3.5 Hz, 1H; B-1), 4.97 (d, J = 3.4 Hz, 1H; D-1), 4.86 (dd, J = 5.6, 1.9 Hz, 2H), 4.34 – 4.25 (m, 6H), 4.22 – 4.18 (m, 5H), 4.11 – 4.05 (m, 3H), 4.02 – 3.93 (m, 7H), 3.82 (s, 3H), 3.74 – 3.66 (m, 7H), 3.66 – 3.54 (m, 6H), 3.43 – 3.37 (m, 3H), 3.33 – 3.35 (m, 2H), 3.30 (d, J = 2.7 Hz, 1H), 2.62 – 2.56 (m, 2H), 2.49 – 2.43 (m, 2H), 2.07 (d, J = 1.7 Hz, 6H). ¹³C NMR (125 MHz, CD₃OD) δ 172.96, 172.92, 170.49, 170.33, 157.48, 143.90, 141.14, 127.38, 126.81, 124.89, 119.48, 99.61, 99.56, 97.23, 96.43, 78.34, 78.26, 74.36, 73.47, 73.09, 71.52, 71.42, 69.99, 69.91, 68.22, 67.76, 67.55, 67.25, 66.49, 66.27, 66.22, 65.91, 64.79, 64.40, 53.60, 53.40, 51.83, 51.75, 50.82, 40.17, 38.67, 36.46, 34.85, 21.74. HRMS: m/z calc. for C₄₁H₆₄N₄O₃₉S₄⁴⁻ [M+H⁺]³⁻: 455.0708; found: 455.0688.



Acetamidoethyl *O*-(4-*O*-carboxyethyl-2-deoxy-2-sulfoamino-6-*O*-sulfonato-1-thio- α -D-glucopyranoside)-(1 \rightarrow 4)-*O*-(6-*O*-carboxyl-2-*O*-sulfonato-1-thio- α -L-idopyranosiduronate)-(1 \rightarrow 4)-*O*-(2-deoxy-2-sulfoamino-6-*O*-sulfonato-1-thio- α -D-glucopyranoside)-(1 \rightarrow 4)-*O*-(6-*O*-carboxyl-2-*O*-sulfonato-1-thio- α -L-idopyranosiduronate)-(1 \rightarrow 4)-*O*-(2-deoxy-2-sulfoamino-6-*O*-sulfonato-1-thio- α -D-glucopyranoside)-(1 \rightarrow 4)-*O*-(6-*O*-carboxyl-2-*O*-sulfonato-1-thio- α -L-idopyranosiduronate) (**50**).

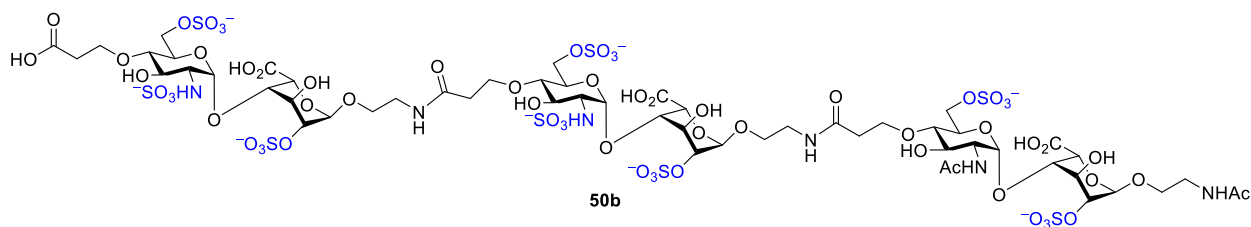
The starting material (5.8 mg, 0.004 mmol) was treated according to the general procedures of NH-Fmoc deprotection, pseudo-hexasaccharide preparation with HBTU and saponification of methyl esters to give compound **50** (3.8 mg, 51% for 3 steps). ¹H NMR (500 MHz, D₂O) δ 5.22 (d, J = 3.6 Hz, 1H; A-1), 5.16 (t, J = 4.2 Hz, 2H; C-1, F-1), 5.00 (d, J = 3.6 Hz, 2H; B-1, D-1), 4.95 (d, J = 2.8 Hz, 1H; E-1), 4.45 (dd, J = 11.5, 2.3 Hz, 2H), 4.41 (d, J = 2.8 Hz, 1H), 4.17 (dd, J = 11.0, 2.1 Hz, 1H), 4.13-4.08 (m, 5H), 4.07 – 3.99 (m, 4H), 3.94 – 3.62 (m, 14H), 3.57 – 3.44 (m, 6H), 3.32-3.16 (m, 8H), 3.13-3.05 (m, 3H), 2.53 – 2.34 (m, 6H), 1.82 (s, 3H). ¹³C NMR (125 MHz, D₂O) δ 173.83, 99.07, 98.72, 96.85, 77.81, 77.78, 77.59, 76.06, 75.94, 74.68, 74.55, 70.48, 70.43, 68.84, 68.82, 68.77, 68.62, 68.40, 68.29, 68.08, 67.61, 67.52, 67.30, 66.92, 66.81, 66.20, 66.12, 57.78, 57.77, 57.71, 39.04, 38.91, 36.22, 36.20, 35.30, 21.69. HRMS: m/z calc. for C₅₃H₇₉N₆O₆₅S₉⁹⁻ [M+4Na⁺]⁵⁻: 443.8033; found: 443.8041.



Acetamidoethyl O-(4-O-carboxyethyl-2-deoxy-2-sulfoamino-6-O-sulfonato-1-thio- α -D-glucopyranoside)-(1 \rightarrow 4)-O-(6-O-carboxyl-2-O-sulfonato-1-thio- α -L-idopyranosiduronate)-(1 \rightarrow 4)-O-(2-deoxy-2-sulfoamino-6-O-sulfonato-1-thio- α -D-glucopyranoside)-(1 \rightarrow 4)-O-(6-O-carboxyl-2-O-sulfonato-1-thio- α -L-idopyranosiduronate)-(1 \rightarrow 4)-O-(2-deoxy-2-sulfoamino-1-thio- α -D-glucopyranoside)-(1 \rightarrow 4)-O-(6-O-carboxyl-1-thio- α -L-idopyranosiduronate) (50a**).**

The starting material (6.5 mg, 0.004 mmol) was treated according to the general procedures of NH-Fmoc deprotection, pseudo-hexasaccharide preparation with HBTU and

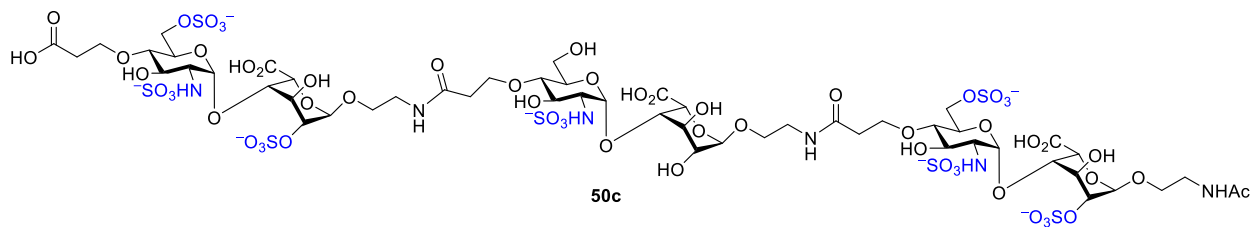
saponification of methyl esters to give compound **50a** (3.7 mg, 48% for 3 steps). ^1H NMR (500 MHz, D_2O) δ 5.19 (d, $J = 3.6$ Hz, 1H; A-1), 5.15 (dd, $J = 6.2, 3.6$ Hz, 2H; C-1, F-1), 5.01 – 4.96 (m, 2H; B-1, D-1), 4.73 – 4.70 (m, 1H; E-1), 4.44 – 4.33 (m, 3H), 4.18 – 4.13 (m, 1H), 4.12 – 4.05 (m, 5H), 4.04–3.99 (m, 2H), 3.98–3.93 (m, 1H), 3.92 – 3.71 (m, 12H), 3.70 – 3.44 (m, 14H), 3.32 – 3.15 (m, 9H), 3.12 – 3.00 (m, 4H), 2.50 – 2.35 (m, 6H), 1.82 (s, 3H). ^{13}C NMR (125 MHz, D_2O) δ 173.84, 100.61, 98.90, 98.70, 97.47, 97.09, 95.60, 78.04, 77.82, 77.64, 75.98, 75.95, 75.38, 74.69, 74.43, 70.68, 70.54, 70.47, 68.79, 68.46, 68.27, 68.22, 68.18, 67.78, 67.66, 67.52, 66.77, 66.71, 66.16, 59.75, 57.77, 57.75, 57.72, 39.05, 38.97, 38.91, 36.19, 21.70. HRMS: m/z calc. for $\text{C}_{53}\text{H}_{81}\text{N}_6\text{O}_{59}\text{S}_7^-$ [$\text{M}+2\text{Na}^+$] $^{5-}$: 403.0278; found: 403.0291.



Acetamidoethyl *O*-(4-*O*-carboxyethyl-2-deoxy-2-sulfoamino-6-*O*-sulfonato-1-thio- α -D-glucopyranoside)-(1 \rightarrow 4)-*O*-(6-*O*-carboxyl-2-*O*-sulfonato-1-thio- α -L-idopyranosiduronate)-(1 \rightarrow 4)-*O*-(2-deoxy-2-sulfoamino-6-*O*-sulfonato-1-thio- α -D-glucopyranoside)-(1 \rightarrow 4)-*O*-(6-*O*-carboxyl-2-*O*-sulfonato-1-thio- α -L-idopyranosiduronate)-(1 \rightarrow 4)-*O*-(2-acetamido-2-deoxy-6-*O*-sulfonato-1-thio- α -D-glucopyranoside)-(1 \rightarrow 4)-*O*-(6-*O*-carboxyl-2-*O*-sulfonato-1-thio- α -L-idopyranosiduronate) (**50b**).

The starting material (5.8 mg, 0.004 mmol) was treated according to the general procedures of NH-Fmoc deprotection, pseudo-hexasaccharide preparation with HBTU and saponification of methyl esters to give compound **50b** (1.4 mg, 19% for 3 steps). ^1H NMR (500

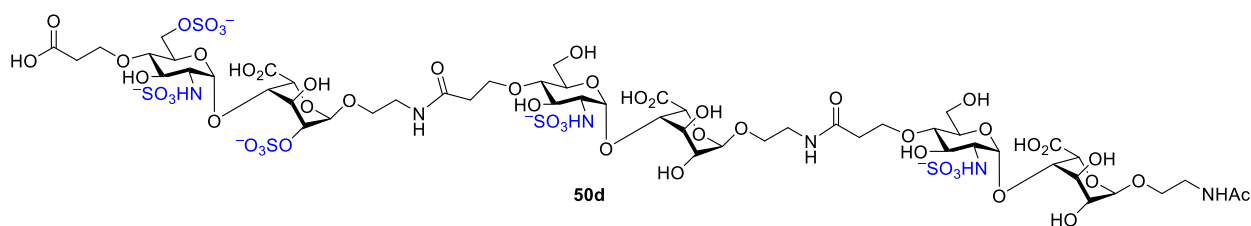
MHz, D₂O) δ 5.17 (dd, $J = 8.9, 3.5$ Hz, 2H; A-1, C-1), 4.98 (s, 2H; F-1, B-1), 4.94 (d, $J = 3.7$ Hz, 1H; D-1), 4.91 (s, 1H; E-1), 4.43 – 4.34 (m, 4H), 4.19 – 3.99 (m, 13H), 3.94 – 3.72 (m, 14H), 3.71 – 3.43 (m, 13H), 3.35 – 3.16 (m, 10H), 3.13 – 3.03 (m, 3H), 2.47 – 2.35 (m, 7H), 1.88 (s, 3H), 1.82 (s, 3H). ¹³C NMR (125 MHz, D₂O) δ 77.87, 75.88, 73.73, 70.49, 70.81, 68.86, 68.76, 68.61, 66.85, 66.91, 66.28, 66.16, 57.76, 39.01, 38.90, 36.18, 27.45, 22.07, 21.70. HRMS: m/z calc. for C₅₅H₈₂N₆O₆₃S₈⁸⁻ [M+3Na⁺]⁵⁻: 431.8177; found: 431.8189.



Acetamidoethyl *O*-(4-*O*-carboxyethyl-2-deoxy-2-sulfoamino-6-*O*-sulfonato-1-thio- α -D-glucopyranoside)-(1 \rightarrow 4)-*O*-(6-*O*-carboxyl-2-*O*-sulfonato-1-thio- α -L-idopyranosiduronate)-(1 \rightarrow 4)-*O*-(2-deoxy-2-sulfoamino-1-thio- α -D-glucopyranoside)-(1 \rightarrow 4)-*O*-(6-*O*-carboxyl-1-thio- α -L-idopyranosiduronate)-(1 \rightarrow 4)-*O*-(2-acetamido-2-deoxy-6-*O*-sulfonato-1-thio- α -D-glucopyranoside)-(1 \rightarrow 4)-*O*-(6-*O*-carboxyl-2-*O*-sulfonato-1-thio- α -L-idopyranosiduronate) (**50c**).

The starting material (4.5 mg, 0.003 mmol) was treated according to the general procedures of NH-Fmoc deprotection, pseudo-hexasaccharide preparation with HBTU and saponification of methyl esters to give compound **50c** (1.4 mg, 51% for 3 steps). ¹H NMR (500 MHz, D₂O) δ 5.22 (d, $J = 3.5$ Hz, 1H; A-1), 5.18 (d, $J = 3.6$ Hz, 1H; C-1), 5.14 (d, $J = 3.9$ Hz, 1H; E-1), 4.97 (d, $J = 2.4$ Hz, 1H; B-1), 4.94 (d, $J = 2.9$ Hz, 1H; D-1), 4.73 (d, $J = 2.7$ Hz, 1H; F-1), 4.41 – 4.32 (m, 3H), 4.19 – 3.99 (m, 9H), 3.97 – 3.92 (m, 1H), 3.92 – 3.73 (m, 12H), 3.71 – 3.42

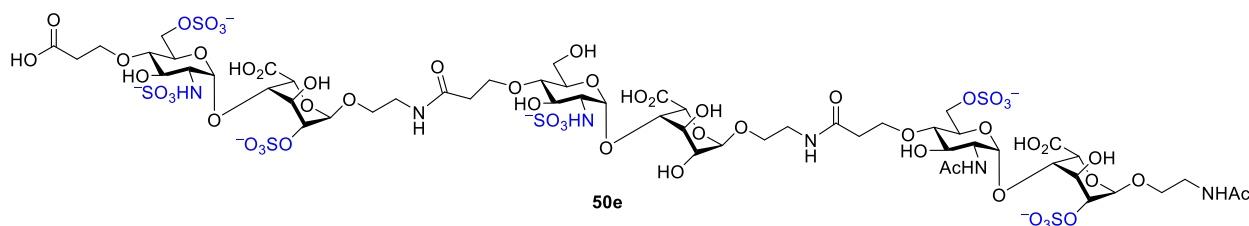
(m, 15H), 3.37 – 3.16 (m, 10H), 3.12 – 3.01 (m, 4H), 2.52 – 2.30 (m, 7H), 1.82 (s, 3H). ¹³C NMR (125 MHz, D₂O) δ 177.77, 173.87, 122.73, 119.89, 109.99, 100.57, 98.83, 97.48, 97.10, 96.74, 95.65, 78.05, 77.75, 77.69, 76.04, 75.93, 74.32, 70.73, 70.58, 70.49, 68.75, 68.70, 68.41, 68.34, 66.87, 66.75, 66.47, 66.20, 57.78, 57.73, 39.05, 38.98, 38.85, 36.35, 21.69. HRMS: m/z calc. for C₅₃H₈₁N₆O₅₉S₇⁷⁻ [M+2Na⁺]⁵⁻: 403.0278; found: 403.0296.



Acetamidoethyl *O*-(4-*O*-carboxyethyl-2-deoxy-2-sulfoamino-6-*O*-sulfonato-1-thio- α -D-glucopyranoside)-(1 \rightarrow 4)-*O*-(6-*O*-carboxyl-2-*O*-sulfonato-1-thio- α -L-idopyranosiduronate)-(1 \rightarrow 4)-*O*-(2-deoxy-2-sulfoamino-1-thio- α -D-glucopyranoside)-(1 \rightarrow 4)-*O*-(6-*O*-carboxyl-1-thio- α -L-idopyranosiduronate)-(1 \rightarrow 4)-*O*-(2-deoxy-2-sulfonato-1-thio- α -D-glucopyranoside)-(1 \rightarrow 4)-*O*-(6-*O*-carboxyl-1-thio- α -L-idopyranosiduronate) (**50d**).

The starting material (4.5 mg, 0.003 mmol) was treated according to the general procedures of NH-Fmoc deprotection, pseudo-hexasaccharide preparation with HBTU and saponification of methyl esters to give compound **50d** (3.0 mg, 56% for 3 steps). ¹H NMR (500 MHz, D₂O) δ 5.18 (d, J = 3.7 Hz, 1H; A-1), 5.14 (dd, J = 3.9, 1.4 Hz, 2H; C-1, E-1), 4.97 (d, J = 2.5 Hz, 1H; B-1), 4.74 – 4.71 (m, 2H; D-1, F-1), 4.39 – 4.32 (m, 3H), 4.18 – 4.14 (m, 1H), 4.12 – 3.99 (m, 4H), 3.97 – 3.92 (m, 2H), 3.91 – 3.72 (m, 11H), 3.70 – 3.45 (m, 18H), 3.31 – 3.16 (m, 10H), 3.10 – 2.98 (m, 4H), 2.48 – 2.33 (m, 7H), 1.82 (s, 3H). ¹³C NMR (125 MHz, D₂O) δ 173.93, 173.85, 100.61, 98.85, 97.11, 95.65, 95.57, 78.12, 78.05, 77.97, 75.94, 74.45, 74.30,

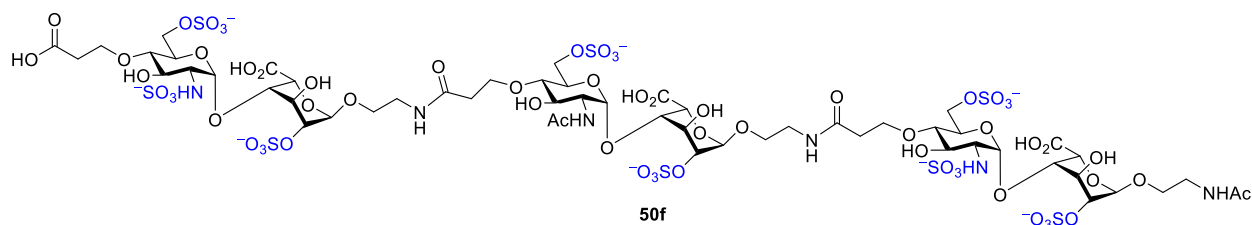
70.71, 70.55, 70.50, 68.78, 68.39, 68.27, 68.12, 67.83, 67.58, 67.38, 66.75, 66.69, 66.49, 66.19, 59.76, 57.78, 57.74, 38.99, 39.06, 36.26, 36.15, 21.70. HRMS: m/z calc. for $C_{53}H_{83}N_6O_{53}S_5^{5-}$ $[M+Na^+]^4$: 458.5627; found: 458.5641.



Acetamidoethyl *O*-(4-*O*-carboxyethyl-2-deoxy-2-sulfoamino-6-*O*-sulfonato-1-thio- α -D-glucopyranoside)-(1 \rightarrow 4)-*O*-(6-*O*-carboxyl-2-*O*-sulfonato-1-thio- α -L-idopyranosiduronate)-(1 \rightarrow 4)-*O*-(2-deoxy-2-sulfoamino-1-thio- α -D-glucopyranoside)-(1 \rightarrow 4)-*O*-(6-*O*-carboxyl-1-thio- α -L-idopyranosiduronate)-(1 \rightarrow 4)-*O*-(2-acetamido-2-deoxy-1-thio- α -D-glucopyranoside)-(1 \rightarrow 4)-*O*-(6-*O*-carboxyl-1-thio- α -L-idopyranosiduronate) (**50e**).

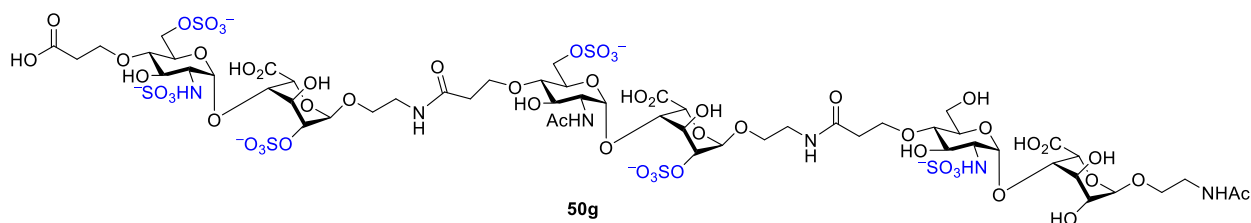
The starting material (4.5 mg, 0.003 mmol) was treated according to the general procedures of NH-Fmoc deprotection, pseudo-hexasaccharide preparation with HBTU and saponification of methyl esters to give compound **50e** (2.9 mg, 50% for 3 steps). 1H NMR (500 MHz, D_2O) δ 7.96 (d, J = 9.8 Hz, 1H; NHAc), 5.18 (d, J = 3.7 Hz, 1H; A-1), 5.14 (d, J = 3.7 Hz, 1H; C-1), 4.98 – 4.90 (m, 3H; D-1, B-1, E-1), 4.75 – 4.71 (m, 1H; F-1), 4.39 (d, J = 2.3 Hz, 1H), 4.35 (dd, J = 6.9, 2.4 Hz, 2H), 4.17 – 4.00 (m, 8H), 3.97 – 3.74 (m, 13H), 3.70 – 3.44 (m, 13H), 3.35 – 3.17 (m, 9H), 3.10 – 3.01 (m, 2H), 2.46 – 2.34 (m, 6H), 1.88 (s, 3H), 1.83 (s, 3H). ^{13}C NMR (125 MHz, D_2O) δ 190.14, 109.99, 109.71, 99.00, 98.65, 98.64, 96.97, 95.61, 93.51, 78.11, 77.77, 75.88, 75.41, 74.39, 73.67, 70.85, 70.73, 70.81, 70.53, 68.83, 68.71, 68.59, 68.26, 68.10, 67.42, 66.85, 66.44, 66.18, 63.81, 57.70, 53.04, 39.00, 38.87, 36.28, 36.13, 22.07, 21.70. HRMS:

m/z calc. for C₅₅H₈₄N₆O₅₇S₆⁶⁻ [M+Na⁺]⁵⁻: 391.0422; found: 391.0433.



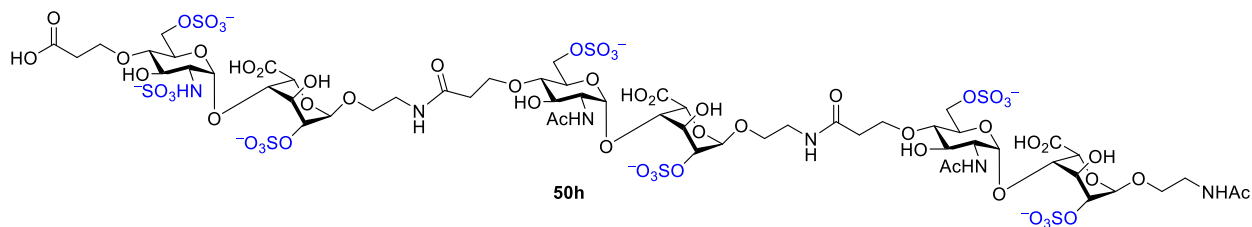
Acetamidoethyl *O*-(4-*O*-carboxyethyl-2-deoxy-2-sulfoamino-6-*O*-sulfonato-1-thio- α -D-glucopyranoside)-(1 \rightarrow 4)-*O*-(6-*O*-carboxyl-2-*O*-sulfonato-1-thio- α -L-idopyranosiduronate)-(1 \rightarrow 4)-*O*-(2-acetamido-2-deoxy-6-*O*-sulfonato-1-thio- α -D-glucopyranoside)-(1 \rightarrow 4)-*O*-(6-*O*-carboxyl-2-*O*-sulfonato-1-thio- α -L-idopyranosiduronate)-(1 \rightarrow 4)-*O*-(2-deoxy-2-sulfonato-6-*O*-sulfonato-1-thio- α -D-glucopyranoside)-(1 \rightarrow 4)-*O*-(6-*O*-carboxyl-2-*O*-sulfonato-1-thio- α -L-idopyranosiduronate) (**50f**).

The starting material (5.2 mg, 0.003 mmol) was treated according to the general procedures of NH-Fmoc deprotection, pseudo-hexasaccharide preparation with HBTU and saponification of methyl esters to give compound **50f** (3.7 mg, 55% for 3 steps). ¹H NMR (500 MHz, D₂O) δ 5.22 (d, J = 3.5 Hz, 1H; A-1), 5.16 (d, J = 3.5 Hz, 1H; C-1), 5.00 – 4.97 (m, 1H; E-1), 4.94 (m, 3H; B-1, D-1, F-1), 4.46 – 4.38 (m, 3H), 4.20 – 3.98 (m, 11H), 3.97 – 3.71 (m, 12H), 3.66 (m, 3H), 3.60 – 3.44 (m, 6H), 3.38 – 3.15 (m, 9H), 3.09 (m, 2H), 2.54 – 2.45 (m, 2H), 2.44 – 2.35 (m, 4H), 1.88 (s, 3H), 1.82 (s, 3H). ¹³C NMR (125 MHz, D₂O) δ 99.08, 98.74, 98.58, 97.49, 96.82, 93.69, 90.46, 77.83, 77.61, 76.03, 75.95, 73.19, 70.78, 70.51, 70.45, 68.80, 68.76, 68.67, 68.63, 68.41, 68.14, 67.70, 66.80, 66.91, 66.71, 66.20, 66.12, 57.79, 57.73, 53.01, 39.04, 38.93, 38.84, 36.24, 36.15, 22.11, 21.69. HRMS: m/z calc. for C₅₅H₈₂N₆O₆₃S₈⁸⁻ [M+Na⁺]⁷⁻: 301.8728; found: 301.8744.



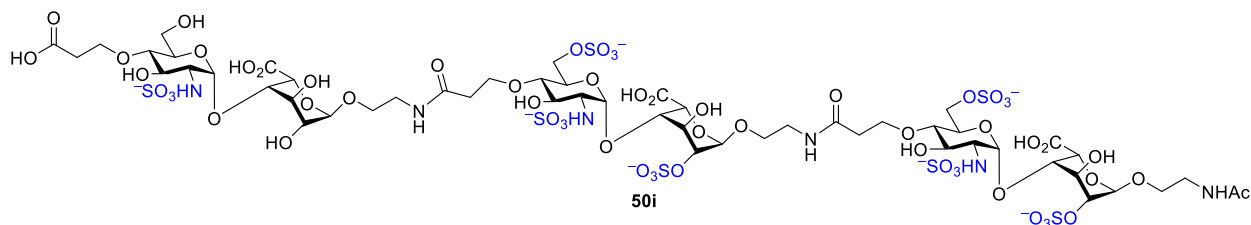
Acetamidoethyl *O*-(4-*O*-carboxyethyl-2-deoxy-2-sulfoamino-6-*O*-sulfonato-1-thio- α -D-glucopyranoside)-(1 \rightarrow 4)-*O*-(6-*O*-carboxyl-2-*O*-sulfonato-1-thio- α -L-idopyranosiduronate)-(1 \rightarrow 4)-*O*-(2-acetamido-2-deoxy-6-*O*-sulfonato-1-thio- α -D-glucopyranoside)-(1 \rightarrow 4)-*O*-(6-*O*-carboxyl-2-*O*-sulfonato-1-thio- α -L-idopyranosiduronate)-(1 \rightarrow 4)-*O*-(2-deoxy-2-sulfonato-1-thio- α -D-glucopyranoside)-(1 \rightarrow 4)-*O*-(6-*O*-carboxyl-1-thio- α -L-idopyranosiduronate) (50g).

The starting material (4.8 mg, 0.003 mmol) was treated according to the general procedures of NH-Fmoc deprotection, pseudo-hexasaccharide preparation with HBTU and saponification of methyl esters to give compound **50g** (2.5 mg, 44% for 3 steps). ^1H NMR (500 MHz, D_2O) δ 5.17 (d, $J = 3.7$ Hz, 1H; A-1), 5.14 (d, $J = 3.6$ Hz, 1H; C-1), 4.99 – 4.97 (m, 1H; E-1), 4.93 (d, $J = 3.1$ Hz, 2H; B-1, D-1), 4.73 – 4.69 (m, 1H; F-1), 4.39 (dd, $J = 13.7, 2.3$ Hz, 2H), 4.33 (d, $J = 2.4$ Hz, 1H), 4.18 – 3.99 (m, 8H), 3.95 (t, $J = 3.9$ Hz, 2H), 3.92 – 3.72 (m, 11H), 3.70 – 3.42 (m, 13H), 3.36 – 3.17 (m, 9H), 3.13-3.01 (m, 3H), 2.51 – 2.32 (m, 6H), 1.88 (s, 3H), 1.81 (s, 3H). ^{13}C NMR (125 MHz, D_2O) δ 174.21, 173.90, 109.99, 100.60, 97.21, 95.57, 93.54, 78.03, 77.85, 77.70, 75.91, 75.02, 74.45, 73.45, 70.69, 70.49, 68.75, 68.32, 68.17, 67.60, 66.69, 66.15, 63.59, 59.74, 57.74, 39.05, 38.93, 36.13, 22.09, 21.70. HRMS: m/z calc. for $\text{C}_{55}\text{H}_{84}\text{N}_6\text{O}_{57}\text{S}_6^{6-}$ $[\text{M}+\text{Na}^+]^5$: 391.0422; found: 391.0435.



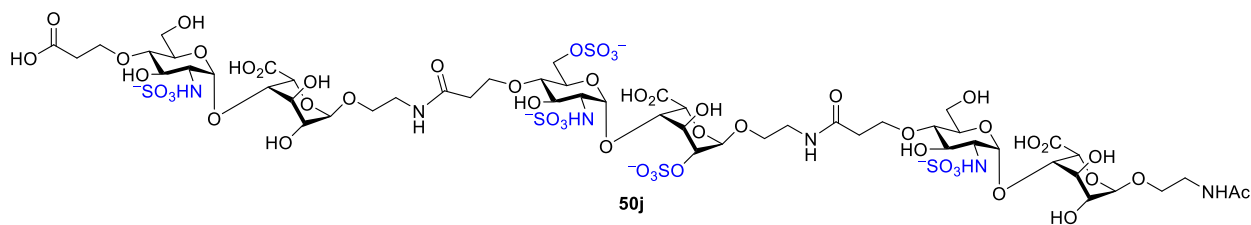
Acetamidoethyl *O*-(4-*O*-carboxyethyl-2-deoxy-2-sulfoamino-6-*O*-sulfonato-1-thio- α -D-glucopyranoside)-(1 \rightarrow 4)-*O*-(6-*O*-carboxyl-2-*O*-sulfonato-1-thio- α -L-idopyranosiduronate)-(1 \rightarrow 4)-*O*-(2-acetamido-2-deoxy-6-*O*-sulfonato-1-thio- α -D-glucopyranoside)-(1 \rightarrow 4)-*O*-(6-*O*-carboxyl-2-*O*-sulfonato-1-thio- α -L-idopyranosiduronate)-(1 \rightarrow 4)-*O*-(2-acetamido-2-deoxy-6-*O*-sulfonato-1-thio- α -D-glucopyranoside)-(1 \rightarrow 4)-*O*-(6-*O*-carboxyl-2-*O*-sulfonato-1-thio- α -L-idopyranosiduronate) (**50h**).

The starting material (5.2 mg, 0.003 mmol) was treated according to the general procedures of NH-Fmoc deprotection, pseudo-hexasaccharide preparation with HBTU and saponification of methyl esters to give compound **50h** (2.8 mg, 42% for 3 steps). ^1H NMR (500 MHz, D_2O) δ 5.16 (d, $J = 3.7$ Hz, 1H; A-1), 4.98 (s, 1H; C-1), 4.93 (m, 4H; B-1, D-1, E-1, F-1), 4.46 – 4.38 (m, 3H), 4.22 – 3.99 (m, 12H), 3.94 – 3.71 (m, 14H), 3.69 – 3.62 (m, 3H), 3.60 – 3.41 (m, 7H), 3.35 – 3.19 (m, 9H), 3.17 (s, 1H), 3.08 (dd, $J = 10.6, 3.5$ Hz, 1H), 2.52 – 2.28 (m, 7H), 1.88 (s, 6H), 1.82 (s, 3H). ^{13}C NMR (125 MHz, D_2O) δ 174.62, 174.15, 173.87, 98.73, 98.67, 98.58, 97.46, 93.65, 93.54, 77.82, 77.62, 76.01, 74.77, 73.65, 73.26, 70.83, 70.78, 70.45, 68.88, 68.79, 68.62, 68.58, 68.48, 68.15, 67.72, 66.87, 66.79, 66.70, 66.22, 66.10, 63.79, 57.77, 53.01, 39.00, 38.93, 38.86, 36.20, 36.15, 35.39, 22.09, 21.69. HRMS: m/z calc. for $\text{C}_{57}\text{H}_{85}\text{N}_6\text{O}_{61}\text{S}_7^-$ [$\text{M}+2\text{Na}^+$] $^{5-}$: 419.8320; found: 419.8341.



Acetamidoethyl *O*-(4-*O*-carboxyethyl-2-deoxy-2-sulfoamino-1-thio- α -D-glucopyranoside)-(1 \rightarrow 4)-*O*-(6-*O*-carboxyl-1-thio- α -L-idopyranosiduronate)-(1 \rightarrow 4)-*O*-(2-deoxy-2-sulfoamino-6-*O*-sulfonato-1-thio- α -D-glucopyranoside)-(1 \rightarrow 4)-*O*-(6-*O*-carboxyl-2-*O*-sulfonato-1-thio- α -L-idopyranosiduronate)-(1 \rightarrow 4)-*O*-(2-deoxy-2-sulfoamino-6-*O*-sulfonato-1-thio- α -D-glucopyranoside)-(1 \rightarrow 4)-*O*-(6-*O*-carboxyl-2-*O*-sulfonato-1-thio- α -L-idopyranosiduronate) (50i).

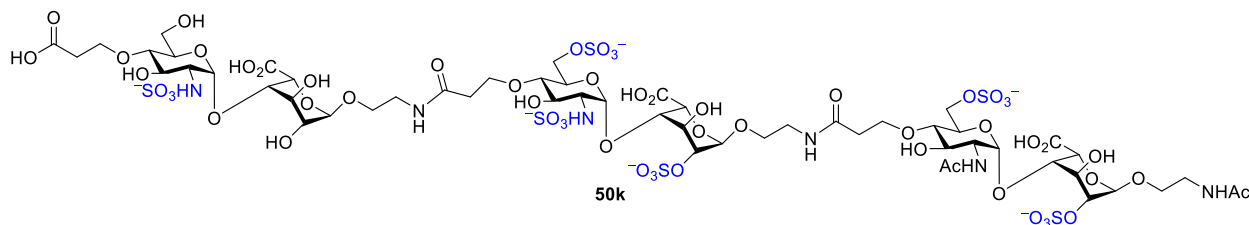
The starting material (4.6 mg, 0.003 mmol) was treated according to the general procedures of NH-Fmoc deprotection, pseudo-hexasaccharide preparation with HBTU and saponification of methyl esters to give compound **50i** (1.2 mg, 20% for 3 steps). ^1H NMR (500 MHz, D_2O) δ 5.24 (s, 1H; A-1), 5.15 (d, $J = 12.9$ Hz, 2H; C-1, E-1), 4.99 (s, 1H; B-1), 4.93 (s, 2H; D-1, F-1), 4.38 – 4.31 (m, 3H), 4.14 – 3.99 (m, 8H), 3.96 – 3.71 (m, 13H), 3.69 – 3.42 (m, 14H), 3.36 – 3.15 (m, 9H), 3.12 – 3.01 (m, 4H), 2.44 – 2.32 (m, 6H), 1.82 (d, $J = 1.8$ Hz, 3H). HRMS: m/z calc. for $\text{C}_{53}\text{H}_{81}\text{N}_6\text{O}_{59}\text{S}_7^{7-}$ $[\text{M}+2\text{Na}^+]^{5-}$: 403.0278; found: 403.0296.



Acetamidoethyl *O*-(4-*O*-carboxyethyl-2-deoxy-2-sulfoamino-1-thio- α -D-glucopyranoside)-

(1→4)-O-(6-O-carboxyl-1-thio- α -L-idopyranosiduronate)-(1→4)-O-(2-deoxy-2-sulfoamino-6-O-sulfonato-1-thio- α -D-glucopyranoside)-(1→4)-O-(6-O-carboxyl-2-O-sulfonato-1-thio- α -L-idopyranosiduronate)-(1→4)-O-(2-deoxy-2-sulfoamino-1-thio- α -D-glucopyranoside)-(1→4)-O-(6-O-carboxyl-1-thio- α -L-idopyranosiduronate) (50j).

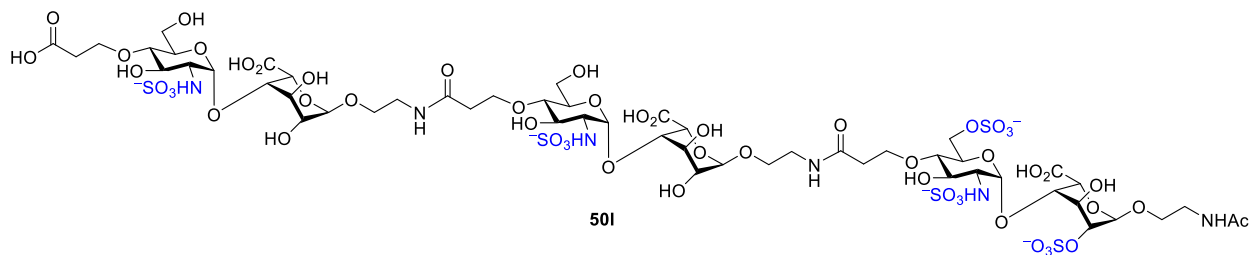
The starting material (4.2 mg, 0.003 mmol) was treated according to the general procedures of NH-Fmoc deprotection, pseudo-hexasaccharide preparation with HBTU and saponification of methyl esters to give compound **50j** (2.4 mg, 48% for 3 steps). ^1H NMR (500 MHz, D_2O) δ 5.17 (d, $J = 2.9$ Hz, 1H; A-1), 5.14 (t, $J = 2.5$ Hz, 2H; C-1, E-1), 4.98 (s, 1H; B-1), 4.72 (dd, $J = 5.4, 2.5$ Hz, 2H; D-1, F-1), 4.46 – 4.35 (m, 3H), 4.12 – 4.05 (m, 3H), 4.03 – 3.83 (m, 9H), 3.83 – 3.69 (m, 5H), 3.68 – 3.44 (m, 15H), 3.36 – 3.13 (m, 9H), 3.11 – 2.99 (m, 3H), 2.46 – 2.34 (m, 6H), 1.81 (d, $J = 1.9$ Hz, 3H). ^{13}C NMR (125 MHz, D_2O) δ 173.88, 170.07, 100.62, 100.60, 98.86, 97.38, 95.63, 77.98, 77.81, 77.66, 76.06, 75.08, 74.38, 74.22, 70.75, 70.66, 70.57, 70.51, 68.79, 68.19, 68.15, 68.09, 67.97, 67.91, 67.64, 67.41, 67.28, 66.82, 66.73, 66.54, 66.11, 59.73, 57.81, 57.70, 39.04, 38.98, 38.88, 36.33, 36.18, 35.58, 21.69. HRMS: m/z calc. for $\text{C}_{53}\text{H}_{83}\text{N}_6\text{O}_{53}\text{S}_5^{5-}$ [$\text{M}+\text{Na}^+$] $^{4+}$: 458.5627; found: 458.5641.



Acetamidoethyl O-(4-O-carboxyethyl-2-deoxy-2-sulfoamino-1-thio- α -D-glucopyranoside)-(1→4)-O-(6-O-carboxyl-1-thio- α -L-idopyranosiduronate)-(1→4)-O-(2-deoxy-2-sulfoamino-6-O-sulfonato-1-thio- α -D-glucopyranoside)-(1→4)-O-(6-O-carboxyl-2-O-sulfonato-1-thio- α -

L-idopyranosiduronate)-(1→4)-O-(2-acetamido-2-deoxy-6-O-sulfonato-1-thio- α -D-glucopyranoside)-(1→4)-O-(6-O-carboxyl-2-O-sulfonato-1-thio- α -L-idopyranosiduronate) (50k).

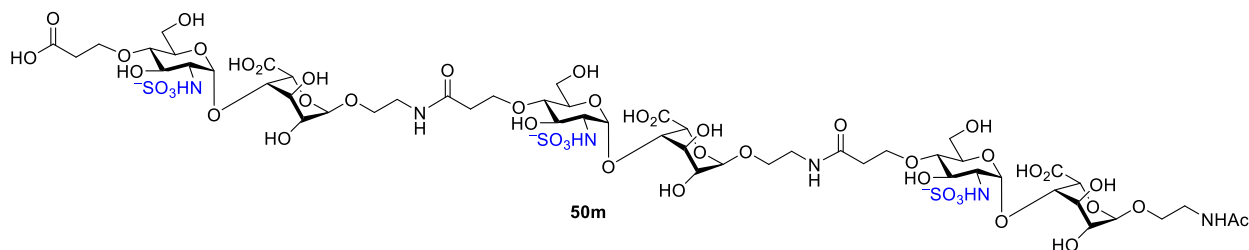
The starting material (6.6 mg, 0.004 mmol) was treated according to the general procedures of NH-Fmoc deprotection, pseudo-hexasaccharide preparation with HBTU and saponification of methyl esters to give compound **50k** (5.0 mg, 59% for 3 steps). ^1H NMR (500 MHz, D_2O) δ 5.15 (m, 2H; A-1, C-1), 4.99 (s, 1H; E-1), 4.94 – 4.90 (m, 2H; D-1, B-1), 4.72 (s, 1H; F-1), 4.45 – 4.36 (m, 3H), 4.13 – 3.99 (m, 8H), 3.95 (t, $J = 3.7$ Hz, 1H), 3.91 – 3.70 (m, 12H), 3.70 – 3.60 (m, 5H), 3.60 – 3.43 (m, 8H), 3.36 – 3.17 (m, 9H), 3.12 – 2.96 (m, 3H), 2.44 – 2.34 (m, 6H), 1.88 (s, 3H), 1.82 (s, 3H). ^{13}C NMR (125 MHz, D_2O) δ 174.62, 173.88, 100.60, 98.77, 98.68, 95.61, 93.54, 77.84, 77.68, 76.04, 74.81, 74.70, 74.23, 73.63, 70.82, 70.76, 70.56, 70.49, 68.88, 68.80, 68.58, 68.40, 68.20, 68.00, 67.72, 67.32, 66.88, 66.81, 66.53, 66.25, 66.14, 63.77, 59.70, 57.82, 57.69, 53.00, 39.00, 38.88, 36.33, 36.17, 22.07, 21.69. HRMS: m/z calc. for $\text{C}_{55}\text{H}_{84}\text{N}_6\text{O}_{57}\text{S}_6^{6-}$ $[\text{M}+\text{Na}^+]^{5-}$: 391.0422; found: 391.0430.



Acetamidoethyl O-(4-O-carboxyethyl-2-deoxy-2-sulfoamino-1-thio- α -D-glucopyranoside)-(1→4)-O-(6-O-carboxyl-1-thio- α -L-idopyranosiduronate)-(1→4)-O-(2-deoxy-2-sulfoamino-1-thio- α -D-glucopyranoside)-(1→4)-O-(6-O-carboxyl-1-thio- α -L-idopyranosiduronate)-

(1→4)-O-(2-deoxy-2-sulfoamino-6-O-sulfonato-1-thio- α -D-glucopyranoside)-(1→4)-O-(6-O-carboxyl-2-O-sulfonato-1-thio- α -L-idopyranosiduronate) (50l).

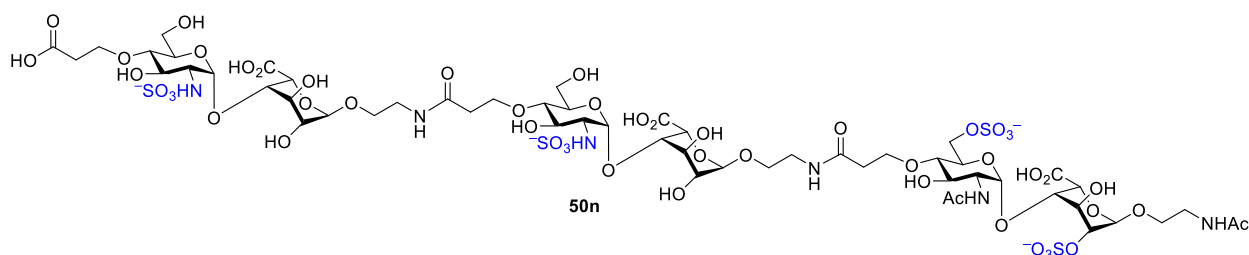
The starting material (2.5 mg, 0.002 mmol) was treated according to the general procedures of NH-Fmoc deprotection, pseudo-hexasaccharide preparation with HBTU and saponification of methyl esters to give compound **50l** (1.4 mg, 42% for 3 steps). ^1H NMR (500 MHz, D_2O) δ 5.22 (d, $J = 3.5$ Hz, 1H; A-1), 5.19 – 5.06 (m, 2H; C-1, E-1), 4.94 (s, 1H; B-1), 4.77 – 4.71 (m, 2H; D-1, F-1), 4.38 – 4.30 (m, 3H), 4.13 – 4.07 (m, 2H), 4.05 – 3.99 (m, 2H), 3.95 (t, $J = 3.9$ Hz, 2H), 3.93 – 3.83 (m, 6H), 3.82 – 3.71 (m, 4H), 3.70 – 3.41 (m, 16H), 3.34 – 3.15 (m, 9H), 3.11 – 3.01 (m, 4H), 2.44 – 2.31 (m, 6H), 1.82 (s, 3H). HRMS: m/z calc. for $\text{C}_{53}\text{H}_{83}\text{N}_6\text{O}_{53}\text{S}_5^{5-}$ $[\text{M}+\text{Na}]^{4+}$: 458.5627; found: 458.5623.



Acetamidoethyl O-(4-O-carboxyethyl-2-deoxy-2-sulfoamino-1-thio- α -D-glucopyranoside)-(1→4)-O-(6-O-carboxyl-1-thio- α -L-idopyranosiduronate)-(1→4)-O-(2-deoxy-2-sulfoamino-1-thio- α -D-glucopyranoside)-(1→4)-O-(6-O-carboxyl-1-thio- α -L-idopyranosiduronate)-(1→4)-O-(2-deoxy-2-sulfoamino-1-thio- α -D-glucopyranoside)-(1→4)-O-(6-O-carboxyl-1-thio- α -L-idopyranosiduronate) (50m).

The starting material (3.0 mg, 0.002 mmol) was treated according to the general procedures of NH-Fmoc deprotection, pseudo-hexasaccharides preparation with HATU and

saponification of methyl esters to give compound **50m** (0.8 mg, 22% for 3 steps). ¹H NMR (500 MHz, D₂O) δ 5.15 (d, J = 3.6 Hz, 3H; A-1, C-1, E-1), 4.73 (d, J = 4.1 Hz, 3H; B-1, D-1, F-1), 4.38 – 4.28 (m, 3H), 3.93 – 3.99 (m, 3H), 3.91-3.82 (m, 6H), 3.80 – 3.73 (m, 4H), 3.70 – 3.44 (m, 20H), 3.33 – 3.17 (m, 9H), 3.11 – 2.99 (m, 4H), 2.46 – 2.33 (m, 6H), 1.82 (s, 2H). HRMS: m/z calc. for C₅₃H₈₅N₆O₄₇S₃³⁻ [M]³⁻: 551.1208; found: 551.1201.

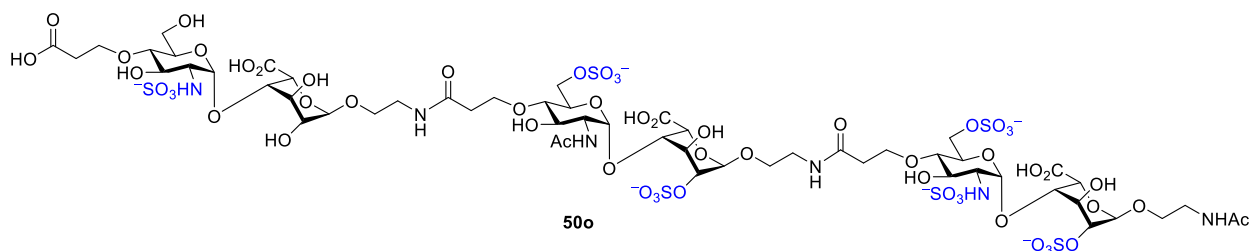


Acetamidoethyl O-(4-O-carboxyethyl-2-deoxy-2-sulfoamino-1-thio- α -D-glucopyranoside)-(1 \rightarrow 4)-O-(6-O-carboxyl-1-thio- α -L-idopyranosiduronate)-(1 \rightarrow 4)-O-(2-deoxy-2-sulfoamino-1-thio- α -D-glucopyranoside)-(1 \rightarrow 4)-O-(6-O-carboxyl-1-thio- α -L-idopyranosiduronate)-(1 \rightarrow 4)-O-(2-acetamido-2-deoxy-6-O-sulfonato-1-thio- α -D-glucopyranoside)-(1 \rightarrow 4)-O-(6-O-carboxyl-2-O-sulfonato-1-thio- α -L-idopyranosiduronate) (50n**).**

The starting material (3.8 mg, 0.003 mmol) was treated according to the general procedures of NH-Fmoc deprotection, pseudo-hexasaccharide preparation with HATU and saponification of methyl esters to give compound **50n** (2.6 mg, 52% for 3 steps). ¹H NMR (500 MHz, D₂O) δ 5.19 – 5.05 (m, 2H; A-1, C-1), 4.95 – 4.91 (m, 2H; E-1, B-1), 4.73 (m, 2H; D-1, F-1), 4.43 – 4.35 (m, 3H), 4.12 – 4.01 (m, 4H), 3.95 (d, J = 4.0 Hz, 2H), 3.92 – 3.72 (m, 12H), 3.70 – 3.42 (m, 18H), 3.32 – 3.19 (m, 9H), 3.08-2.98 (m, 3H), 2.47 – 2.33 (m, 7H), 1.88 (s, 3H), 1.81 (s, 3H). ¹³C NMR (125 MHz, D₂O) δ 174.62, 173.88, 100.61, 98.65, 95.67, 95.59, 93.61, 77.90,

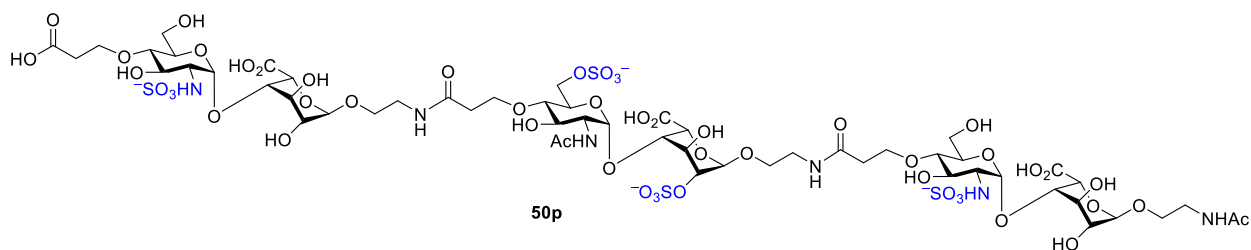
77.86, 77.75, 74.30, 74.27, 73.59, 70.85, 70.75, 70.71, 70.55, 68.87, 68.56, 68.18, 68.08, 67.37, 67.28, 66.88, 66.52, 63.77, 59.72, 57.77, 57.70, 53.04, 39.00, 38.89, 36.29, 36.23, 22.07, 21.70.

HRMS: m/z calc. for $C_{55}H_{86}N_6O_{51}S_4^{4-}$ $[M]^{4-}$: 443.5806; found: 443.5810.



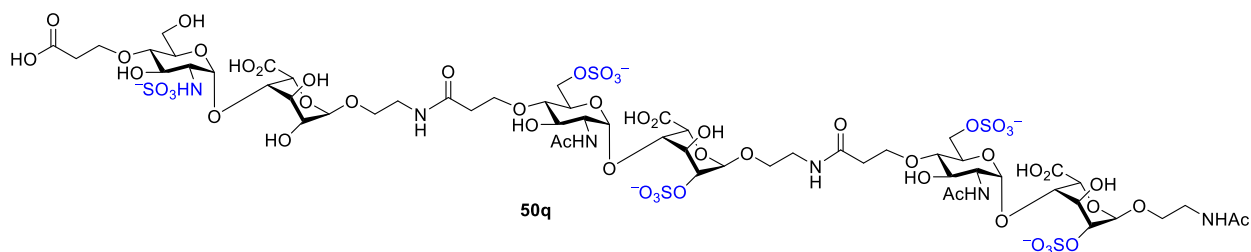
Acetamidoethyl *O*-(4-*O*-carboxyethyl-2-deoxy-2-sulfoamino-1-thio- α -D-glucopyranoside)-(1 \rightarrow 4)-*O*-(6-*O*-carboxyl-1-thio- α -L-idopyranosiduronate)-(1 \rightarrow 4)-*O*-(2-acetamido-2-deoxy-1-thio- α -D-glucopyranoside)-(1 \rightarrow 4)-*O*-(6-*O*-carboxyl-1-thio- α -L-idopyranosiduronate)-(1 \rightarrow 4)-*O*-(2-acetamido-2-deoxy-6-*O*-sulfonato-1-thio- α -D-glucopyranoside)-(1 \rightarrow 4)-*O*-(6-*O*-carboxyl-2-*O*-sulfonato 1-thio- α -L-idopyranosiduronate) (50o).

The starting material (3.9 mg, 0.003 mmol) was treated according to the general procedures of NH-Fmoc deprotection, pseudo-hexasaccharide preparation with HATU and saponification of methyl esters to give compound **50o** (1.7 mg, 34% for 3 steps). 1H NMR (500 MHz, D_2O) δ 5.21 (d, $J = 3.7$ Hz, 1H; A-1), 5.14 (d, $J = 3.7$ Hz, 1H; C-1), 4.97 – 4.91 (m, 3H; B-1, D-1, E-1), 4.73 (s, 1H; F-1), 4.48 – 4.36 (m, 3H), 4.14 – 3.99 (m, 8H), 3.98 – 3.71 (m, 13H), 3.70 – 3.44 (m, 13H), 3.36 – 3.15 (m, 9H), 3.14 – 3.00 (m, 3H), 2.47 – 2.33 (m, 6H), 1.88 (s, 3H), 1.82 (s, 3H). HRMS: m/z calc. for $C_{55}H_{84}N_6O_{57}S_6^{6-}$ $[M+2Na^+]^{4-}$: 494.5500; found: 494.5502.



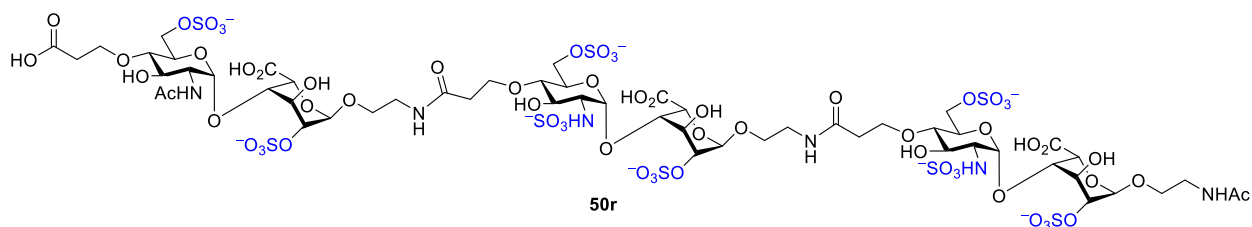
Acetamidoethyl *O*-(4-*O*-carboxyethyl-2-deoxy-2-sulfoamino-1-thio- α -D-glucopyranoside)-(1 \rightarrow 4)-*O*-(6-*O*-carboxyl-1-thio- α -L-idopyranosiduronate)-(1 \rightarrow 4)-*O*-(2-acetamido-2-deoxy-6-*O*-sulfonato-1-thio- α -D-glucopyranoside)-(1 \rightarrow 4)-*O*-(6-*O*-carboxyl-2-*O*-sulfonato-1-thio- α -L-idopyranosiduronate)-(1 \rightarrow 4)-*O*-(2-deoxy-2-sulfoamino-1-thio- α -D-glucopyranoside)-(1 \rightarrow 4)-*O*-(6-*O*-carboxyl-1-thio- α -L-idopyranosiduronate) (50p).

The starting material (7.1 mg, 0.005 mmol) was treated according to the general procedures of NH-Fmoc deprotection, pseudo-hexasaccharide preparation with HATU and saponification of methyl esters to give compound **50p** (4.4 mg, 51% for 3 steps). ^1H NMR (500 MHz, D_2O) δ 5.19 – 5.04 (m, 2H; A-1, C-1), 4.96 – 4.92 (m, 2H; B-1, E-1), 4.74 – 4.71 (m, 2H; D-1, F-1), 4.45 (d, $J = 2.1$ Hz, 1H), 4.40 (dd, $J = 4.4, 2.5$ Hz, 2H), 4.12 – 4.00 (m, 5H), 3.95 (d, $J = 4.3$ Hz, 2H), 3.91 – 3.73 (m, 12H), 3.71 – 3.44 (m, 19H), 3.38 – 3.17 (m, 10H), 3.07 – 3.01 (m, 3H), 2.47 – 2.36 (m, 6H), 1.89 (s, 3H), 1.81 (s, 3H). ^{13}C NMR (125 MHz, D_2O) δ 174.65, 174.47, 174.15, 173.94, 100.65, 98.65, 95.66, 93.79, 77.94, 77.78, 77.71, 74.37, 74.22, 73.35, 70.92, 70.82, 70.73, 70.67, 70.59, 68.92, 68.54, 68.17, 68.13, 67.98, 67.40, 67.27, 66.79, 66.75, 66.59, 66.19, 63.57, 59.73, 59.70, 57.72, 53.05, 39.04, 38.93, 36.28, 36.21, 35.40, 22.09, 21.69. HRMS: m/z calc. for $\text{C}_{55}\text{H}_{86}\text{N}_6\text{O}_{51}\text{S}_4^+$ $[\text{M}]^4$: 443.5806; found: 443.5805.



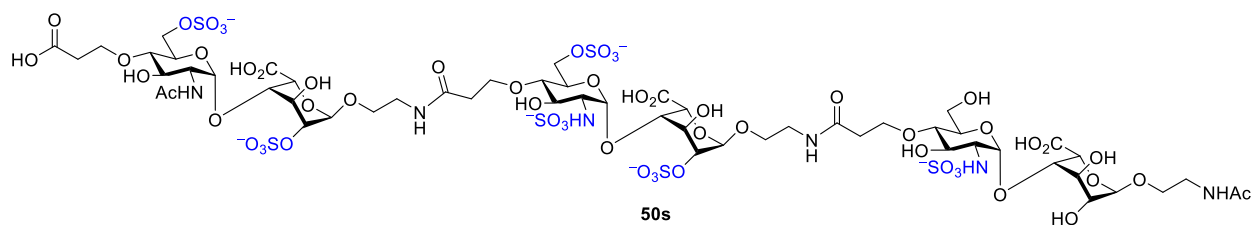
Acetamidoethyl *O*-(4-*O*-carboxyethyl-2-deoxy-2-sulfoamino-1-thio- α -D-glucopyranoside)-(1 \rightarrow 4)-*O*-(6-*O*-carboxyl-1-thio- α -L-idopyranosiduronate)-(1 \rightarrow 4)-*O*-(2-acetamido-2-deoxy-6-*O*-sulfonato-1-thio- α -D-glucopyranoside)-(1 \rightarrow 4)-*O*-(6-*O*-carboxyl-2-*O*-sulfonato-1-thio- α -L-idopyranosiduronate)-(1 \rightarrow 4)-*O*-(2-acetamido-2-deoxy-6-*O*-sulfonato-1-thio- α -D-glucopyranoside)-(1 \rightarrow 4)-*O*-(6-*O*-carboxyl-2-*O*-sulfonato-1-thio- α -L-idopyranosiduronate) (50q).

The starting material (6.9 mg, 0.005 mmol) was treated according to the general procedures of NH-Fmoc deprotection, pseudo-hexasaccharide preparation with HATU and saponification of methyl esters to give compound **50q** (4.0 mg, 45% for 3 steps). ^1H NMR (500 MHz, D_2O) δ 7.99 – 7.88 (m, 3H, NHAc), 5.14 (d, J = 3.6 Hz, 1H; A-1), 4.96 – 4.91 (m, 4H; B-1, C-1, D-1, E-1), 4.39 (d, J = 2.4 Hz, 2H; F-1), 4.32 (s, 1H), 4.15 – 4.02 (m, 9H), 3.96 – 3.73 (m, 16H), 3.69 – 3.42 (m, 16H), 3.38 – 3.19 (m, 11H), 3.05 (dd, J = 10.4, 3.5 Hz, 2H), 2.46 – 2.31 (m, 6H), 1.89 (s, 6H), 1.83 (s, 3H). ^{13}C NMR (125 MHz, D_2O) δ 174.63, 98.68, 98.54, 95.59, 93.55, 93.50, 78.13, 77.86, 77.75, 74.38, 73.74, 73.33, 70.85, 70.72, 70.57, 69.28, 68.85, 68.63, 68.18, 67.52, 66.86, 66.65, 66.46, 66.27, 63.89, 63.47, 59.81, 59.70, 57.66, 53.05, 39.03, 38.89, 36.28, 36.21, 22.12, 22.09, 21.72. HRMS: m/z calc. for $\text{C}_{57}\text{H}_{87}\text{N}_6\text{O}_{55}\text{S}_5^{5-}$ $[\text{M}+\text{Li}^+]^{4-}$: 475.5745; found: 475.5755.



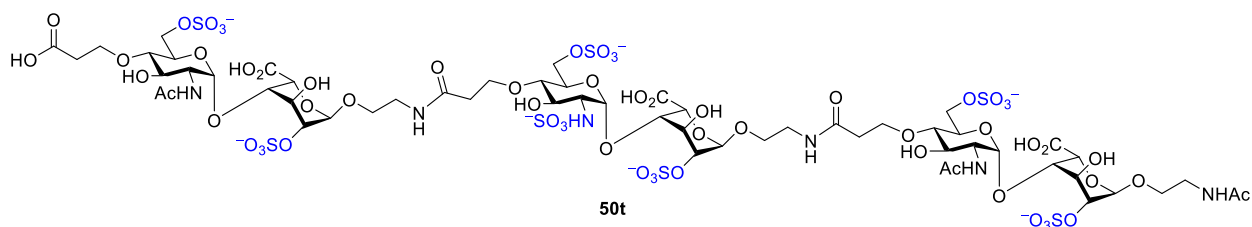
Acetamidoethyl ***O*-(2-acetamido-4-*O*-carboxyethyl-2-deoxy-6-*O*-sulfonato-1-thio- α -D-glucopyranoside)-(1 \rightarrow 4)-*O*-(6-*O*-carboxyl-2-*O*-sulfonato-1-thio- α -L-idopyranosiduronate)-(1 \rightarrow 4)-*O*-(2-deoxy-2-sulfoamino-6-*O*-sulfonato-1-thio- α -D-glucopyranoside)-(1 \rightarrow 4)-*O*-(6-*O*-carboxyl-2-*O*-sulfonato-1-thio- α -L-idopyranosiduronate)-(1 \rightarrow 4)-*O*-(2-deoxy-2-sulfoamino-6-*O*-sulfonato-1-thio- α -D-glucopyranoside)-(1 \rightarrow 4)-*O*-(6-*O*-carboxyl-2-*O*-sulfonato-1-thio- α -L-idopyranosiduronate) (**50r**).**

The starting material (5.5 mg, 0.003 mmol) was treated according to the general procedures of NH-Fmoc deprotection, pseudo-hexasaccharide preparation with HBTU and saponification of methyl esters to give compound **50r** (2.4 mg, 34% for 3 steps). ^1H NMR (500 MHz, D_2O) δ 5.22 (d, $J = 3.3$ Hz, 1H; A-1), 5.16 (d, $J = 3.6$ Hz, 1H; C-1), 5.00 (s, 2H; E-1), 4.96 – 4.89 (m, 3H; B-1, D-1, F-1), 4.48 – 4.39 (m, 3H), 4.19 – 3.98 (m, 10H), 3.93 – 3.45 (m, 20H), 3.34 – 3.04 (m, 11H), 2.52 – 2.33 (m, 6H), 1.89 (s, 3H), 1.82 (s, 3H). ^{13}C NMR (125 MHz, D_2O) δ 173.79, 171.71, 109.99, 99.08, 98.56, 97.59, 93.80, 91.93, 91.61, 77.81, 77.76, 77.61, 76.07, 75.96, 74.67, 74.22, 73.18, 72.85, 70.86, 70.79, 70.49, 68.91, 68.78, 68.37, 67.62, 66.93, 66.13, 57.72, 53.00, 45.75, 38.87, 57.72, 39.05, 38.87, 36.23, 22.10, 21.70. HRMS: m/z calc. for $\text{C}_{55}\text{H}_{82}\text{N}_6\text{O}_{63}\text{S}_8^{8-}$ $[\text{M}+3\text{Na}^+]^{5-}$: 431.8177; found: 431.8196.



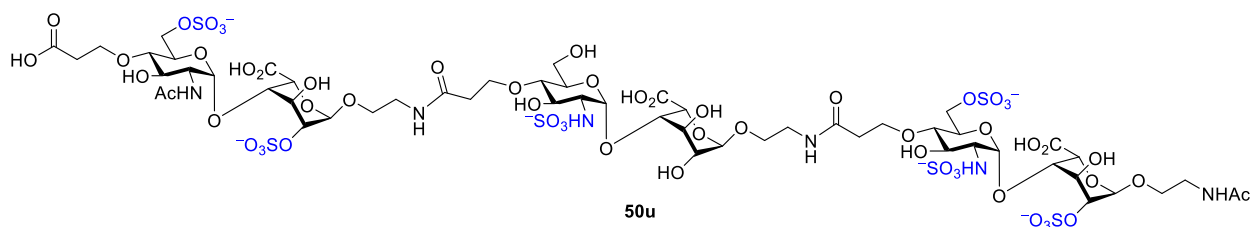
Acetamidoethyl ***O*-(2-acetamido-4-*O*-carboxyethyl-2-deoxy-6-*O*-sulfonato-1-thio- α -D-glucopyranoside)-(1 \rightarrow 4)-*O*-(6-*O*-carboxyl-2-*O*-sulfonato-1-thio- α -L-idopyranosiduronate)-(1 \rightarrow 4)-*O*-(2-deoxy-2-sulfoamino-6-*O*-sulfonato-1-thio- α -D-glucopyranoside)-(1 \rightarrow 4)-*O*-(6-*O*-carboxyl-2-*O*-sulfonato-1-thio- α -L-idopyranosiduronate)-(1 \rightarrow 4)-*O*-(2-deoxy-2-sulfoamino-1-thio- α -D-glucopyranoside)-(1 \rightarrow 4)-*O*-(6-*O*-carboxyl-1-thio- α -L-idopyranosiduronate) (50s).**

The starting material (8.2 mg, 0.005 mmol) was treated according to the general procedures of NH-Fmoc deprotection, pseudo-hexasaccharide preparation with HBTU and saponification of methyl esters to give compound **50s** (5.0 mg, 51% for 3 steps). ^1H NMR (500 MHz, D_2O) δ 5.19 (d, $J = 3.6$ Hz, 1H; A-1), 5.14 (d, $J = 3.7$ Hz, 1H; C-1), 4.98 (d, $J = 2.1$ Hz, 1H; E-1), 4.96 – 4.91 (m, 2H; B-1, D-1), 4.73 – 4.70 (m, 1H; F-1), 4.43 (d, $J = 2.0$ Hz, 2H), 4.37 (d, $J = 2.4$ Hz, 1H), 4.19 – 3.99 (m, 9H), 3.96 (t, $J = 3.9$ Hz, 2H), 3.92 – 3.44 (m, 29H), 3.35 – 3.16 (m, 10H), 3.12 – 3.02 (m, 3H), 2.50 – 2.33 (m, 6H), 1.89 (s, 3H), 1.81 (s, 3H). ^{13}C NMR (125 MHz, D_2O) δ 174.66, 174.16, 173.87, 100.63, 98.91, 98.56, 97.22, 95.62, 93.76, 78.01, 77.77, 77.61, 76.01, 75.29, 74.41, 73.18, 70.83, 70.79, 70.67, 70.56, 68.90, 68.81, 68.41, 68.24, 68.17, 68.09, 67.72, 67.48, 66.81, 66.73, 66.16, 66.13, 63.42, 59.74, 57.77, 57.72, 52.99, 39.05, 38.97, 38.87, 36.25, 36.18, 35.51, 22.09, 21.70. HRMS: m/z calc. for $\text{C}_{55}\text{H}_{84}\text{N}_6\text{O}_{57}\text{S}_6^{6-}$ $[\text{M}+2\text{Na}^+]^4$: 494.5500; found: 494.5519.



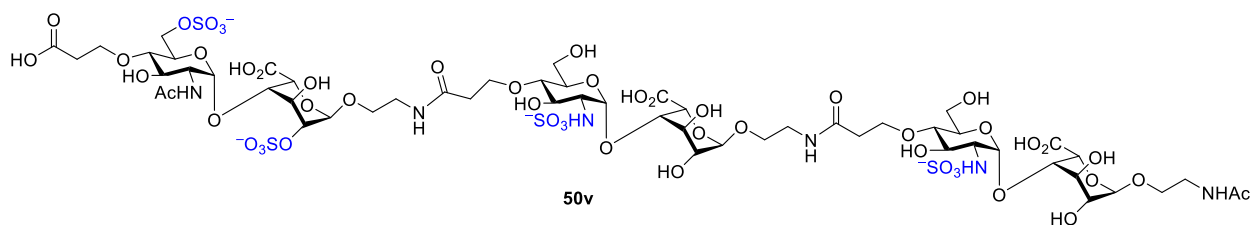
Acetamidoethyl ***O*-(2-acetamido-4-*O*-carboxyethyl-2-deoxy-6-*O*-sulfonato-1-thio- α -D-glucopyranoside)-(1 \rightarrow 4)-*O*-(6-*O*-carboxyl-2-*O*-sulfonato-1-thio- α -L-idopyranosiduronate)-(1 \rightarrow 4)-*O*-(2-deoxy-2-sulfoamino-6-*O*-sulfonato-1-thio- α -D-glucopyranoside)-(1 \rightarrow 4)-*O*-(6-*O*-carboxyl-2-*O*-sulfonato-1-thio- α -L-idopyranosiduronate)-(1 \rightarrow 4)-*O*-(2-acetamido-2-deoxy-6-*O*-sulfonato-1-thio- α -D-glucopyranoside)-(1 \rightarrow 4)-*O*-(6-*O*-carboxyl-2-*O*-sulfonato-1-thio- α -L-idopyranosiduronate) (50t).**

The starting material (7.1 mg, 0.004 mmol) was treated according to the general procedures of NH-Fmoc deprotection, pseudo-hexasaccharide preparation with HBTU and saponification of methyl esters to give compound **50t** (4.5 mg, 50% for 3 steps). ^1H NMR (500 MHz, D_2O) δ 5.17 (d, J = 3.5 Hz, 1H; A-1), 4.99 (s, 1H; C-1), 4.97 – 4.90 (m, 4H; B-1, D-1, E-1, F-1), 4.47 – 4.40 (m, 3H), 4.16 (dd, J = 11.1, 2.7 Hz, 1H), 4.13 – 3.99 (m, 10H), 3.95 – 3.42 (m, 24H), 3.35 – 3.18 (m, 9H), 3.09 (dd, J = 10.5, 3.5 Hz, 2H), 2.53 – 2.32 (m, 6H), 1.88 (s, 6H), 1.82 (s, 3H). ^{13}C NMR (125 MHz, D_2O) δ 199.58, 177.66, 174.62, 174.16, 173.84, 98.77, 98.68, 98.56, 97.48, 93.80, 93.57, 77.84, 77.75, 77.61, 76.04, 74.83, 73.63, 73.17, 70.85, 70.78, 70.46, 68.90, 68.84, 68.58, 68.44, 68.36, 67.74, 66.89, 66.83, 66.75, 66.26, 66.13, 63.79, 63.43, 57.78, 53.00, 39.00, 38.93, 36.24, 36.18, 35.43, 22.09, 21.70. HRMS: m/z calc. for $\text{C}_{57}\text{H}_{85}\text{N}_6\text{O}_{61}\text{S}_7^{7-}$ [$\text{M}+2\text{Na}^+$] $^{5-}$: 419.8320; found: 419.8333.



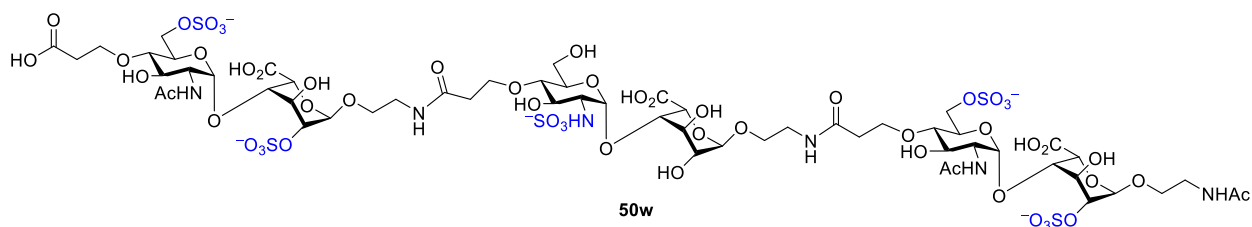
Acetamidoethyl ***O*-(2-acetamido-4-*O*-carboxyethyl-2-deoxy-6-*O*-sulfonato-1-thio- α -D-glucopyranoside)-(1 \rightarrow 4)-*O*-(6-*O*-carboxyl-2-*O*-sulfonato-1-thio- α -L-idopyranosiduronate)-(1 \rightarrow 4)-*O*-(2-deoxy-2-sulfoamino-1-thio- α -D-glucopyranoside)-(1 \rightarrow 4)-*O*-(6-*O*-carboxyl-thio- α -L-idopyranosiduronate)-(1 \rightarrow 4)-*O*-(2-deoxy-2-sulfoamino-6-*O*-sulfonato-1-thio- α -D-glucopyranoside)-(1 \rightarrow 4)-*O*-(6-*O*-carboxyl-2-*O*-sulfonato-1-thio- α -L-idopyranosiduronate) (50u).**

The starting material (6.8 mg, 0.005 mmol) was treated according to the general procedures of NH-Fmoc deprotection, pseudo-hexasaccharide preparation with HBTU and saponification of methyl esters to give compound **50u** (4.0 mg, 45% for 3 steps). ^1H NMR (500 MHz, D_2O) δ 5.21 (d, $J = 3.5$ Hz, 1H; A-1), 5.14 (d, $J = 3.7$ Hz, 1H; C-1), 4.96 – 4.91 (m, 3H; E-1, B-1, D-1), 4.75 – 4.71 (m, 1H; F-1), 4.39 (dd, $J = 13.1, 2.4$ Hz, 3H), 4.20 – 3.99 (m, 9H), 3.96 (t, $J = 3.8$ Hz, 1H), 3.93 – 3.73 (m, 13H), 3.70 – 3.43 (m, 15H), 3.39 – 3.16 (m, 11H), 3.06 (m, 3H), 2.49 – 2.33 (m, 6H), 1.89 (s, 3H), 1.82 (s, 3H). ^{13}C NMR (125 MHz, D_2O) δ 174.64, 173.89, 99.03, 98.60, 96.80, 95.65, 93.68, 78.02, 77.74, 77.66, 75.95, 74.31, 73.36, 70.84, 70.57, 68.86, 68.72, 68.57, 68.41, 68.19, 66.89, 66.74, 66.48, 66.15, 63.58, 59.74, 57.78, 57.74, 52.97, 39.05, 36.35, 35.78, 22.09, 21.69. HRMS: m/z calc. for $\text{C}_{55}\text{H}_{84}\text{N}_6\text{O}_{57}\text{S}_{66}^-$ $[\text{M}+\text{Na}^+]^5^-$: 391.0422; found: 391.0437.



Acetamidoethyl ***O*-(2-acetamido-4-*O*-carboxyethyl-2-deoxy-6-*O*-sulfonato-1-thio- α -D-glucopyranoside)-(1 \rightarrow 4)-*O*-(6-*O*-carboxyl-2-*O*-sulfonato-1-thio- α -L-idopyranosiduronate)-(1 \rightarrow 4)-*O*-(2-deoxy-2-sulfoamino-1-thio- α -D-glucopyranoside)-(1 \rightarrow 4)-*O*-(6-*O*-carboxyl-thio- α -L-idopyranosiduronate)-(1 \rightarrow 4)-*O*-(2-deoxy-2-sulfoamino-1-thio- α -D-glucopyranoside)-(1 \rightarrow 4)-*O*-(6-*O*-carboxyl-1-thio- α -L-idopyranosiduronate) (50v).**

The starting material (7.3 mg, 0.005 mmol) was treated according to the general procedures of NH-Fmoc deprotection, pseudo-hexasaccharide preparation with HBTU and saponification of methyl esters to give compound **50v** (4.1 mg, 46% for 3 steps). ^1H NMR (500 MHz, D_2O) δ 5.14 (s, 2H; A-1, C-1), 4.93 (s, 2H; B-1, E-1), 4.75 – 4.70 (m, 2H; D-1, F-1), 4.43 – 4.30 (m, 4H), 4.20 – 4.02 (m, 5H), 3.95 (q, $J = 4.1$ Hz, 2H), 3.91 – 3.71 (m, 12H), 3.69 – 3.42 (m, 18H), 3.33 – 3.13 (m, 10H), 3.04 (dd, $J = 10.5, 3.7$ Hz, 3H), 2.48 – 2.30 (m, 6H), 1.88 (s, 3H), 1.81 (s, 3H). ^{13}C NMR (125 MHz, D_2O) δ 174.63, 173.93, 100.60, 98.60, 95.63, 95.58, 93.67, 78.00, 77.94, 77.65, 74.42, 74.33, 73.36, 70.79, 70.69, 70.50, 68.86, 68.54, 68.23, 68.10, 67.52, 66.69, 66.51, 66.14, 63.57, 59.74, 57.77, 57.74, 52.96, 39.05, 38.95, 36.25, 36.17, 22.08, 21.70. HRMS: m/z calc. for $\text{C}_{55}\text{H}_{86}\text{N}_6\text{O}_{51}\text{S}_4^4-$ $[\text{M}]^{4-}$: 443.5806; found: 443.5793.

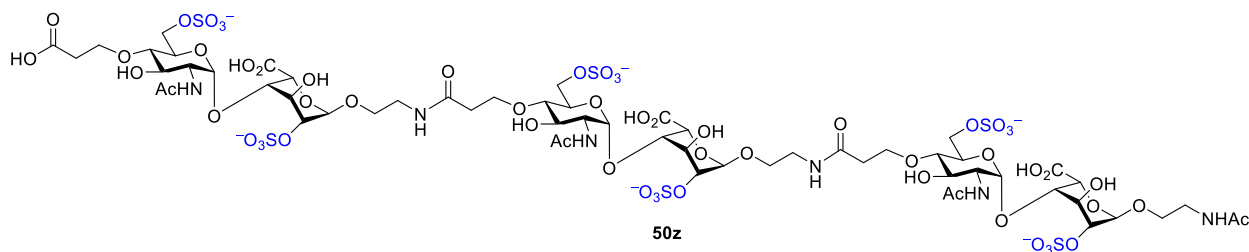


Acetamidoethyl ***O*-(2-acetamido-4-*O*-carboxyethyl-2-deoxy-6-*O*-sulfonato-1-thio- α -D-glucopyranoside)-(1 \rightarrow 4)-*O*-(6-*O*-carboxyl-2-*O*-sulfonato-1-thio- α -L-idopyranosiduronate)-(1 \rightarrow 4)-*O*-(2-deoxy-2-sulfoamino-1-thio- α -D-glucopyranoside)-(1 \rightarrow 4)-*O*-(6-*O*-carboxyl-thio- α -L-idopyranosiduronate)-(1 \rightarrow 4)-*O*-(2-acetamido-2-deoxy-6-*O*-sulfonato-1-thio- α -D-glucopyranoside)-(1 \rightarrow 4)-*O*-(6-*O*-carboxyl-2-*O*-sulfonato-1-thio- α -L-idopyranosiduronate) (**50w**).**

The starting material (7.0 mg, 0.005 mmol) was treated according to the general procedures of NH-Fmoc deprotection, pseudo-hexasaccharide preparation with HBTU and saponification of methyl esters to give compound **50w** (4.5 mg, 50% for 3 steps). ^1H NMR (500 MHz, D_2O) δ 5.14 (d, $J = 3.7$ Hz, 1H; A-1), 4.95 – 4.90 (m, 4H; B-1, C-1, D-1, E-1), 4.75 – 4.71 (m, 1H; F-1), 4.42 – 4.35 (m, 3H), 4.18 – 4.01 (m, 8H), 3.96 (t, $J = 3.7$ Hz, 1H), 3.92 – 3.73 (m, 13H), 3.70 – 3.44 (m, 14H), 3.37 – 3.16 (m, 10H), 3.04 (dd, $J = 10.4, 3.6$ Hz, 1H), 2.51 – 2.30 (m, 6H), 1.88 (s, 6H), 1.82 (s, 3H). ^{13}C NMR (125 MHz, D_2O) δ 174.63, 173.87, 100.56, 98.65, 98.60, 95.66, 93.68, 93.56, 78.00, 77.75, 77.65, 74.32, 73.61, 73.35, 70.84, 70.80, 70.72, 70.58, 68.85, 68.51, 68.16, 66.86, 66.74, 66.49, 66.14, 63.78, 63.57, 59.73, 57.74, 53.04, 52.97, 39.00, 36.29, 36.16, 35.67, 22.07, 21.70. HRMS: m/z calc. for $\text{C}_{57}\text{H}_{87}\text{N}_6\text{O}_{55}\text{S}_5^{5-}$ $[\text{M}]^{5-}$: 379.0565; found: 379.0584.

Acetamidoethyl *O*-(2-acetamido-4-*O*-carboxyethyl-2-deoxy-6-*O*-sulfonato-1-thio- α -D-glucopyranoside)-(1 \rightarrow 4)-*O*-(6-*O*-carboxyl-2-*O*-sulfonato-1-thio- α -L-idopyranosiduronate)-(1 \rightarrow 4)-*O*-(2-acetamido-2-deoxy-6-*O*-sulfonato-1-thio- α -D-glucopyranoside)-(1 \rightarrow 4)-*O*-(6-*O*-carboxyl-2-*O*-sulfonato-thio- α -L-idopyranosiduronate)-(1 \rightarrow 4)-*O*-(2-deoxy-2-sulfoamino-1-thio- α -D-glucopyranoside)-(1 \rightarrow 4)-*O*-(6-*O*-carboxyl-1-thio- α -L-idopyranosiduronate) (**50y**).

The starting material (6.7 mg, 0.004 mmol) was treated according to the general procedures of NH-Fmoc deprotection, pseudo-hexasaccharide preparation with HBTU and saponification of methyl esters to give compound **50y** (4.4 mg, 55% for 3 steps). ^1H NMR (500 MHz, D_2O) δ 5.13 (d, $J = 3.8$ Hz, 1H; A-1), 4.92 (s, 3H; B-1, C-1, E-1), 4.73 – 4.69 (m, 1H; D-1), 4.46 – 4.32 (m, 3H), 4.17 – 3.99 (m, 7H), 3.94 (t, $J = 3.9$ Hz, 1H), 3.91 – 3.70 (m, 11H), 3.69 – 3.43 (m, 11H), 3.34 – 3.14 (m, 8H), 3.03 (dd, $J = 10.5, 3.6$ Hz, 1H), 2.50 – 2.31 (m, 6H), 1.87 (s, 4H), 1.80 (s, 3H). ^{13}C NMR (125 MHz, D_2O) δ 174.64, 173.91, 100.61, 98.63, 98.55, 95.61, 93.74, 93.65, 77.96, 77.78, 77.59, 74.38, 73.37, 73.20, 70.81, 70.66, 70.54, 68.89, 68.33, 68.20, 67.45, 66.73, 66.11, 63.53, 63.42, 59.71, 57.71, 52.98, 39.03, 38.92, 36.19, 35.39, 22.07, 21.68. HRMS: m/z calc. for $\text{C}_{57}\text{H}_{87}\text{N}_6\text{O}_{55}\text{S}_5^{5-}$ $[\text{M}]^{5-}$: 379.0565; found: 379.0574.



Acetamidoethyl *O*-(2-acetamido-4-*O*-carboxyethyl-2-deoxy-6-*O*-sulfonato-1-thio- α -D-glucopyranoside)-(1 \rightarrow 4)-*O*-(6-*O*-carboxyl-2-*O*-sulfonato-1-thio- α -L-idopyranosiduronate)-

(1→4)-O-(2-acetamido-2-deoxy-6-O-sulfonato-1-thio- α -D-glucopyranoside)-(1→4)-O-(6-O-carboxyl-2-O-sulfonato-thio- α -L-idopyranosiduronate)-(1→4)-O-(2-acetamido-2-deoxy-6-O-sulfonato-1-thio- α -D-glucopyranoside)-(1→4)-O-(6-O-carboxyl-2-O-sulfonato-1-thio- α -L-idopyranosiduronate) (50z**).**

The starting material (8.0 mg, 0.005 mmol) was treated according to the general procedures of NH-Fmoc deprotection, pseudo-hexasaccharide preparation with HBTU and saponification of methyl esters to give compound **50z** (4.5 mg, 44% for 3 steps). ^1H NMR (500 MHz, D_2O) δ 4.98 – 4.90 (m, 6H; A-1, B-1, C-1, D-1, E-1, F-1), 4.42 – 4.35 (m, 3H), 4.17 – 4.01 (m, 12H), 3.93 – 3.74 (m, 15H), 3.70 – 3.45 (m, 11H), 3.36 – 3.21 (m, 10H), 2.44 – 2.31 (m, 6H), 1.89 (s, 8H), 1.83 (s, 3H). ^{13}C NMR (125 MHz, D_2O) δ 174.67, 170.33, 109.99, 98.68, 98.57, 93.63, 77.86, 73.74, 73.35, 70.86, 69.21, 68.87, 68.67, 66.87, 66.65, 66.28, 63.90, 63.55, 53.05, 52.91, 39.03, 38.89, 36.22, 22.12, 22.09, 21.72. HRMS: m/z calc. for $\text{C}_{59}\text{H}_{88}\text{N}_6\text{O}_{59}\text{S}_6^{6-}$ $[\text{M}]^{6-}$: 336.0405; found: 336.0412.

APPENDIX

Product Characterization Spectra

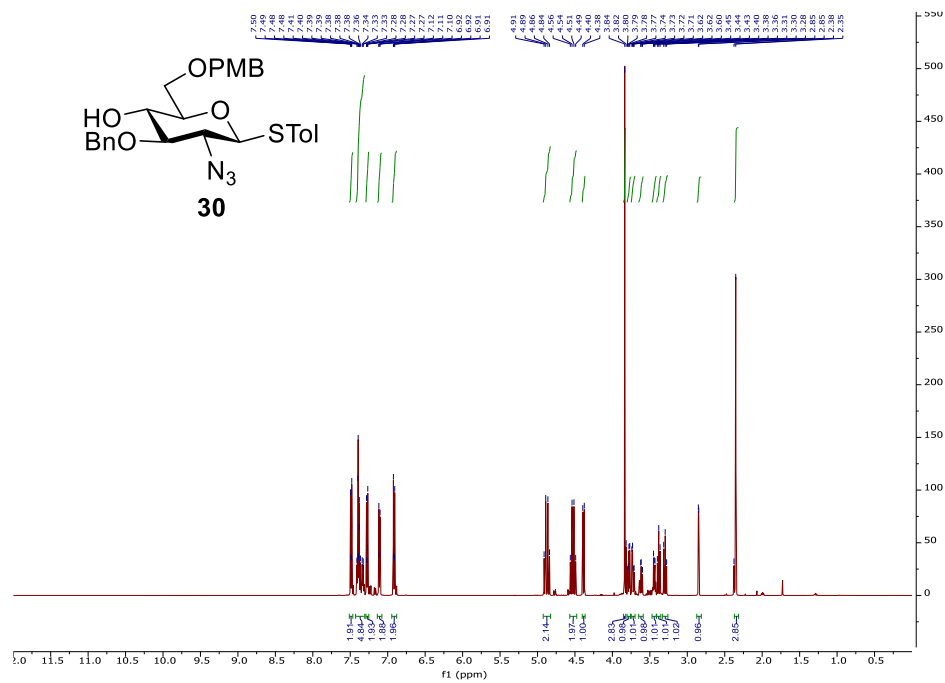
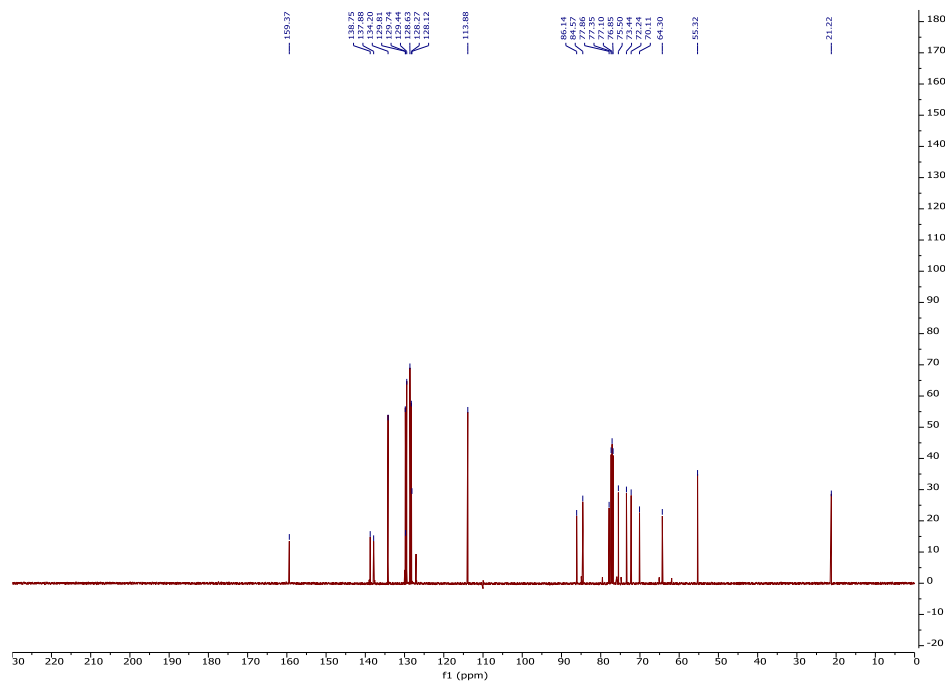


Figure 2.2. ¹H-NMR of **30** (500 MHz CDCl₃)



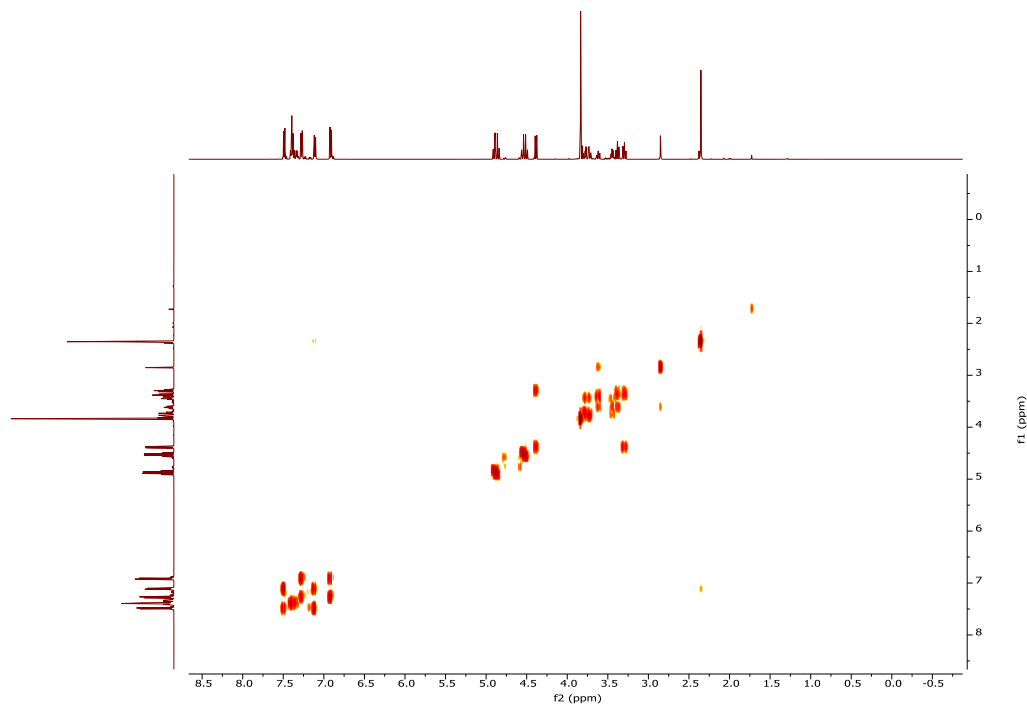


Figure 2.4. ^1H - ^1H gCOSY of **30** (500 MHz CDCl_3)

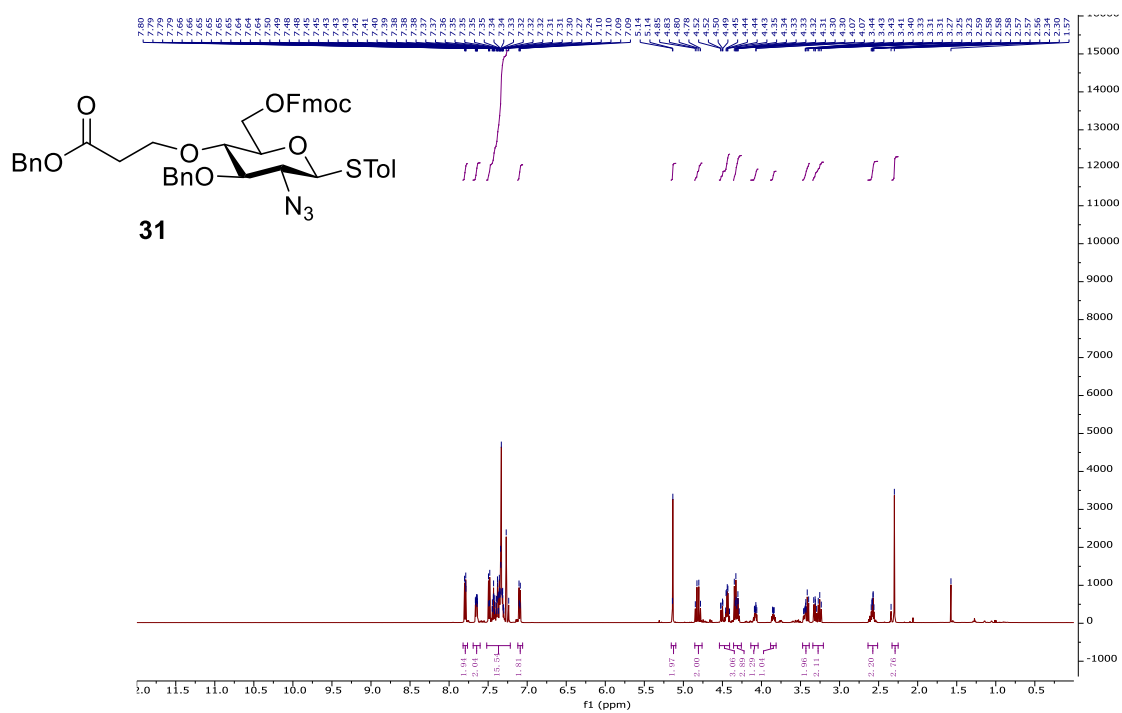


Figure 2.5. ^1H -NMR of **31** (500 MHz CDCl_3)

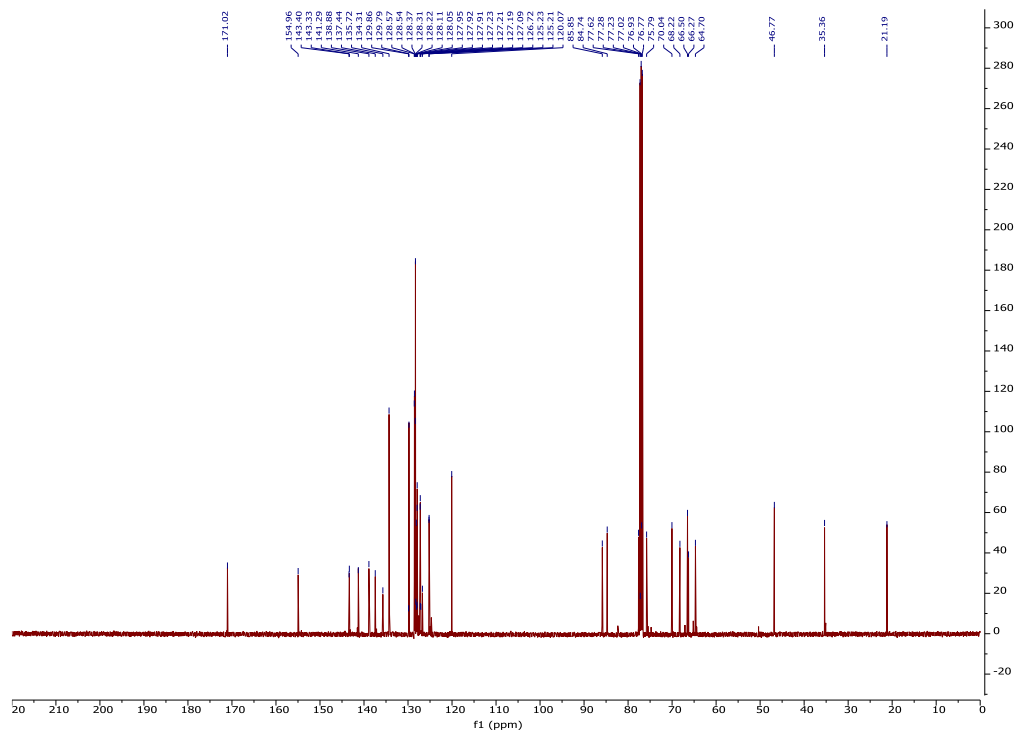


Figure 2.6. ^{13}C -NMR of **31** (125 MHz CDCl_3)

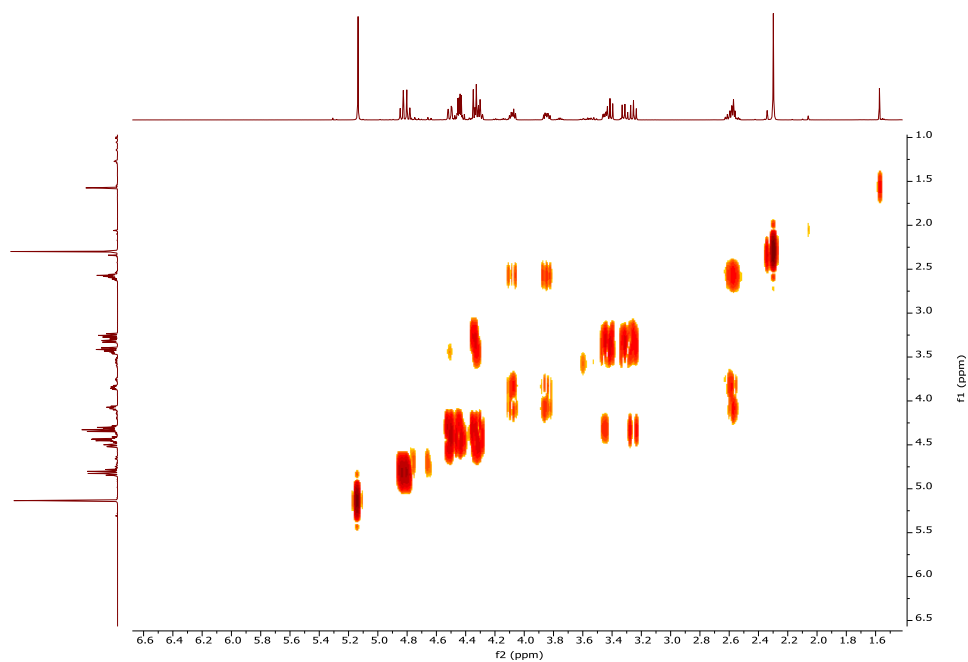
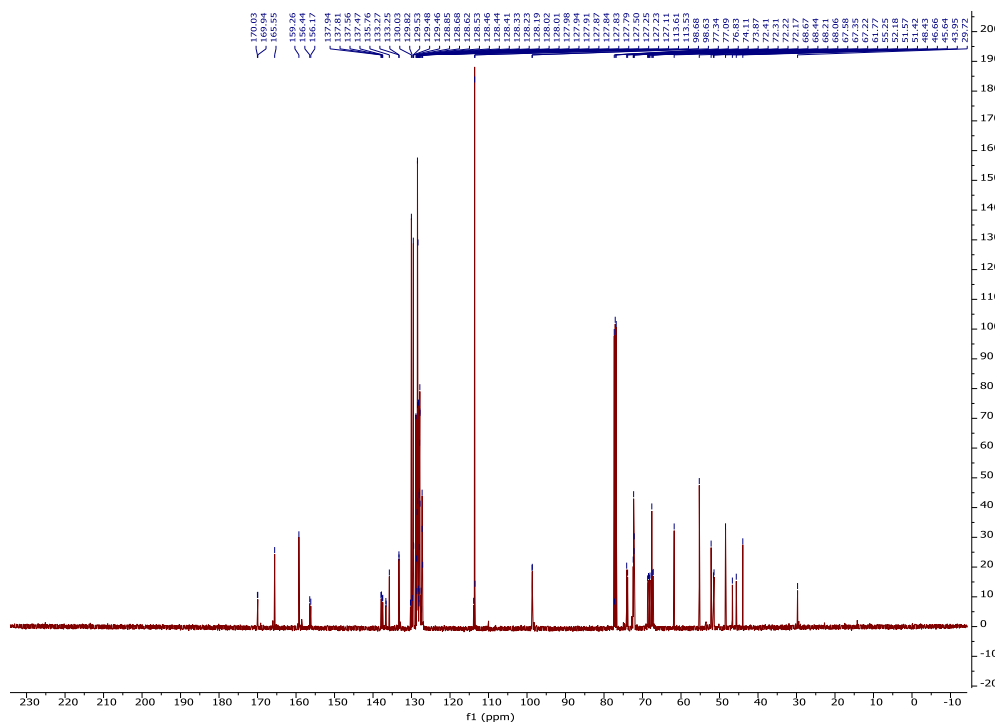
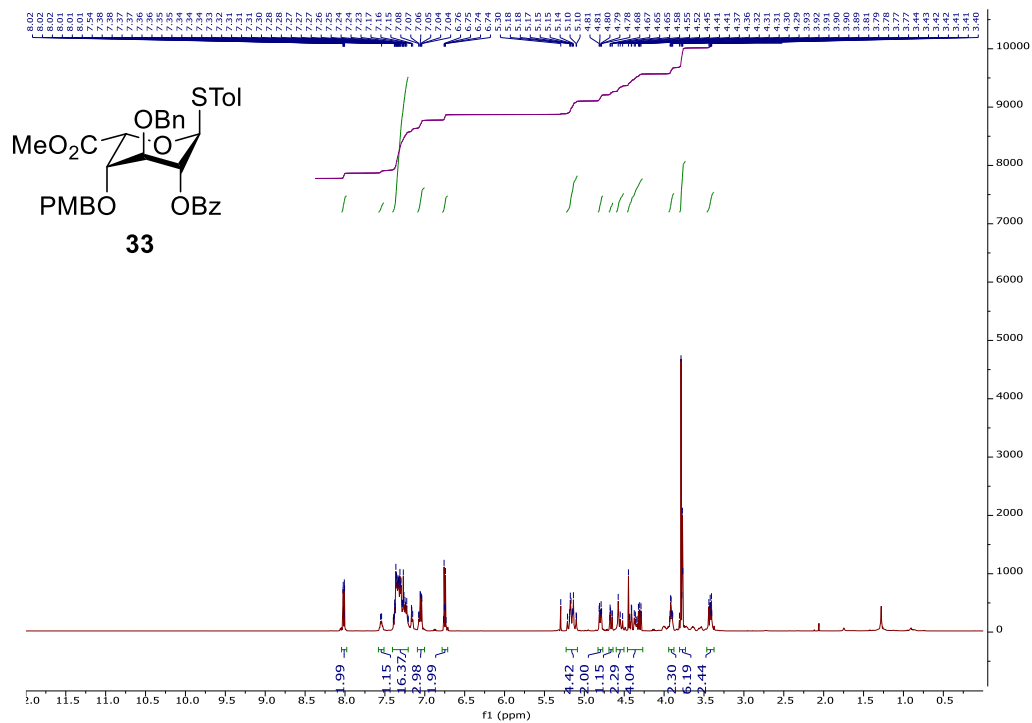


Figure 2.7. ^1H - ^1H gCOSY of **31** (500 MHz CDCl_3)



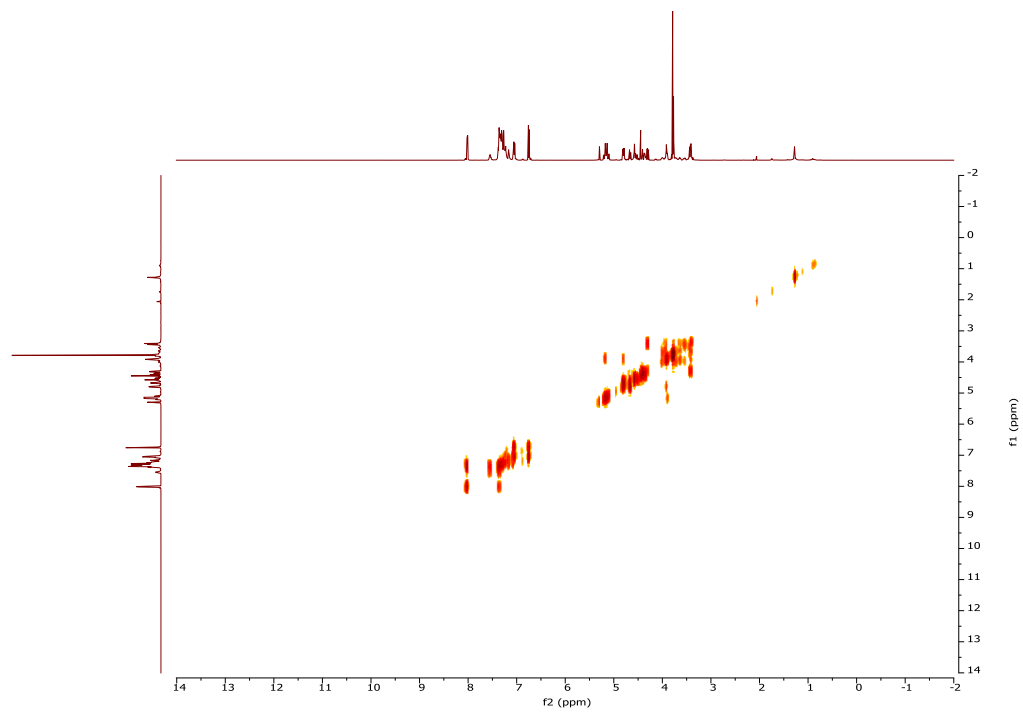


Figure 2.10. ^1H - ^1H gCOSY of **33** (500 MHz CDCl_3)

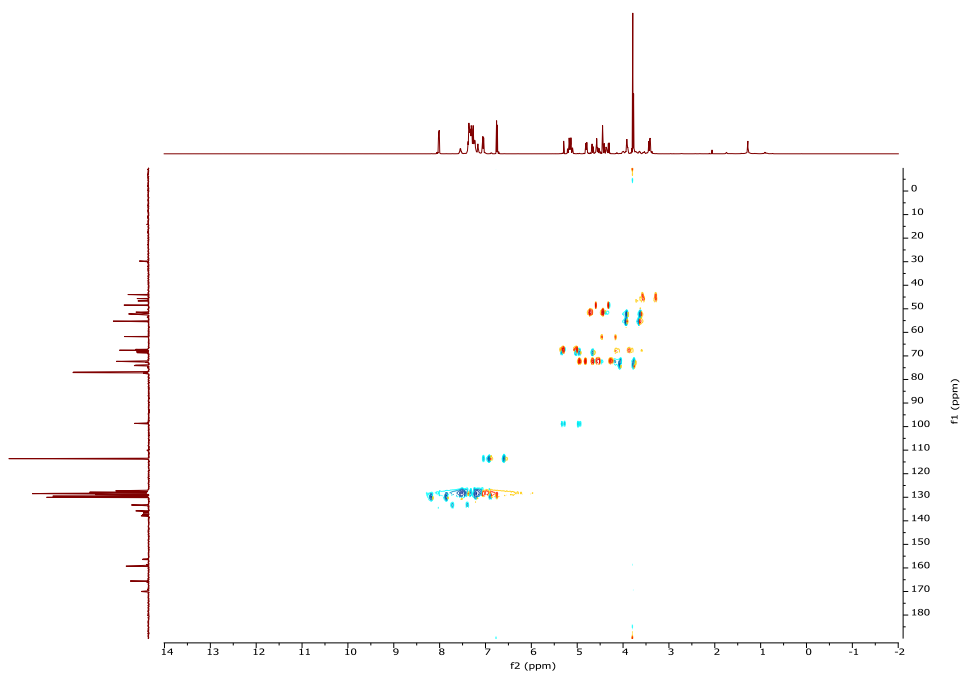
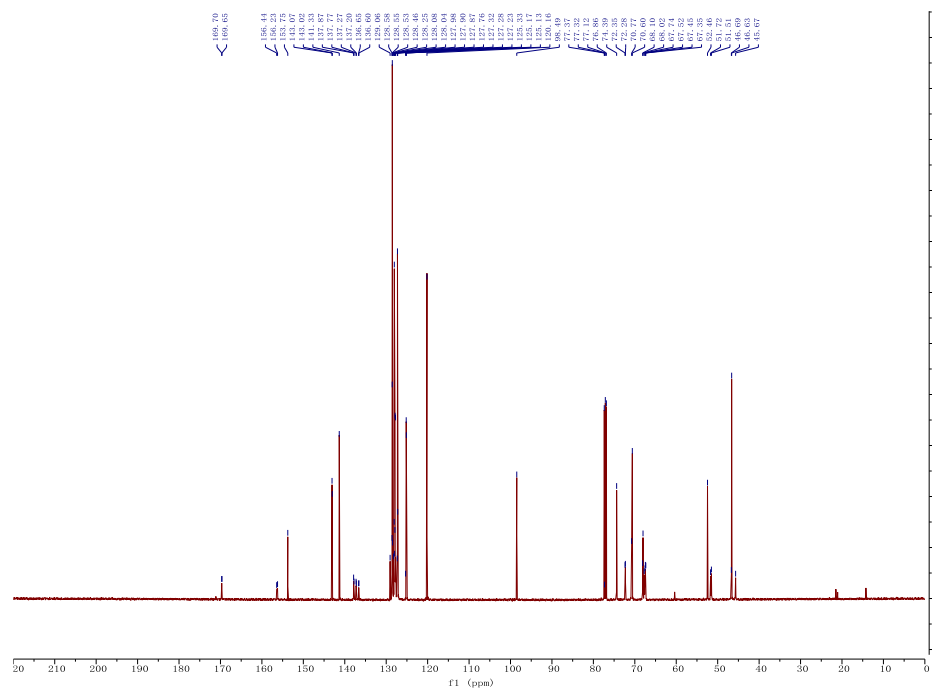
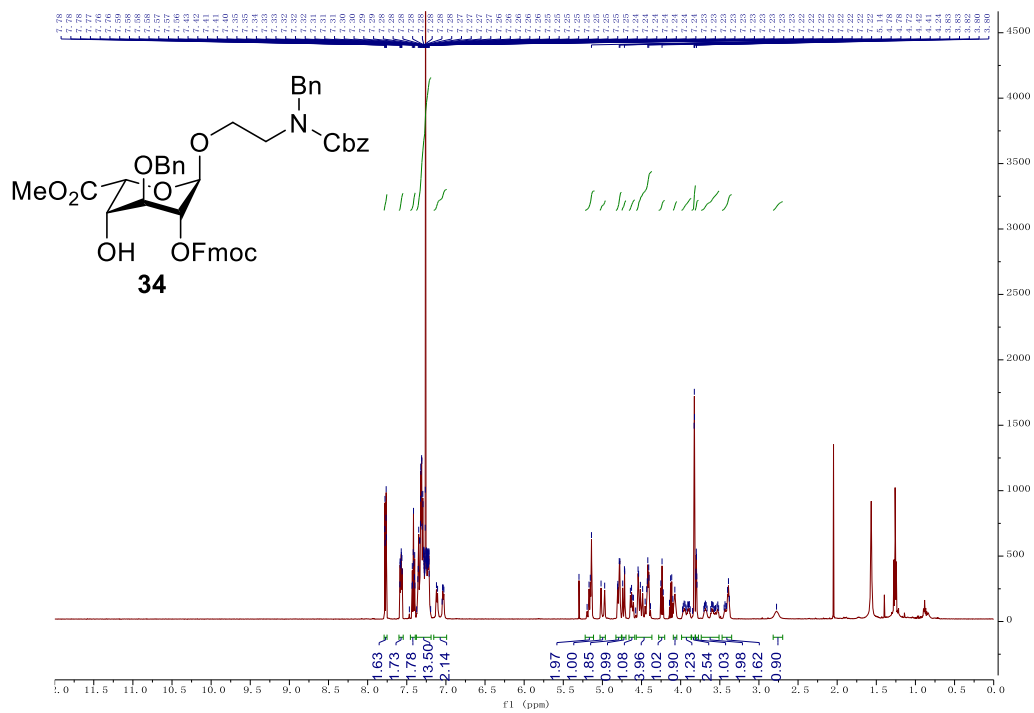


Figure 2.11. ^1H - ^{13}C gHSQCAD of **33** (500 MHz CDCl_3)



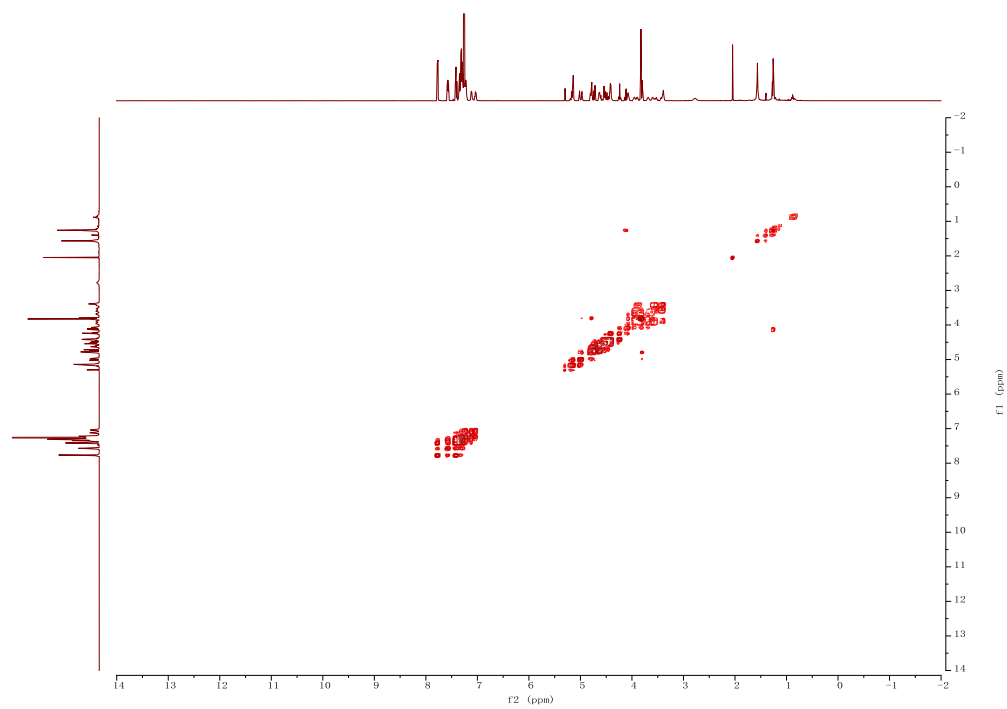


Figure 2.14. ^1H - ^1H gCOSY of **34** (500 MHz CDCl_3)

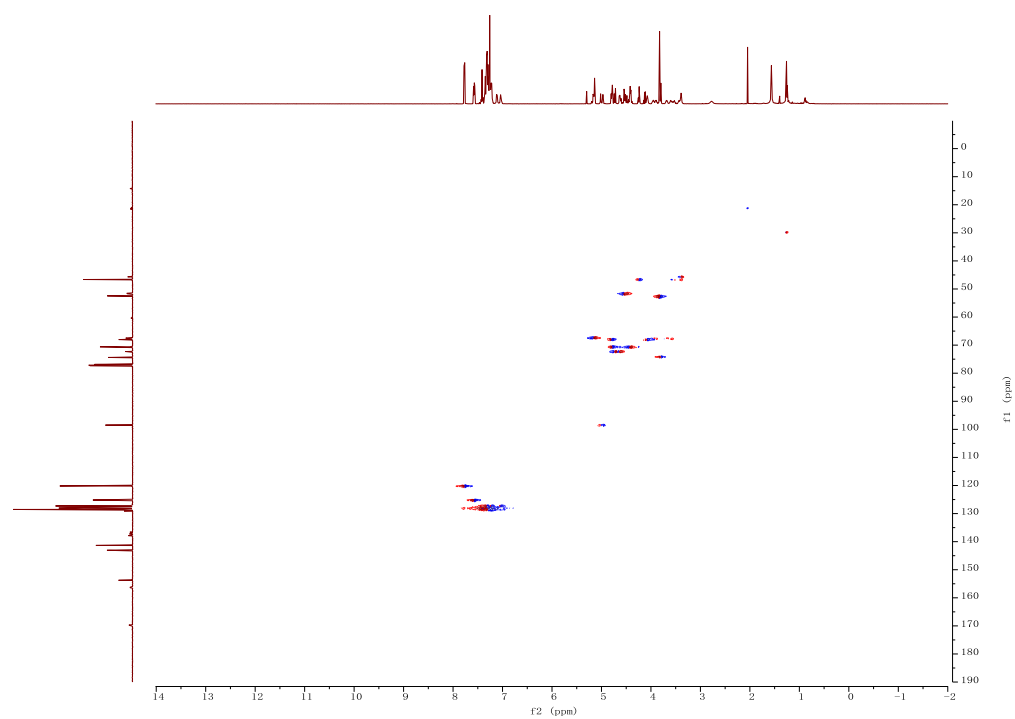


Figure 2.15. ^1H - ^{13}C gHSQCAD of **34** (500 MHz CDCl_3)

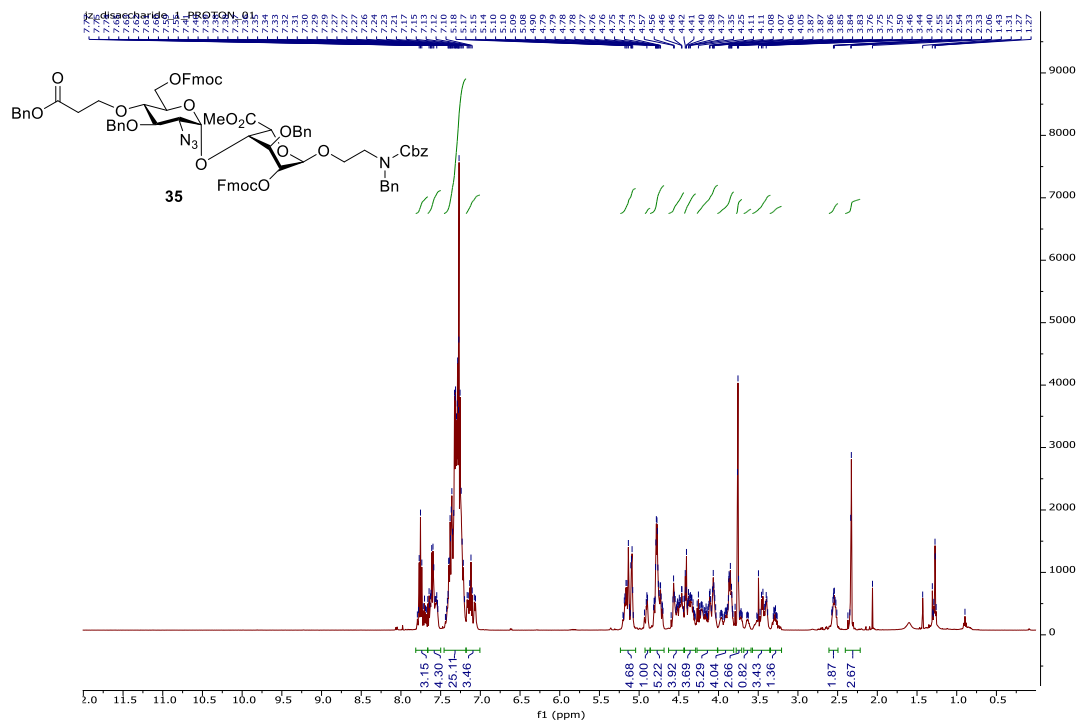


Figure 2.16. $^1\text{H-NMR}$ of **35** (500 MHz CDCl_3)

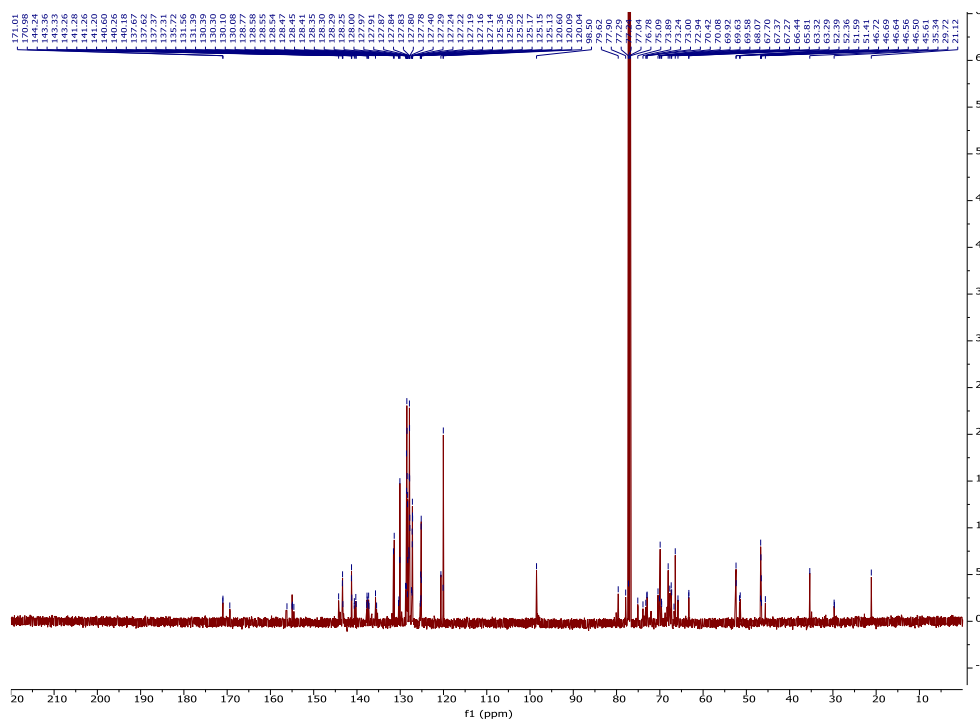


Figure 2.17. $^{13}\text{C-NMR}$ of **35** (125 MHz CDCl_3)

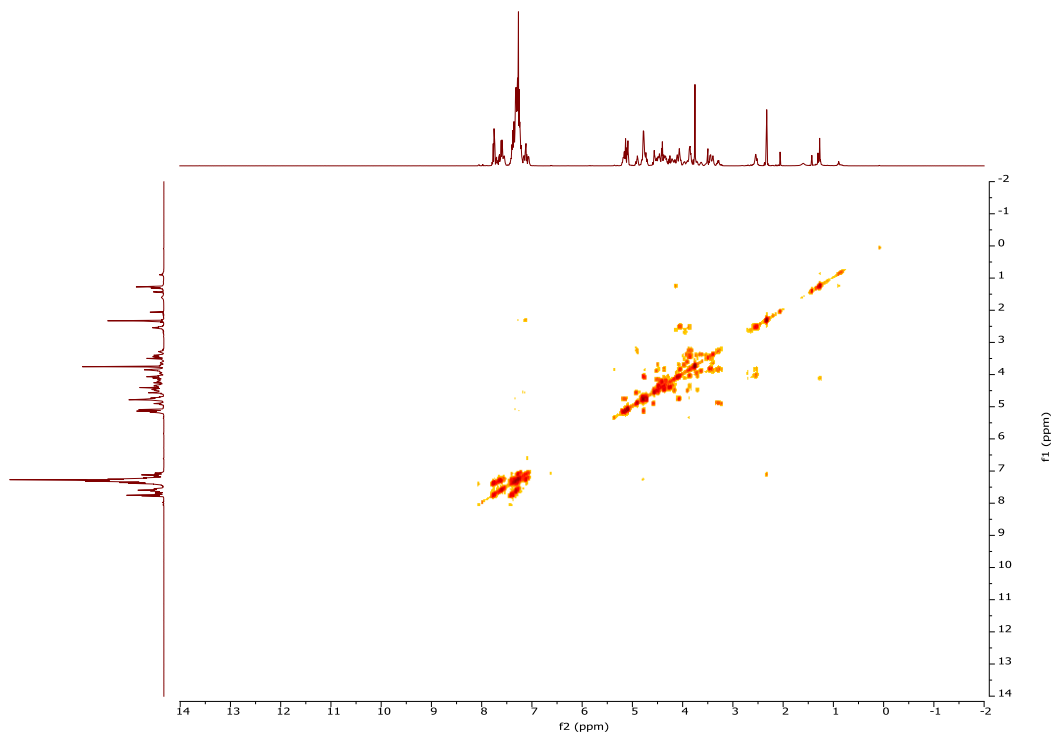


Figure 2.18. ^1H - ^1H gCOSY of **35** (500 MHz CDCl_3)

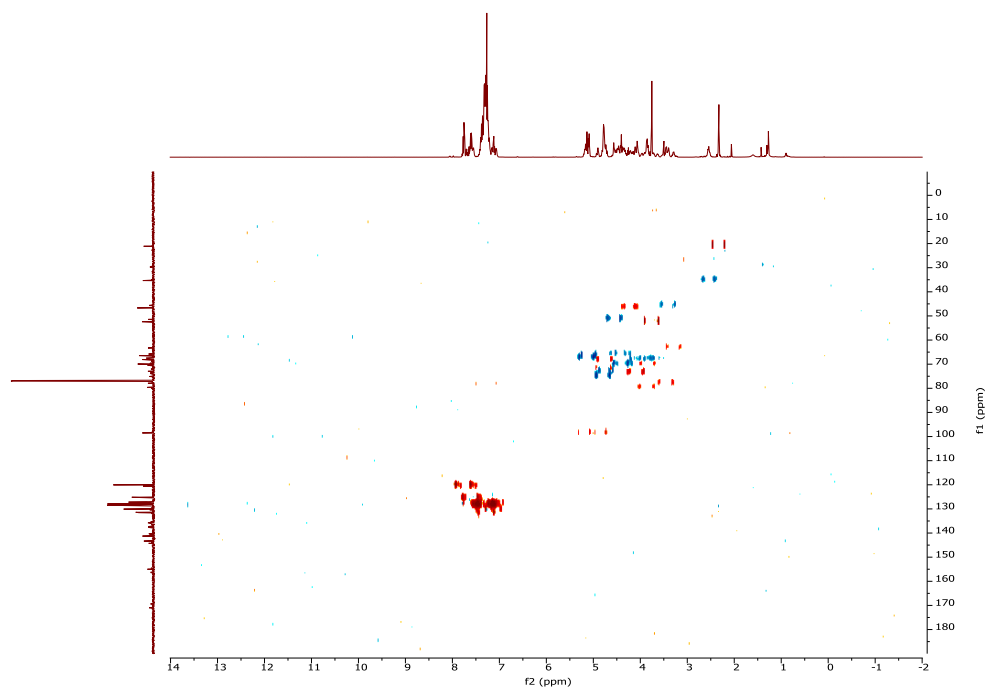


Figure 2.19. ^1H - ^{13}C gHSQCAD of **35** (500 MHz CDCl_3)

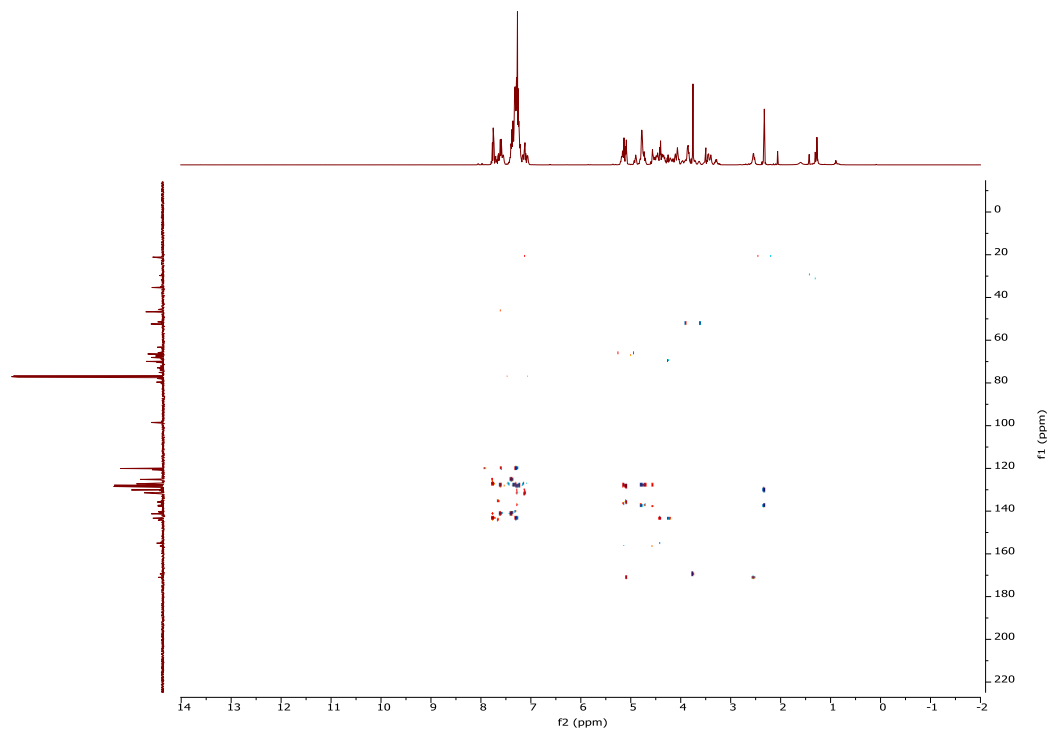


Figure 2.20. ^1H - ^{13}C gHMBCAD of **35** (500 MHz CDCl_3)

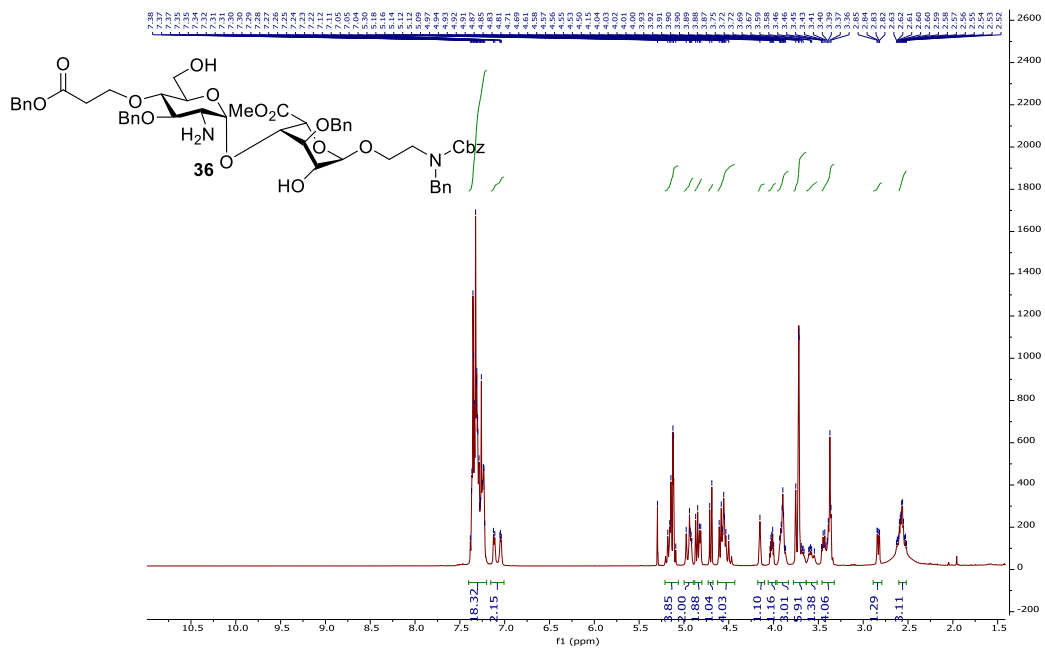


Figure 2.21. ^1H -NMR of **36** (500 MHz CDCl_3)

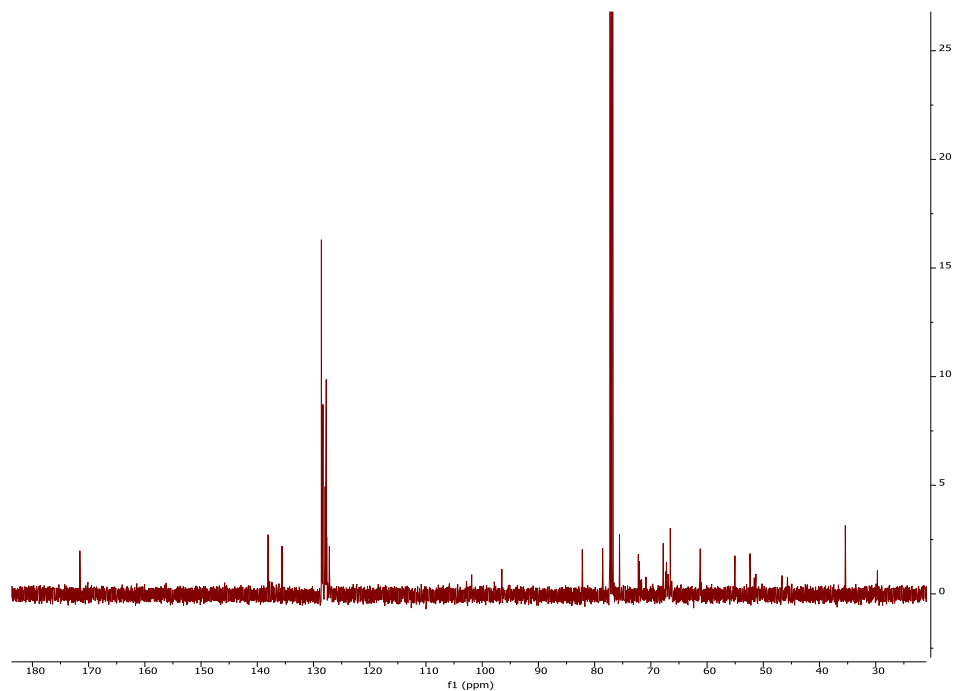


Figure 2.22. ^{13}C -NMR of **36** (125 MHz CDCl_3)

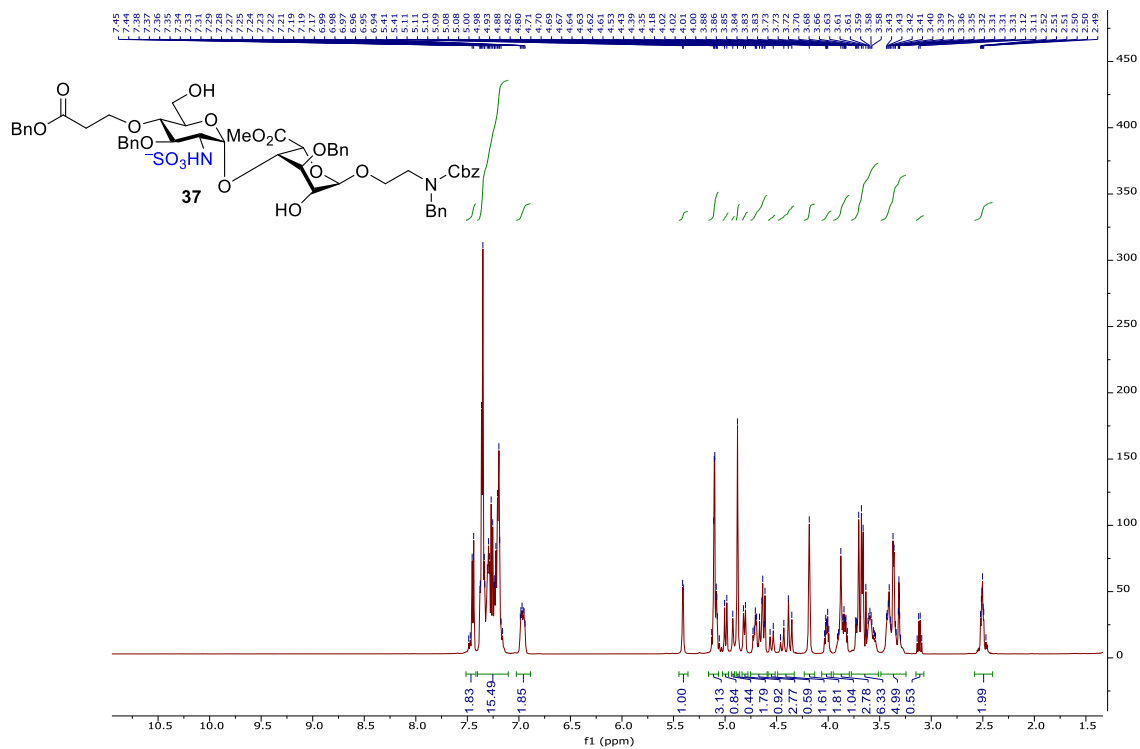


Figure 2.23. ^1H -NMR of **37** (500 MHz CD_3OD)

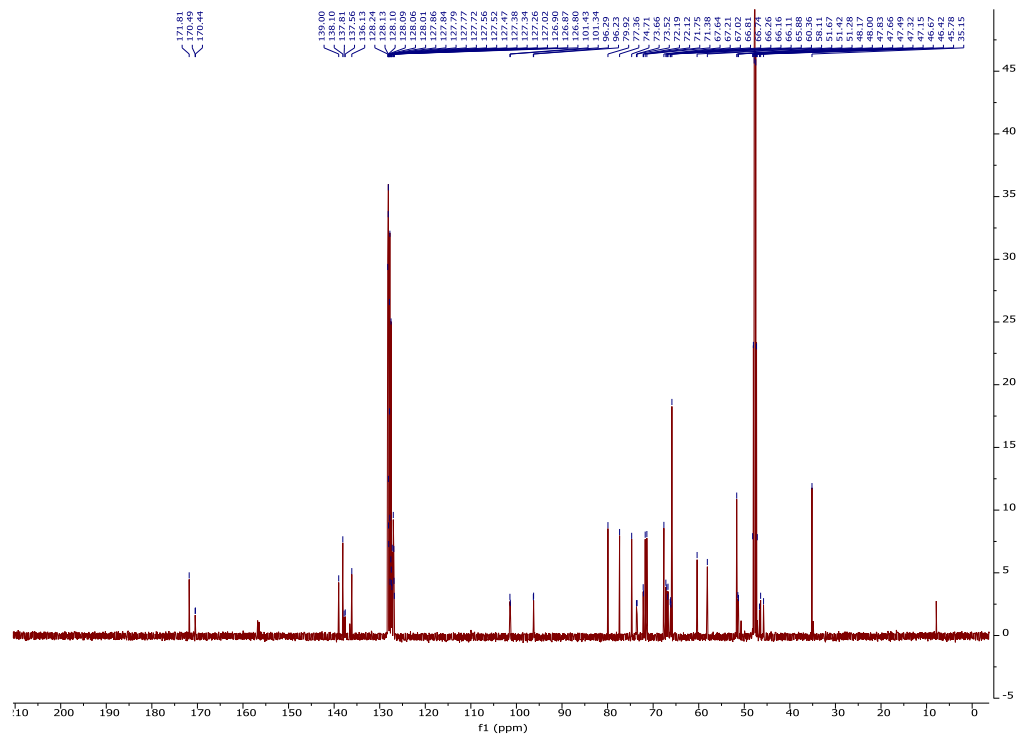


Figure 2.24. ^{13}C -NMR of **37** (125 MHz CD_3OD)

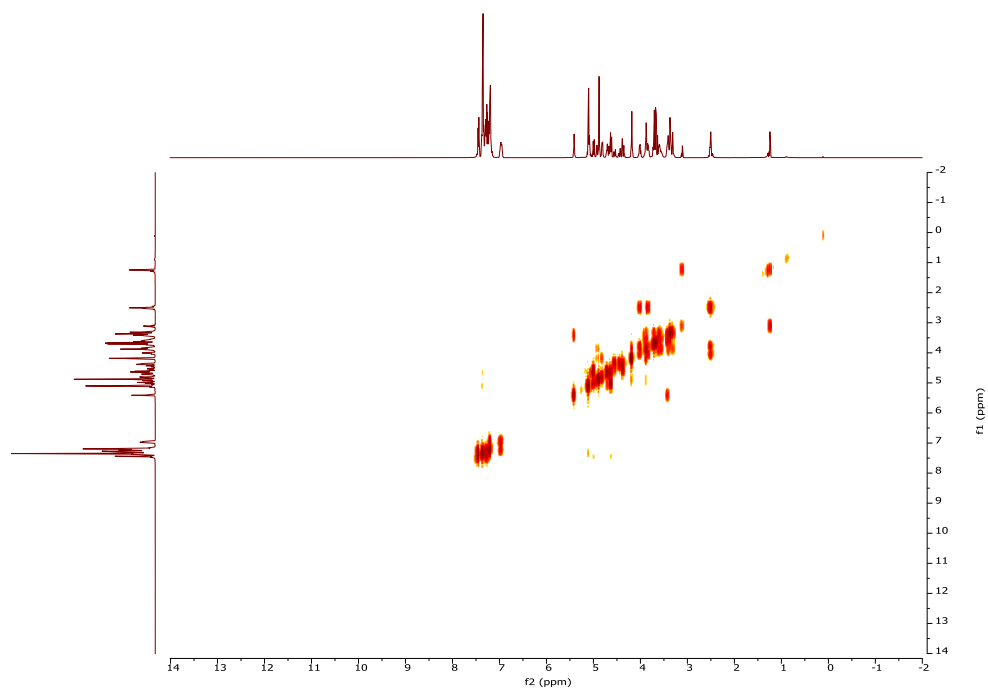


Figure 2.25. ^1H - ^1H gCOSY of **37** (500 MHz CD_3OD)

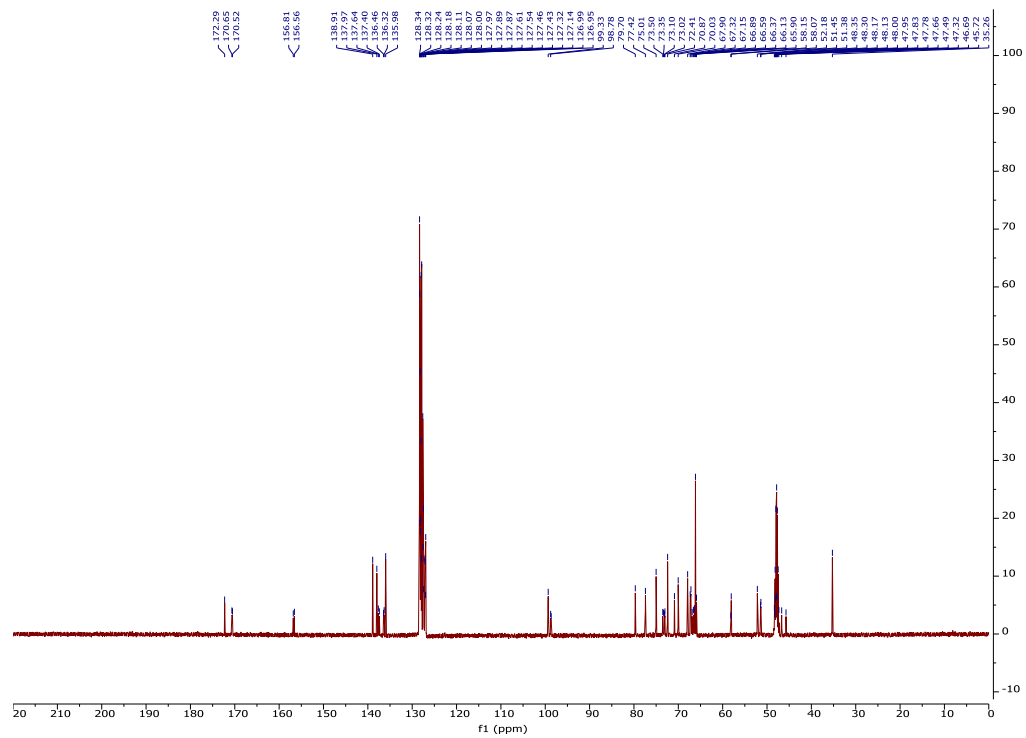


Figure 2.28. ^{13}C -NMR of **39** (125 MHz CD_3OD)

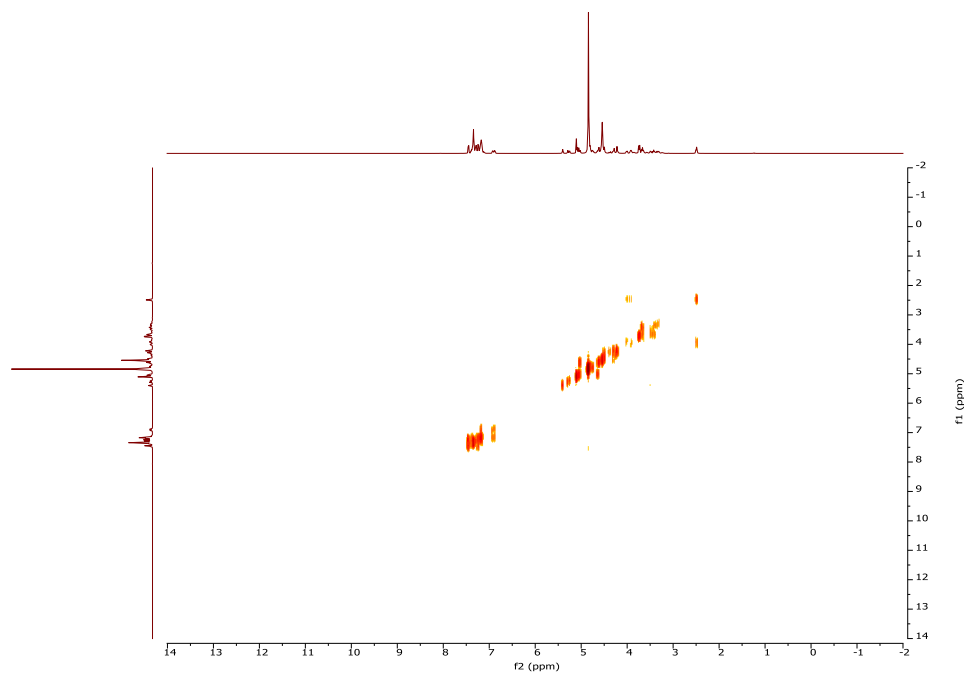


Figure 2.29. ^1H - ^1H gCOSY of **39** (500 MHz CD_3OD)

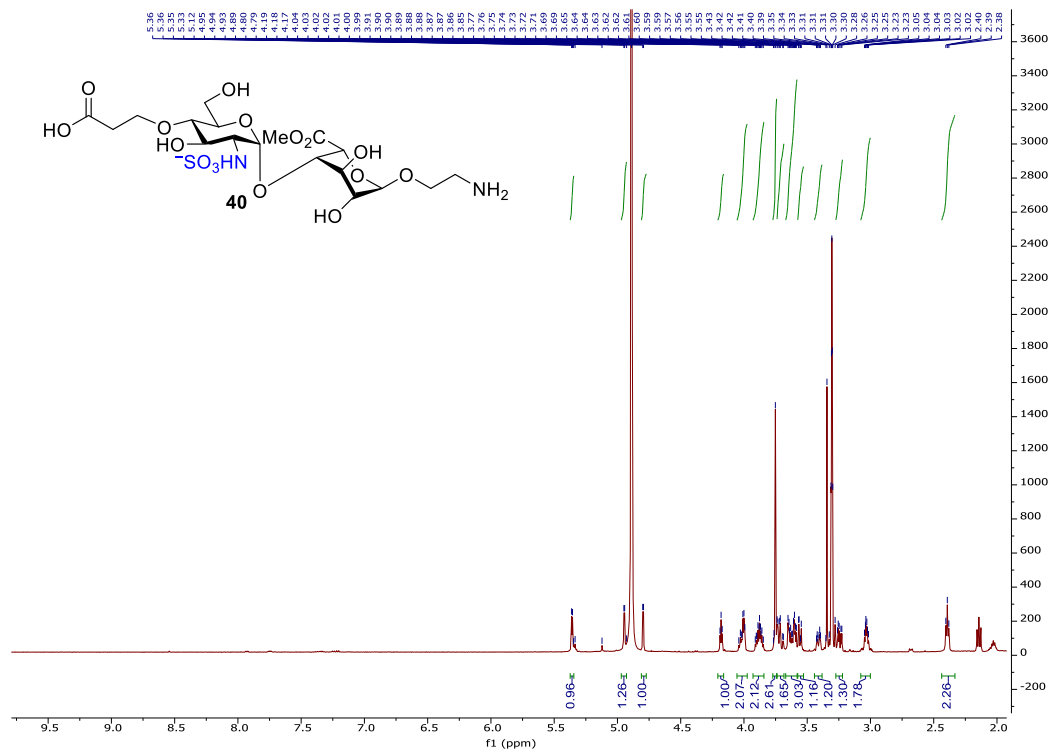


Figure 2.30. ¹H-NMR of **40** (500 MHz CD₃OD)

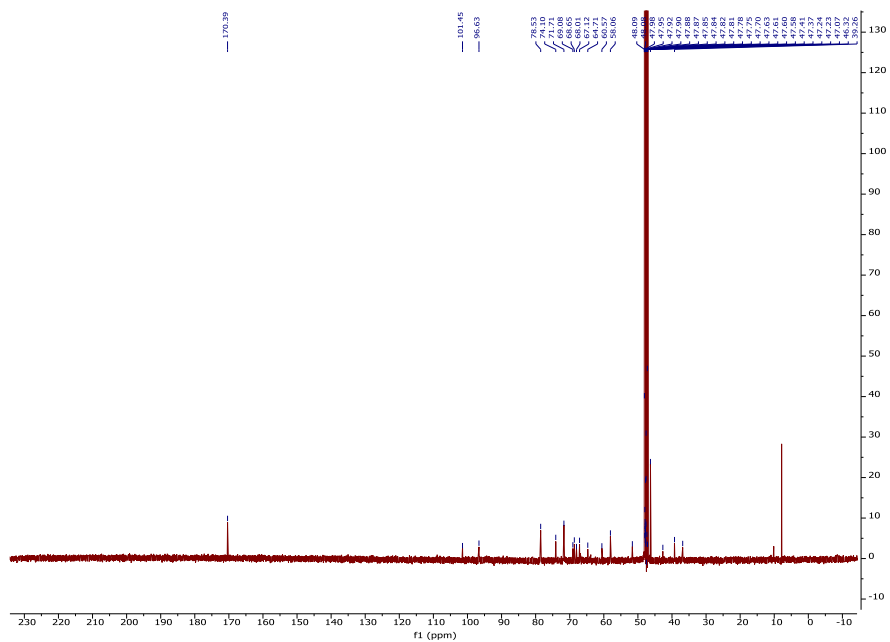


Figure 2.31. ¹³C-NMR of **40** (125 MHz CD₃OD)

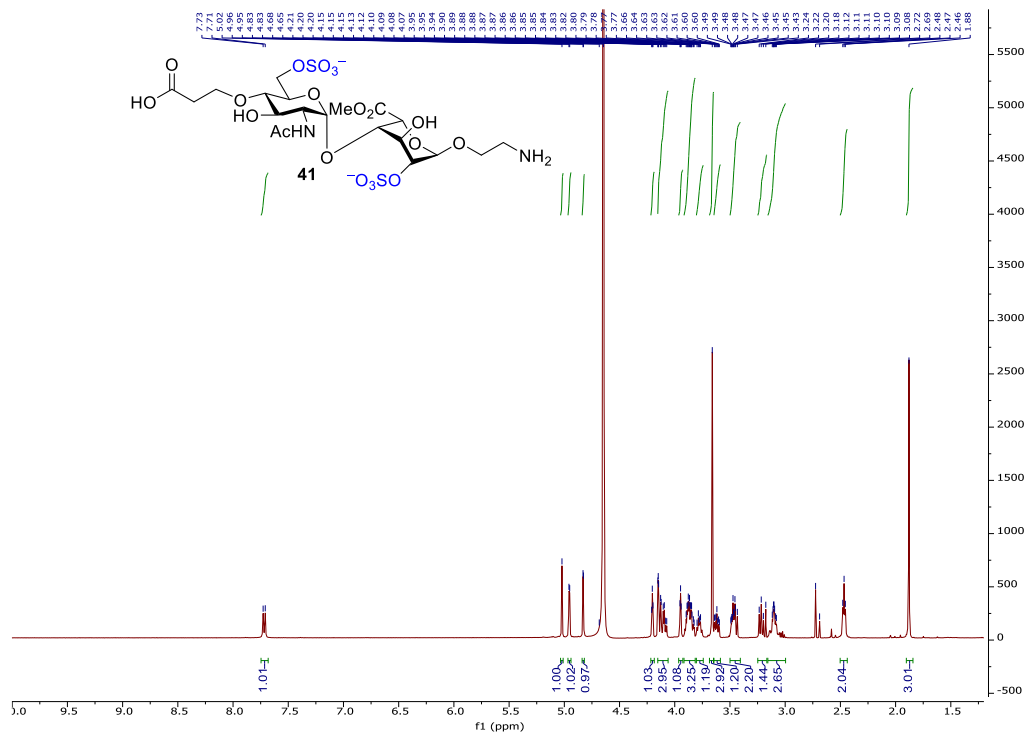


Figure 2.32. $^1\text{H-NMR}$ of **41** (500 MHz D_2O)

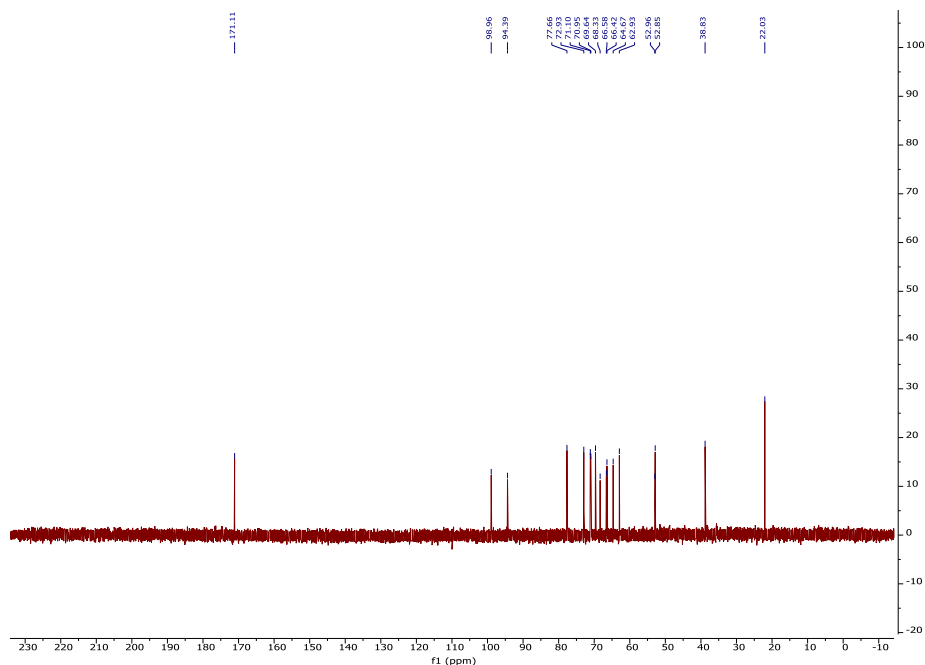


Figure 2.33. $^{13}\text{C-NMR}$ of **41** (125 MHz D_2O)

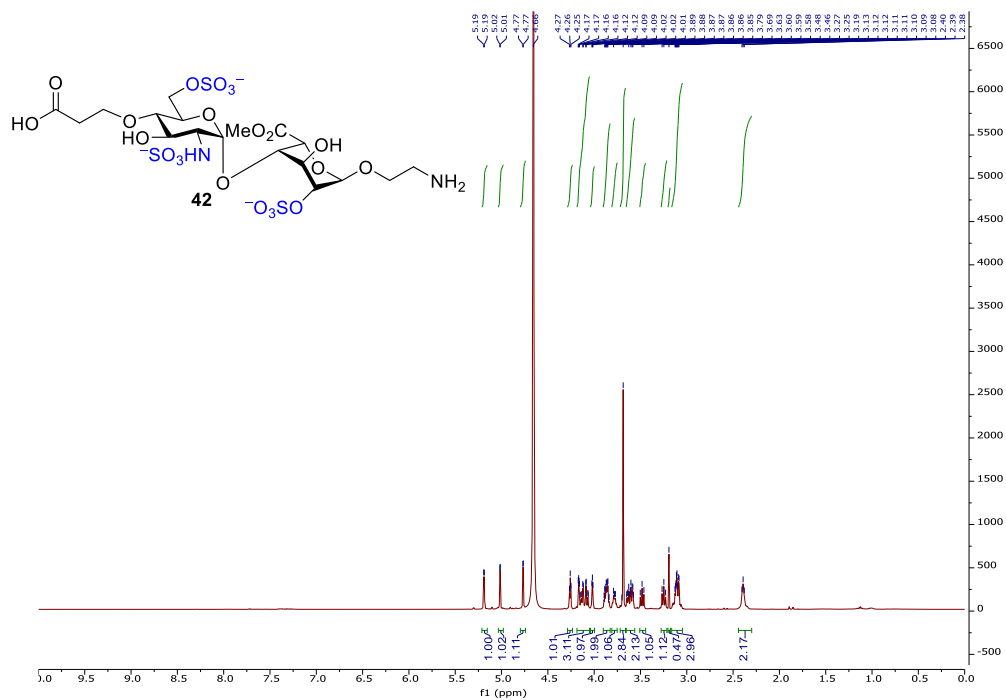


Figure 2.34. ¹H-NMR of 42 (500 MHz D₂O)

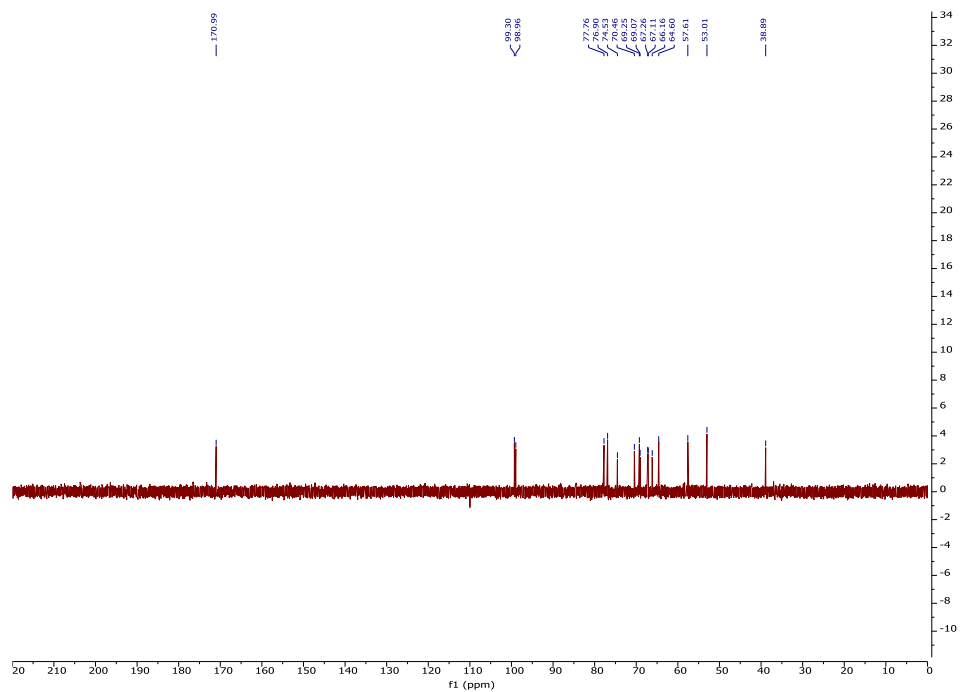


Figure 2.35. ¹³C-NMR of 42 (125 MHz D₂O)

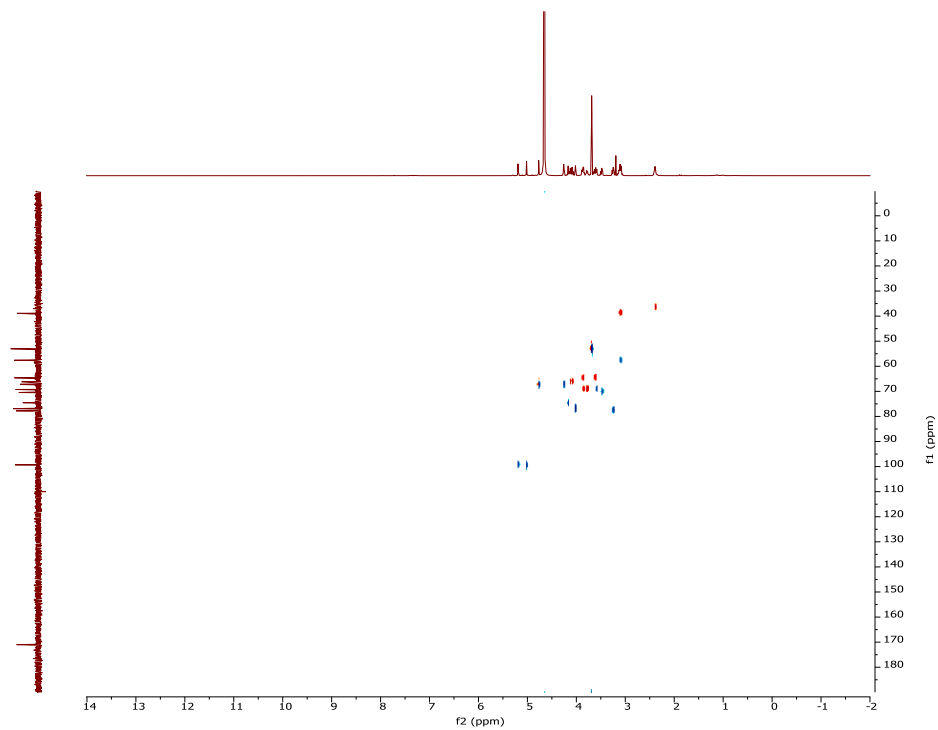


Figure 2.36. ^1H - ^{13}C gHSQCAD of **42** (500 MHz D_2O)

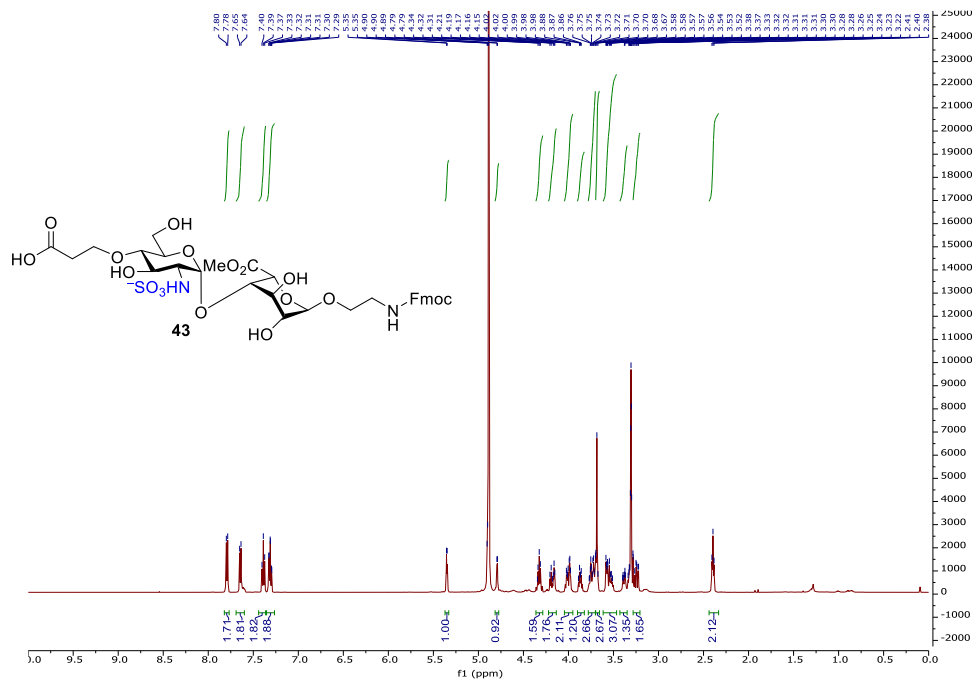
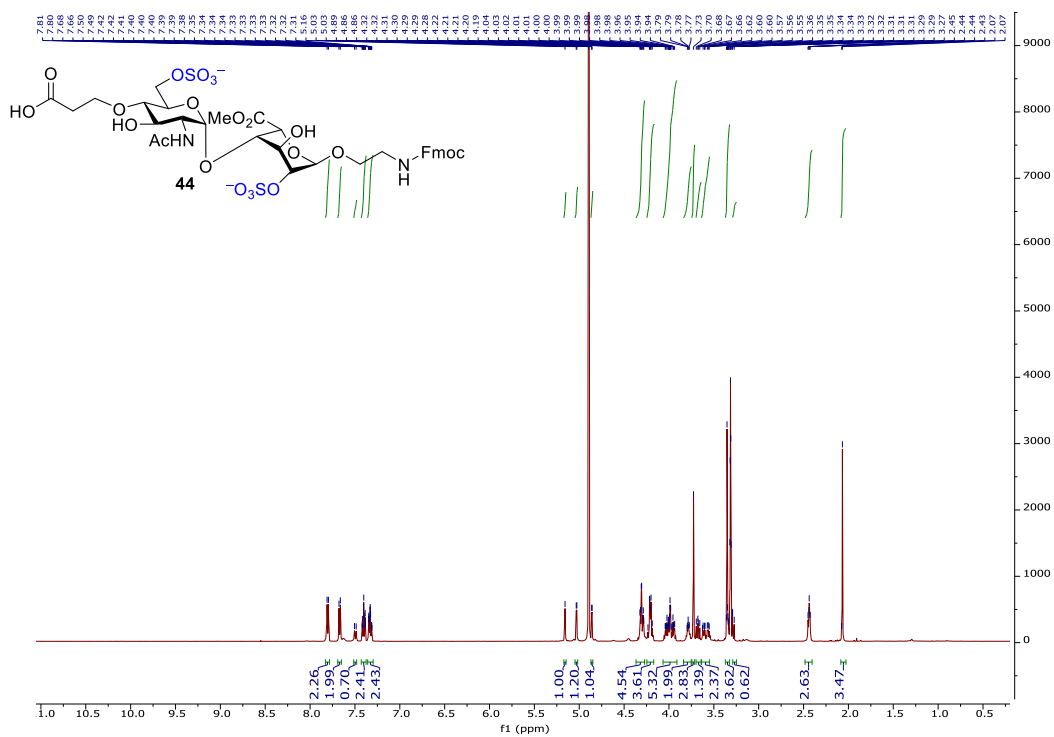
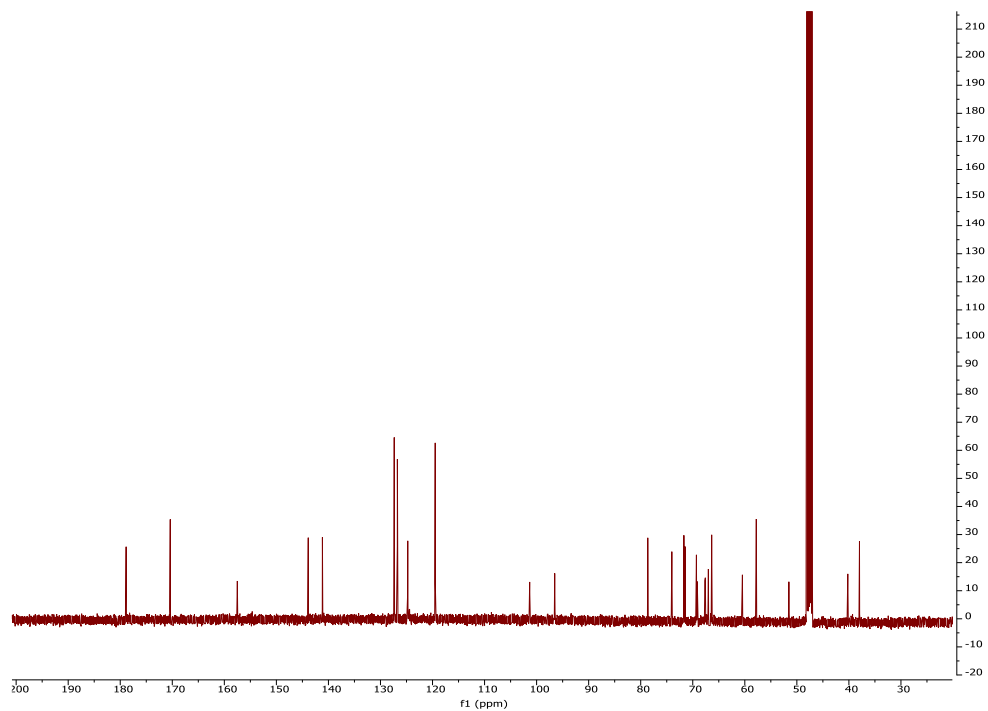


Figure 2.37. ^1H -NMR of **43** (500 MHz CD_3OD)



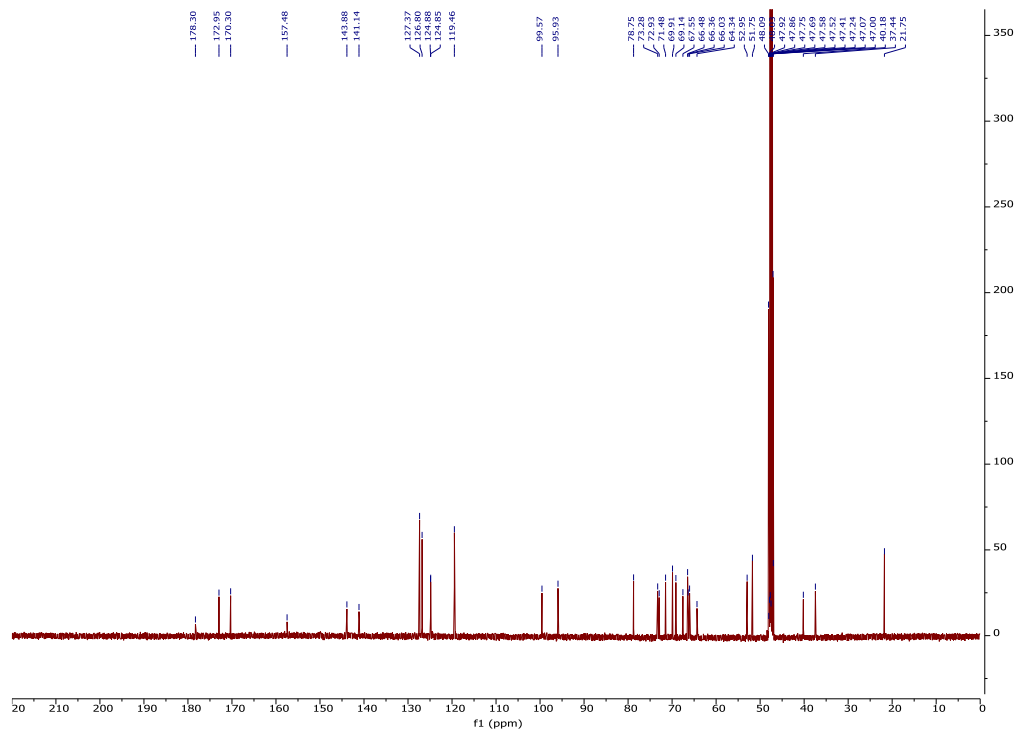


Figure 2.40. ^{13}C -NMR of **44** (125 MHz CD_3OD)

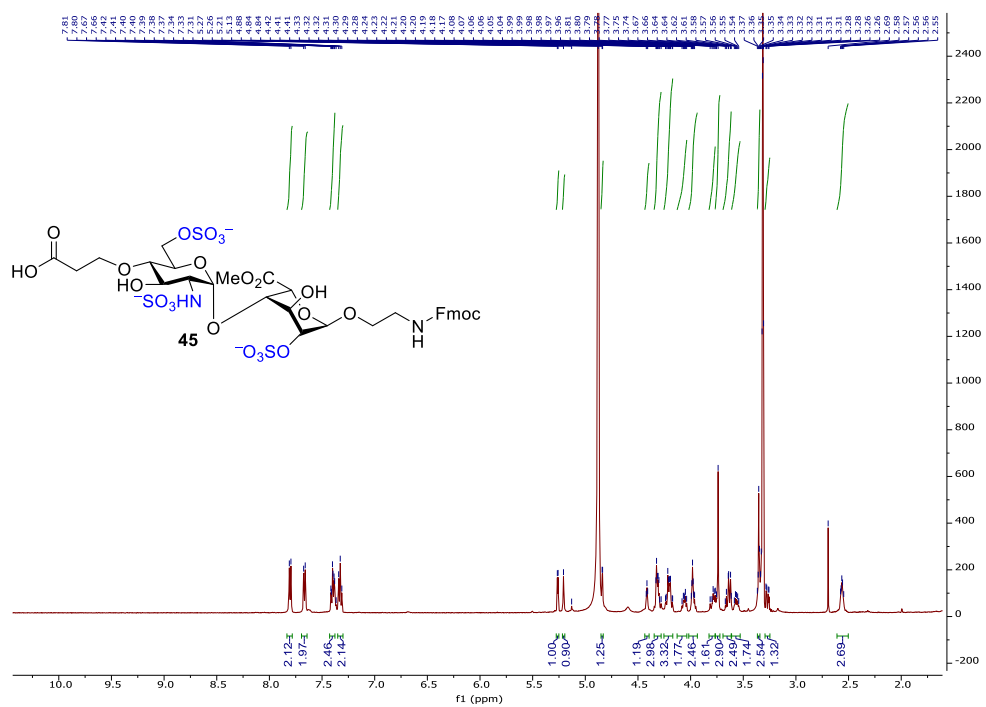


Figure 2.41. ^1H -NMR of **45** (500 MHz CD_3OD)

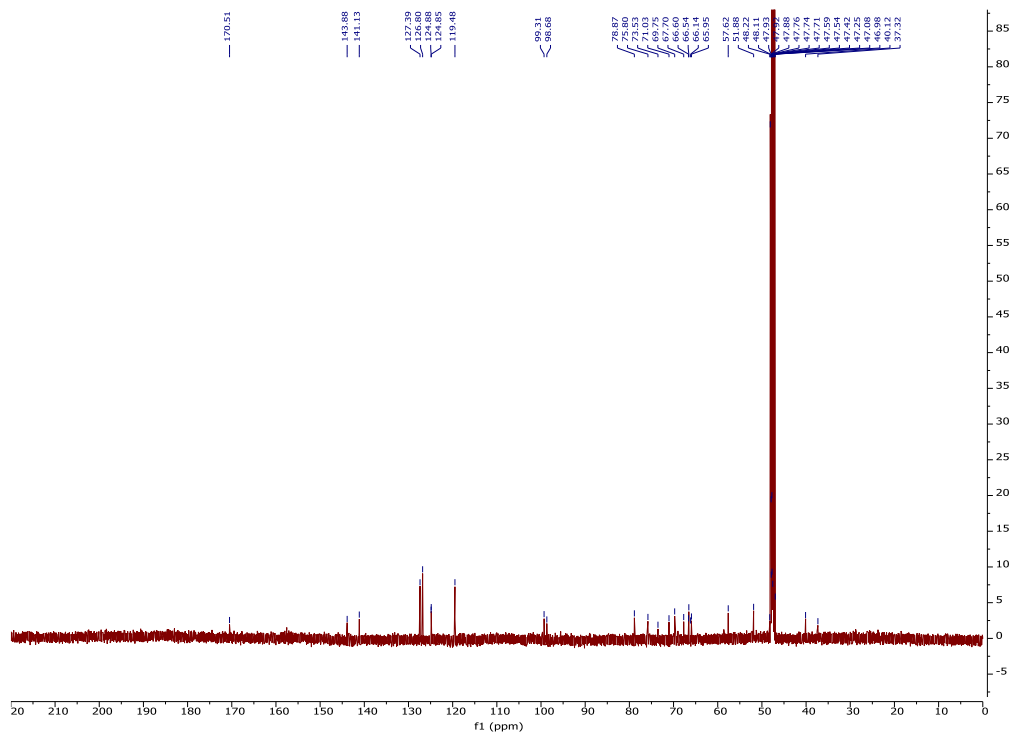


Figure 2.42. ^{13}C -NMR of **45** (125 MHz CD_3OD)

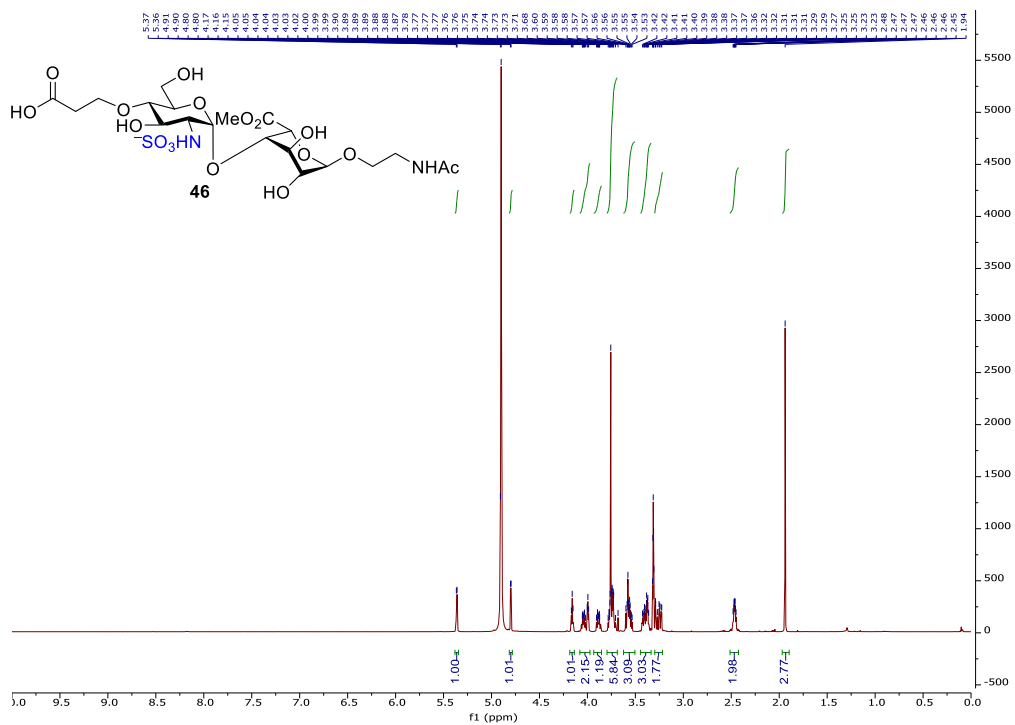


Figure 2.43. ^1H -NMR of **46** (500 MHz CD_3OD)

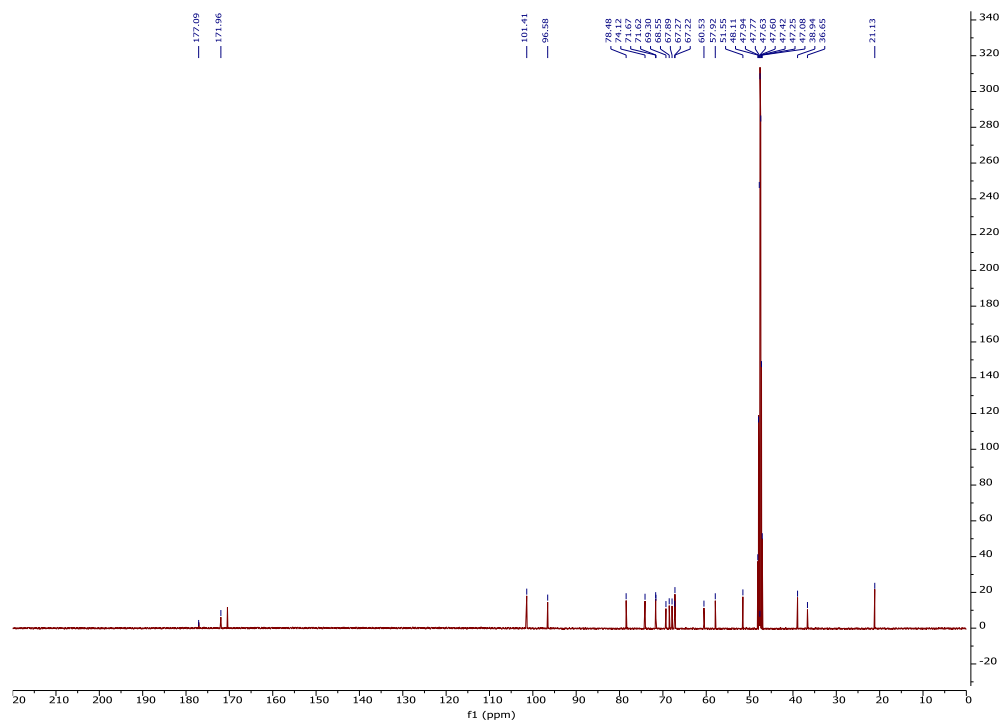


Figure 2.44. ^{13}C -NMR of **46** (125 MHz CD_3OD)

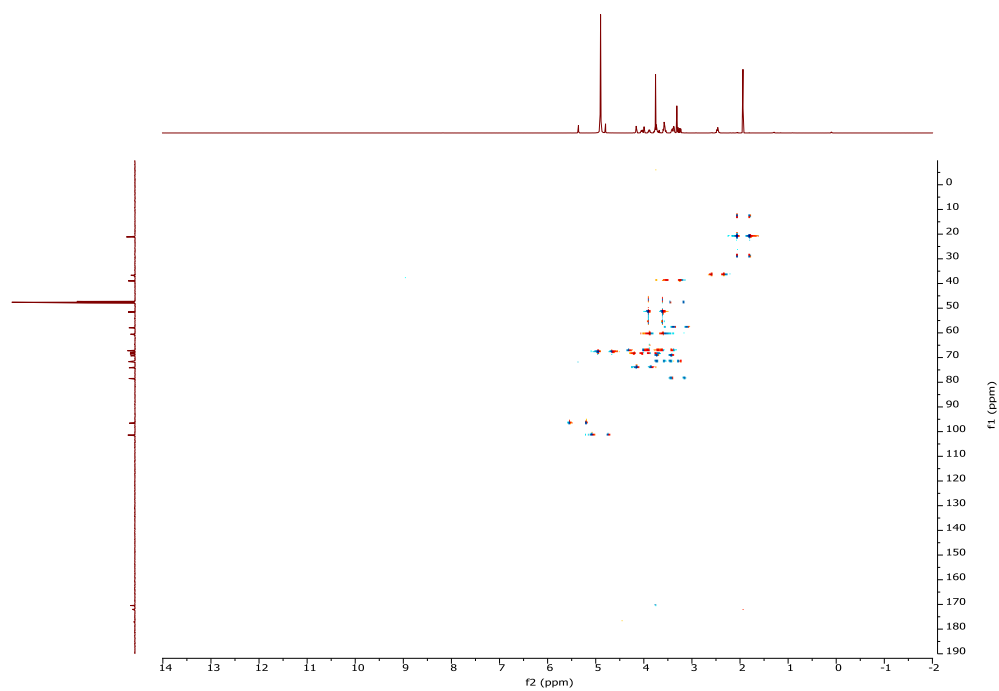


Figure 2.45. ^1H - ^{13}C gHSQCAD of **46** (500 MHz CD_3OD)

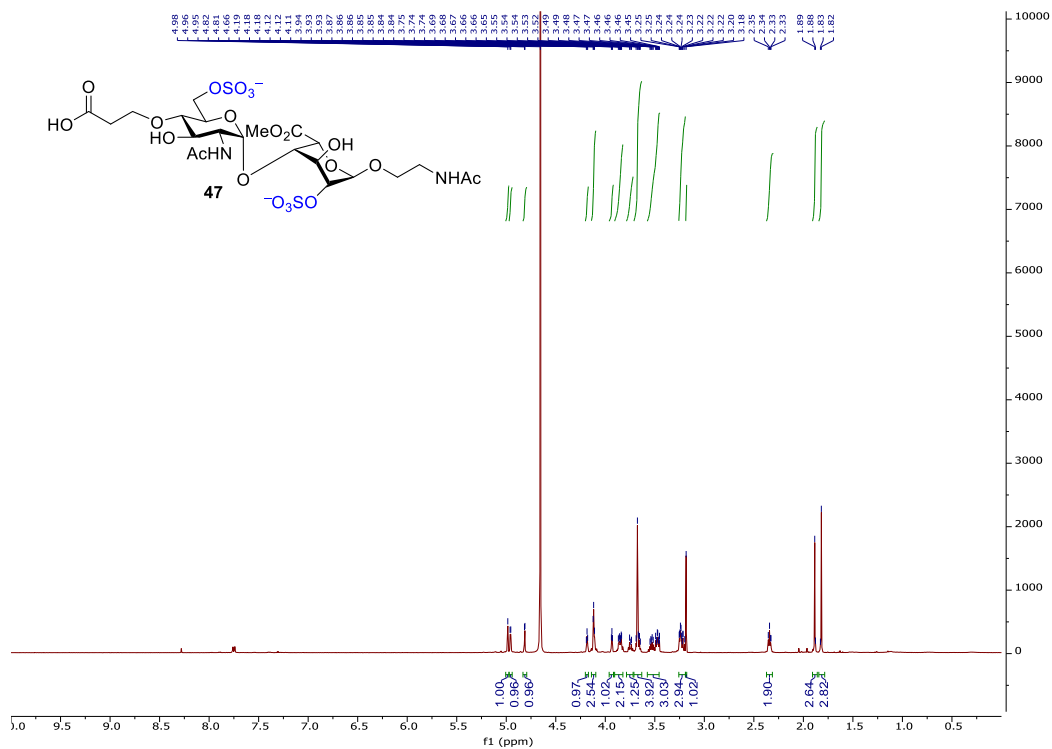


Figure 2.46. ¹H-NMR of 47 (500 MHz D₂O)

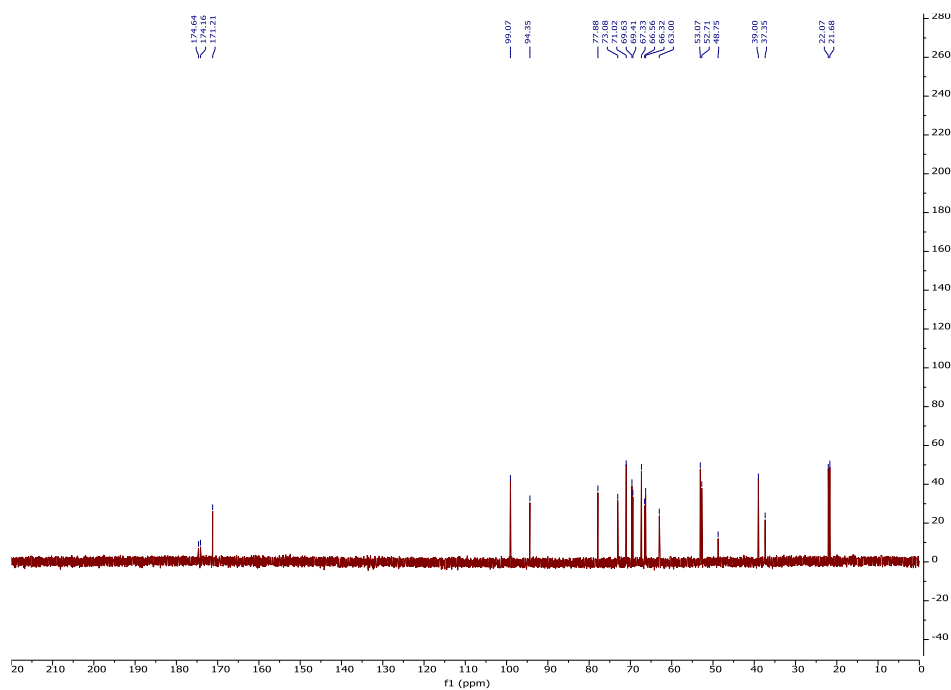
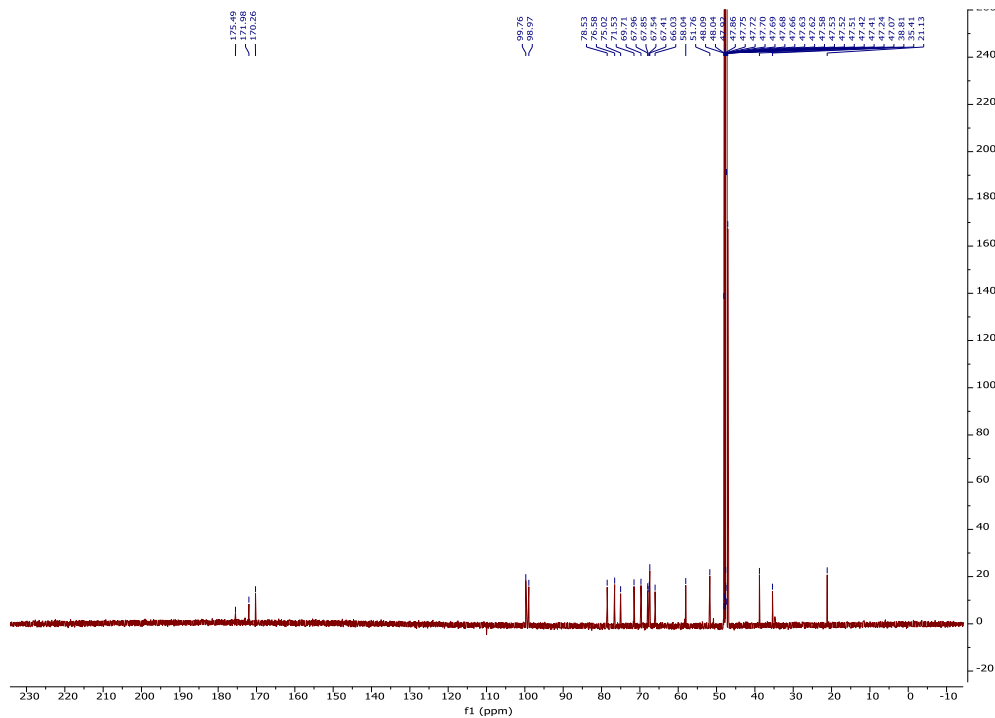
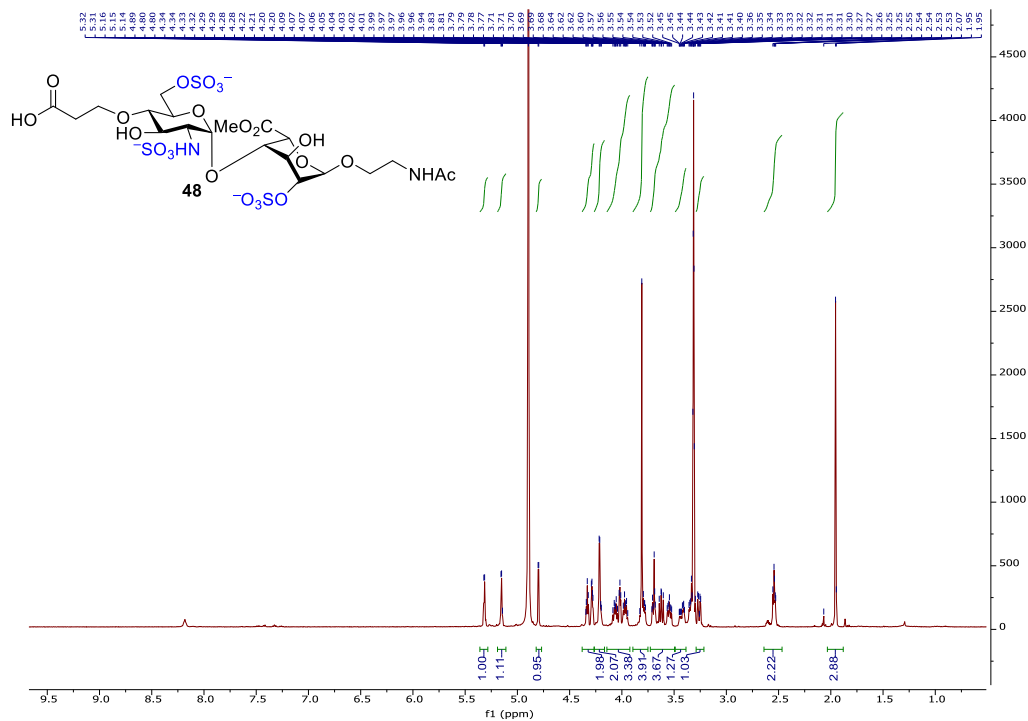


Figure 2.47. ¹³C-NMR of 47 (125 MHz D₂O)



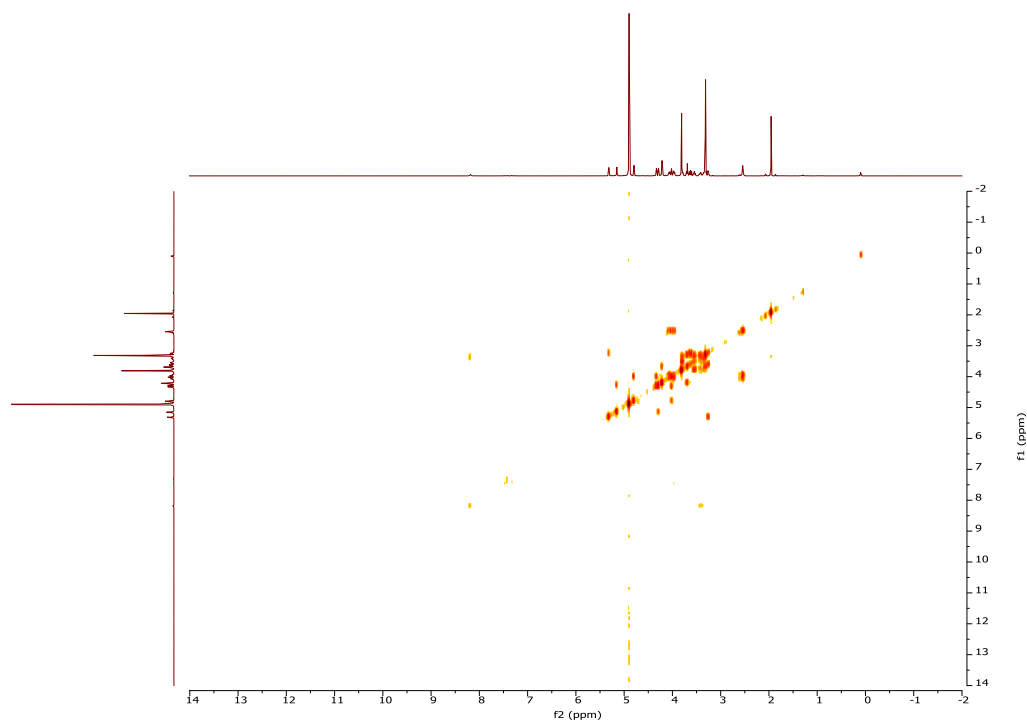


Figure 2.50. ^1H - ^1H gCOSY of **48** (500 MHz CD_3OD)

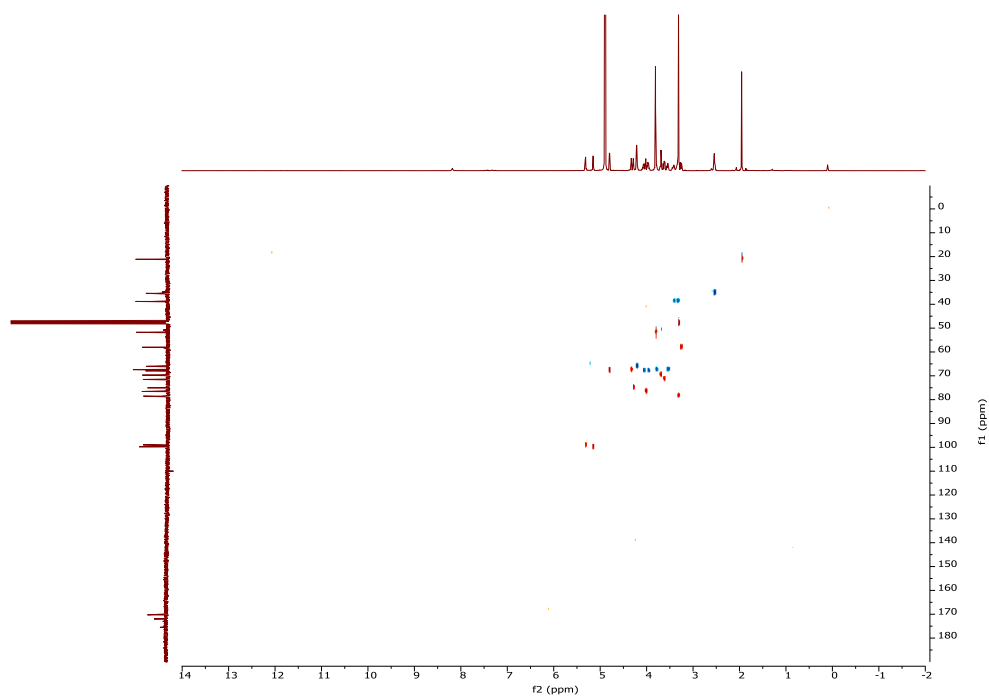


Figure 2.51. ^1H - ^{13}C gHSQCAD of **48** (500 MHz CD_3OD)

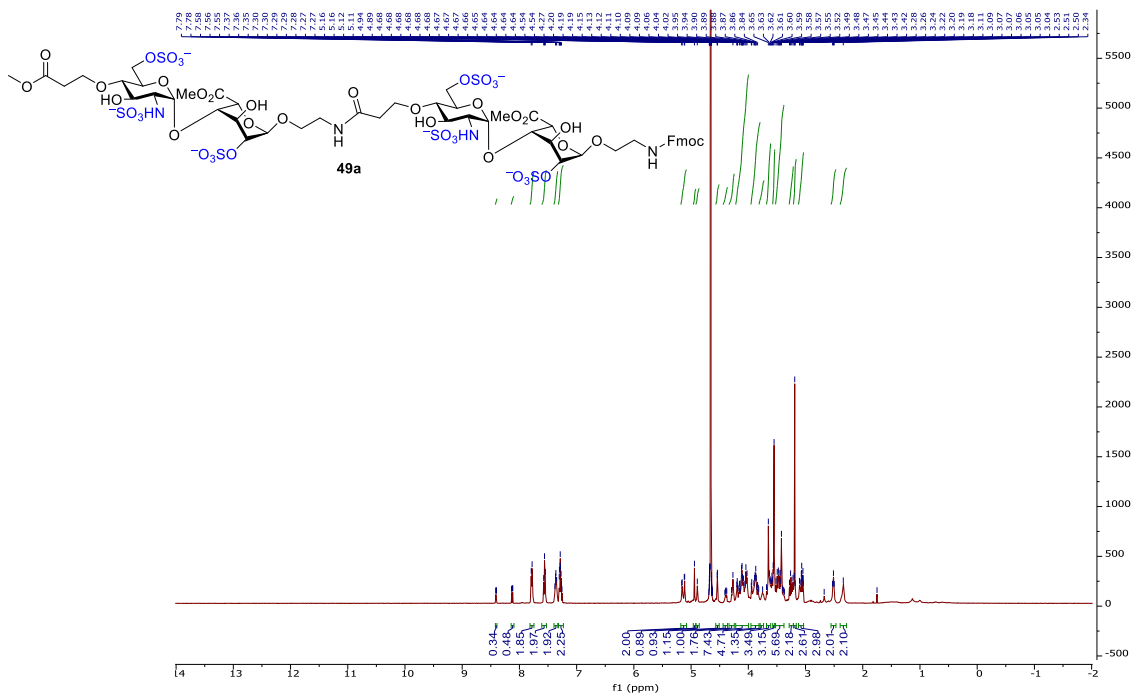


Figure 2.52. $^1\text{H-NMR}$ of 49a (500 MHz D_2O)

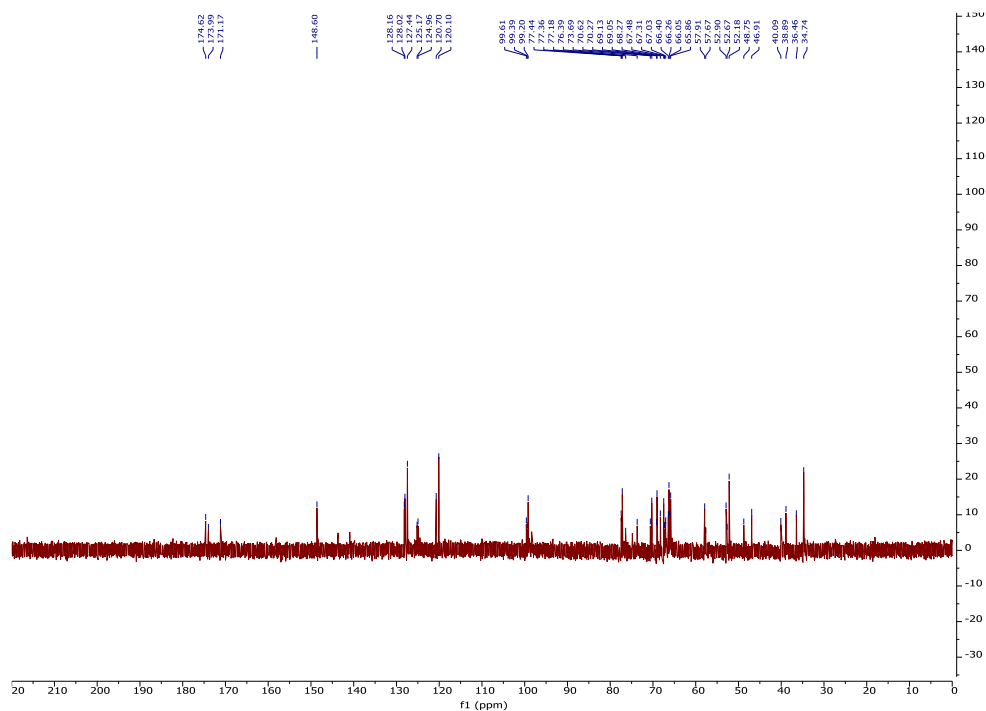
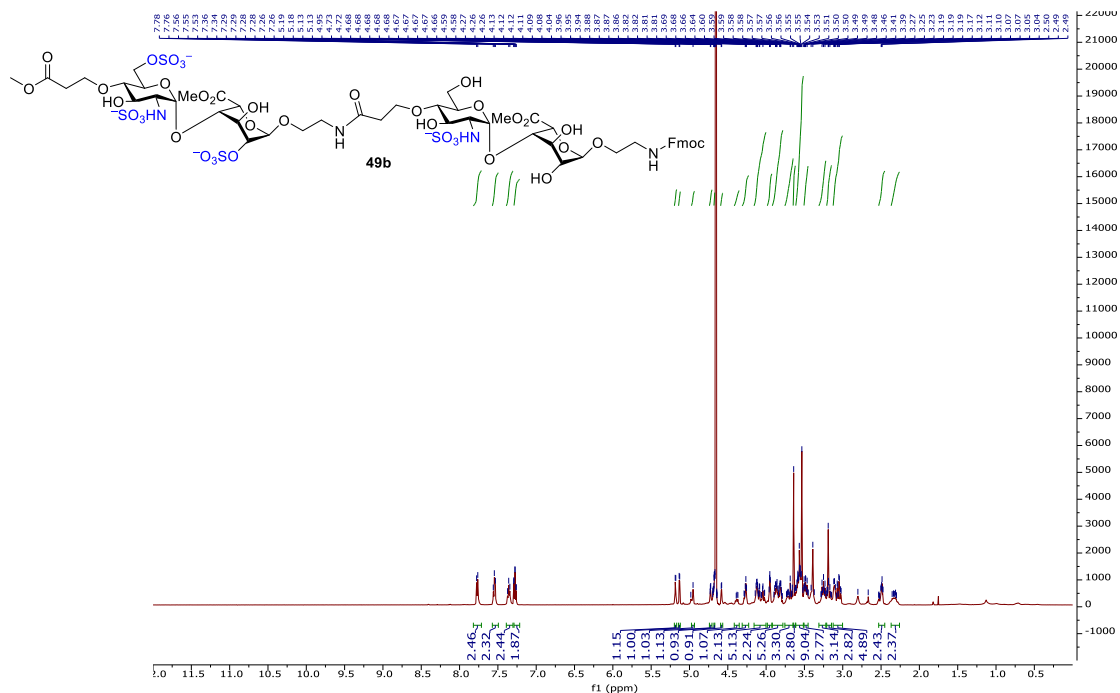


Figure 2.53. $^{13}\text{C-NMR}$ of 49a (125 MHz D_2O)



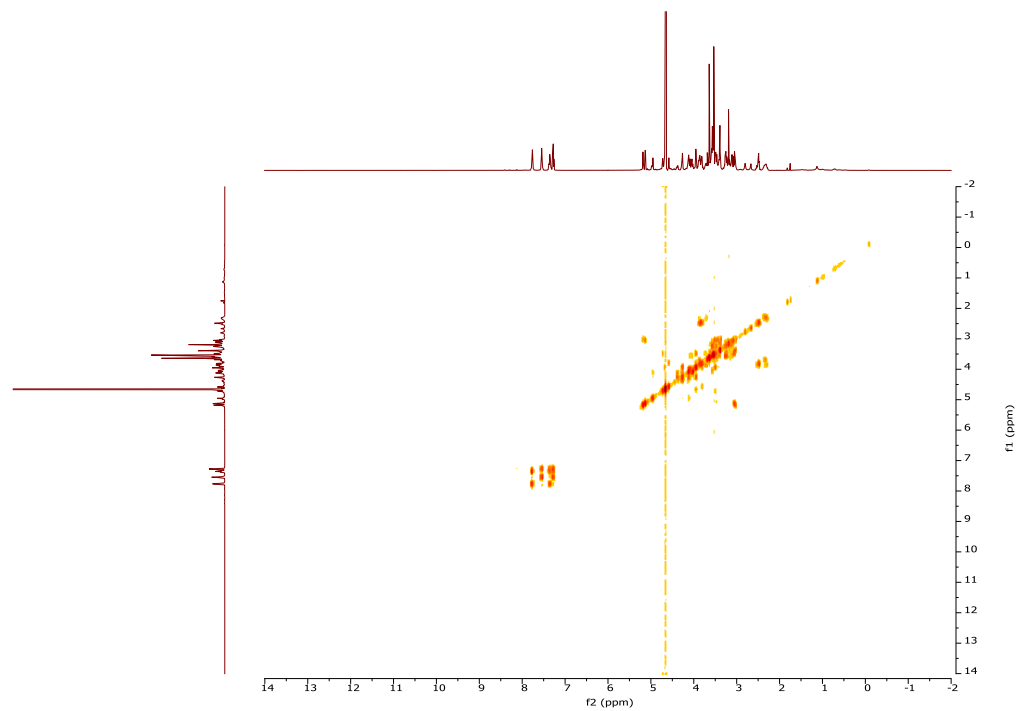


Figure 2.56. ^1H - ^1H gCOSY of **49b** (500 MHz D_2O)

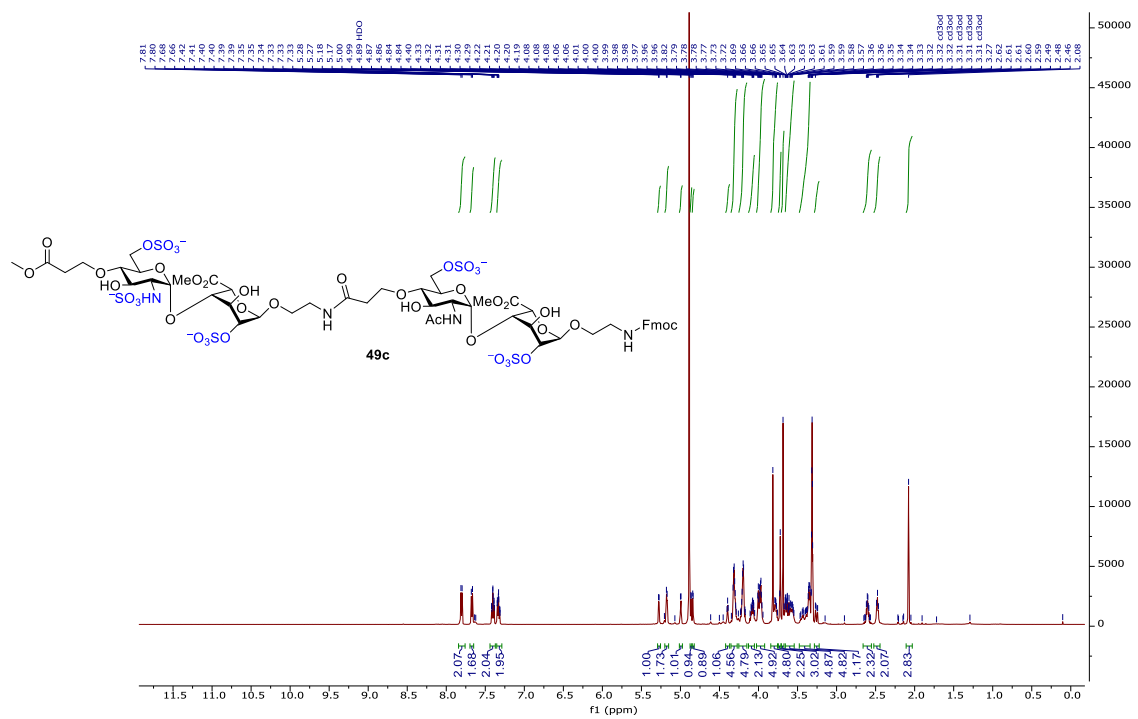


Figure 2.57. ^1H -NMR of **49c** (500 MHz CD_3OD)

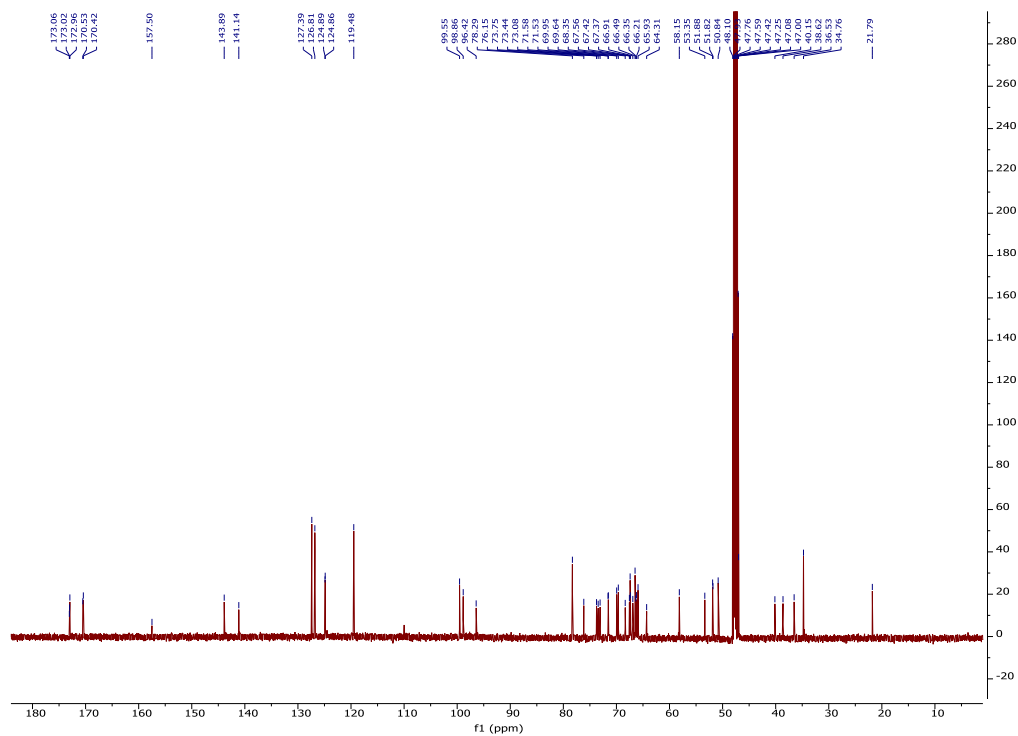


Figure 2.58. ^{13}C -NMR of **49c** (125 MHz CD_3OD)

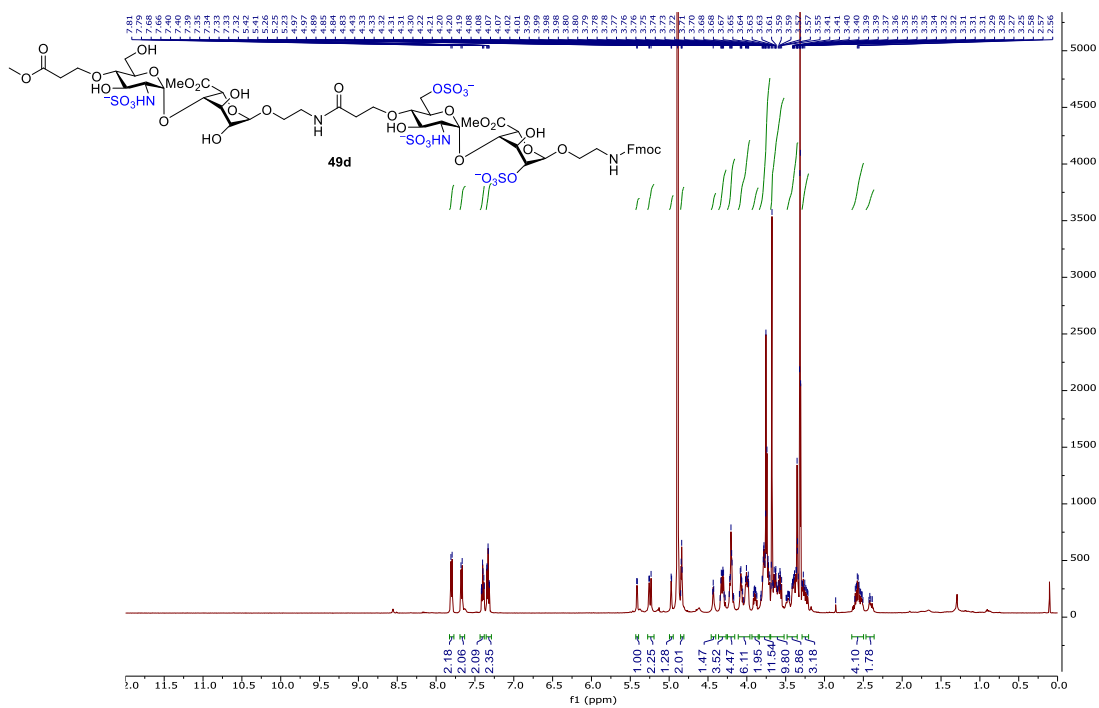


Figure 2.59. ^1H -NMR of **49d** (500 MHz CD_3OD)

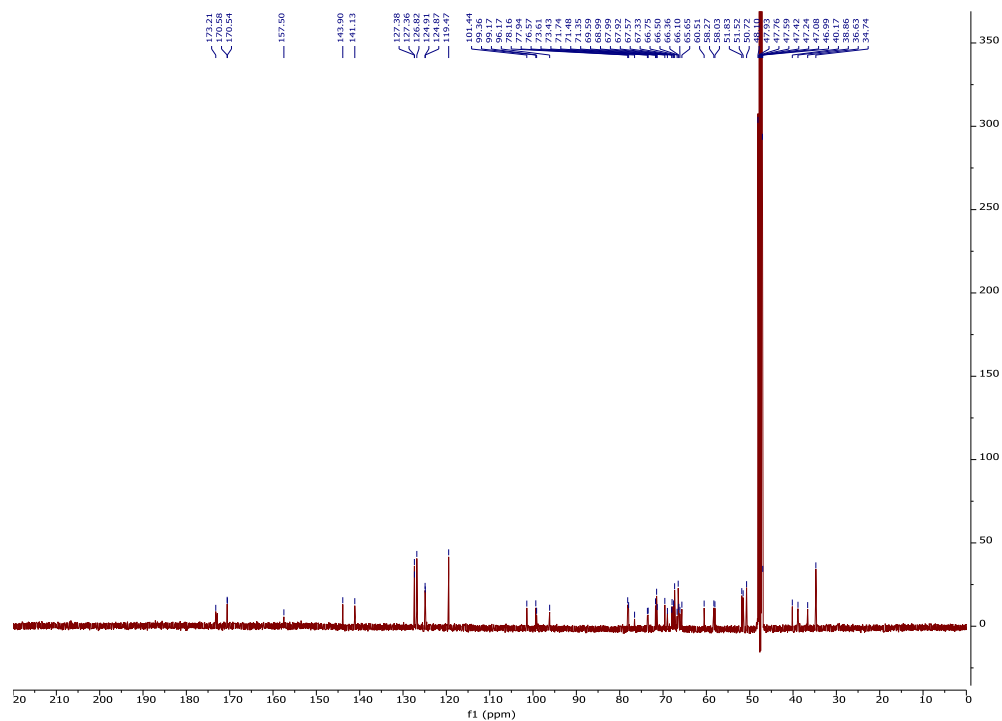


Figure 2.60. ^{13}C -NMR of 49d (125 MHz CD_3OD)

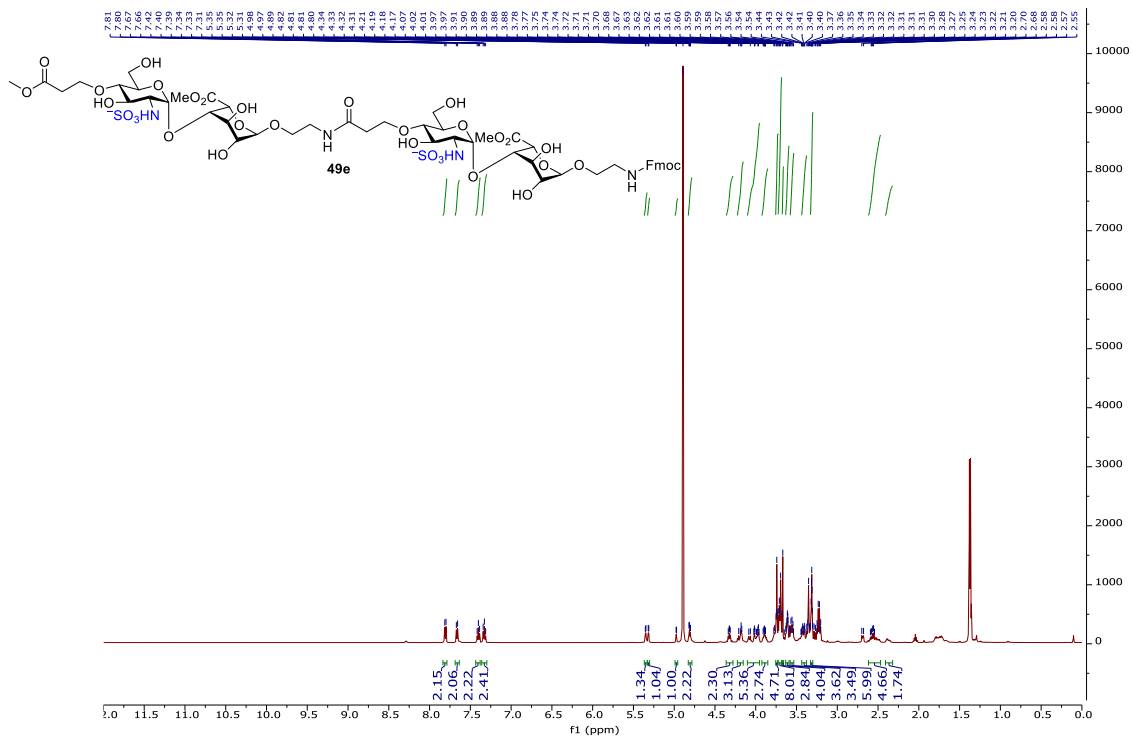


Figure 2.61. ^1H -NMR of 49e (500 MHz CD_3OD)

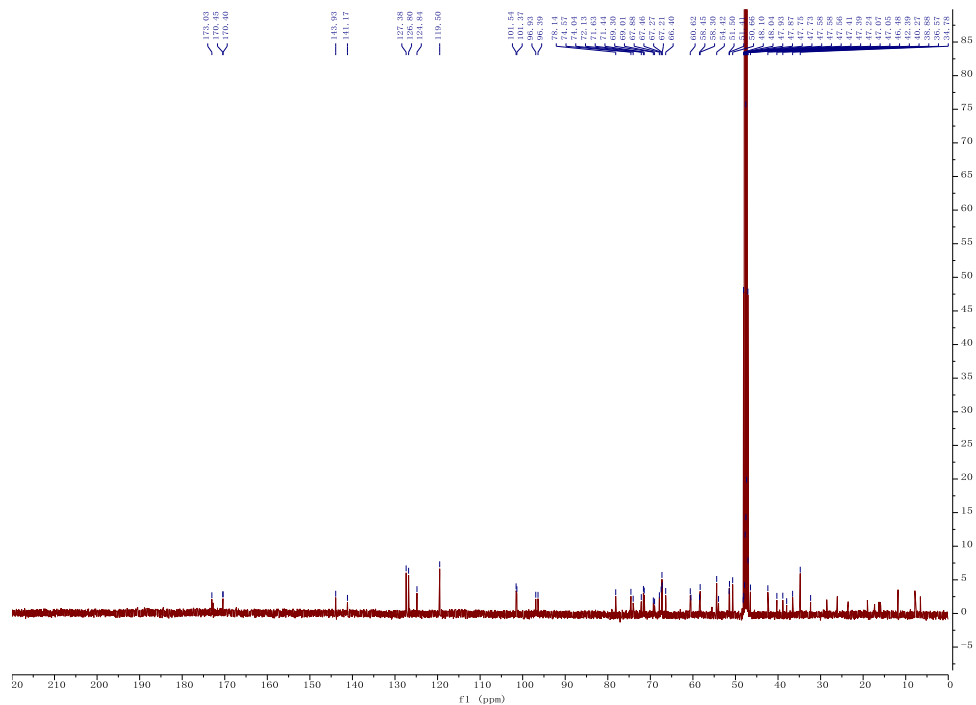


Figure 2.62. ^{13}C -NMR of **49e** (125 MHz CD_3OD)

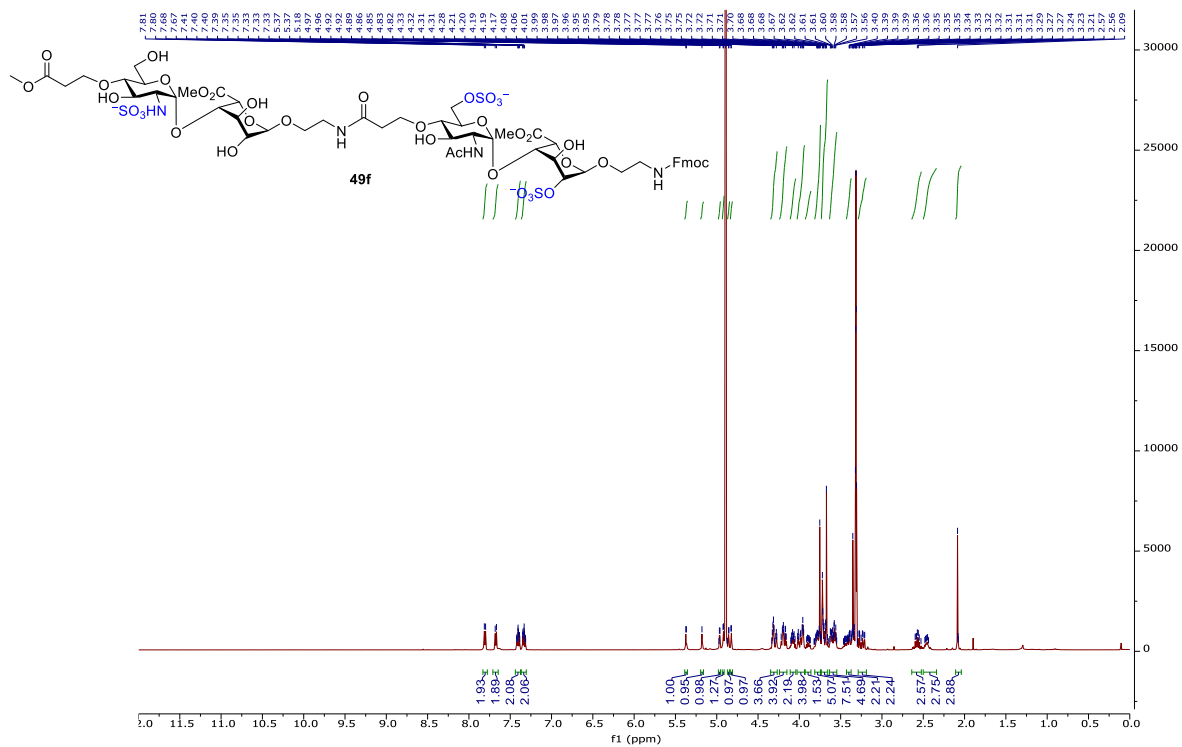


Figure 2.63. ^1H -NMR of **49f** (500 MHz CD_3OD)

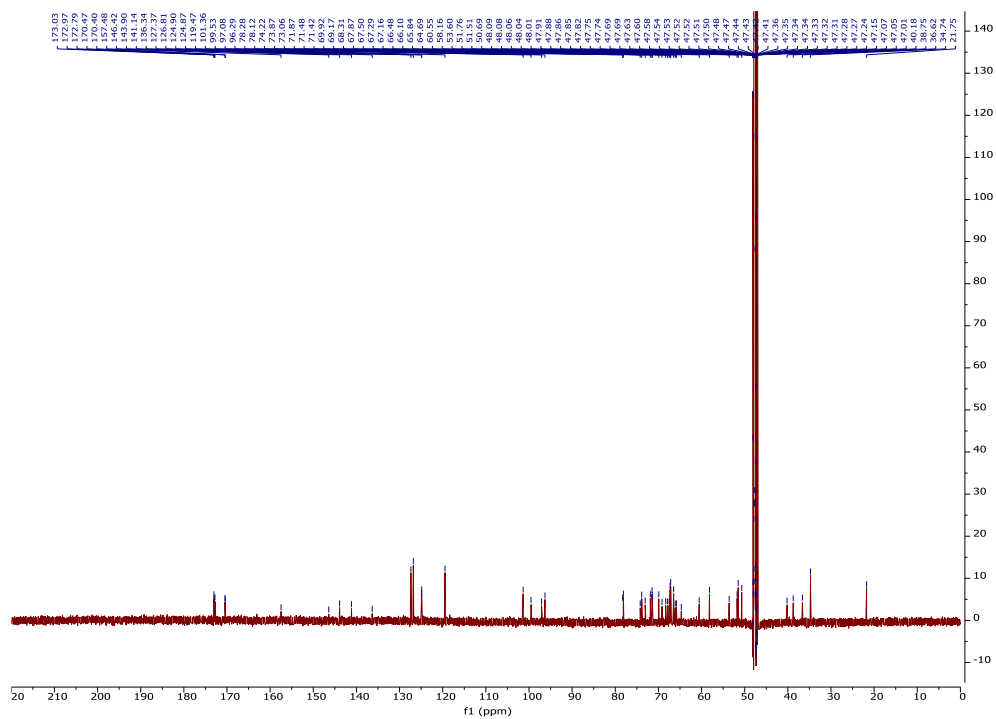


Figure 2.64. ^{13}C -NMR of **49f** (125 MHz CD_3OD)

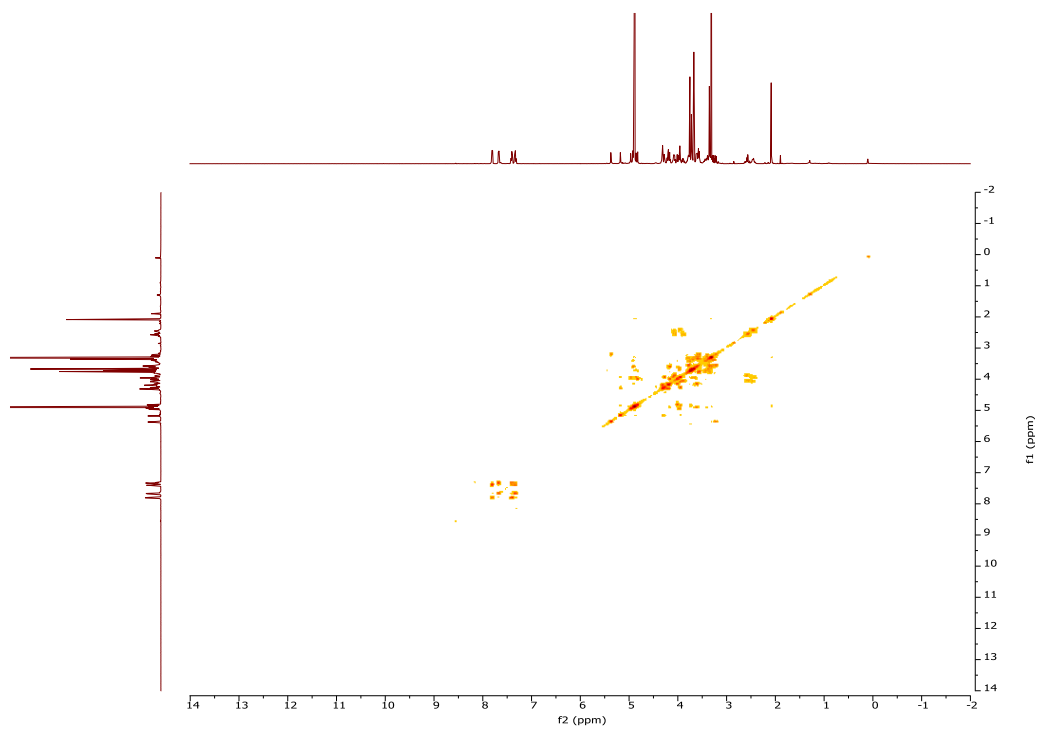


Figure 2.65. ^1H - ^1H gCOSY of **49f** (500 MHz CD_3OD)

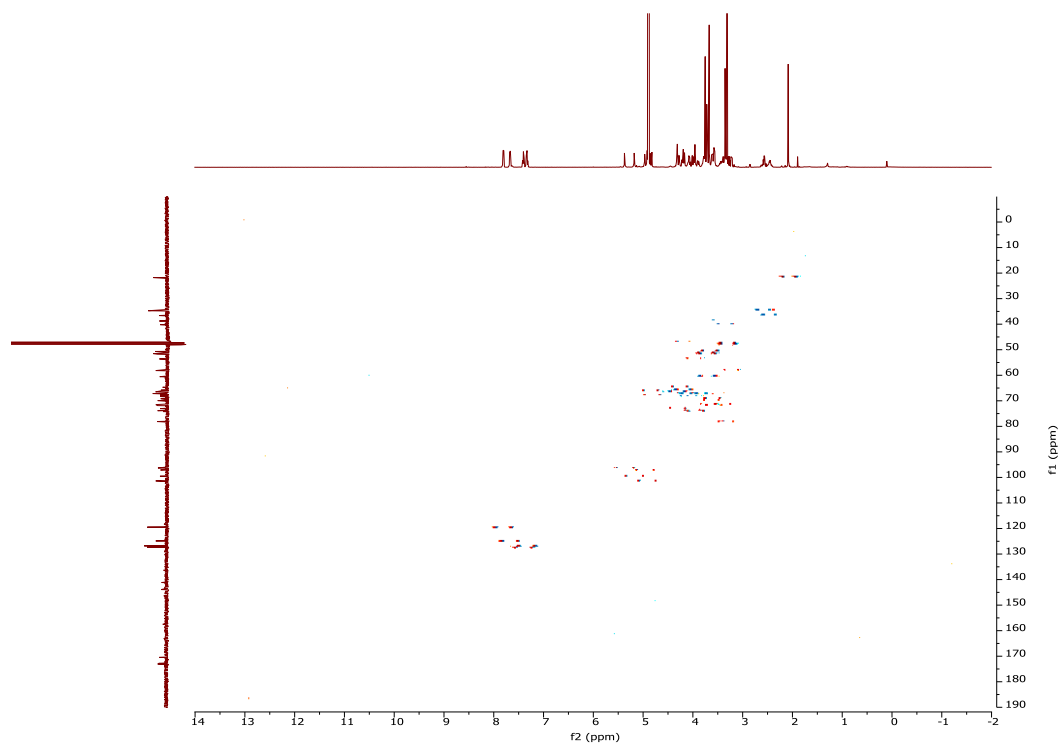


Figure 2.66. ^1H - ^{13}C gHSQCAD of **49f** (500 MHz CD_3OD)

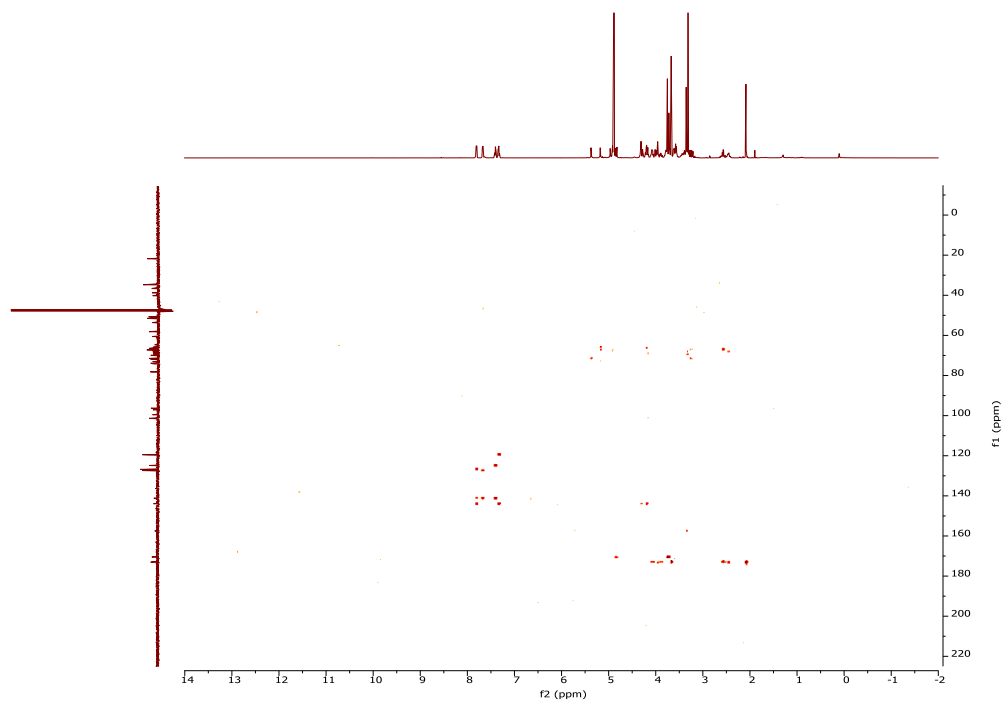
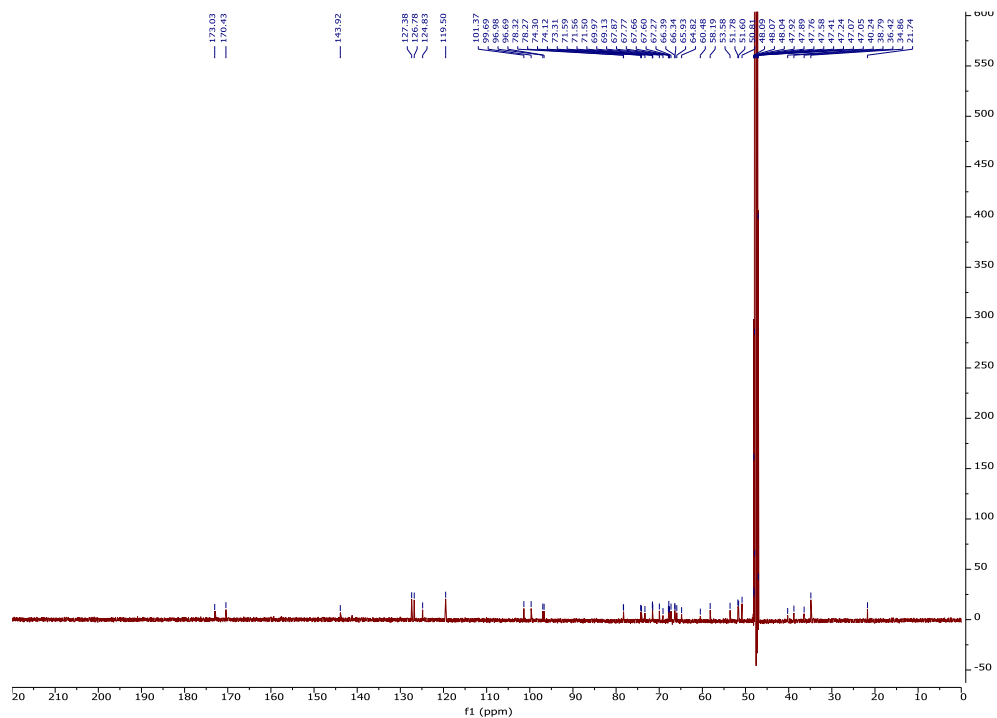
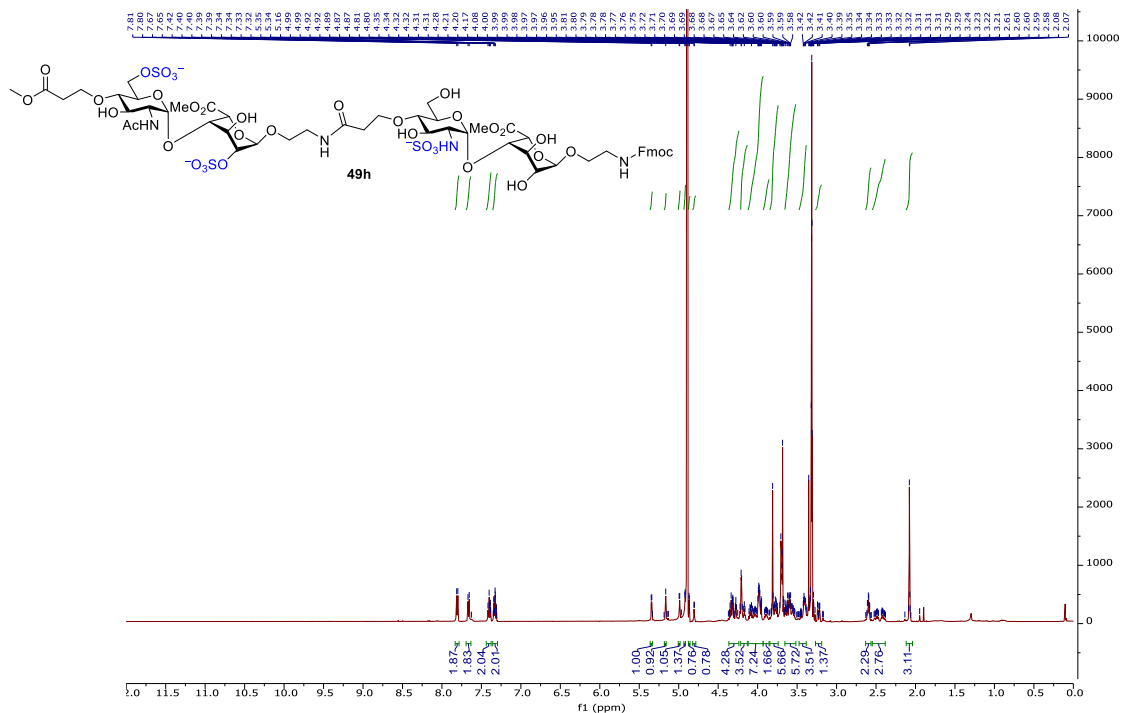


Figure 2.67. ^1H - ^{13}C gHMBCAD of **49f** (500 MHz CD_3OD)



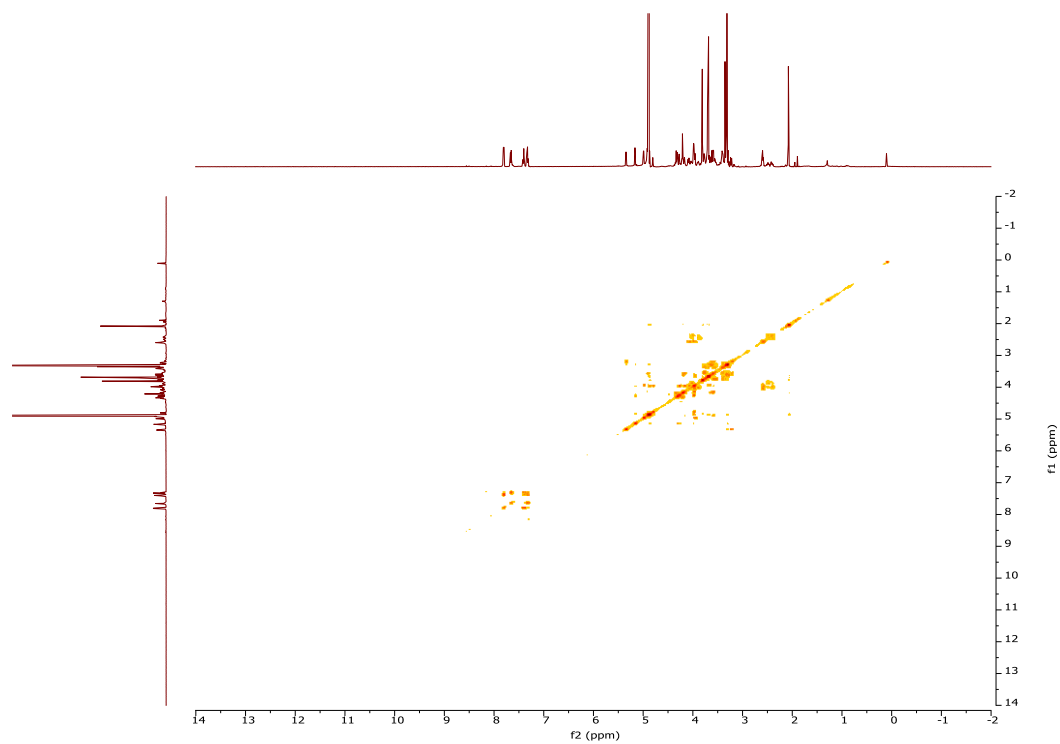


Figure 2.72. ^1H - ^1H gCOSY of **49h** (500 MHz CD_3OD)

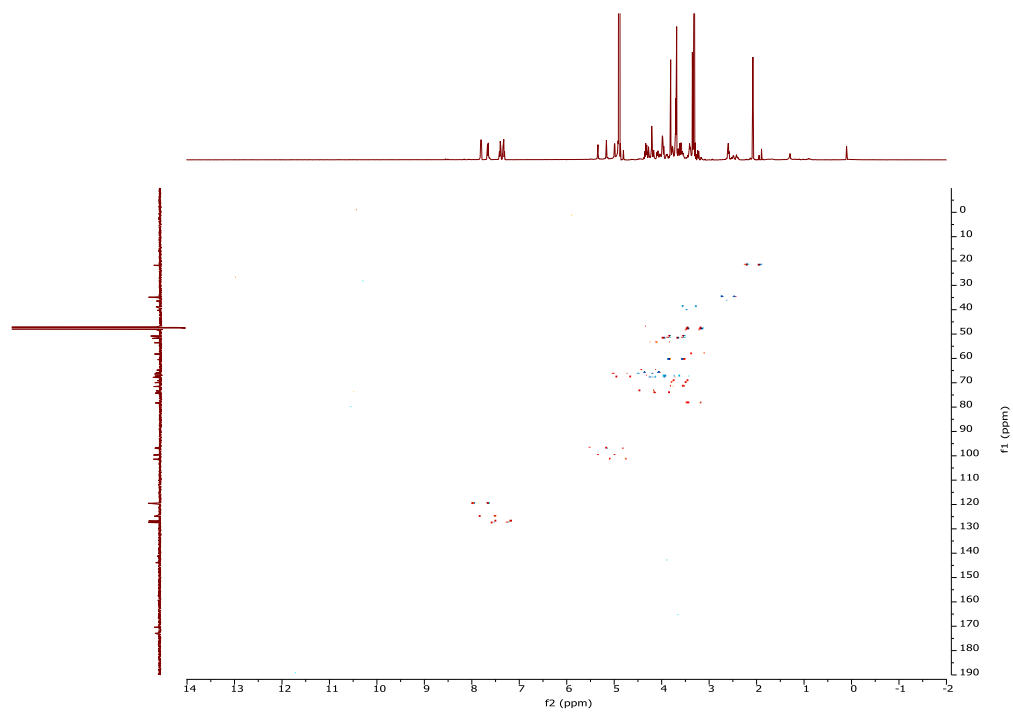


Figure 2.73. ^1H - ^{13}C gHSQC of **49h** (500 MHz CD_3OD)

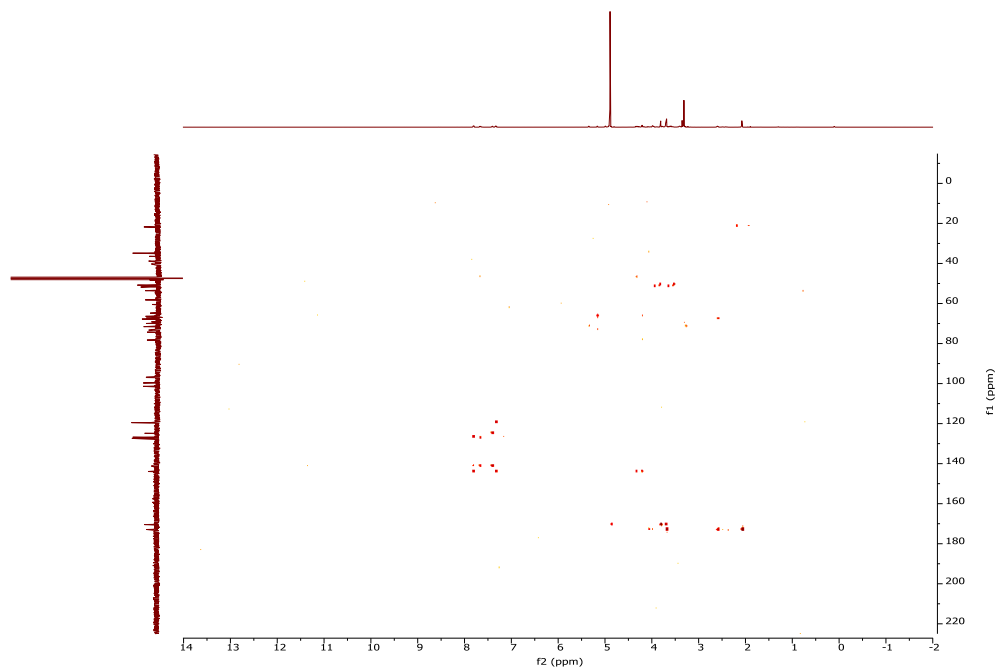


Figure 2.74. ^1H - ^{13}C gHMBCAD of **49h** (500 MHz CD_3OD)

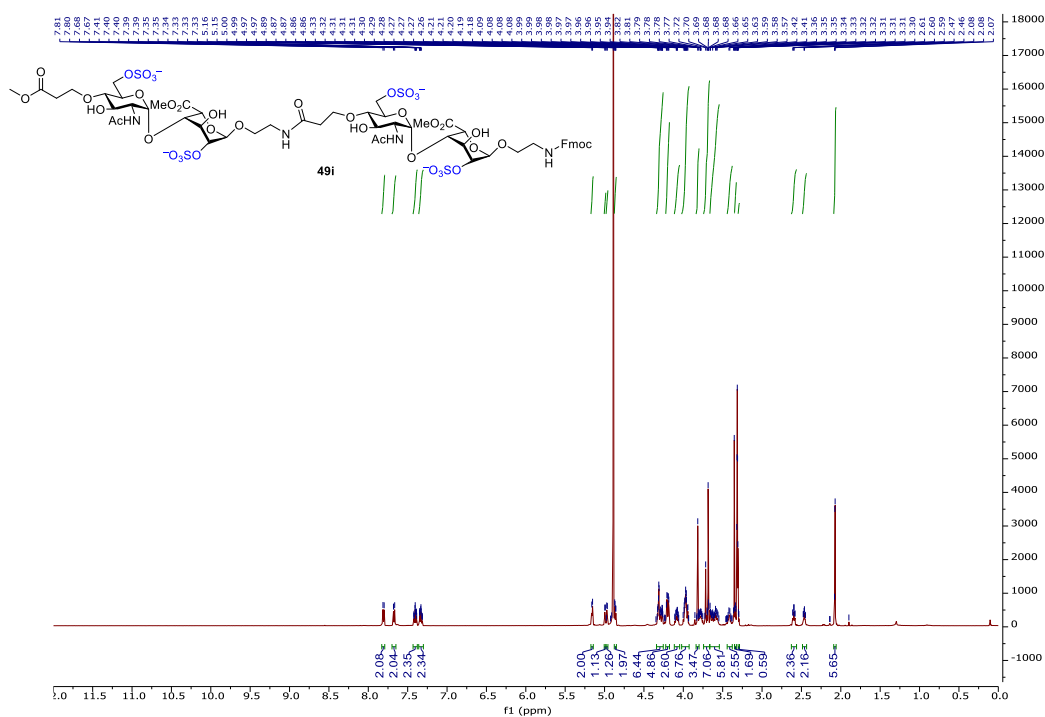


Figure 2.75. ^1H -NMR of **49i** (500 MHz CD_3OD)

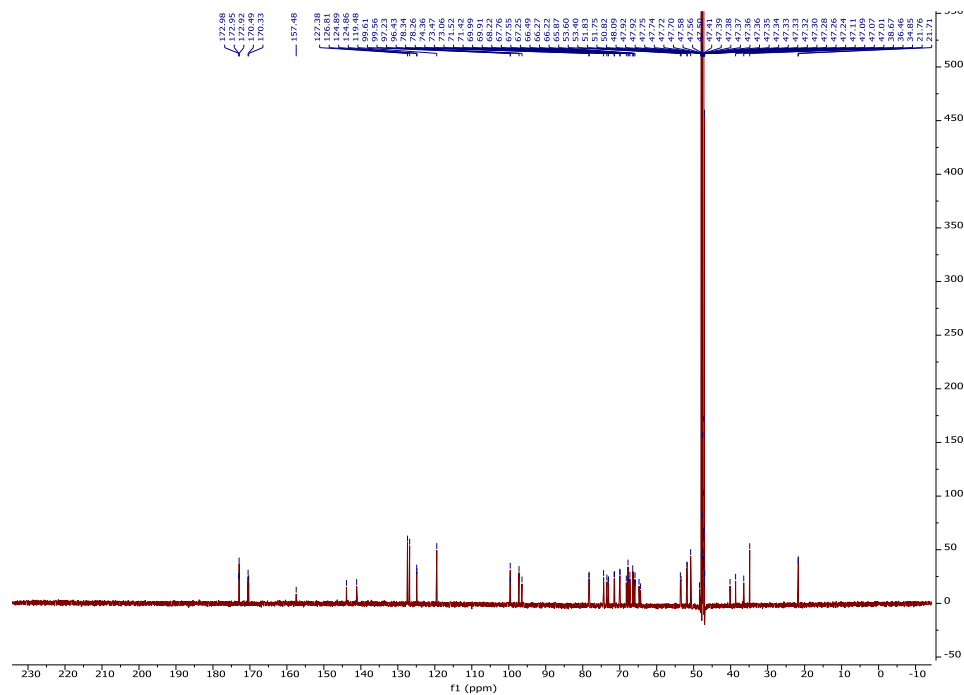


Figure 2.76. ^{13}C -NMR of **49i** (125 MHz CD_3OD)

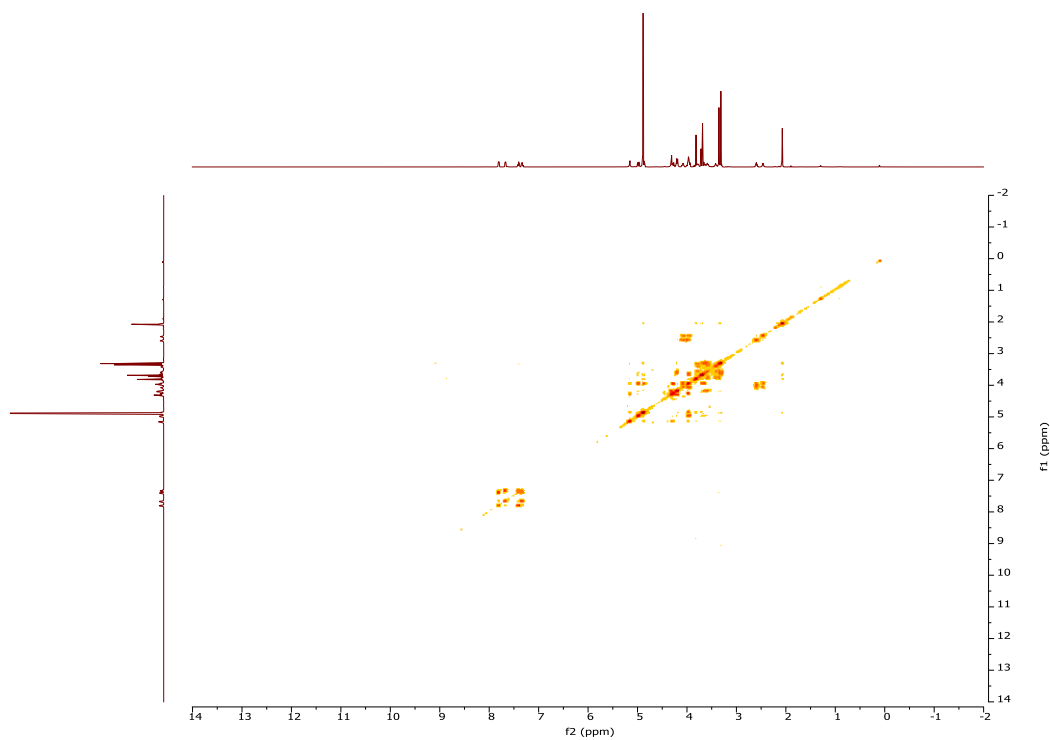


Figure 2.77. ^1H - ^1H gCOSY of **49i** (500 MHz CD_3OD)

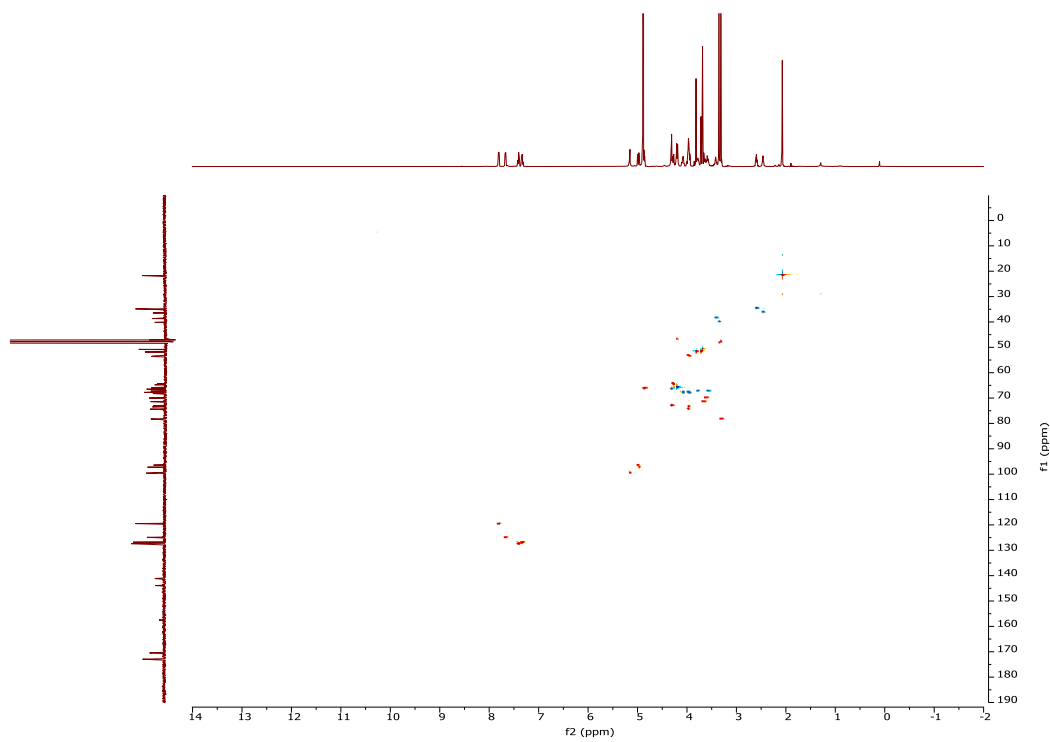


Figure 2.78. ^1H - ^{13}C gHSQCAD of **49i** (500 MHz CD_3OD)

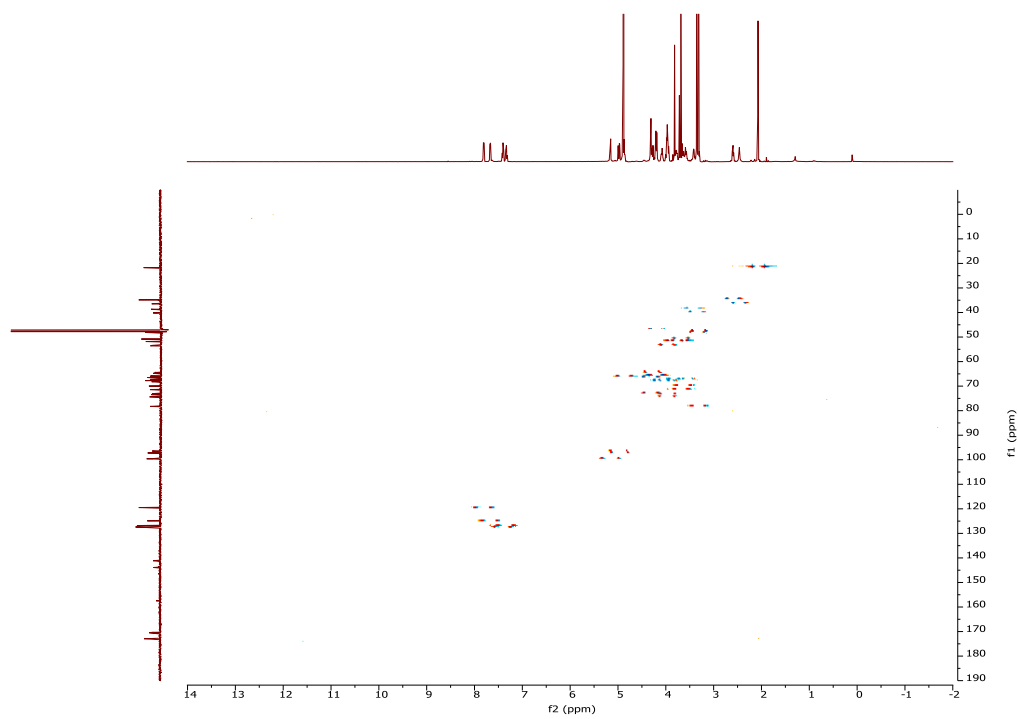


Figure 2.79. ^1H - ^{13}C gHSQCAD of **49i** (500 MHz CD_3OD)

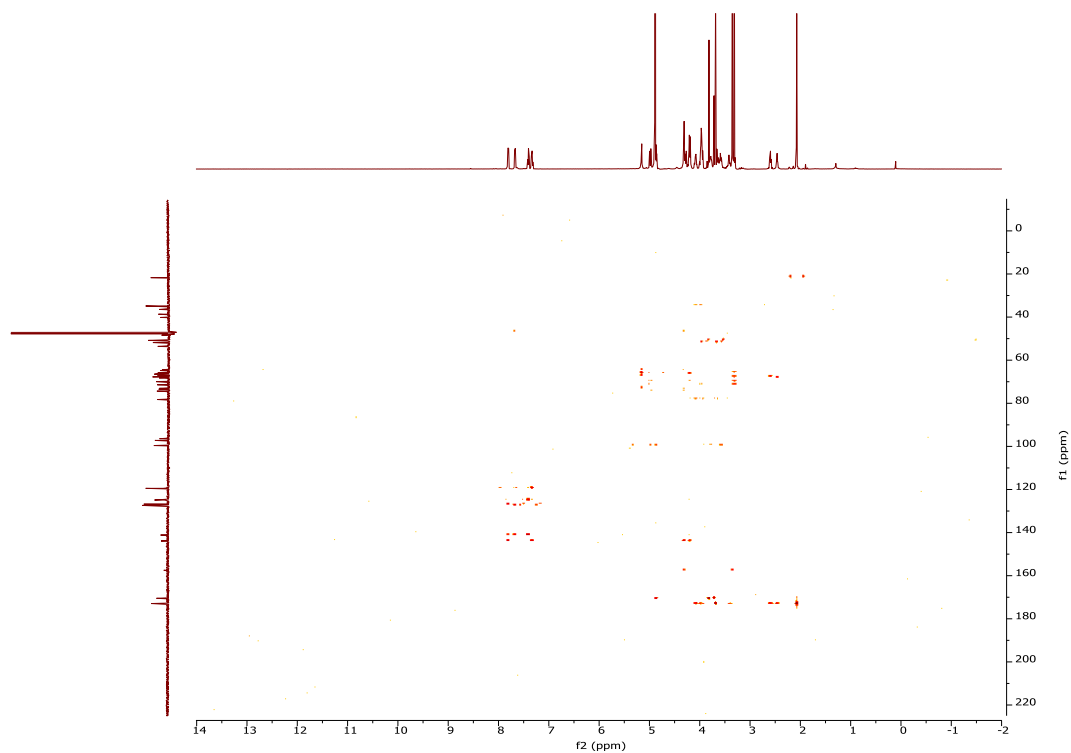


Figure 2.80. ^1H - ^{13}C gHMBCAD of **49i** (500 MHz CD_3OD)

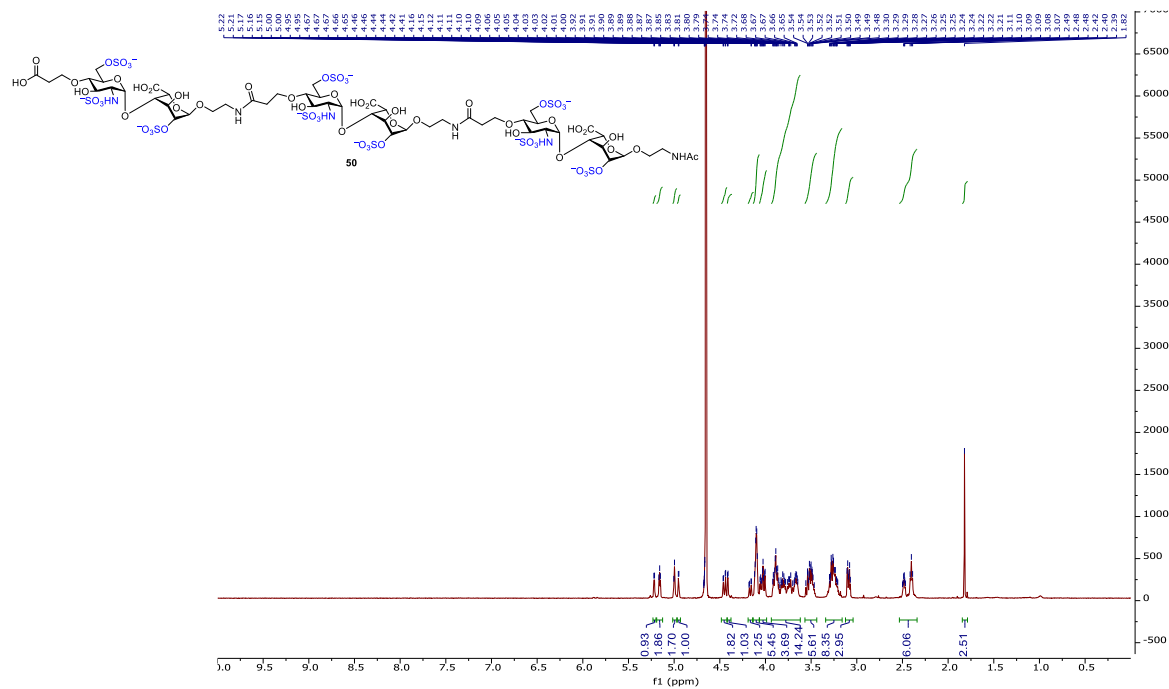


Figure 2.81. ^1H -NMR of **50** (500 MHz D_2O)

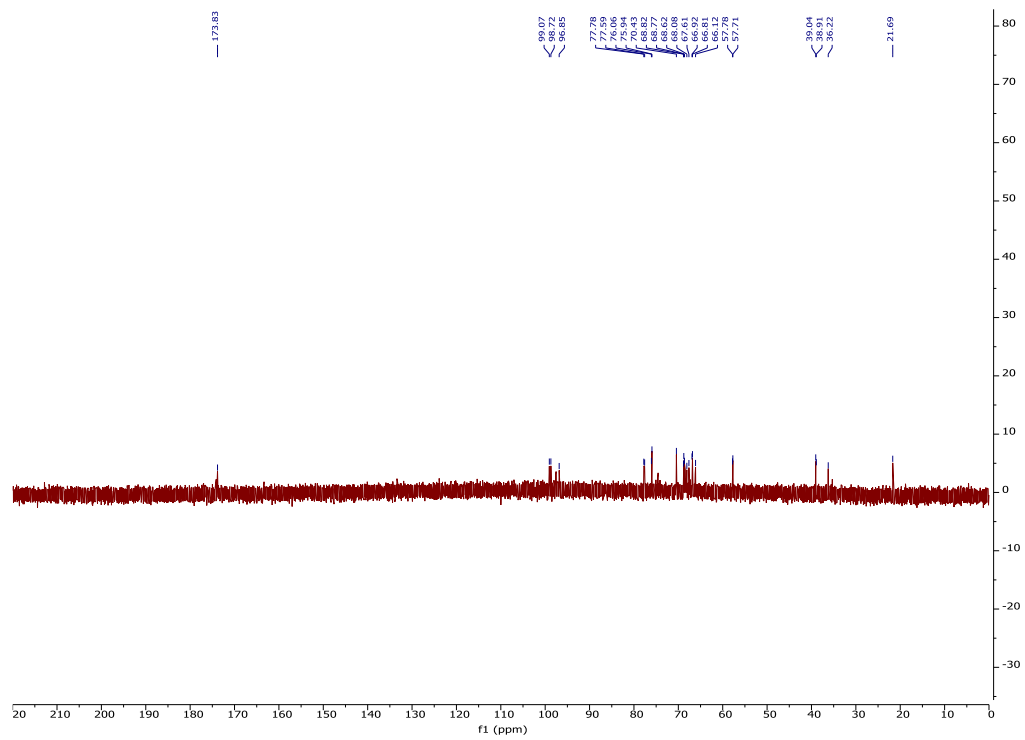


Figure 2.82. ^{13}C -NMR of **50** (125 MHz D_2O)

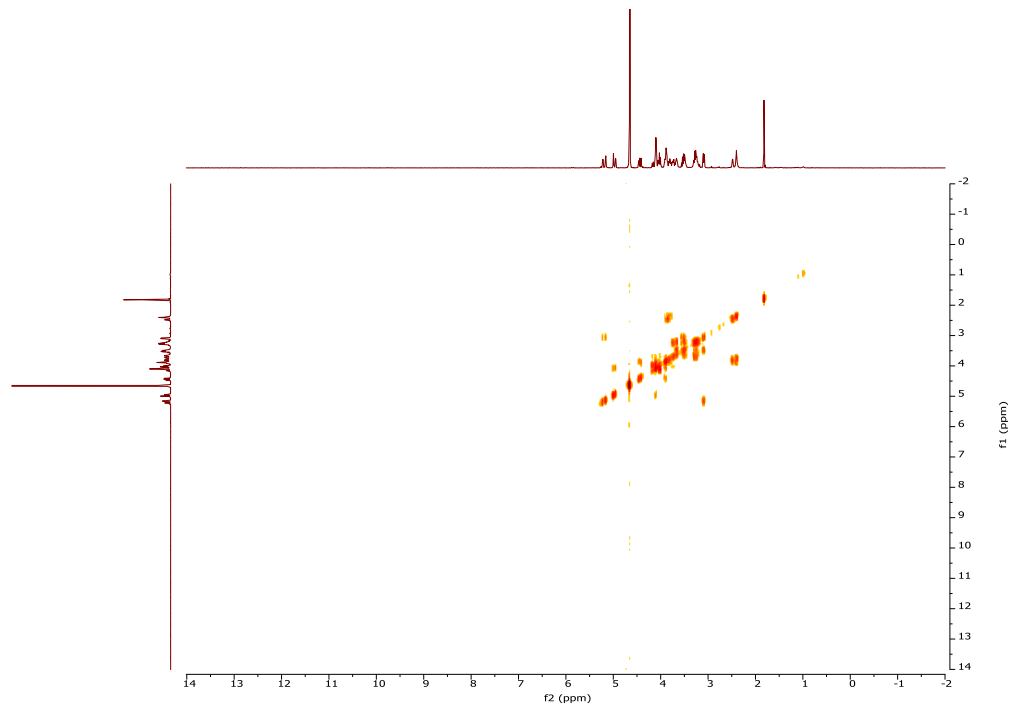


Figure 2.83. ^1H - ^1H gCOSY of **50** (500 MHz D_2O)

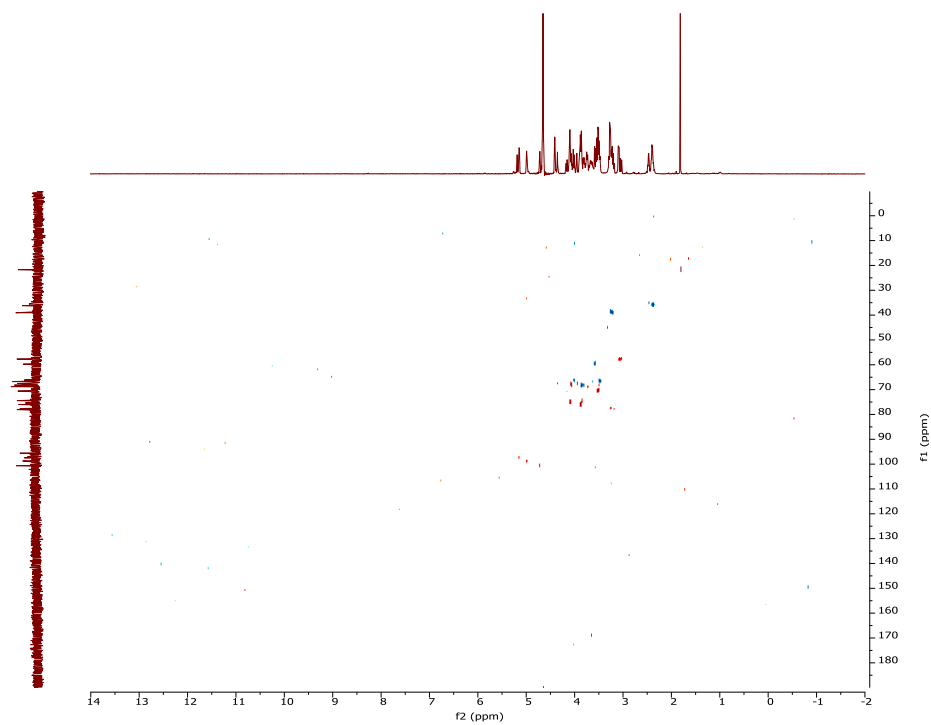


Figure 2.86. ^1H - ^{13}C gHSQCAD of **50a** (500 MHz D_2O)

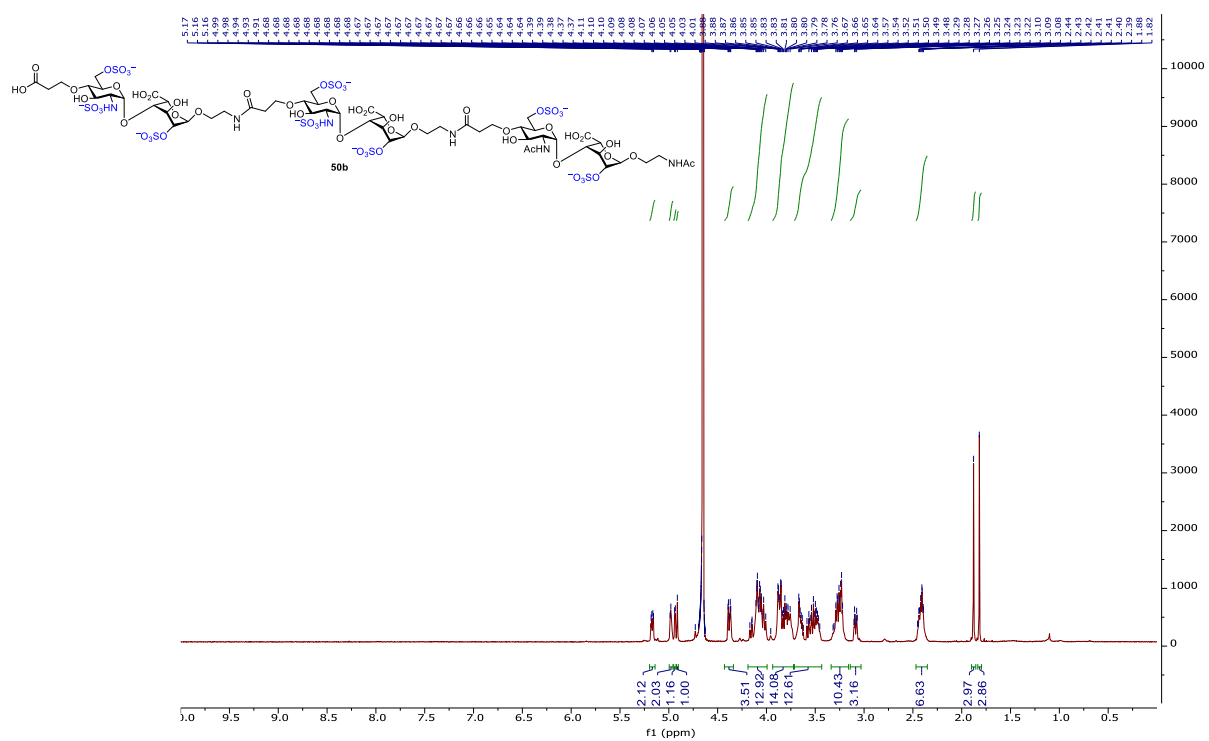


Figure 2.87. ^1H -NMR of **50b** (500 MHz D_2O)

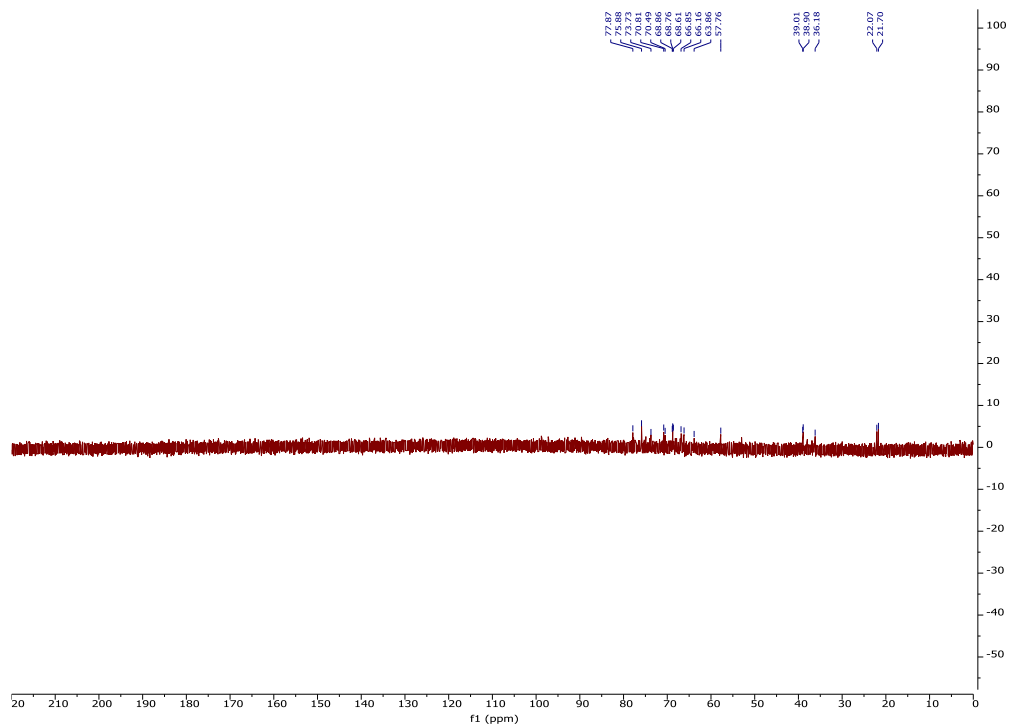


Figure 2.88. ¹³C-NMR of **50b** (125 MHz D₂O)

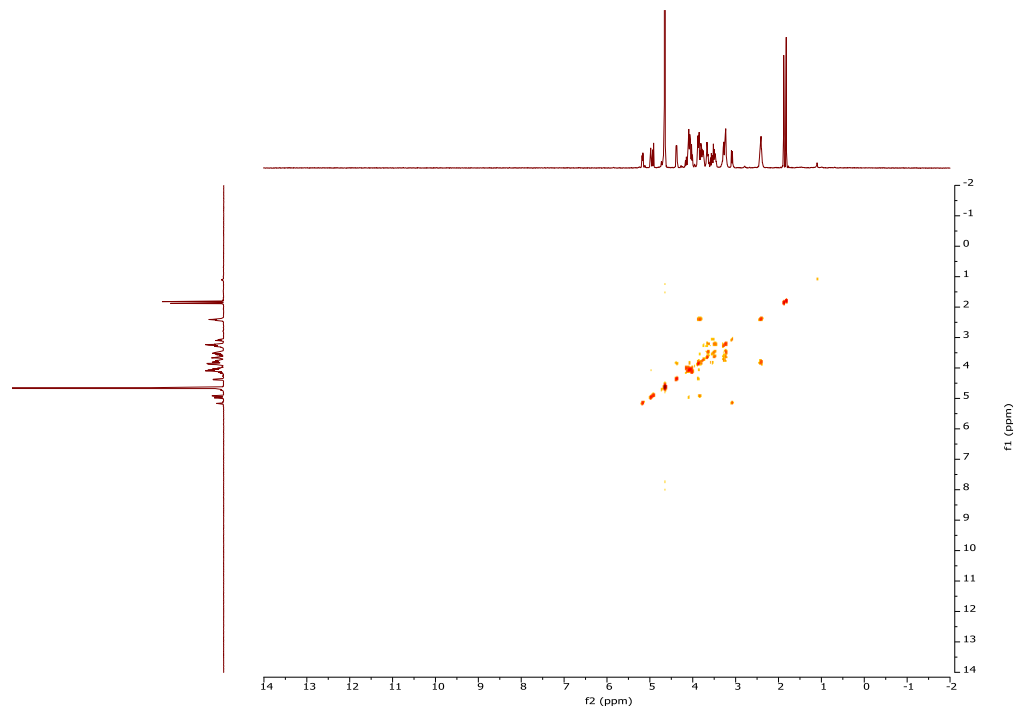


Figure 2.89. ¹H-¹H gCOSY of **50b** (500 MHz D₂O)

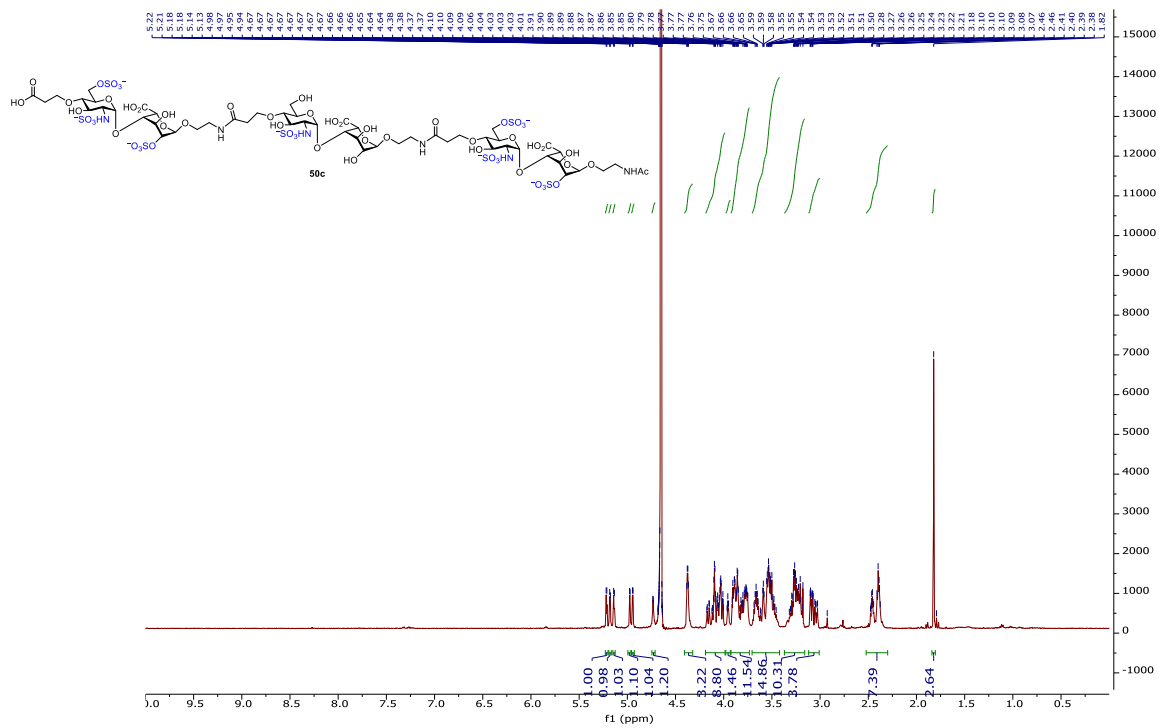


Figure 2.90. $^1\text{H-NMR}$ of 50c (500 MHz D_2O)

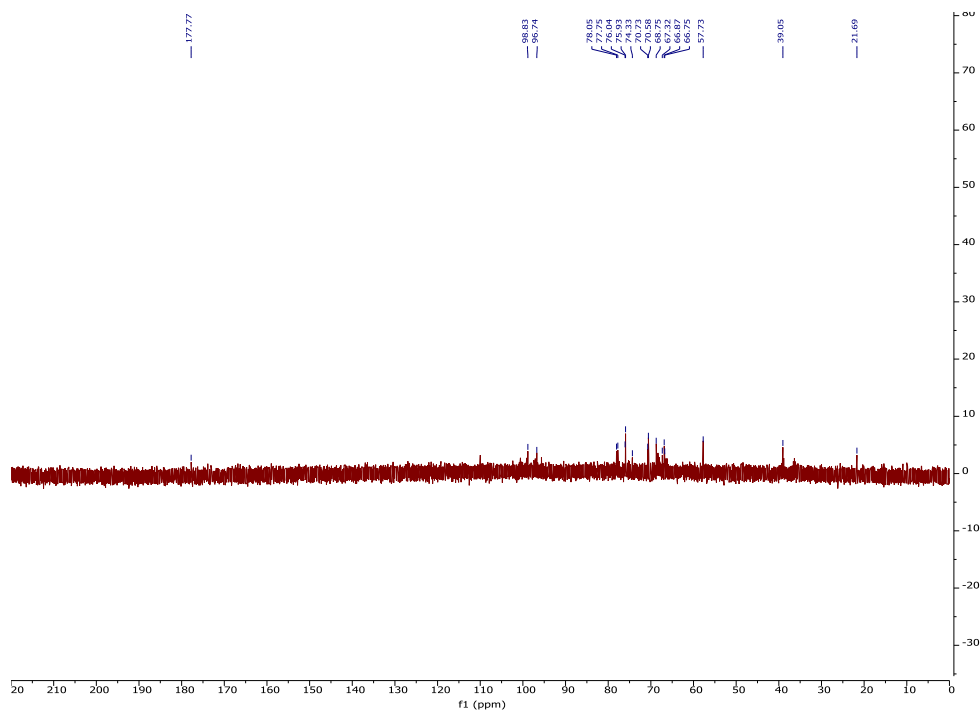


Figure 2.91. $^{13}\text{C-NMR}$ of 50c (125 MHz D_2O)

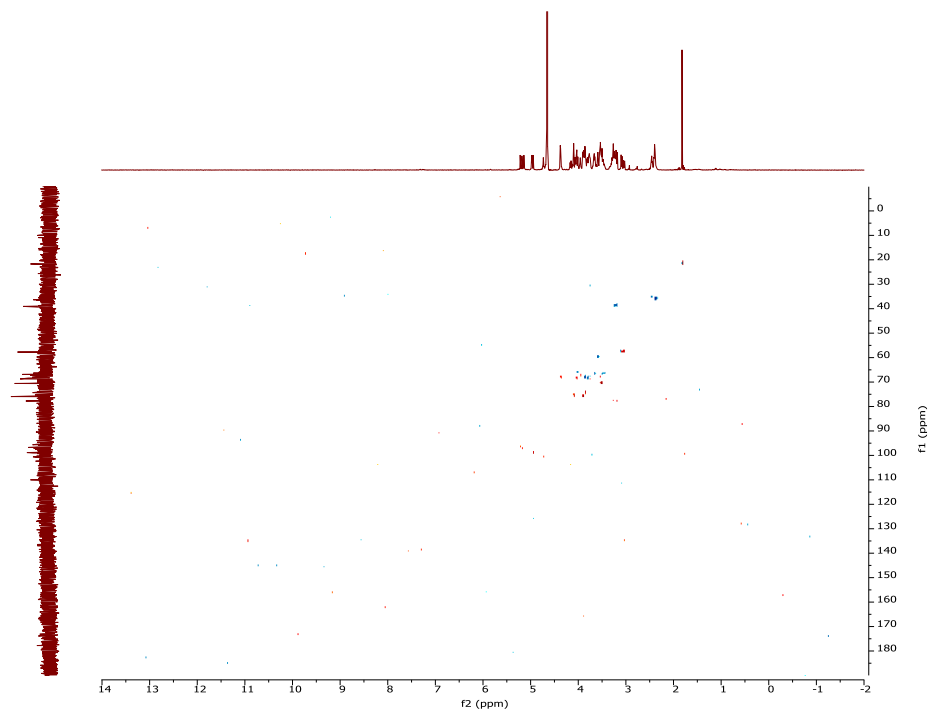


Figure 2.92. ^1H - ^{13}C gHSQCAD of **50c** (500 MHz D_2O)

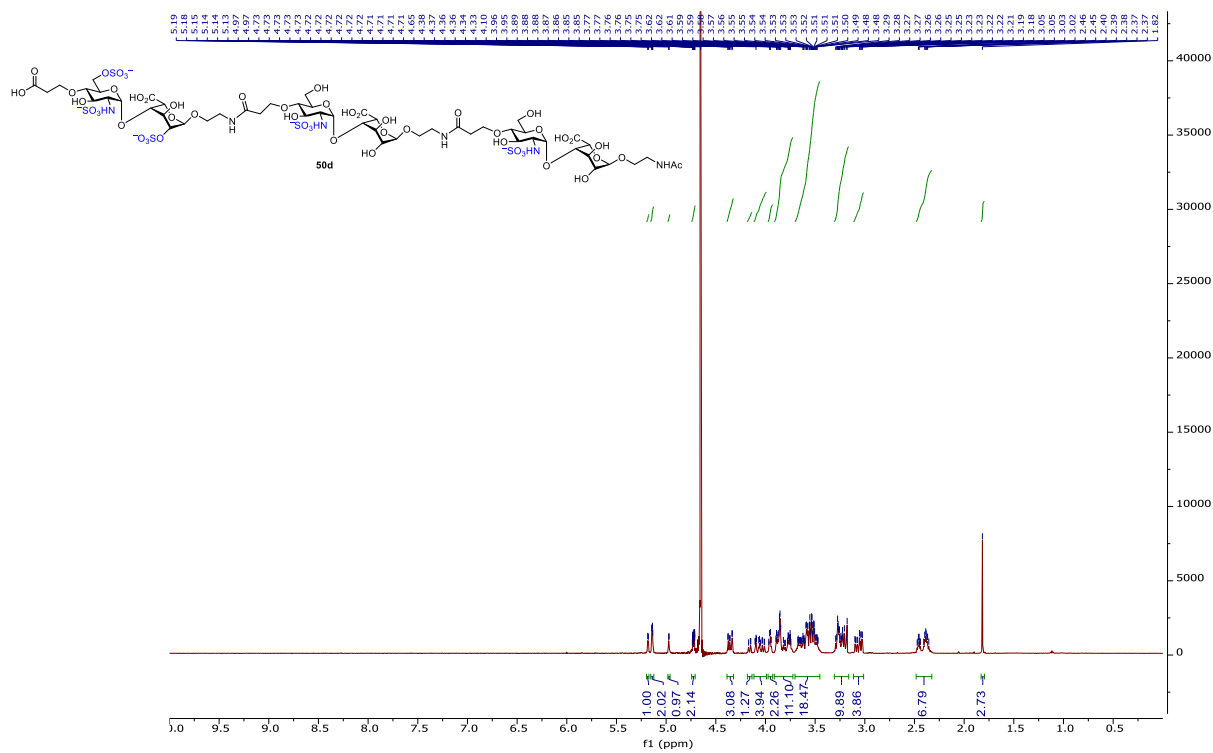


Figure 2.93. ^1H -NMR of **50d** (500 MHz D_2O)

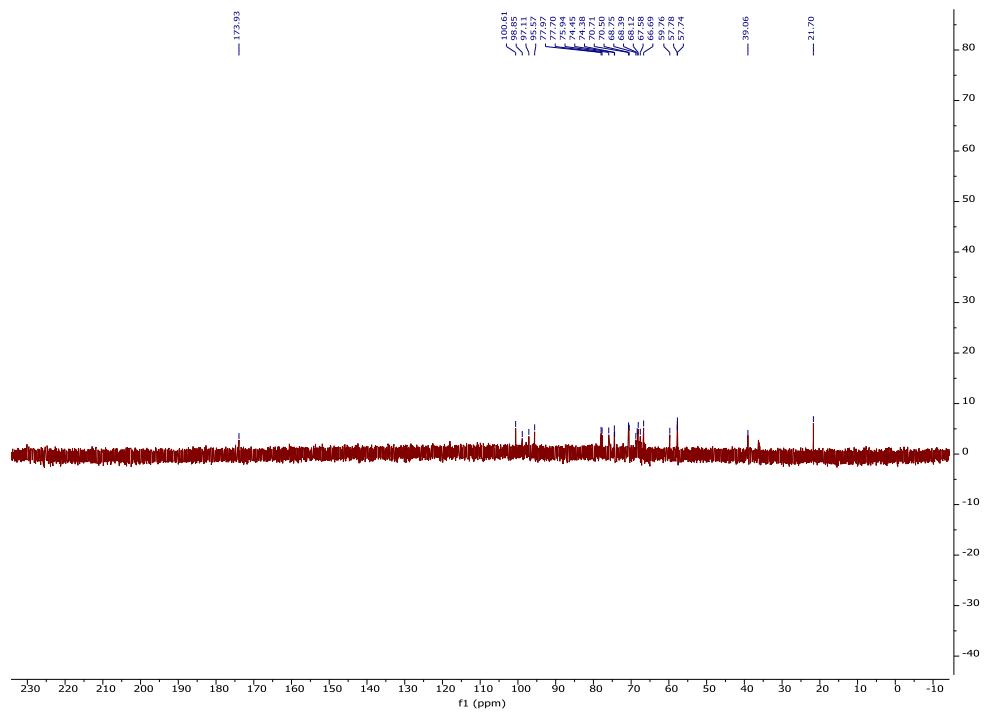


Figure 2.94. ^{13}C -NMR of **50d** (125 MHz D_2O)

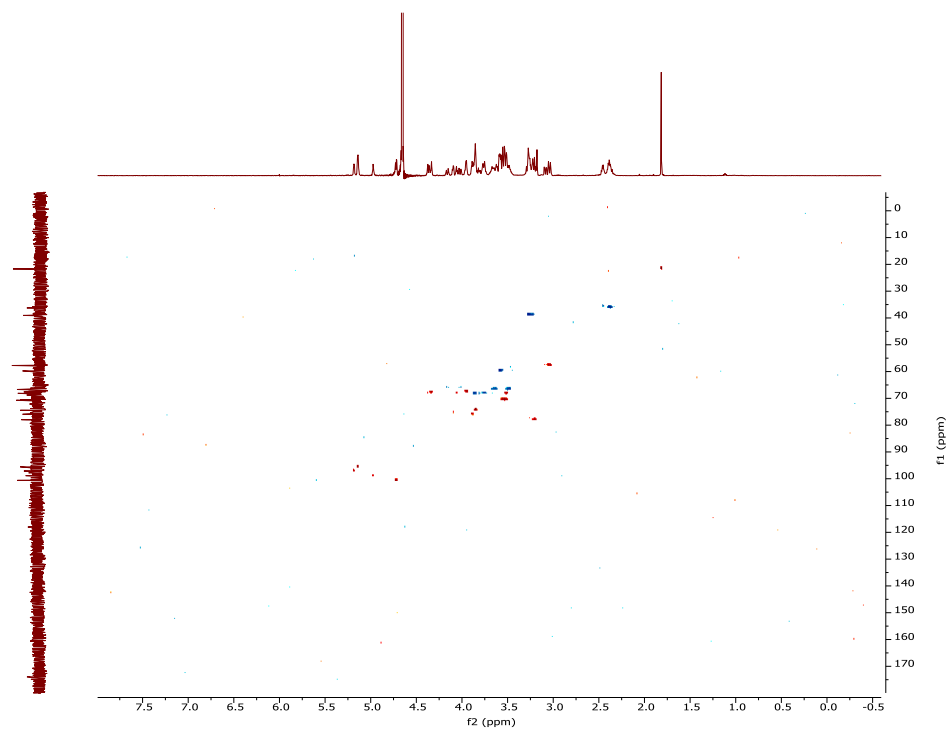
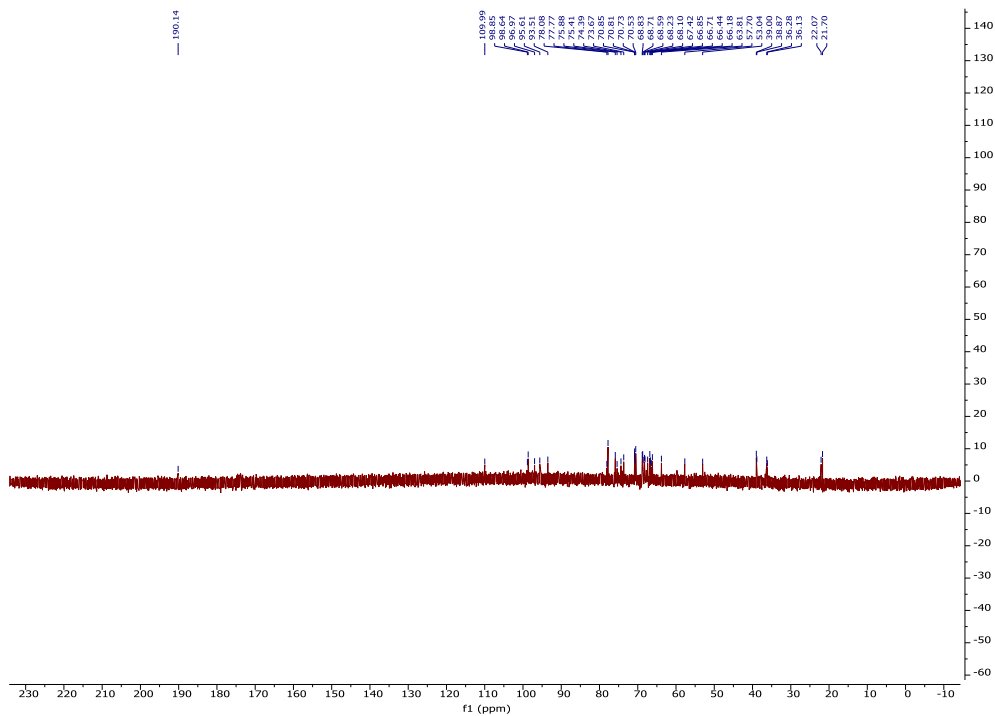
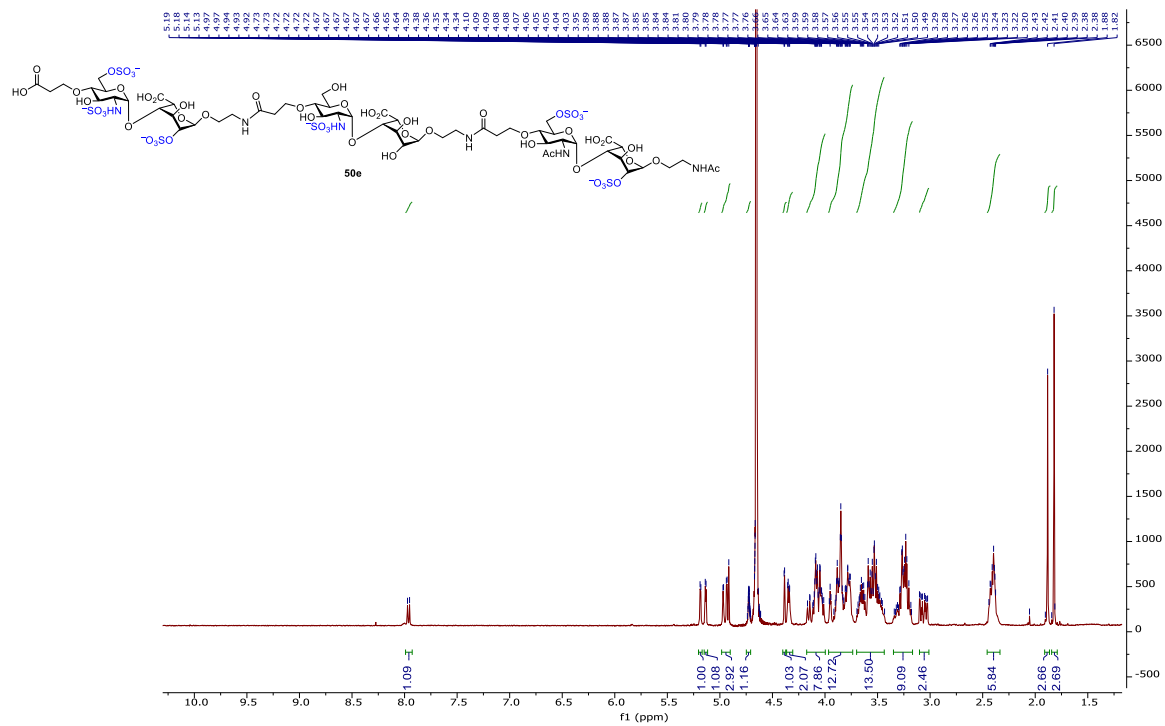


Figure 2.95. ^1H - ^{13}C gHSQCAD of **50d** (500 MHz D_2O)



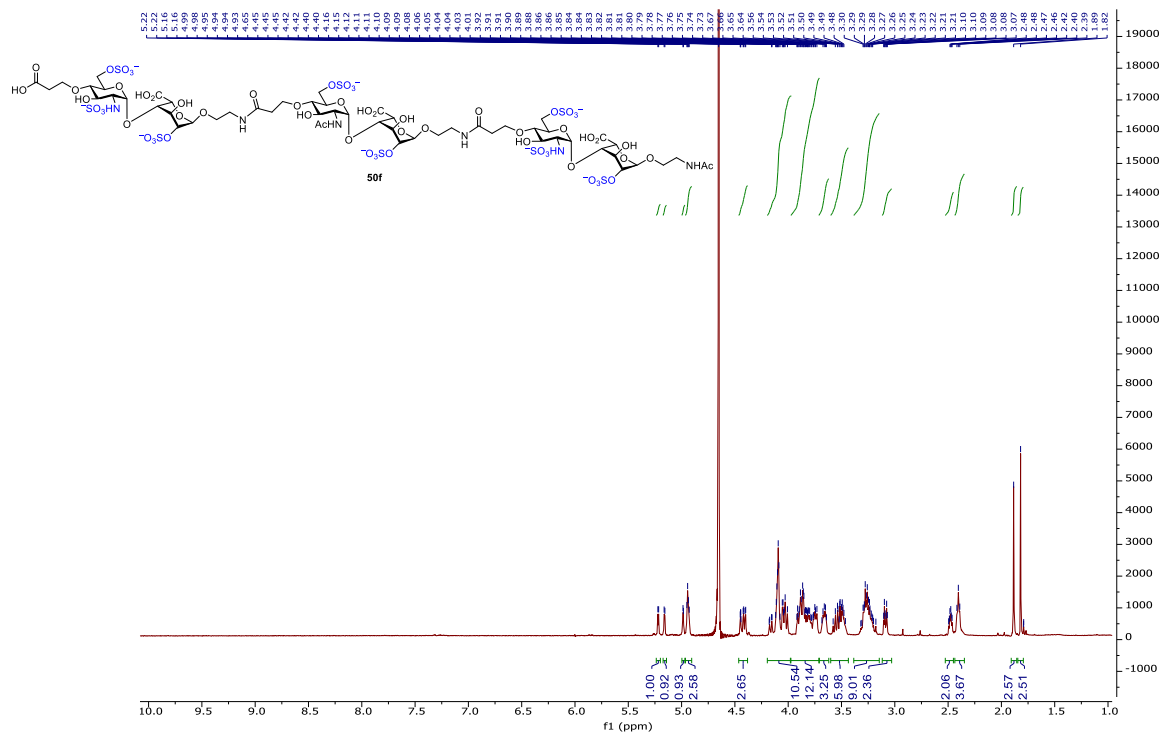


Figure 2.98. $^1\text{H-NMR}$ of **50f** (500 MHz D_2O)

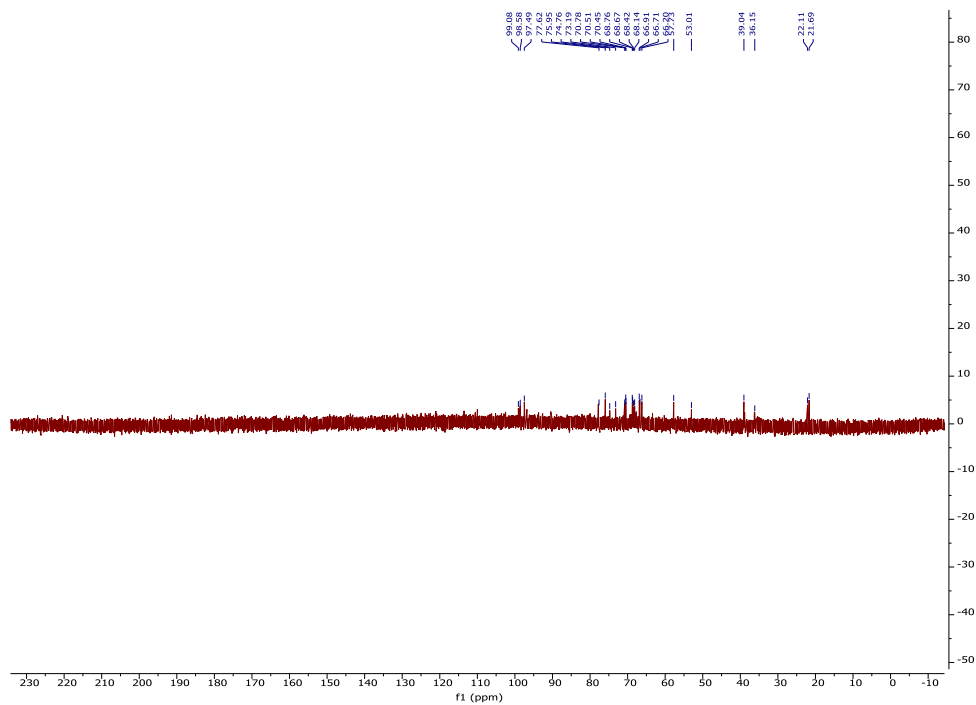


Figure 2.99. $^{13}\text{C-NMR}$ of **50f** (125 MHz D_2O)

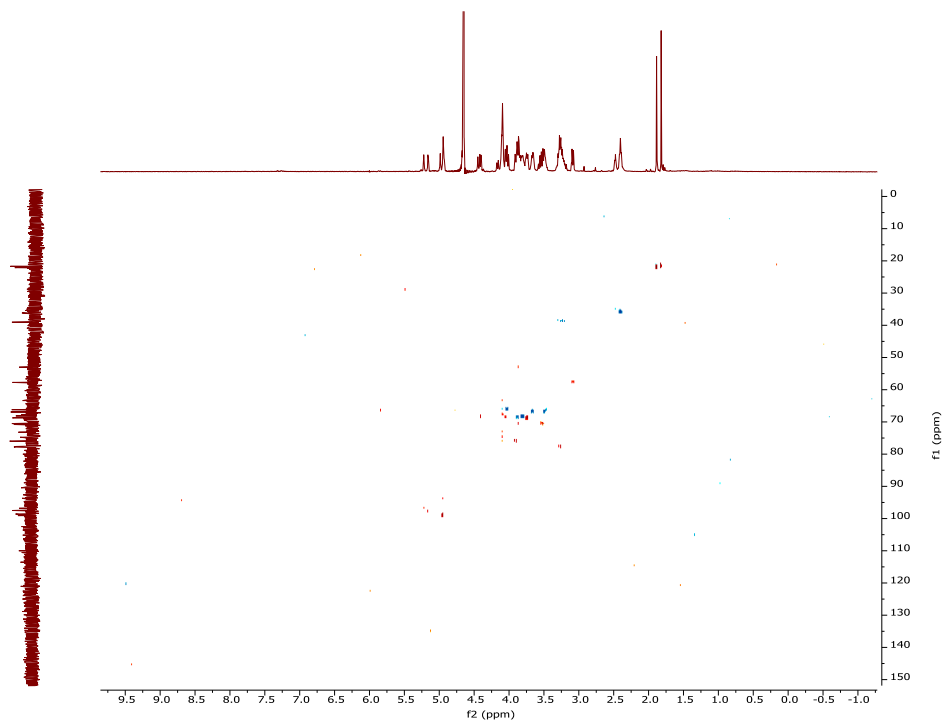


Figure 2.100. ^1H - ^{13}C gHSQCAD of **50f** (500 MHz D_2O)

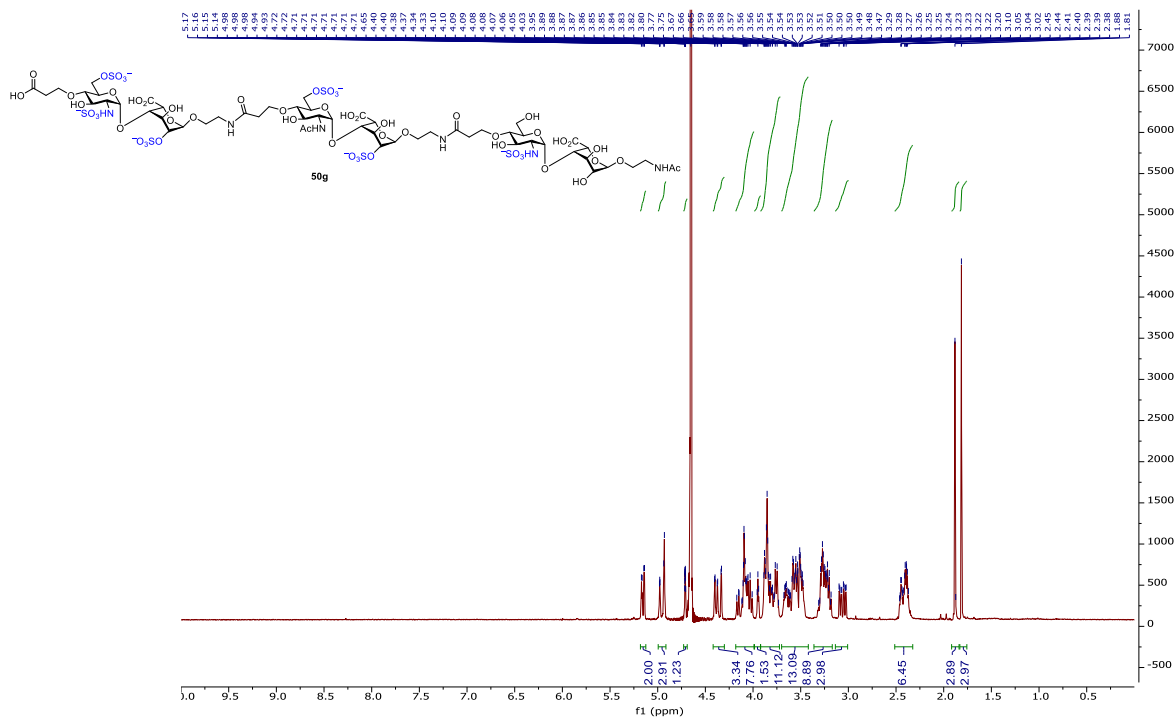


Figure 2.101. ^1H -NMR of **50g** (500 MHz D_2O)

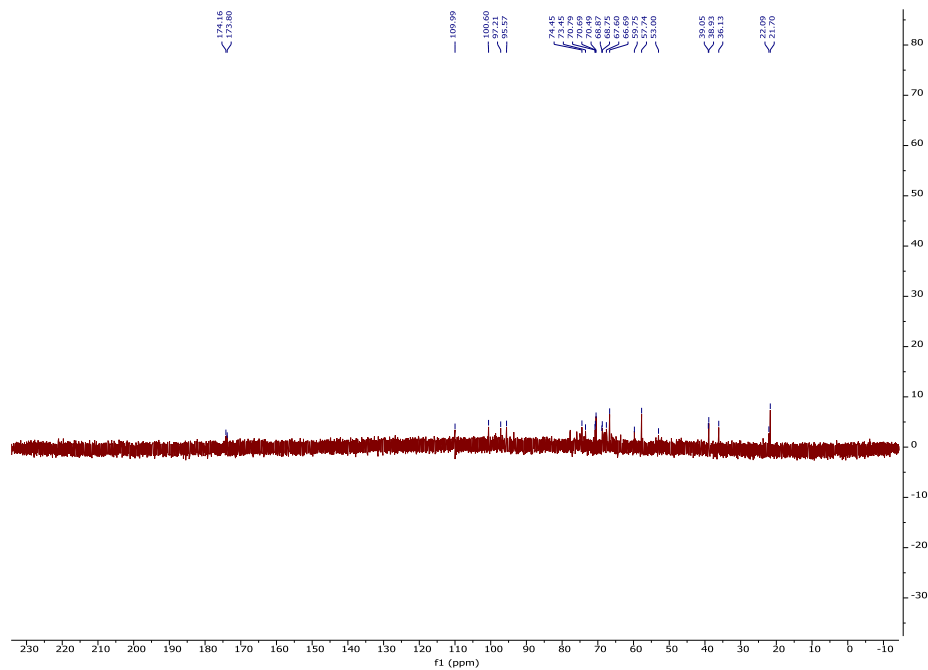


Figure 2.102. ^{13}C -NMR of **50g** (125 MHz D_2O)

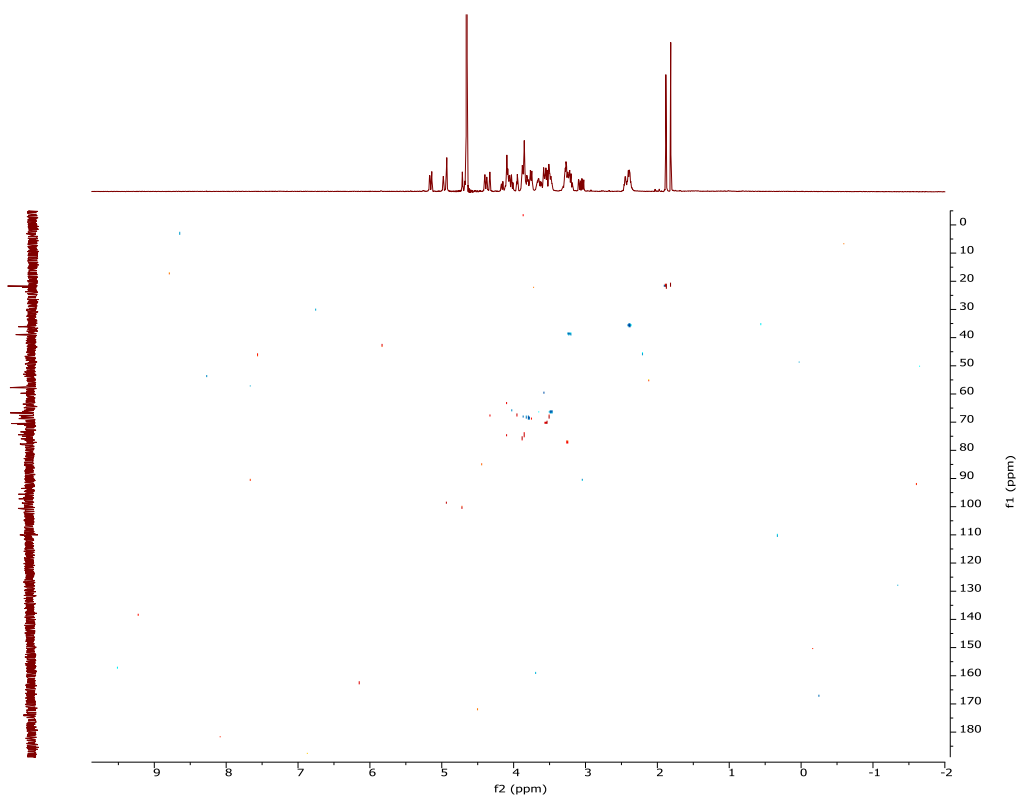


Figure 2.103. ^1H - ^{13}C gHSQCAD of **50g** (500 MHz D_2O)

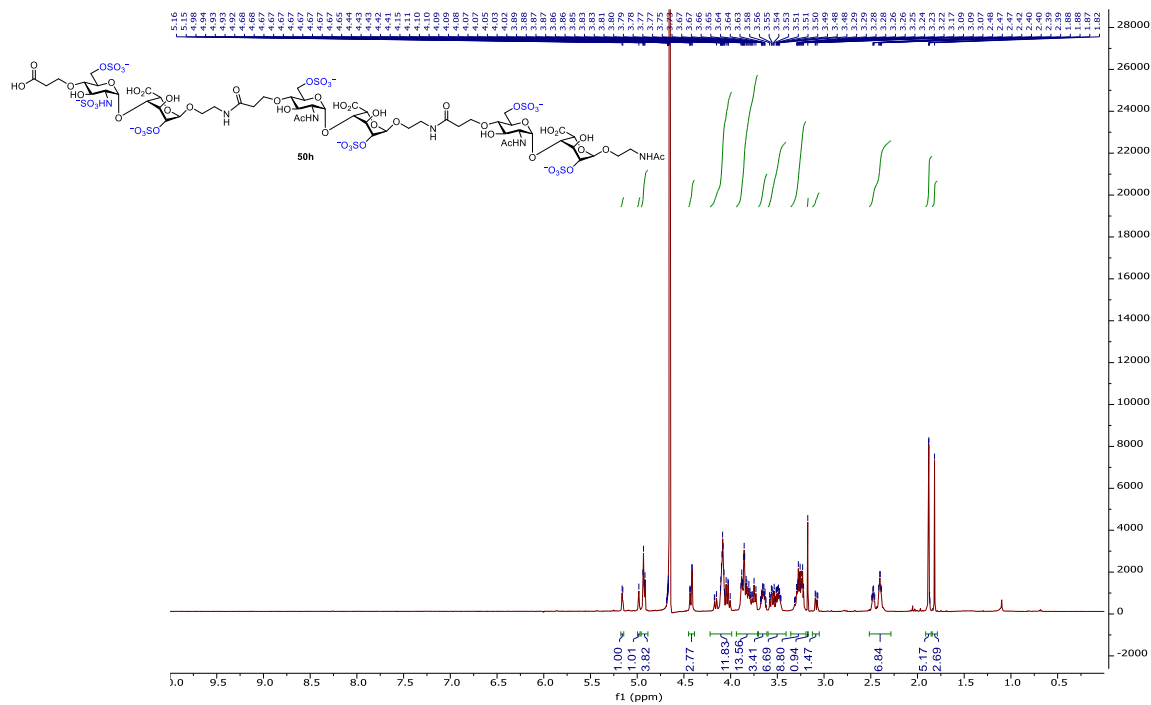


Figure 2.104. $^1\text{H-NMR}$ of 50h (500 MHz D_2O)

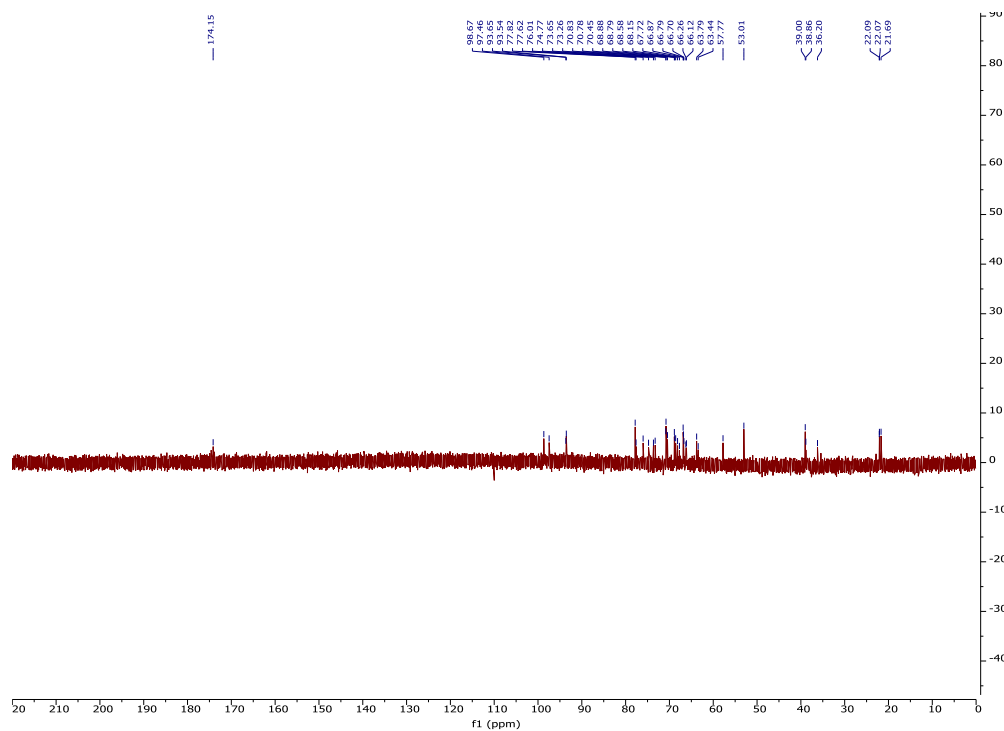


Figure 2.105. $^{13}\text{C-NMR}$ of 50h (125 MHz D_2O)

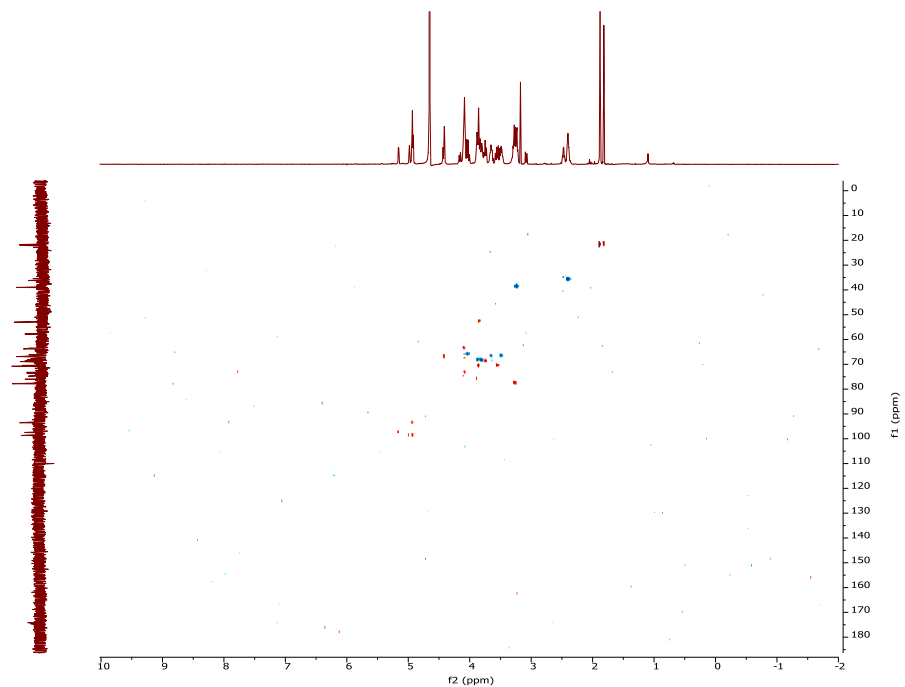


Figure 2.106. ^1H - ^{13}C gHSQCAD of **50h** (500 MHz D_2O)

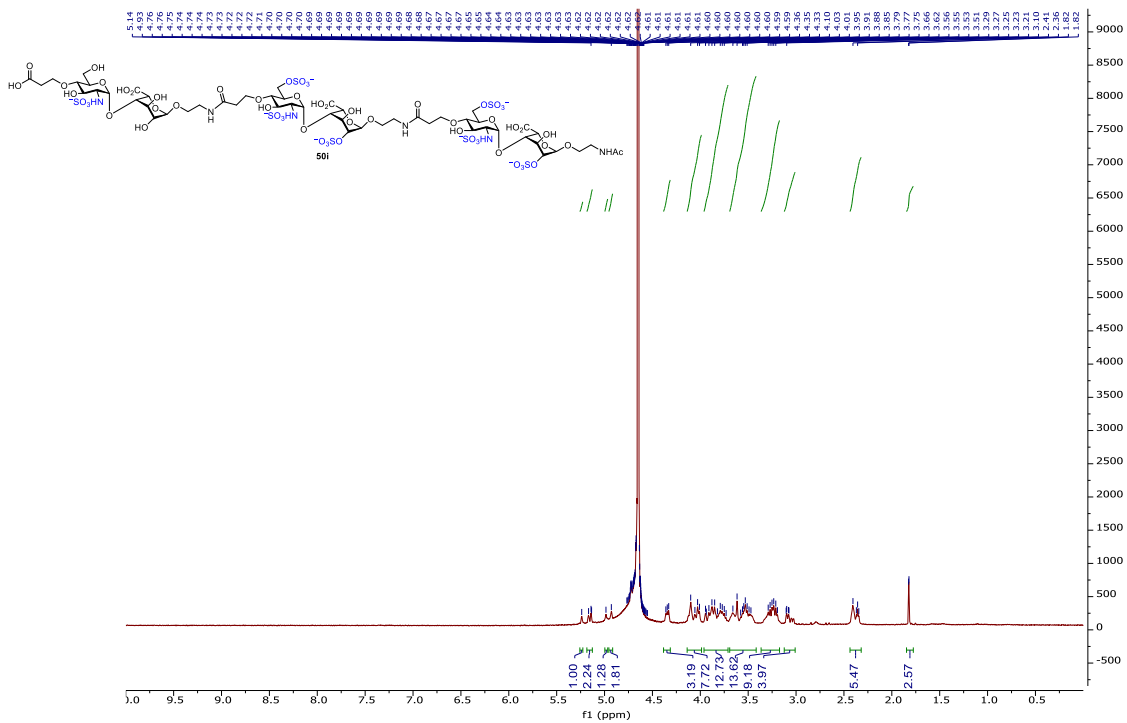


Figure 2.107. ^1H -NMR of **50i** (500 MHz D_2O)

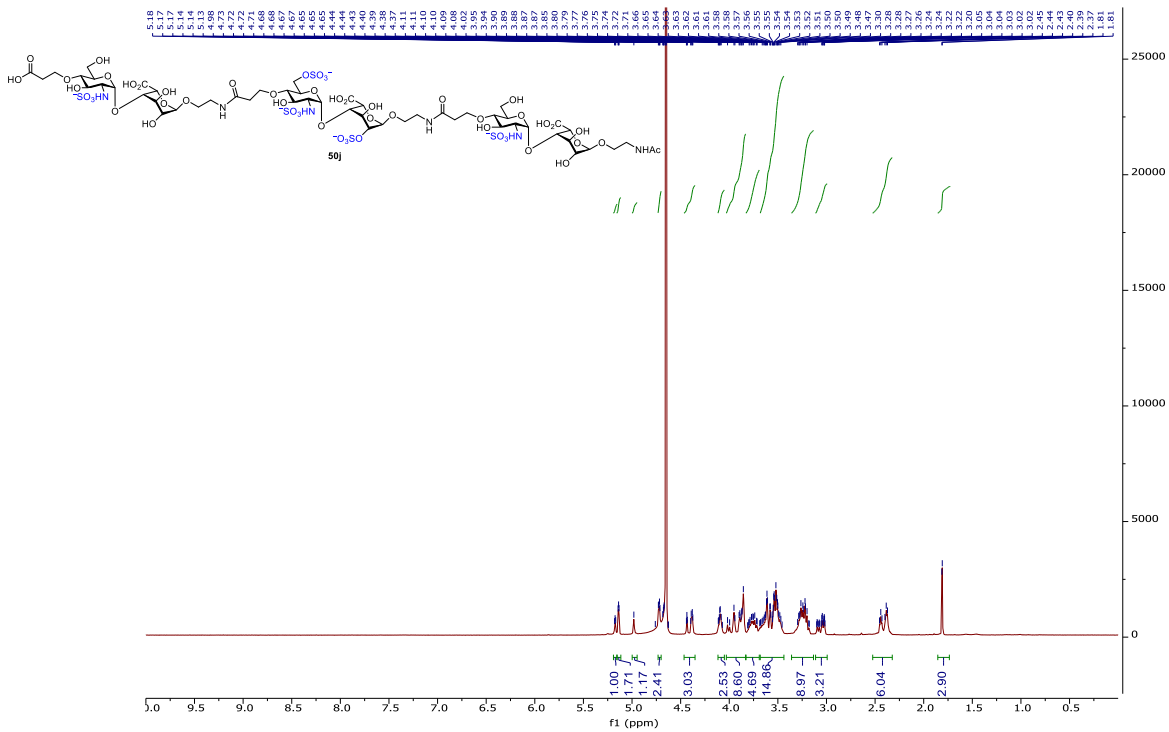


Figure 2.108. ¹H-NMR of 50j (500 MHz D₂O)

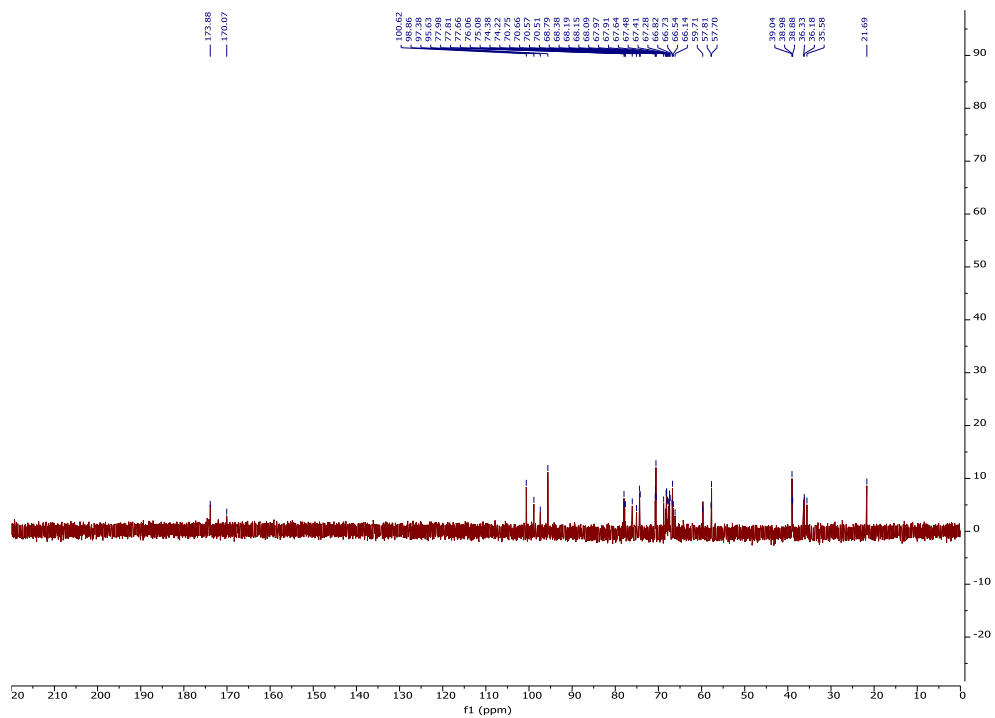


Figure 2.109. ¹³C-NMR of 50j (125 MHz D₂O)

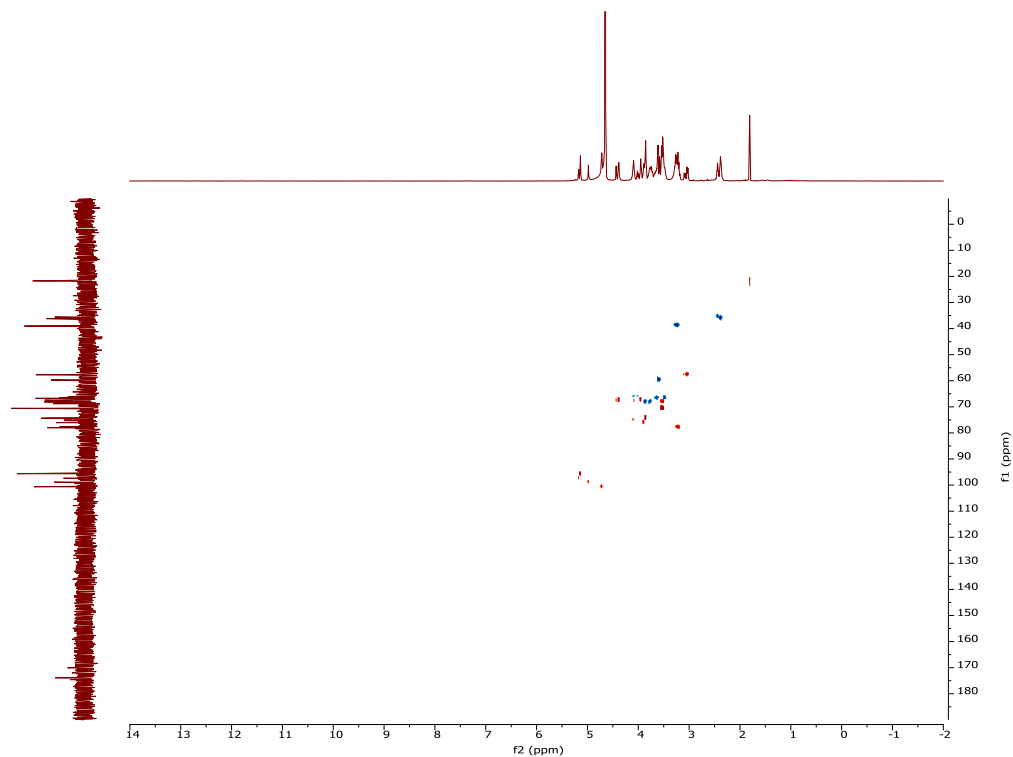


Figure 2.110. ^1H - ^{13}C gHSQCAD of **50j** (500 MHz D_2O)

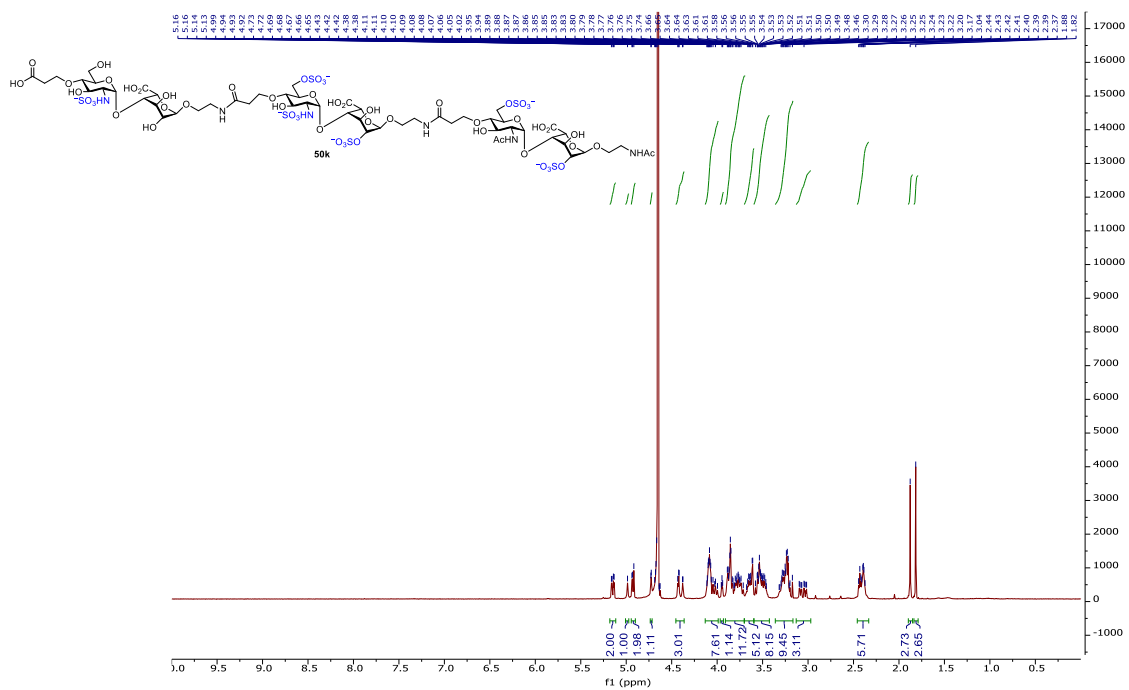


Figure 2.111. ^1H -NMR of **50k** (500 MHz D_2O)

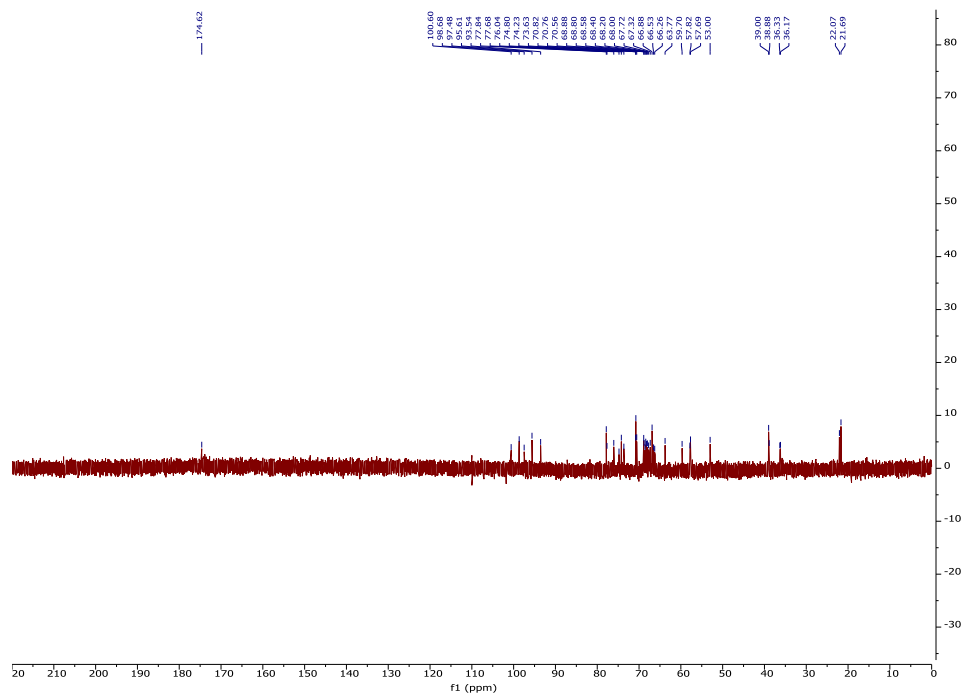


Figure 2.112. ^{13}C -NMR of **50k** (125 MHz D_2O)

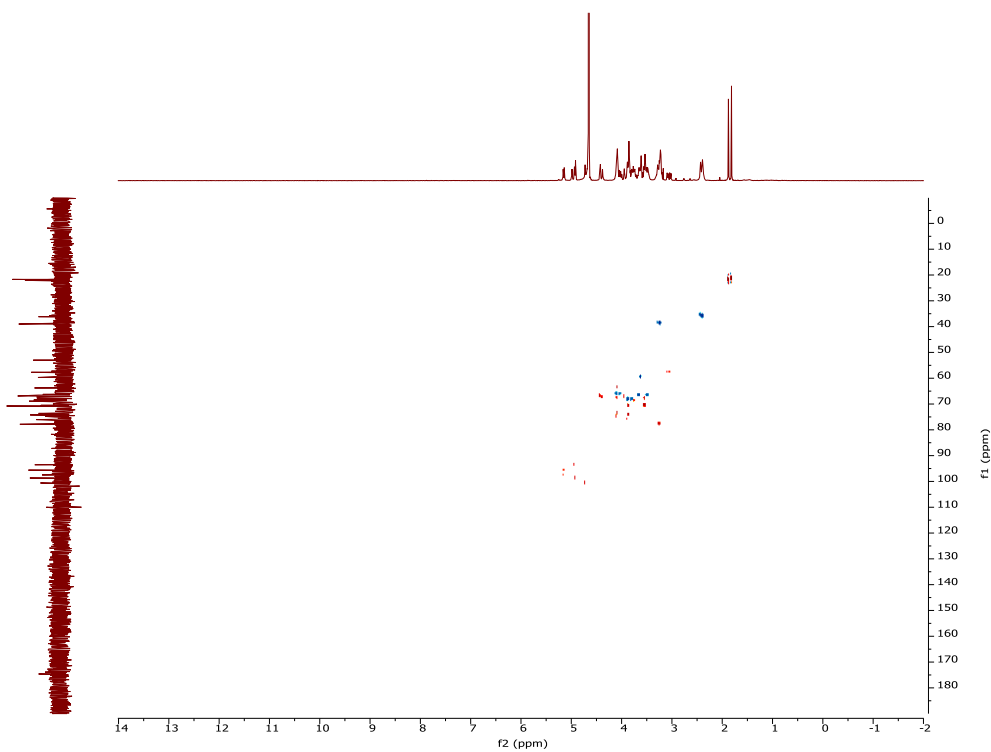


Figure 2.113. ^1H - ^{13}C gHSQCAD of **50k** (500 MHz D_2O)

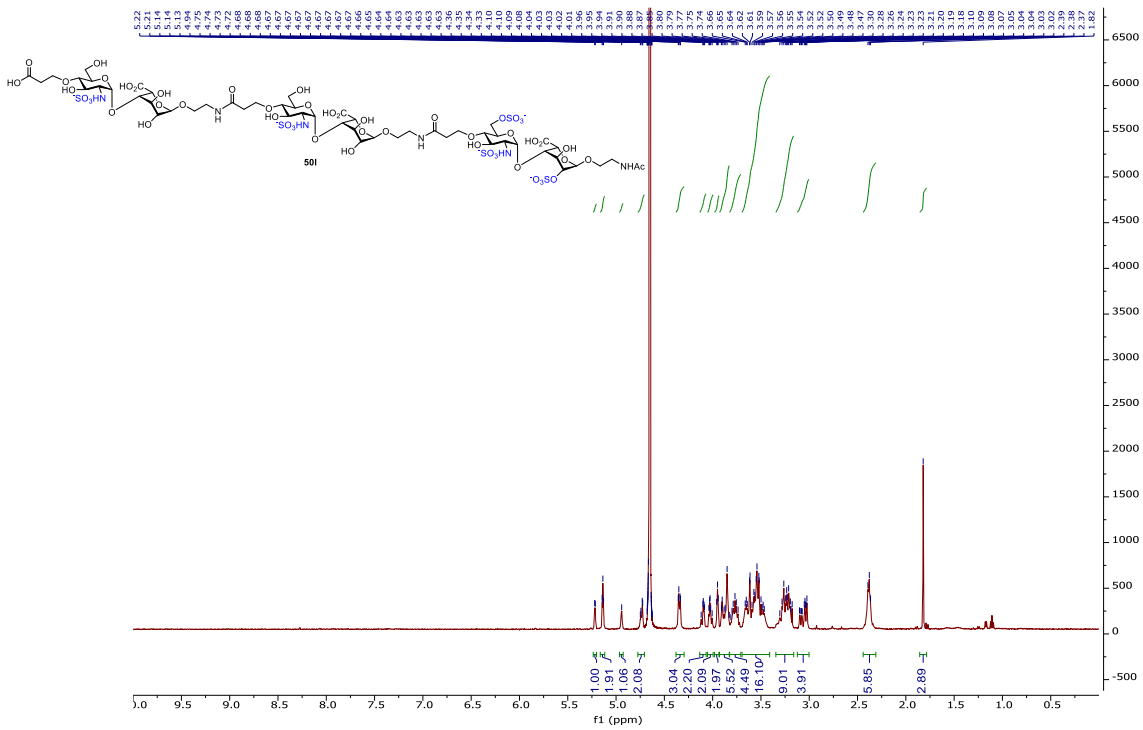


Figure 2.114. $^1\text{H-NMR}$ of **50l** (500 MHz D_2O)

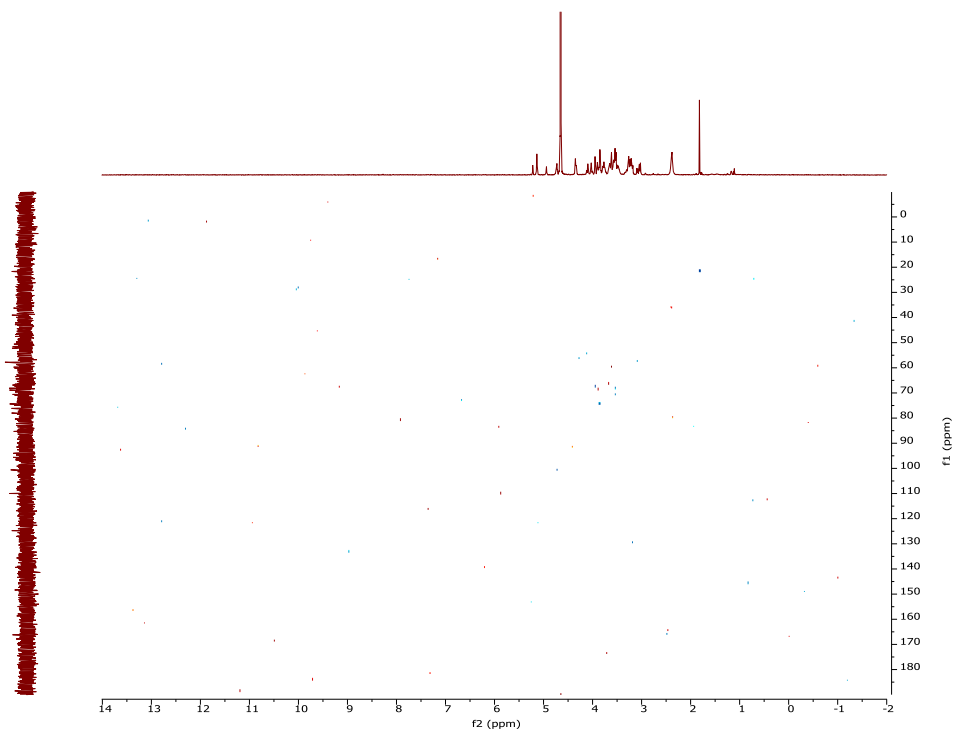


Figure 2.115. $^1\text{H-}^1\text{H}$ gCOSY of **50l** (500 MHz D_2O)

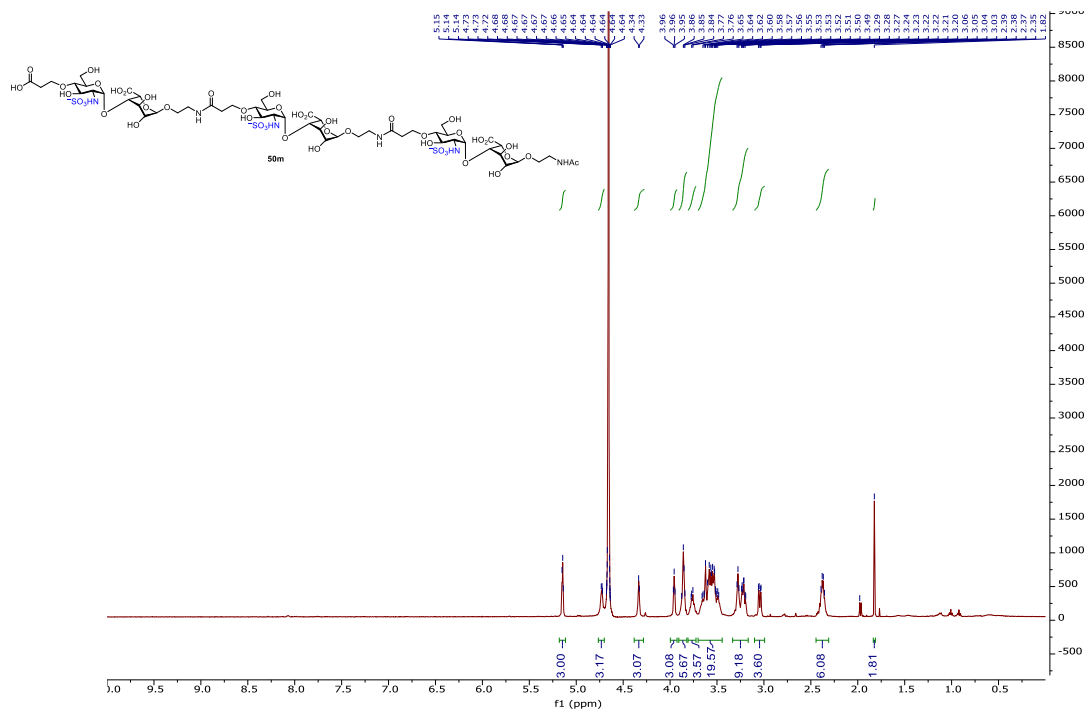


Figure 2.116. ¹H-NMR of 50m (500 MHz D₂O)

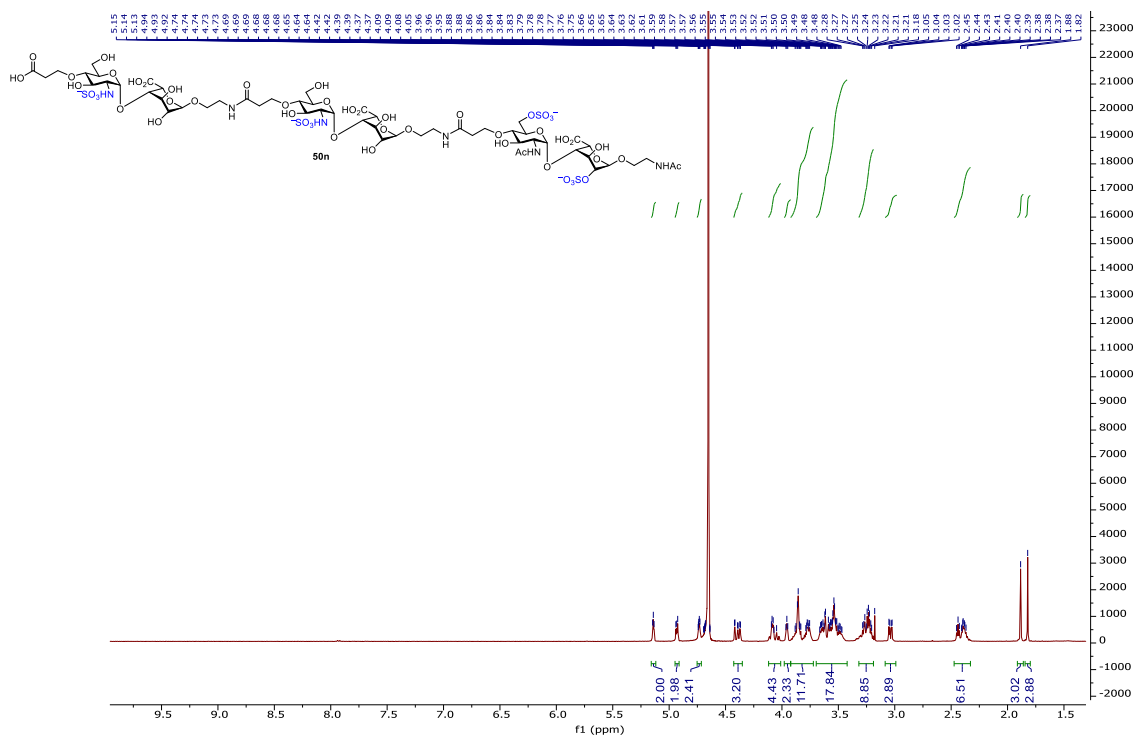


Figure 2.117. ¹H-NMR of 50n (500 MHz D₂O)

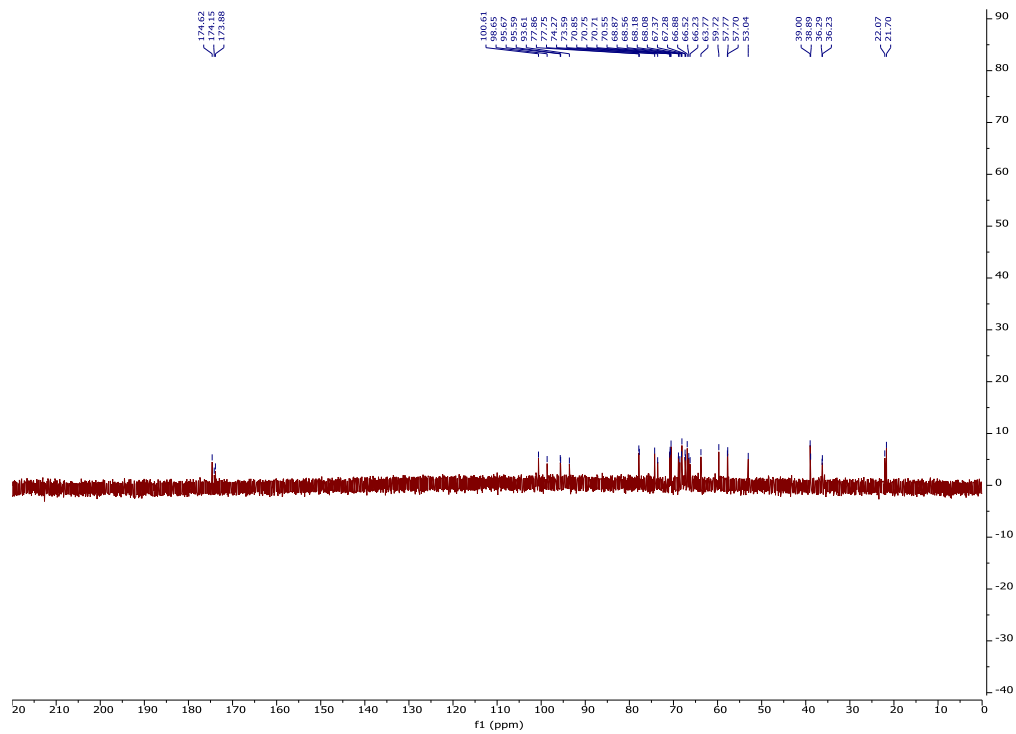


Figure 2.118. ^{13}C -NMR of **50n** (125 MHz D_2O)

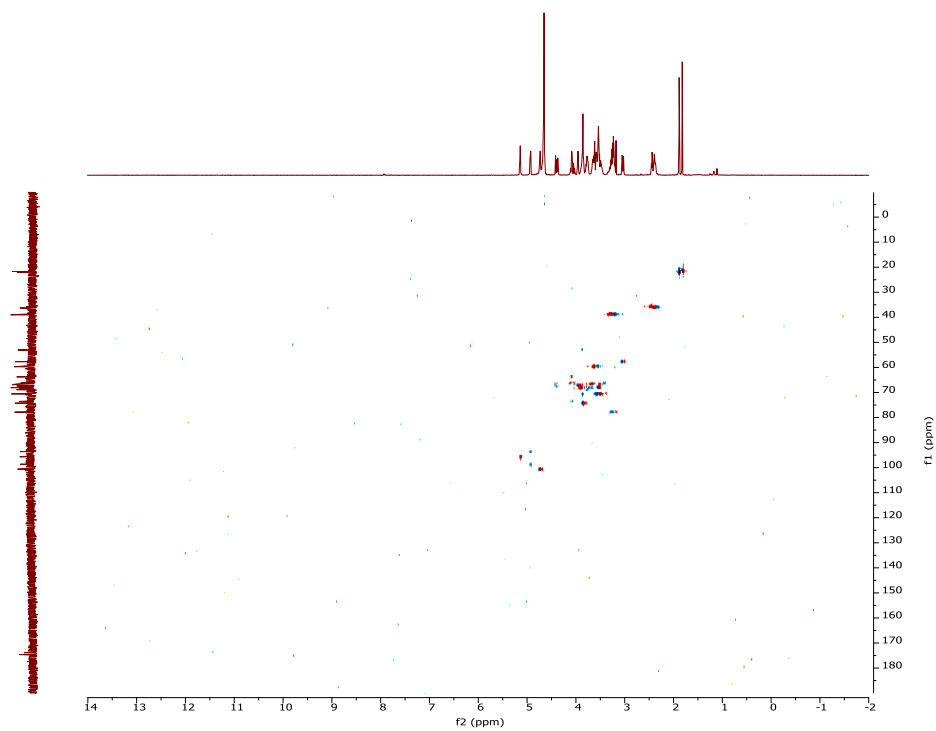


Figure 2.119. ^1H - ^{13}C gHSQCAD of **50n** (500 MHz D_2O)

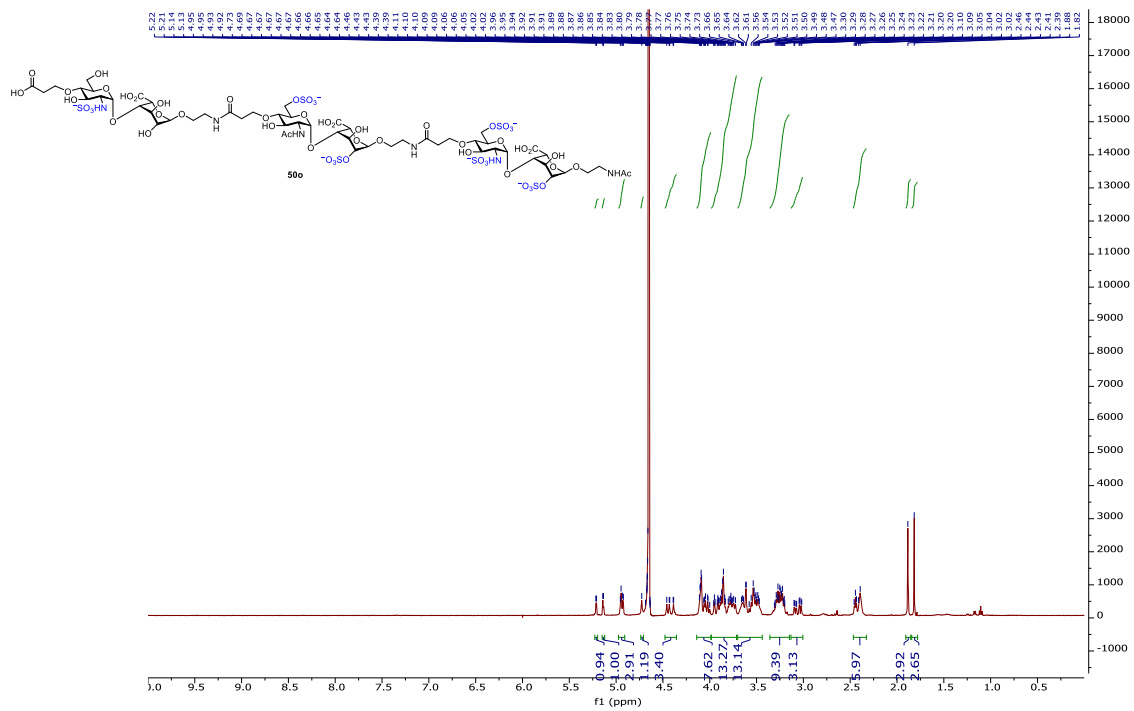


Figure 2.120. $^1\text{H-NMR}$ of **50o** (500 MHz D_2O)

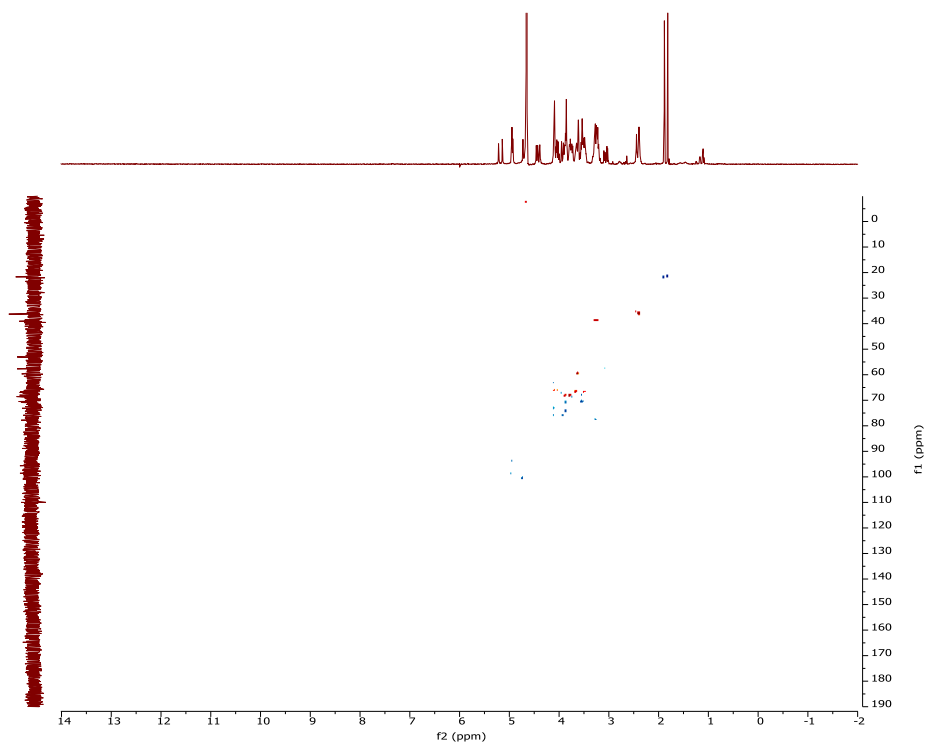


Figure 2.121. $^1\text{H-}^{13}\text{C}$ gHSQCAD of **50o** (500 MHz D_2O)

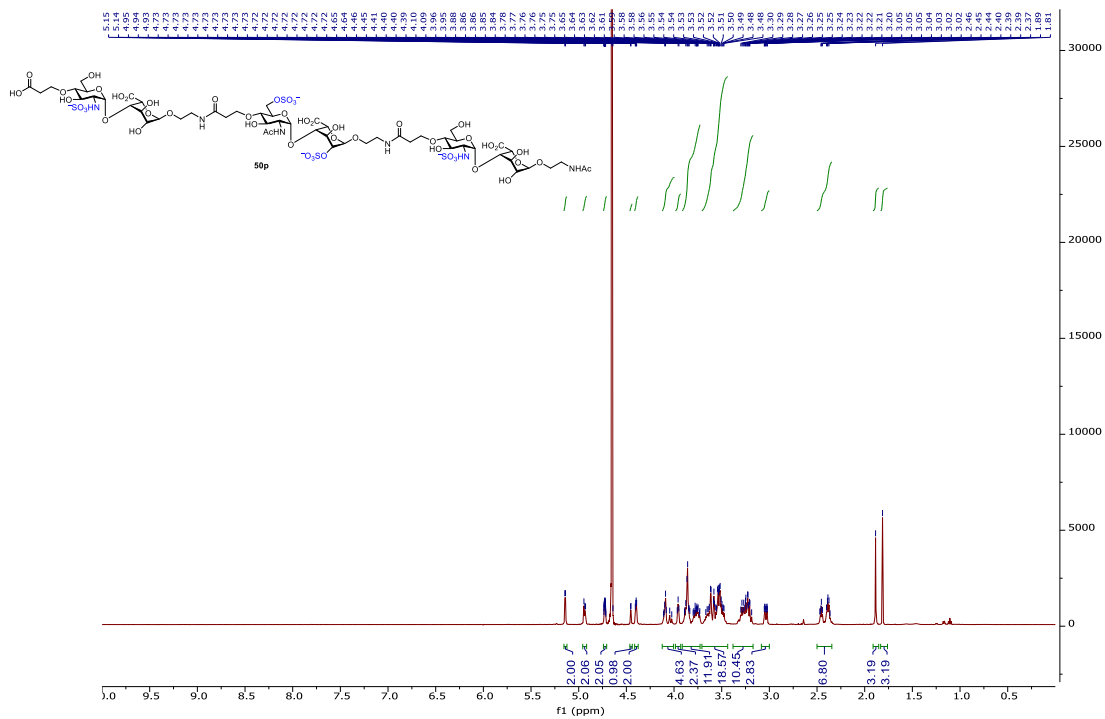


Figure 2.122. ¹H-NMR of 50p (500 MHz D₂O)

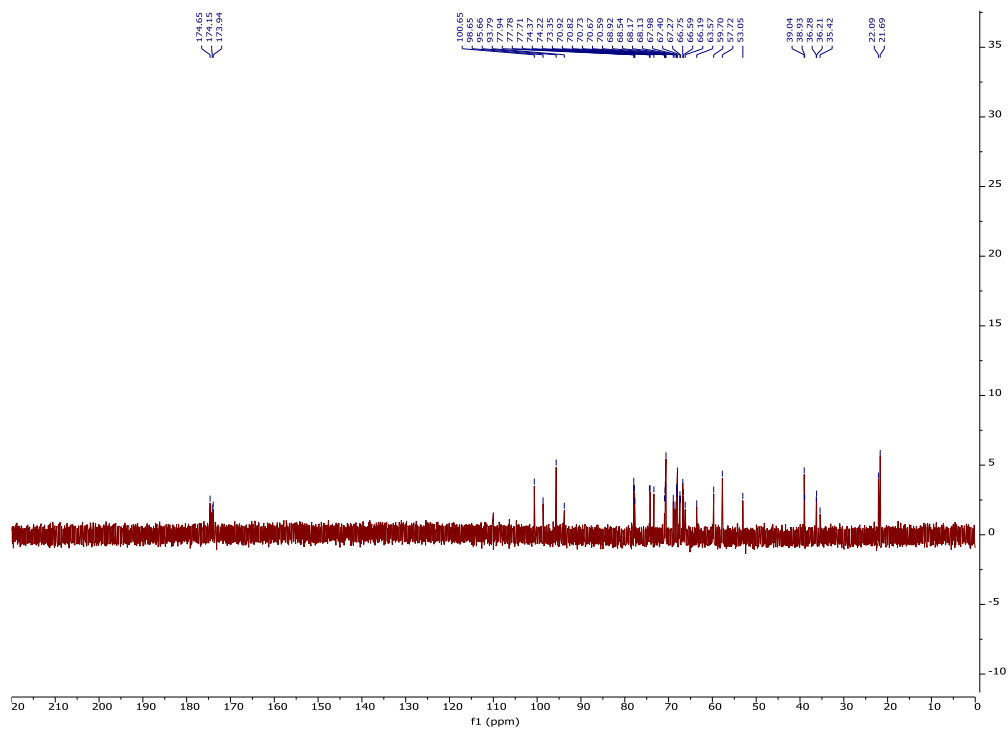


Figure 2.123. ¹³C-NMR of 50p (125 MHz D₂O)

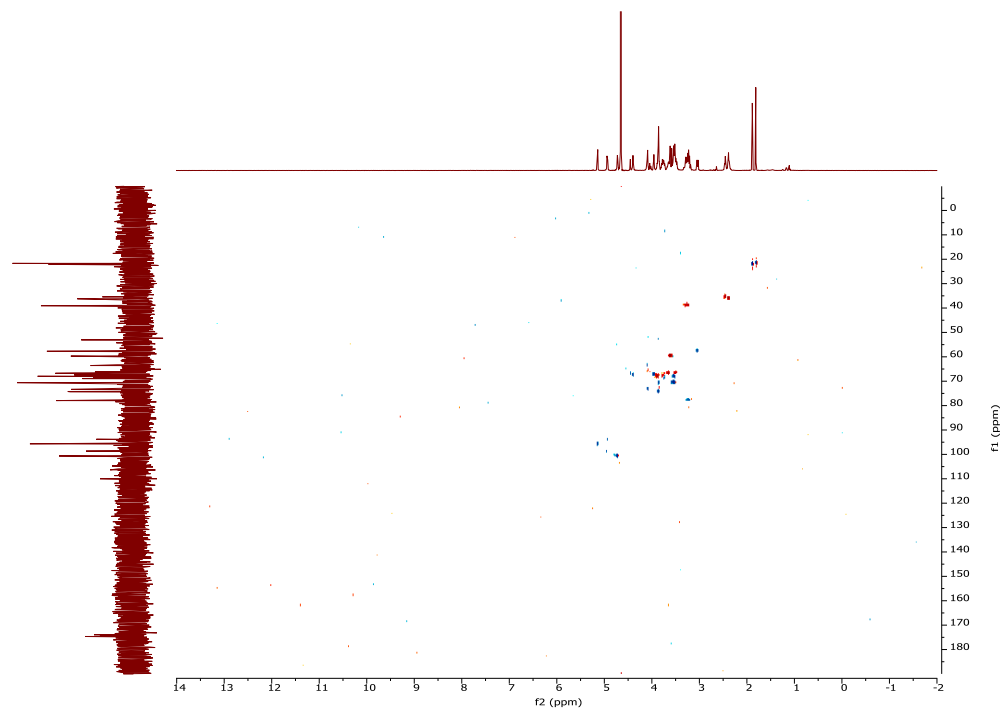


Figure 2.124. ^1H - ^{13}C gHSQCAD of **50p** (500 MHz D_2O)

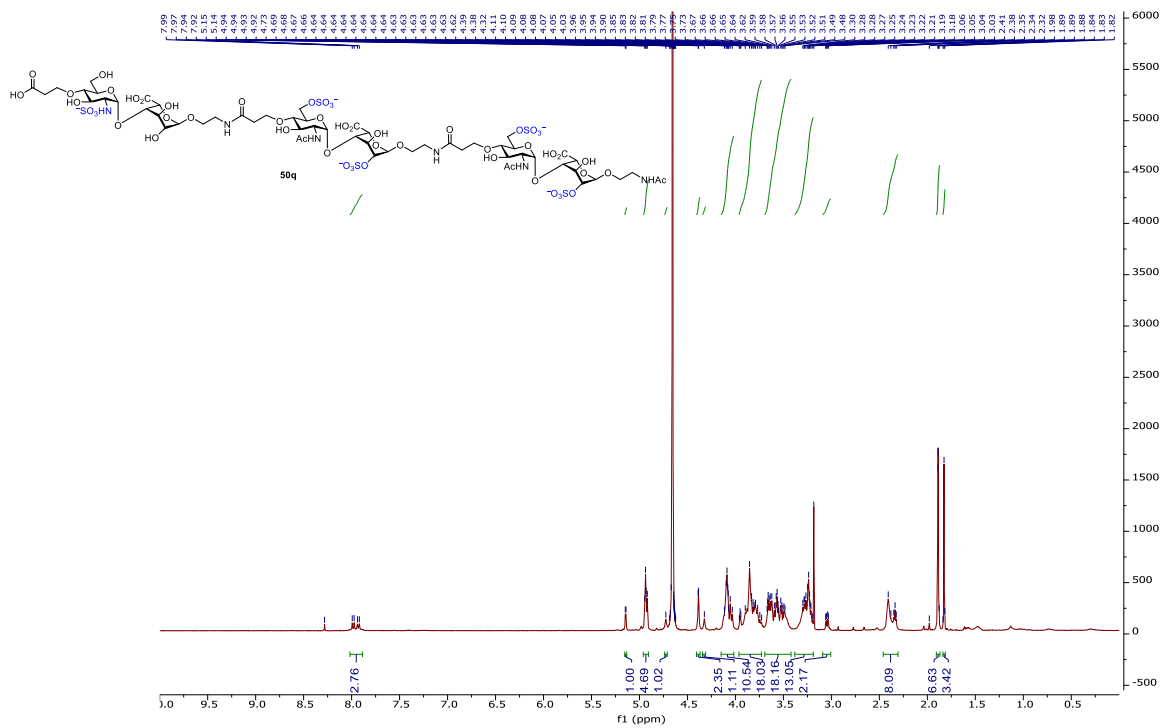


Figure 2.125. ^1H -NMR of **50q** (500 MHz D_2O)

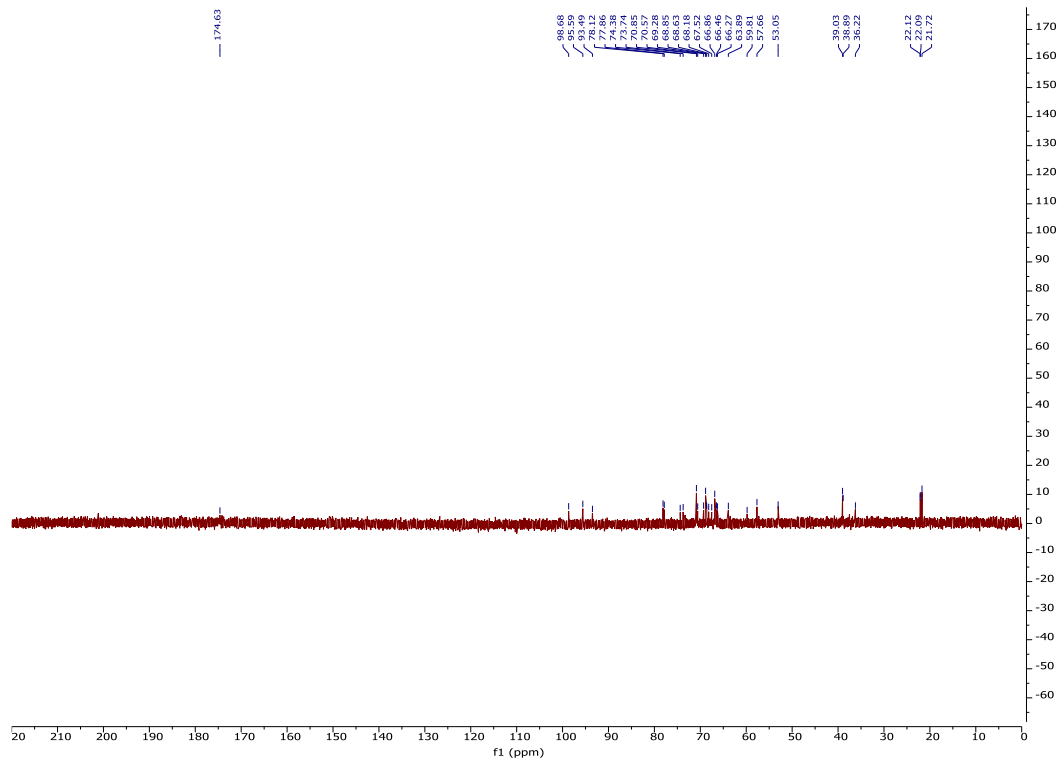


Figure 2.126. ^{13}C -NMR of 50q (125 MHz D_2O)

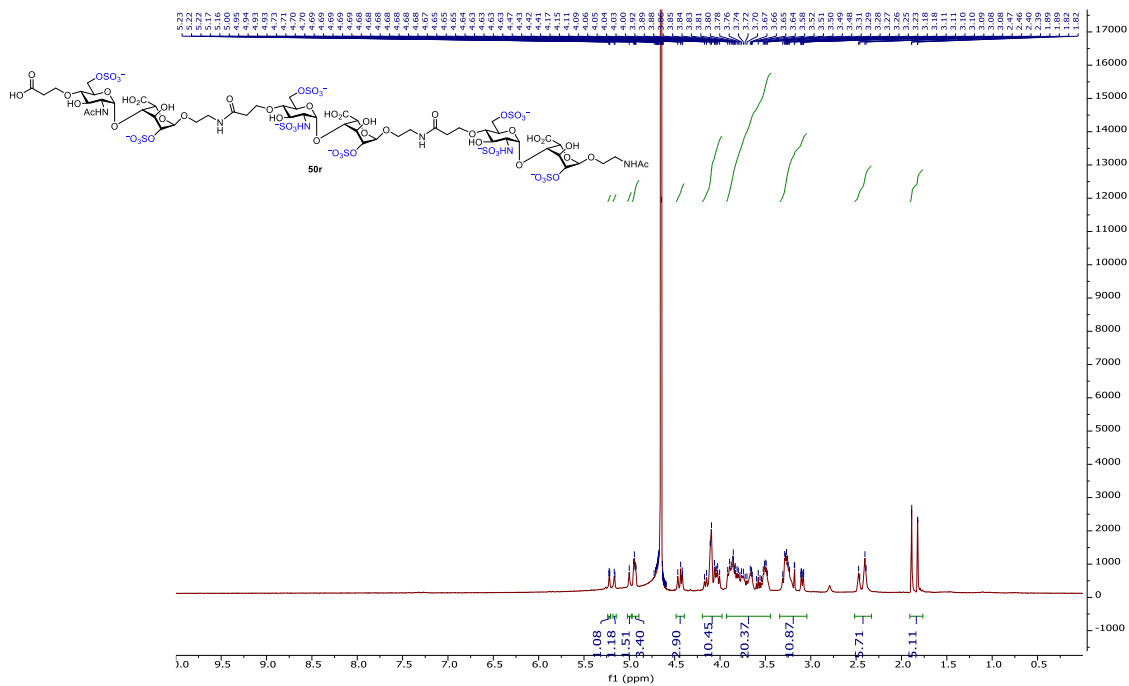


Figure 2.127. ^1H -NMR of 50r (500 MHz D_2O)

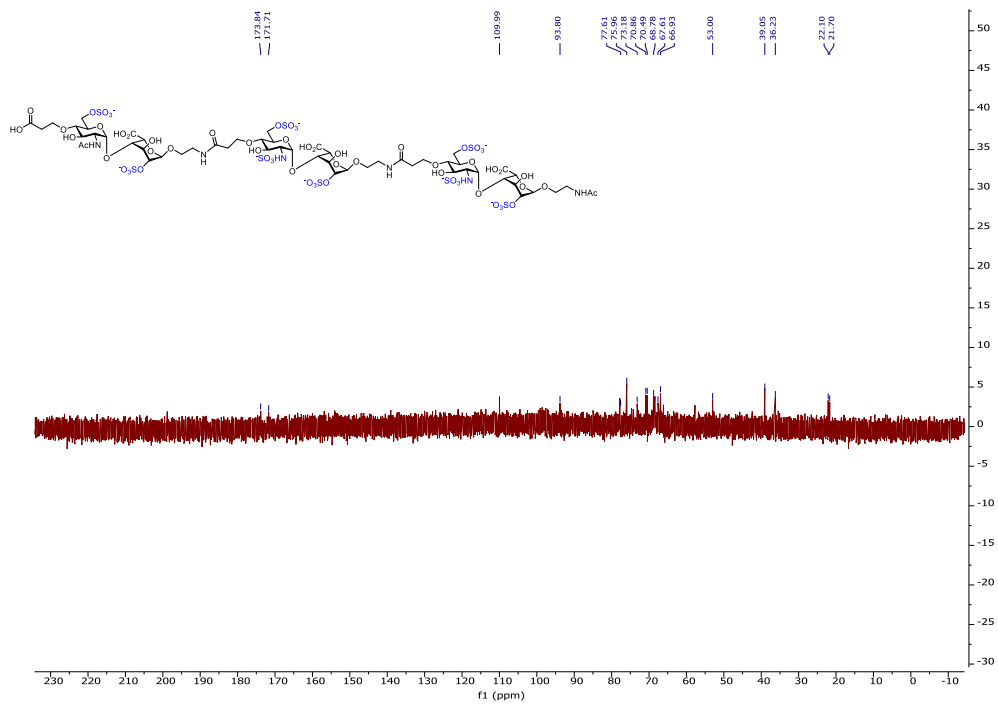


Figure 2.128. ^{13}C -NMR of **50r** (125 MHz D_2O)

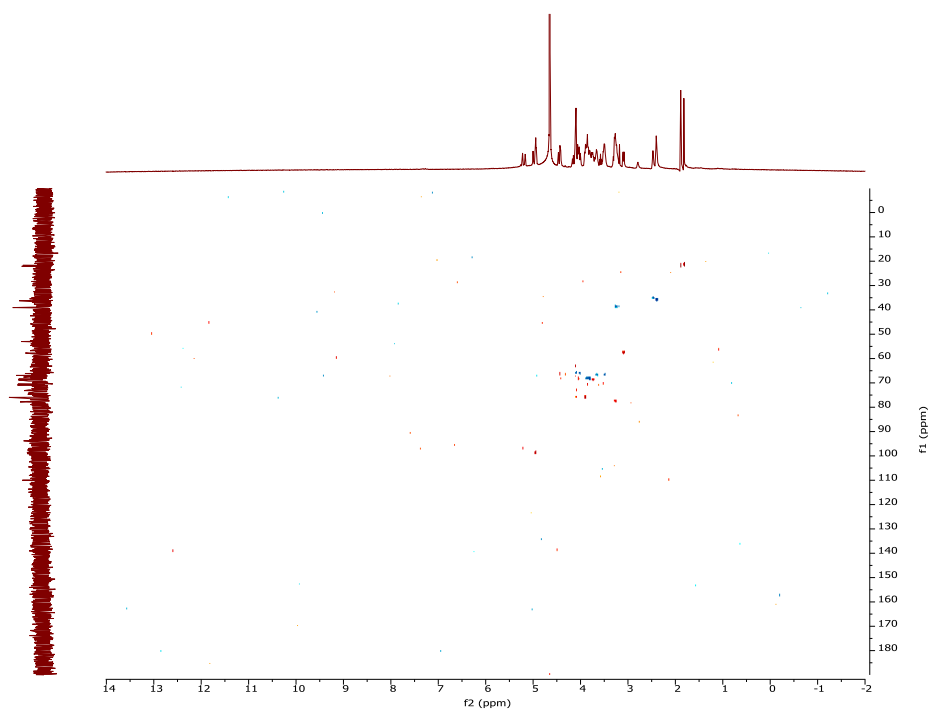


Figure 2.129. ^1H - ^{13}C gHSQCAD of **50r** (500 MHz D_2O)

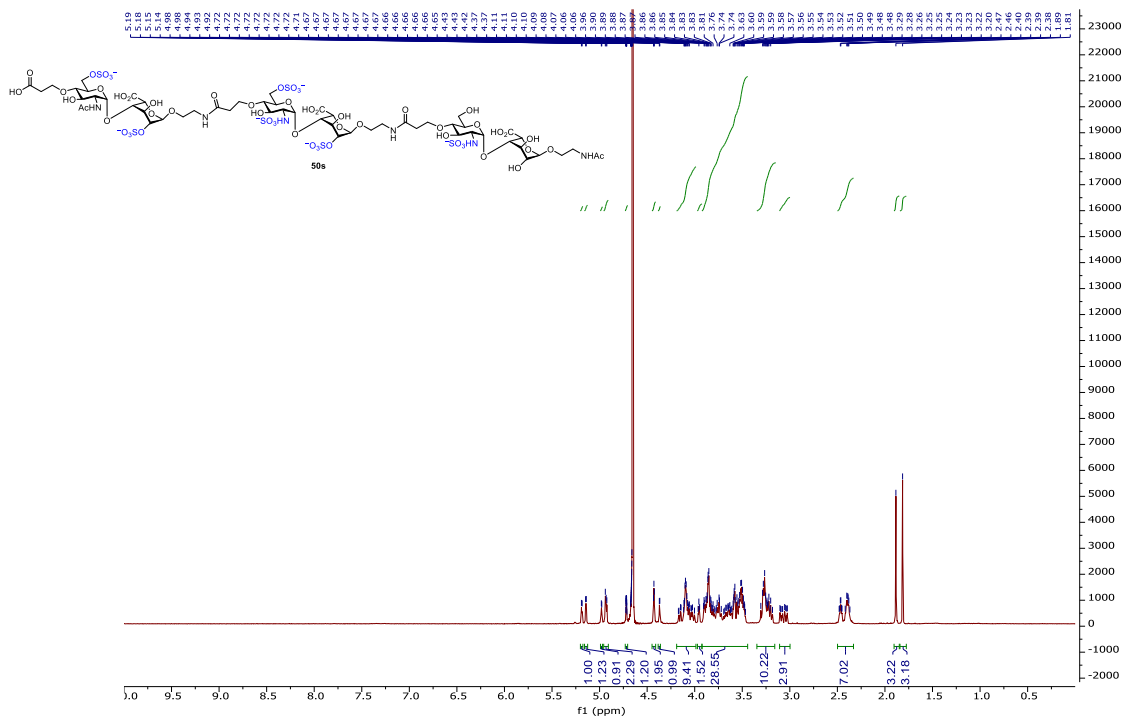
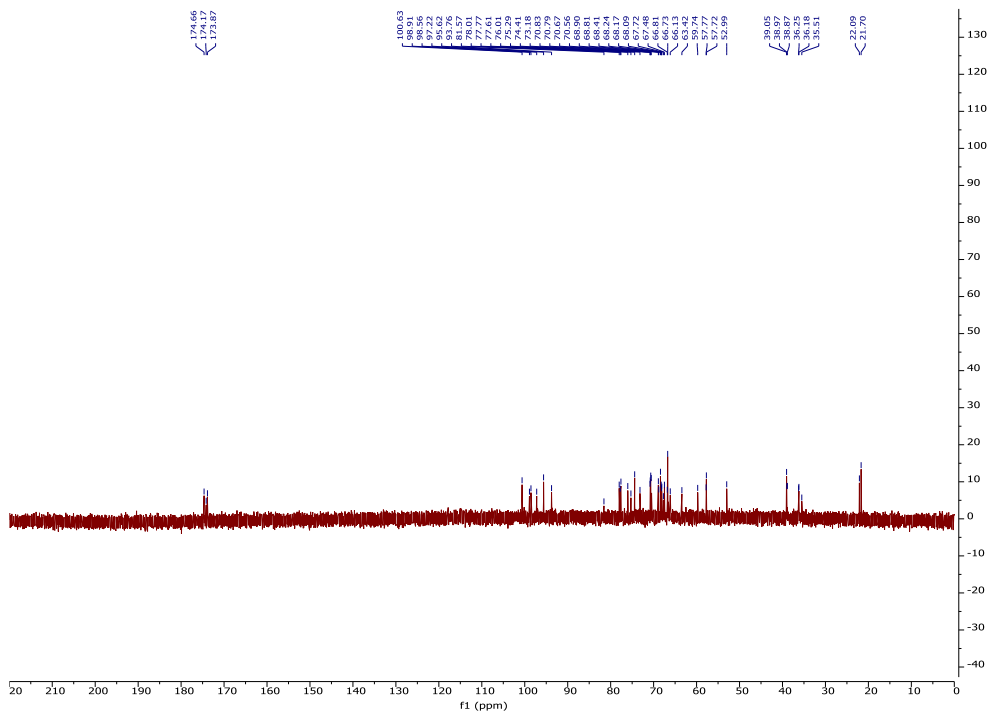


Figure 2.130. $^1\text{H-NMR}$ of 50s (500 MHz D_2O)



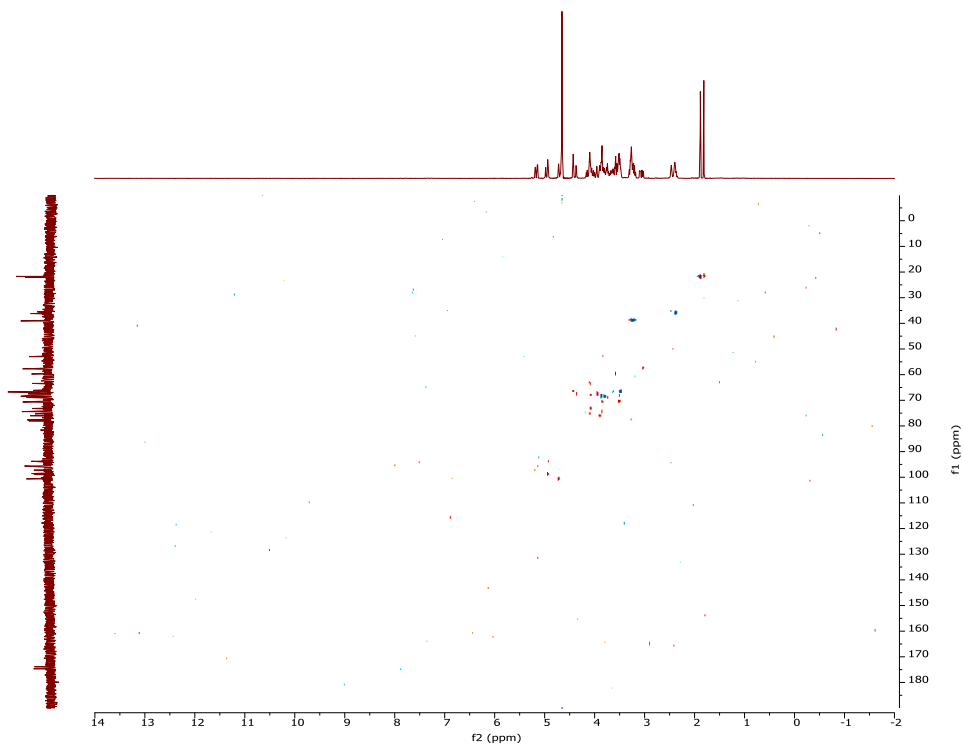


Figure 2.132. ^1H - ^{13}C gHSQCAD of **50s** (500 MHz D_2O)

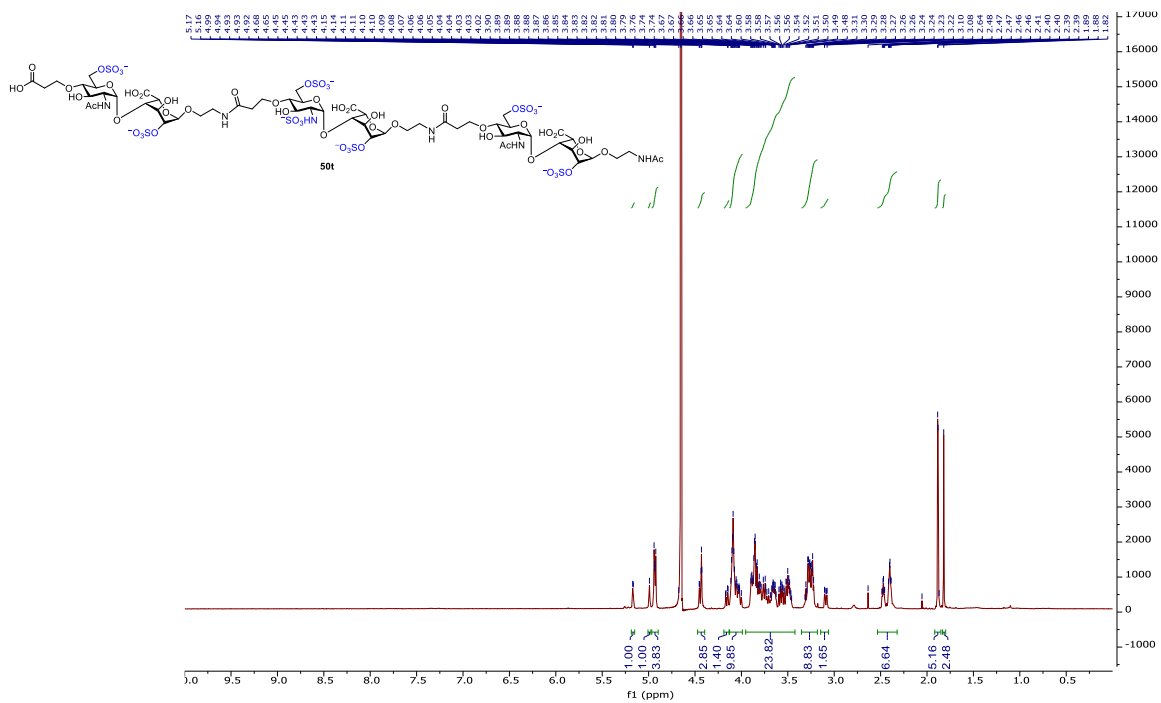


Figure 2.133. ^1H -NMR of **50t** (500 MHz D_2O)

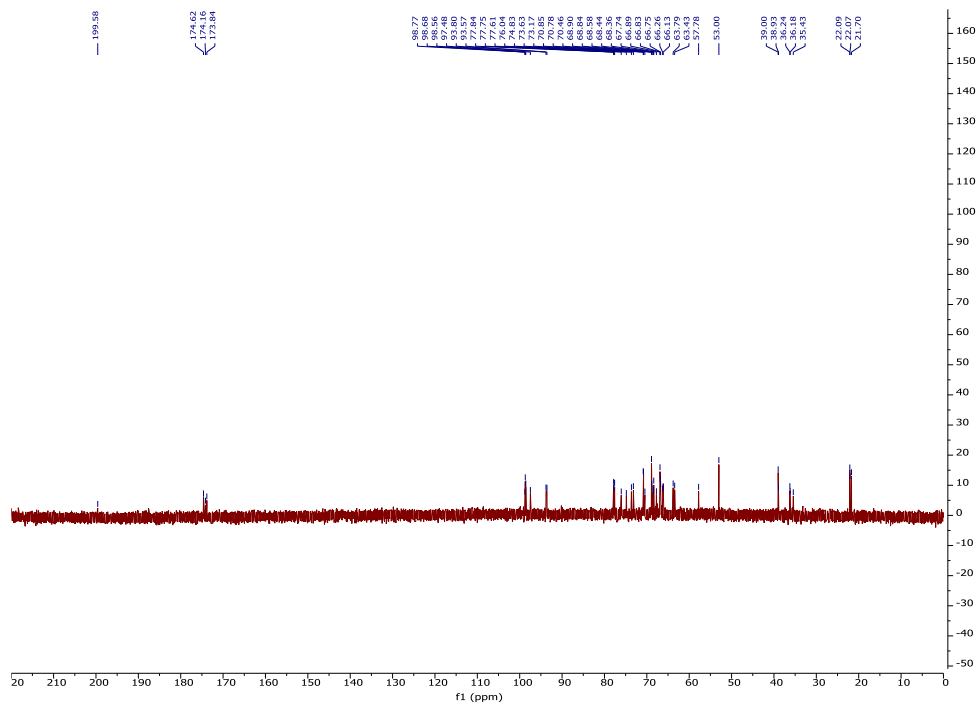


Figure 2.134. ^{13}C -NMR of **50t** (125 MHz D_2O)

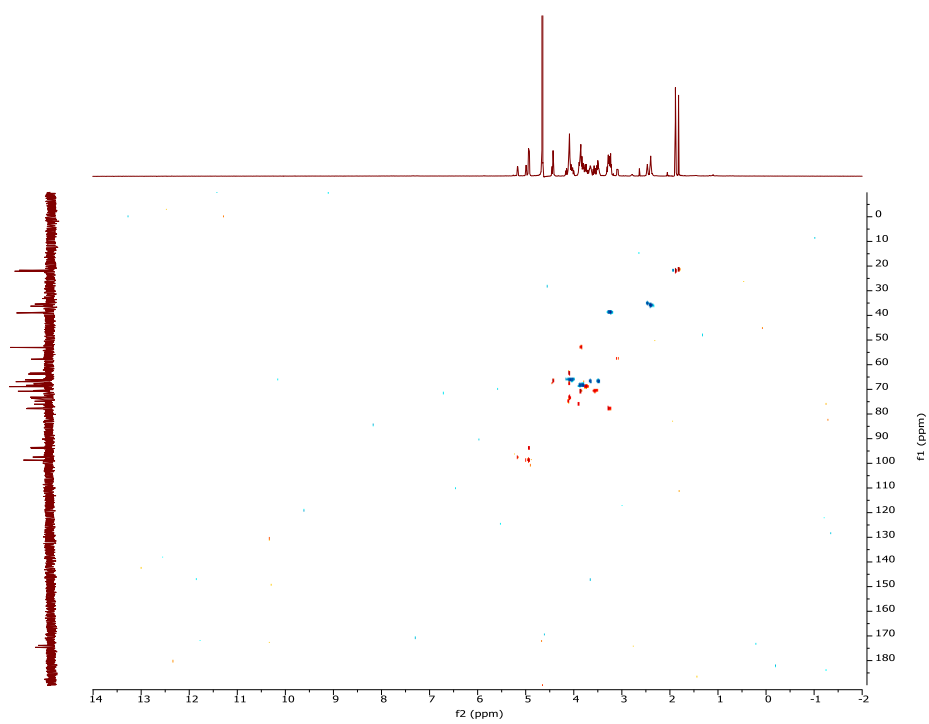


Figure 2.135. ^1H - ^{13}C gHSQCAD of **50t** (500 MHz D_2O)

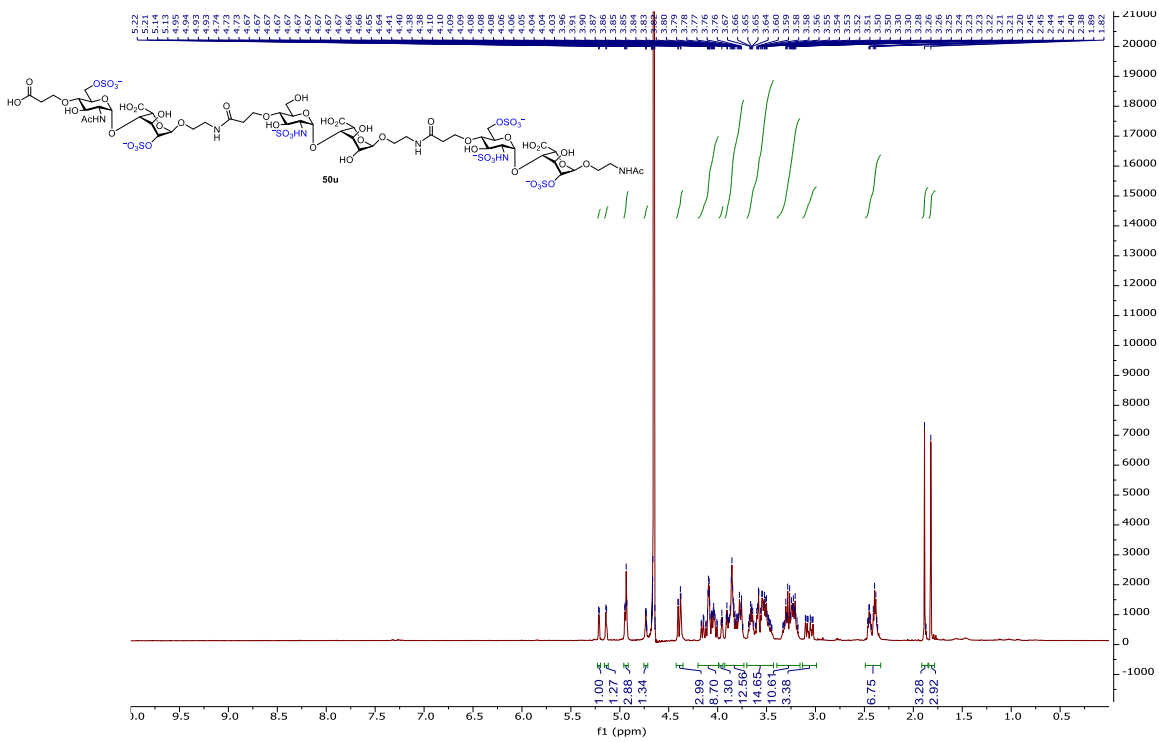


Figure 2.136. ¹H-NMR of 50u (500 MHz D₂O)

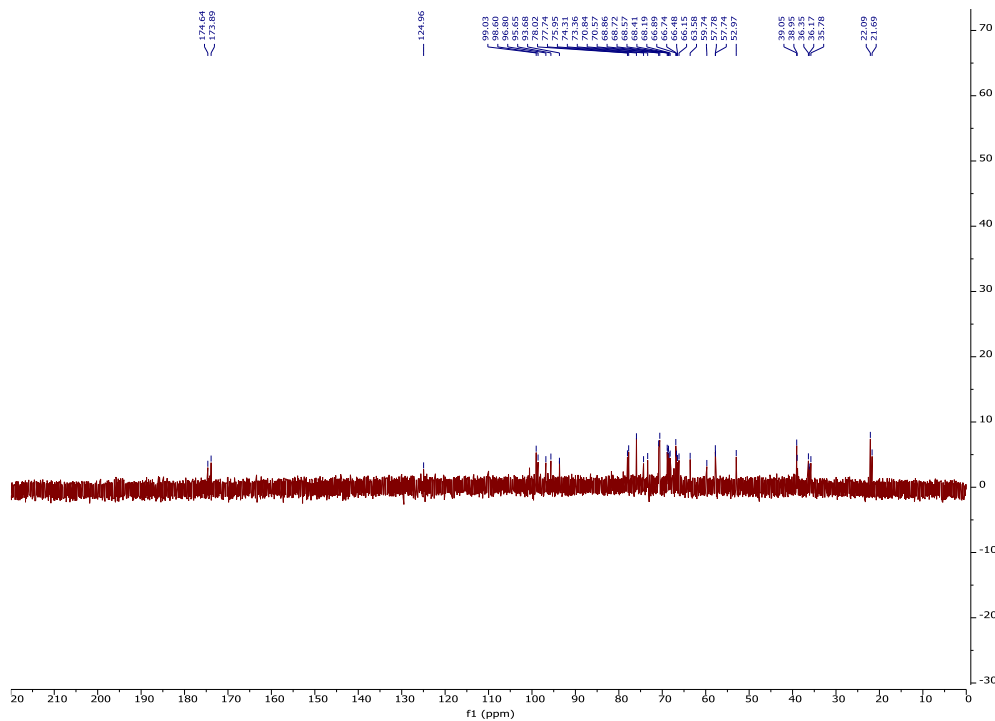


Figure 2.137. ¹³C-NMR of 50u (125 MHz D₂O)

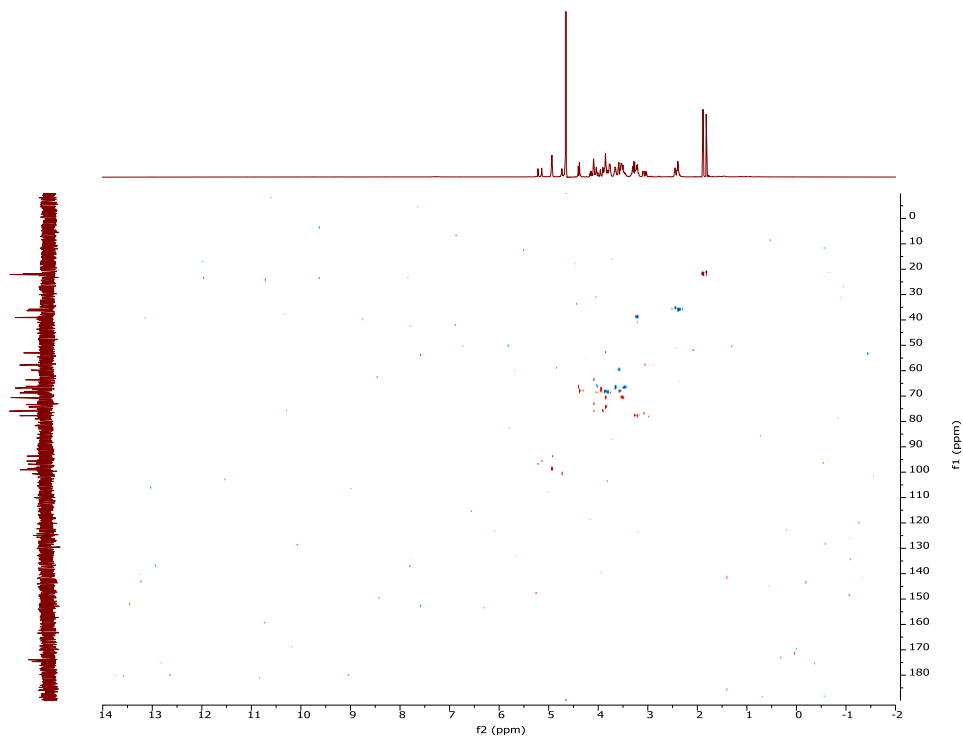


Figure 2.138. ^1H - ^{13}C gHSQCAD of **50u** (500 MHz D_2O)

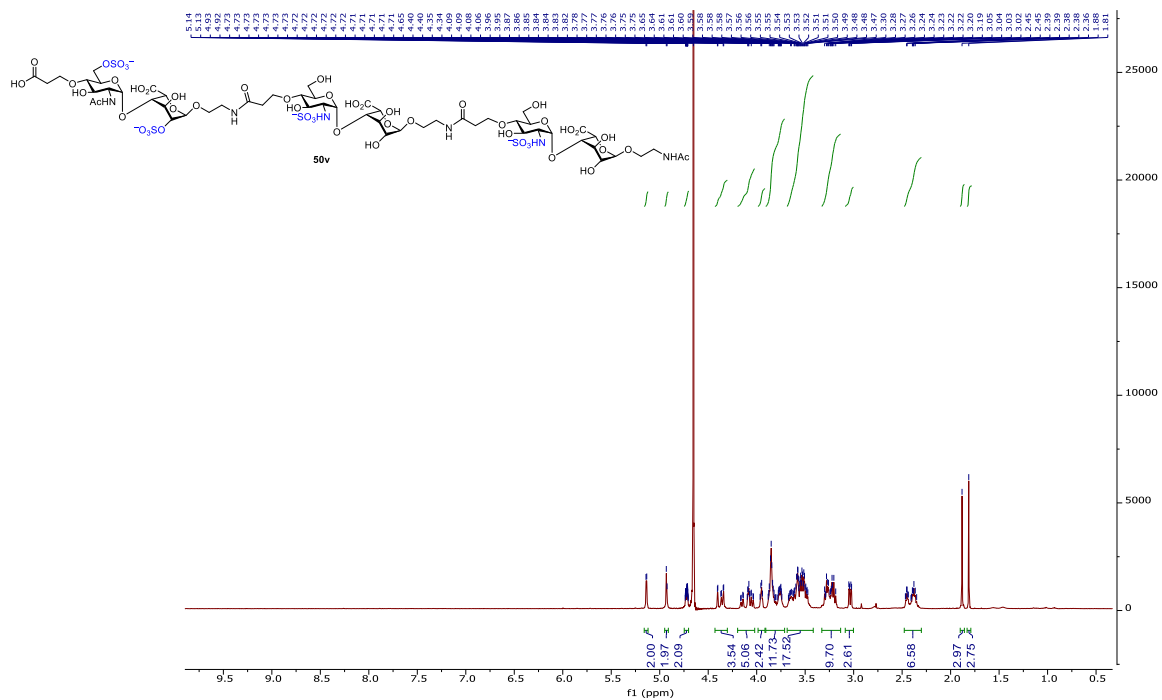


Figure 2.139. ^1H -NMR of **50v** (500 MHz D_2O)

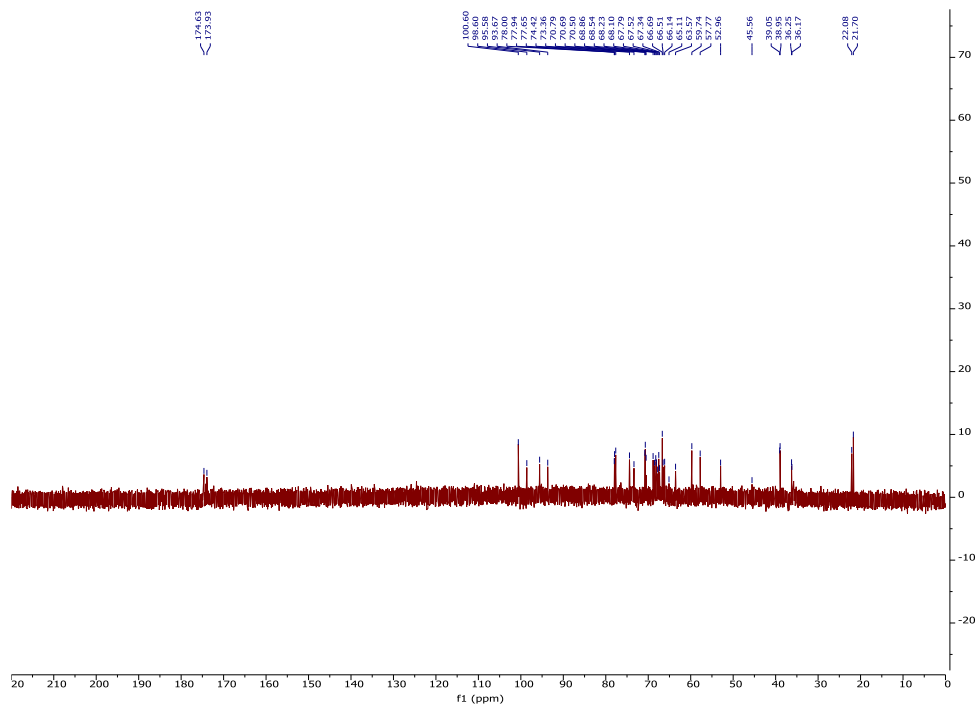


Figure 2.140. ^{13}C -NMR of **50v** (125 MHz D_2O)

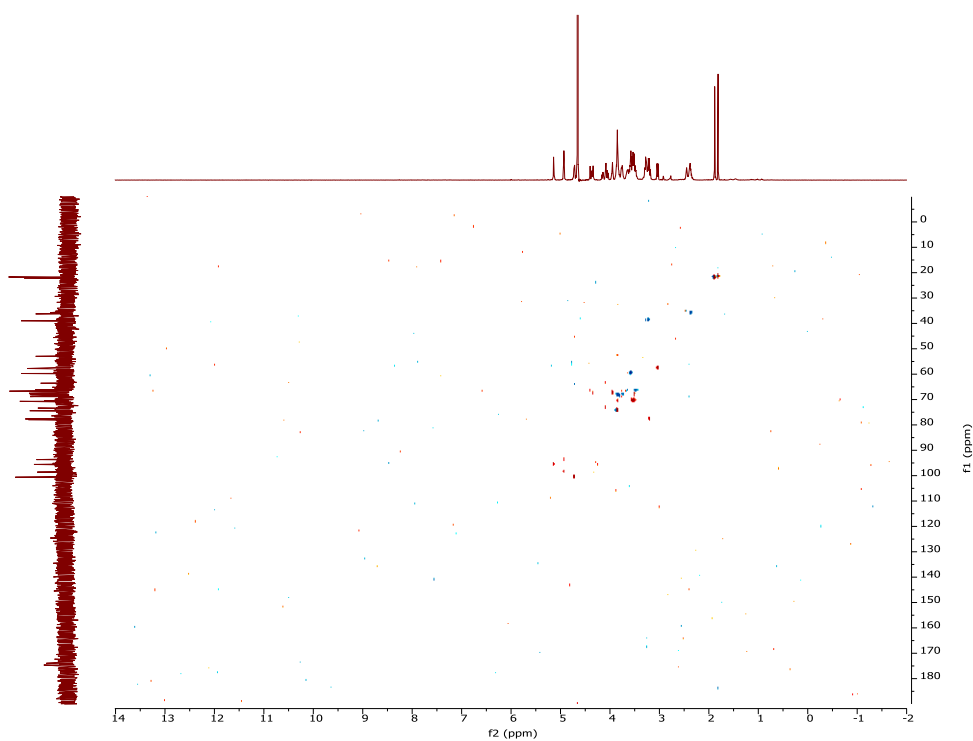


Figure 2.141. ^1H - ^{13}C gHSQCAD of **50v** (500 MHz D_2O)

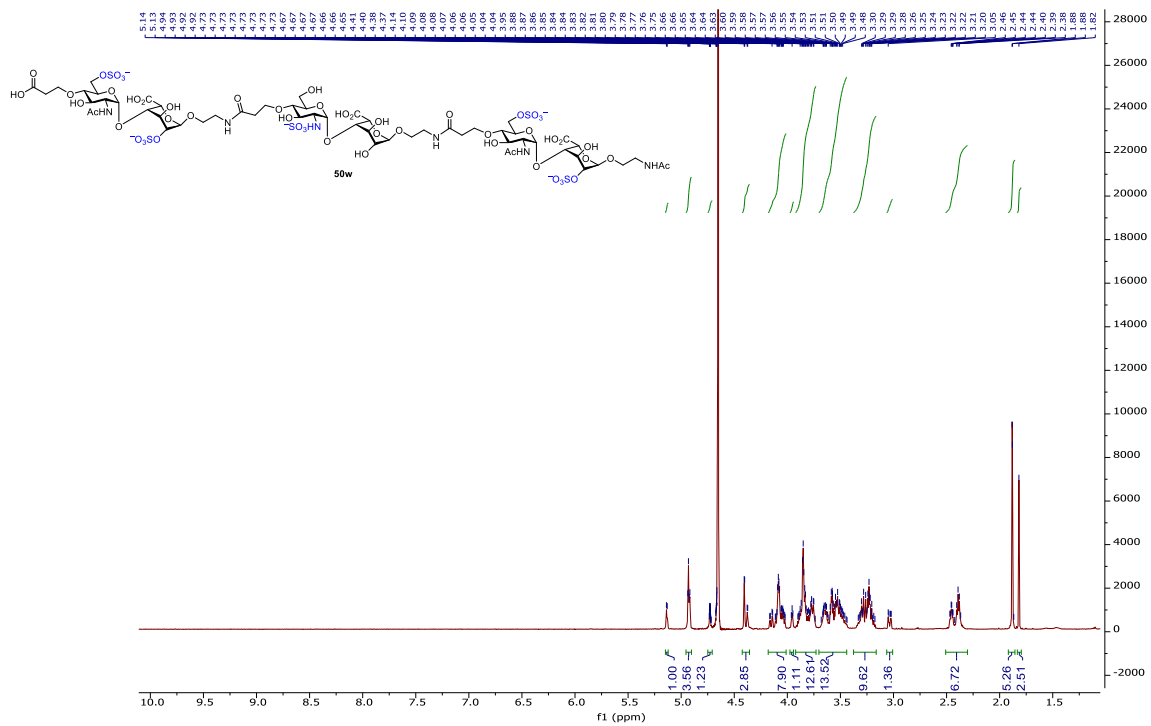


Figure 2.142. ¹H-NMR of **50w** (500 MHz D₂O)

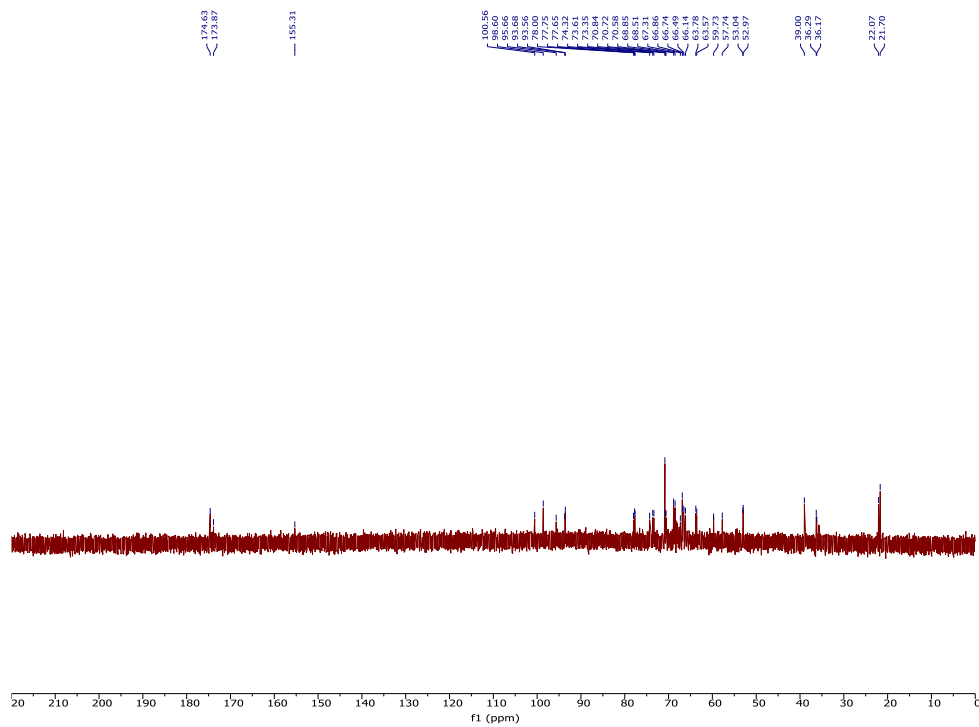


Figure 2.143. ¹³C-NMR of **50w** (125 MHz D₂O)

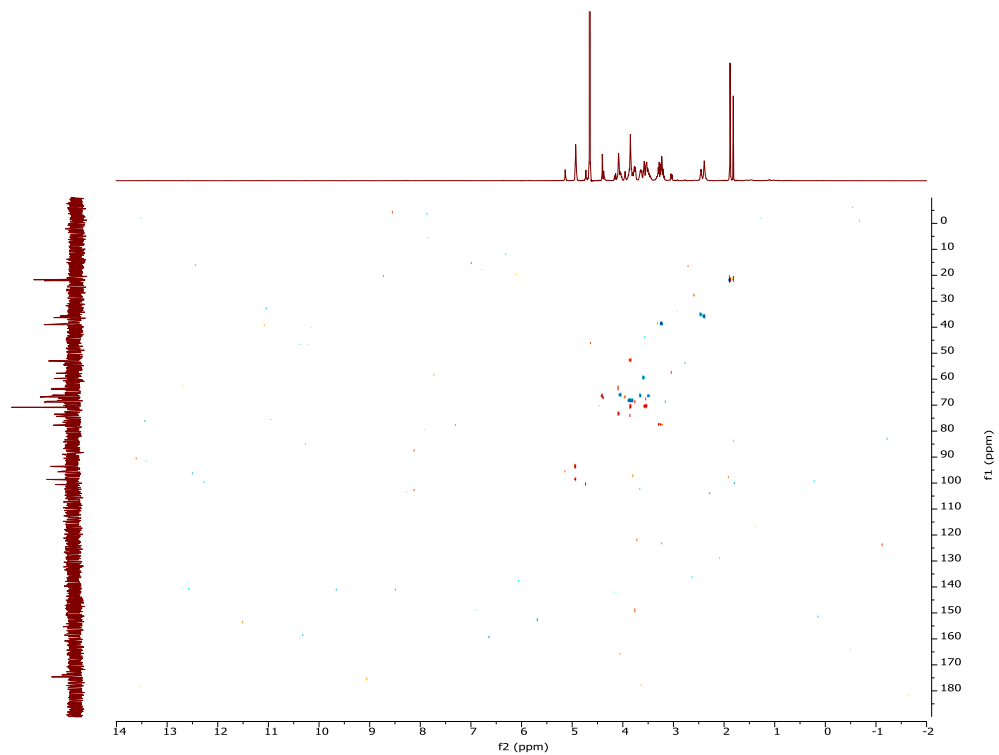


Figure 2.144. ^1H - ^{13}C gHSQCAD of **50w** (500 MHz D_2O)

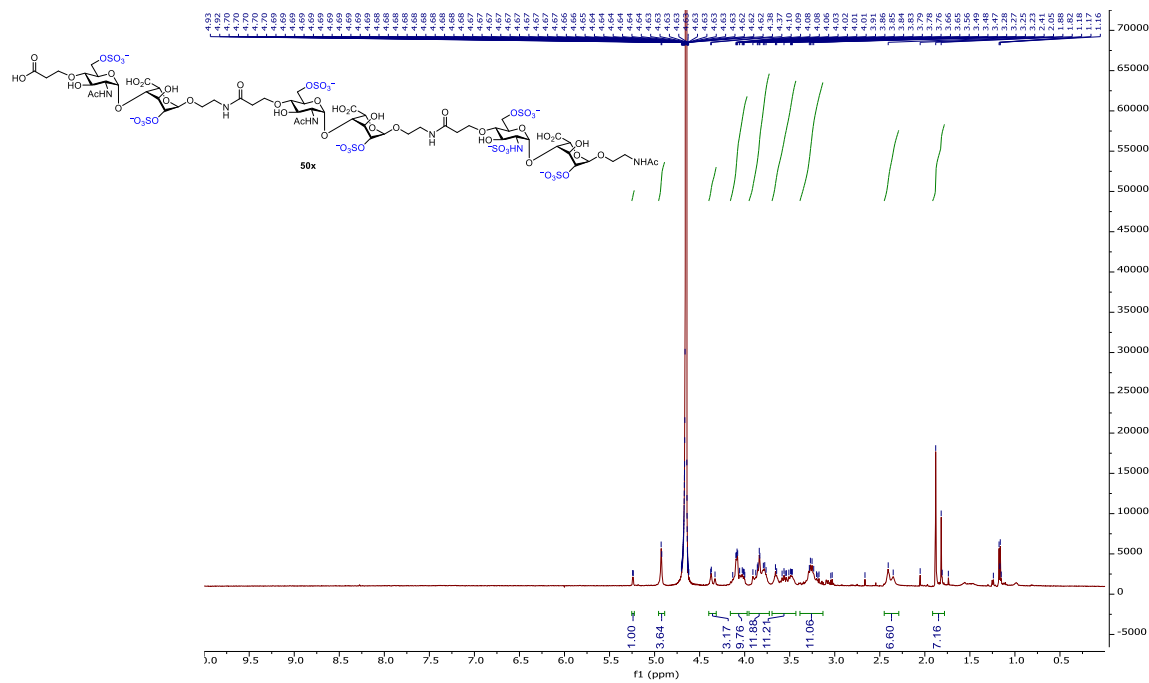


Figure 2.145. ^1H -NMR of **50x** (500 MHz D_2O)

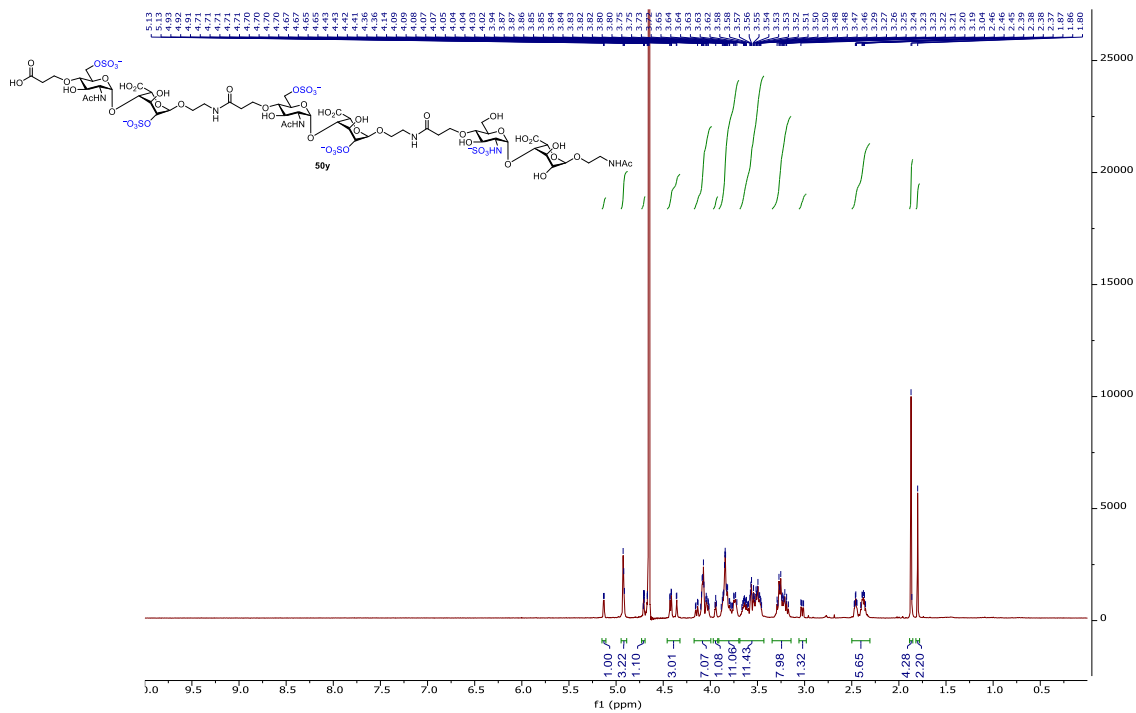


Figure 2.146. $^1\text{H-NMR}$ of 50y (500 MHz D_2O)

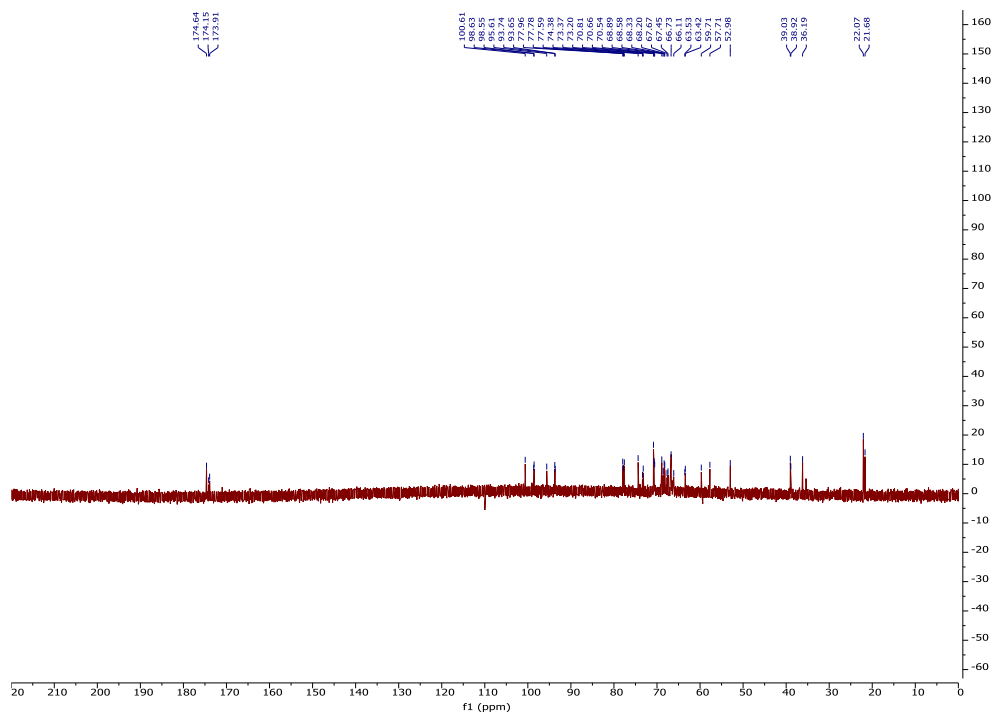


Figure 2.147. $^{13}\text{C-NMR}$ of 50y (125 MHz D_2O)

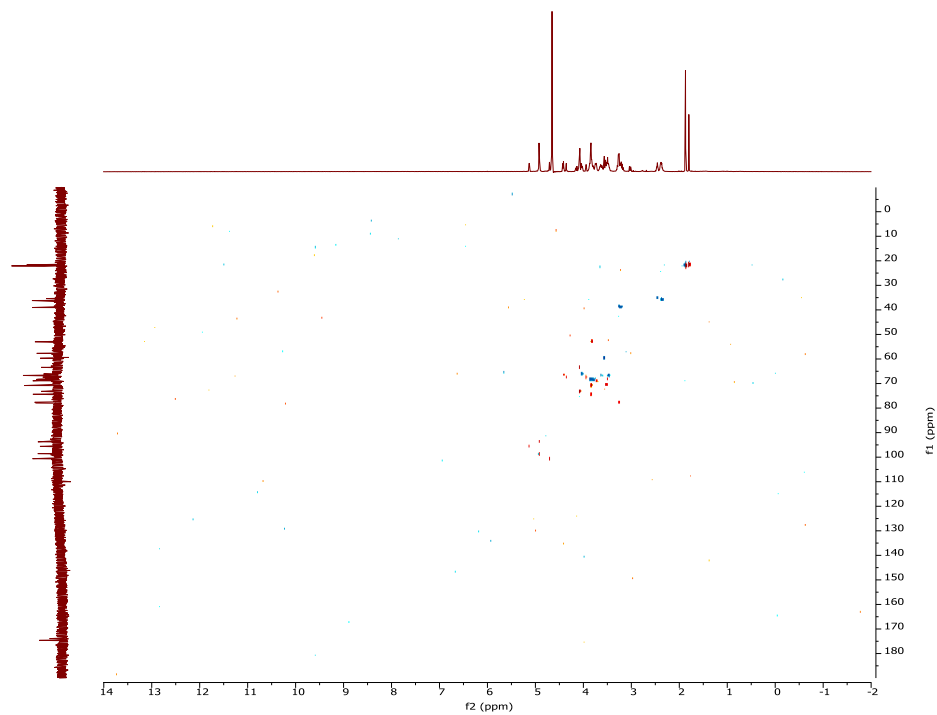


Figure 2.148. ^1H - ^{13}C gHSQCAD of **50y** (500 MHz D_2O)

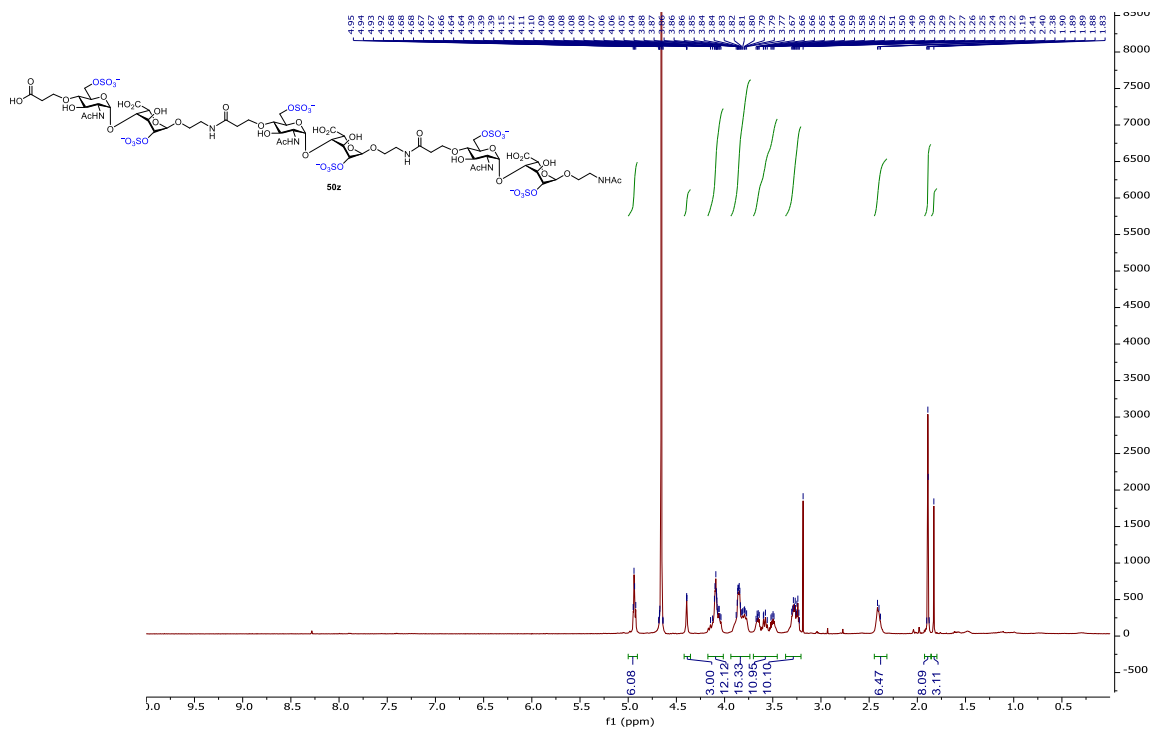


Figure 2.149. ^1H -NMR of **50z** (500 MHz D_2O)

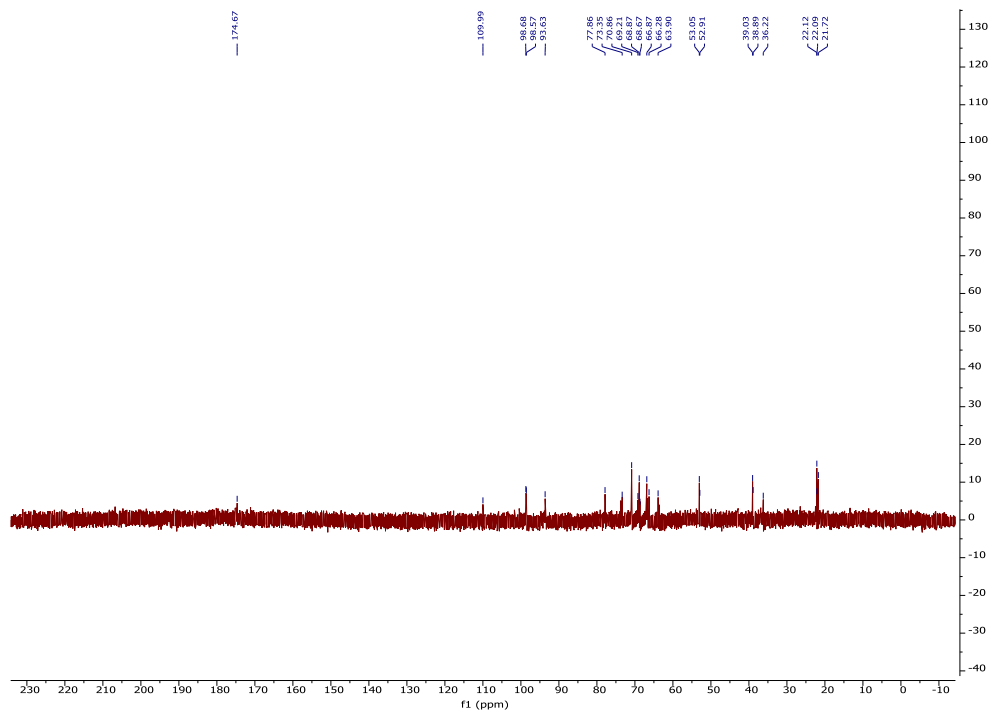


Figure 2.150. ^{13}C -NMR of **50z** (125 MHz D_2O)

Chapter 3. Biological Studies of Pseudo-hexasaccharide Heparin Mimetics

3.1. Bio-Layer Interferometry (BLI) Competition Assay on FGF-2-heparin interaction

With the successful preparation of the library of heparin mimetics, we explored whether the library of pseudo-hexasaccharides could mimic the natural heparin oligosaccharides. We examined the binding with FGF-2 that is essential for normal and cancer biology.¹³¹ FGF-2 is one of the most extensively studied heparin-binding proteins, which can mediate cell growth, differentiation, survival, and patterning.¹¹⁶ FGF-2 has low and high molecular weight isoforms,¹³² and low molecular weight FGF-2 binds with both FGFR and HSPGs on cell surface. The formation of the FGF-2-FGFR-HSPGs ternary structure activates the downstream signaling pathways.¹³³ FGF-2-FGFR1 complexes are also found in the nuclear matrix, promoting cell proliferation.¹³⁴ Dysregulation of FGF-2 signaling is associated with aggressive cancer phenotypes, enhanced chemotherapy resistance, and many acquired forms of cancers.¹³⁵⁻¹³⁷

The binding studies were performed by competition bio-layer interferometry (BLI). Before testing the pseudo-hexasaccharides, heparin-FGF-2 interaction was studied. Biotinylated heparin (27.5 nM) was immobilized on streptavidin (SA) biosensors, and various concentrations of FGF-2 were prepared as analytes. The titration curves fitted well to a 1:1 binding mode, and strong binding was observed as expected with K_D values of 2.7 nM (**Figure 3.1**).

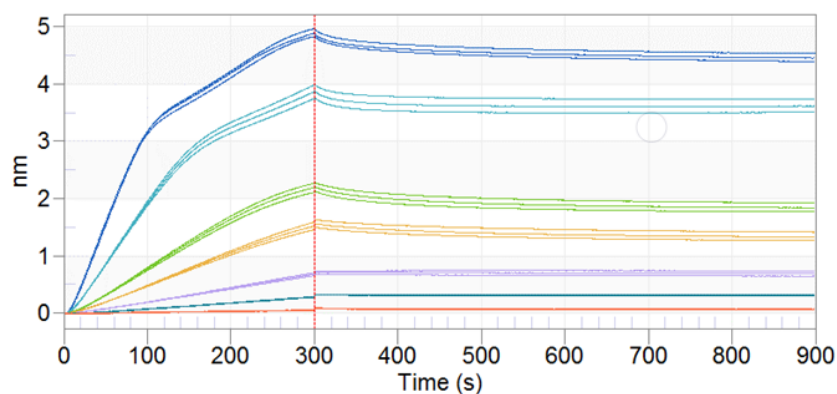


Figure 3.1. The sensorgram of heparin-FGF-2 interaction.

Next, heparin, compounds **50k**, and fondaparinux were selected as inhibitors for competition BLI. Different concentrations of each inhibitor were mixed with FGF-2 (75 nM), and biotinylated heparin was used as the ligand (**Figure 3.2**). Heparin showed potent inhibitory activity against heparin-FGF-2 interaction, and ~80% inhibition was achieved for 6.5 nM heparin. However, both compound **50k** and fondaparinux only exhibited inhibitory activity at high concentrations (> 4 μ M).

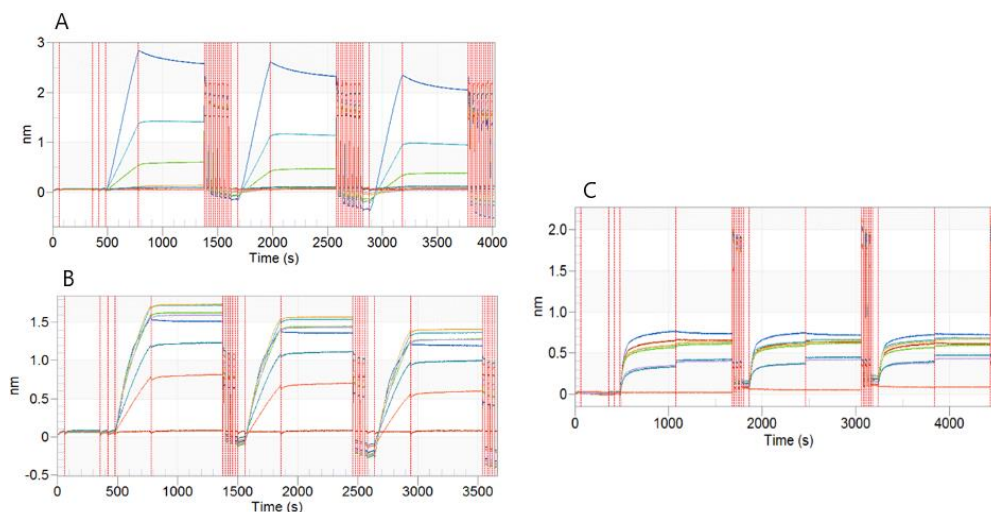


Figure 3.2. The sensorgrams of competition BLI. A: heparin as the inhibitor. Concentrations from top to bottom: 0, 3.2, 6.5, 13.1, 26.1, 51.7, 77.8 nM. B: compound **50k**. Concentrations from top to bottom: 0, 12.5, 25, 50, 100, 500, 1000 μ M. C: fondaparinux. Concentrations from top to bottom: 0, 1.0, 10.0, 25, 50, 1000, 2000 μ M.

3.2. Binding Studies of Pseudo-hexasaccharides and FGF-2 Using Surface Plasmon Resonance (SPR)

Since the pseudo-hexasaccharides did not exhibit potent inhibitory activity against heparin-FGF-2 binding through competition experiments, the direct binding studies were performed by surface plasmon resonance (SPR). FGF-2 was immobilized on CDH sensor chip surface through EDC/NHS coupling, and fully sulfated (**50**), *O*-sulfated (**50z**) and *N*-sulfated (**50m**) pseudo-hexasaccharides were selected as analytes. **50** and **50z** showed strong and moderate binding to FGF-2 with K_D values of 19.6 and 940 nM respectively, and the only weak signal was observed for **50m** (**Figure 3.3**). Delightfully, the SPR results correlated well with that of heparin hexasaccharides²⁵ (**36**, **51**, **52**). Fully sulfated hexasaccharide **36** showed comparable FGF-2 binding ability as that of heparin through microarray assay, and no significant binding signal was observed for *N*-sulfated hexasaccharide **52**. The pseudo-hexasaccharides also exhibited much stronger FGF-2 binding ability in comparison to that of heparin di- and tetrasaccharides (**54**, **53**) (**Figure 3.4**).^{20, 113} **50** is about 20 times more potent than the strongest tetrasaccharide binder **53** based on K_D values acquired from SPR assay.

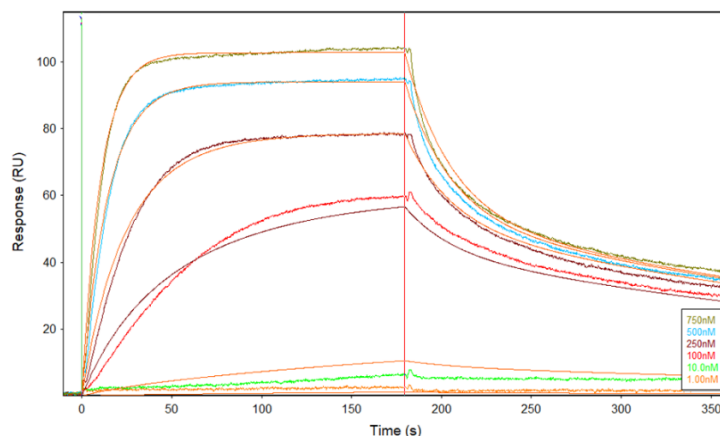


Figure 3.3. The SPR sensorgram of FGF-2 and compound **50** interaction at different concentrations

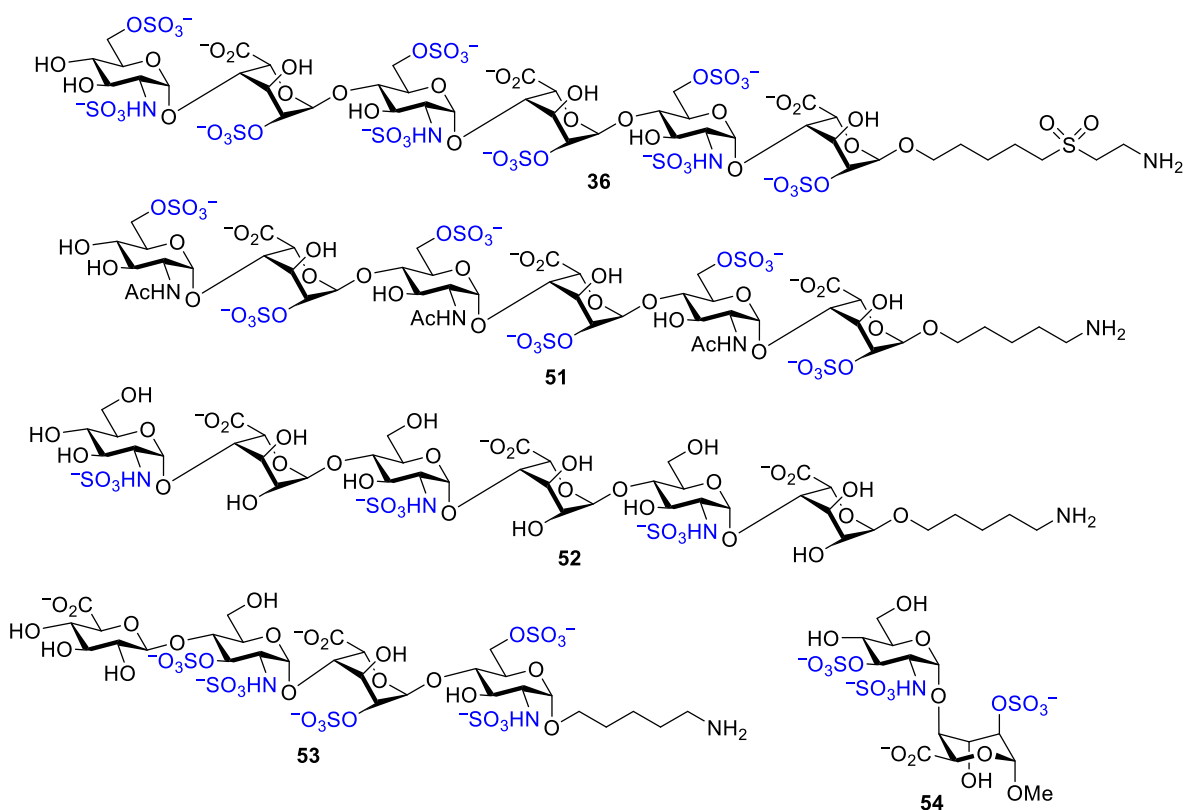


Figure 3.4. Heparin hexa-, tetra- and disaccharides.

In order to gain more insights into the structure-activity relationship between heparin and FGF-2, the competition assay was performed by the Linhardt group (**Figure 3.5**). Biotinylated heparin was immobilized on the biosensor, and 27 pseudo-hexasaccharides (10 μ M) was mixed with FGF-2 (50 nM) individually. As expected, the fully sulfated pseudo-hexasaccharide (**50**) showed the most potent inhibitory activity. Compounds with more sulfate groups showed relatively higher potency. Among 27 pseudo-hexasaccharides, the best inhibitors (**50**, **50a**, **50b**, **50i**, **50r**), which showed about 50-65% inhibition of binding between FGF-2 and heparin contain successive fully sulfated disaccharide modules. For IC_{50} measurements, biotinylated heparin was immobilized on the SA sensor chip as described above, and FGF-2 (50 nM) was pre-mixed with different concentrations of pseudo-hexasaccharides. Fully sulfated pseudo-hexasaccharide **50** displayed the highest IC_{50} value of 1.7 μ M, and **50a**, **50b**, and **50r**

also exhibited potent competitive effect ($IC_{50} = 10.8, 4.0,$ and $3.5 \mu M,$ respectively) (**Figure 3.6**). According to competition SPR results, successive fully sulfated disaccharide modules are required for potent competitive activity.

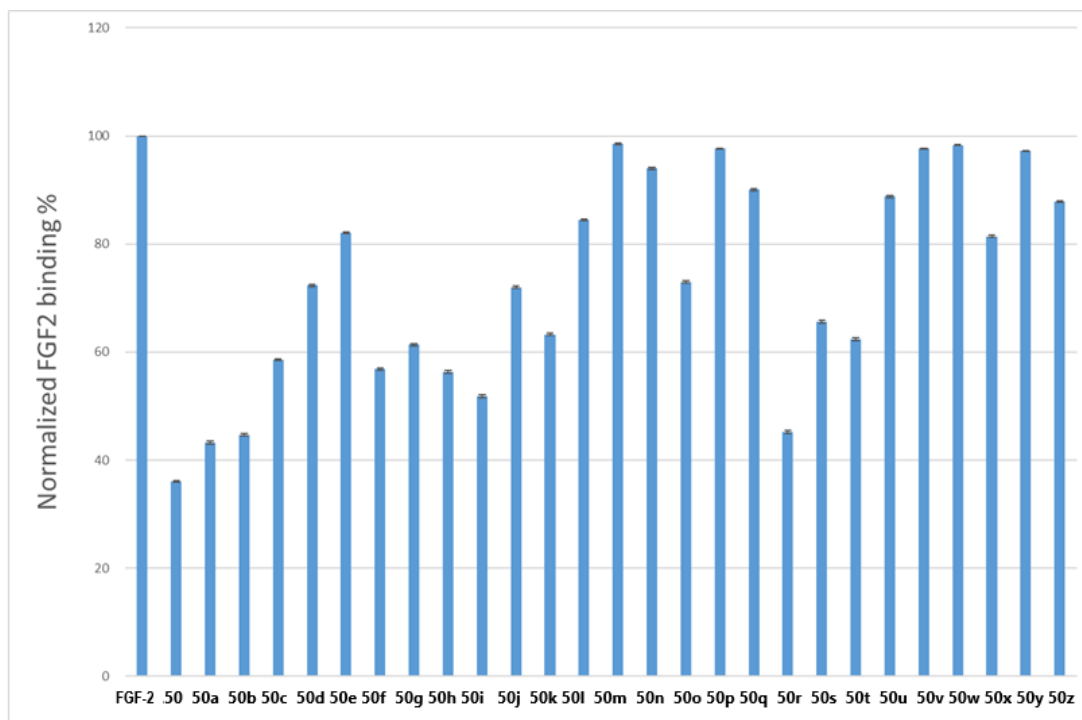


Figure 3.5. Measurement of inhibition of 27 pseudo-hexasaccharides on FGF-2-heparin interaction using competition SPR

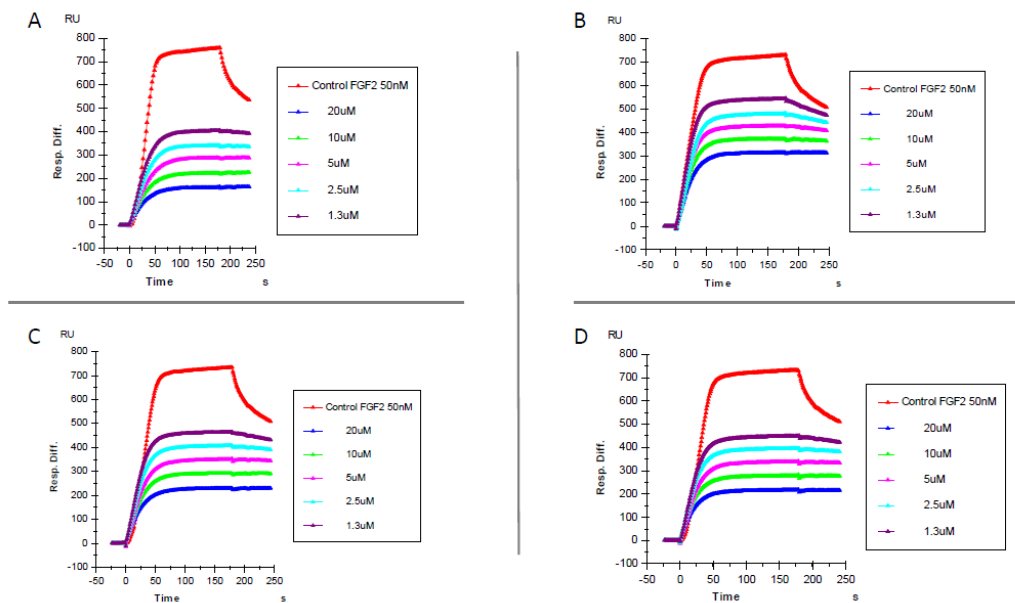


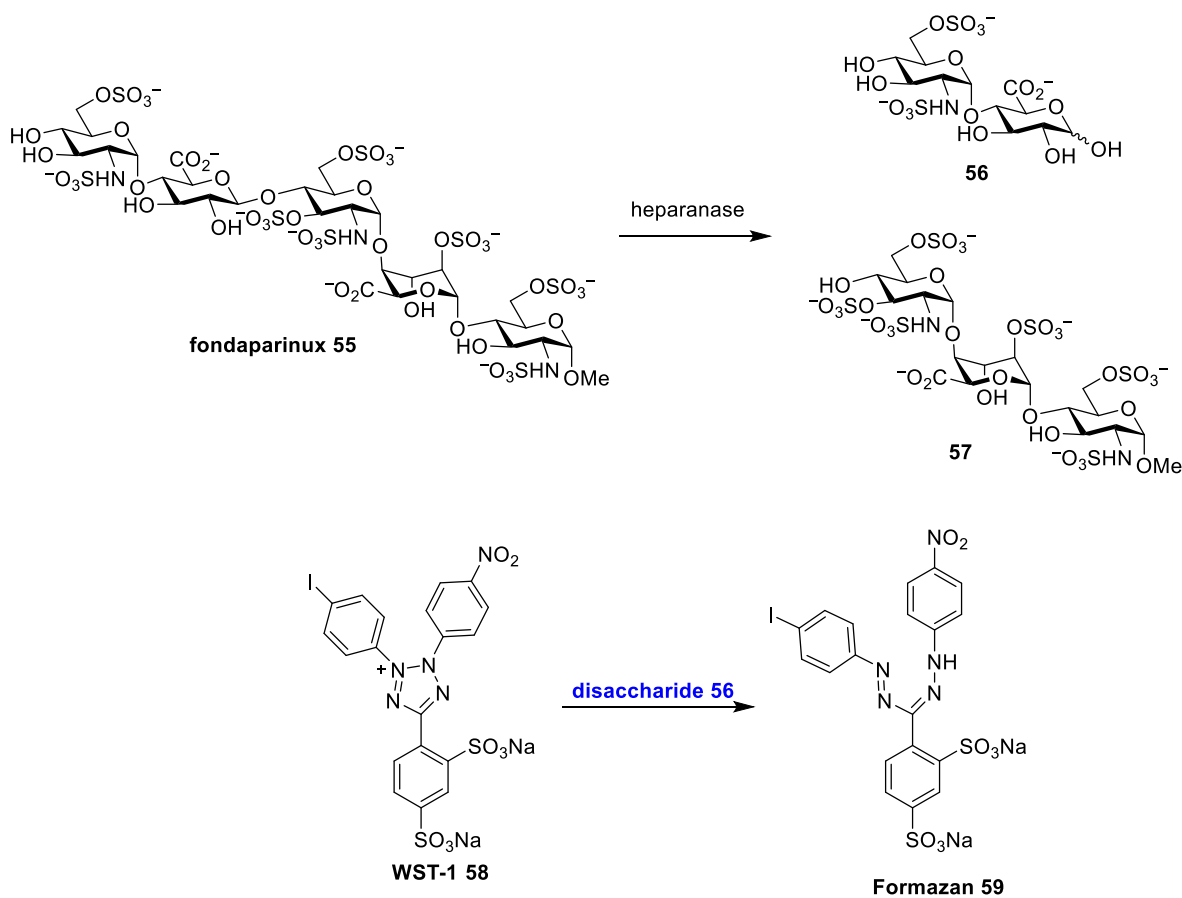
Figure 3.6. Competition SPR for IC_{50} measurements for pseudo-hexasaccharides **50** (A), **50a** (B), **50b** (C), and **50r** (D)

3.3. Heparanase Inhibitory Activity Tests Through the Colorimetric Assay

Next, we investigated the anti-tumor activity of pseudo-hexasaccharides by inhibiting heparanase enzyme that is strongly related to tumor formation, including tumor initiation, growth and metastasis.¹³⁸ Proheparanase was synthesized on the endoplasmic reticulum (ER) and transported to the Golgi apparatus and secreted into the extracellular space. Proheparanase may interact with receptors on the cell surface and upregulate the expression of VEGF, resulting in cell proliferation. On the other hand, proheparanase could also be activated by internalization through binding with cell surface syndecans, and active heparanase may be translocated into the nucleus and secreted into the ECM.^{139, 140} Heparanase is the sole endoglycosidase that degrades HS side chains of HSPGs. The cleavage of HS releases the sequestered growth factors and degrades the structural integrity of the basement membrane and ECM. Thus, heparanase is strongly related to tumor growth and metastasis. Since heparin and HS have the same backbone

arrangement of glucosamine and uronic acid disaccharide repeating units, heparin was considered as a potential potent heparanase inhibitor.¹⁴¹⁻¹⁴³

Heparanase activity was measured by a colorimetric assay. Fondaparinux **55** was used as the substrate, which would be cleaved by heparanase, and the appearance of disaccharide product **56** was measured by the tetrazolium salt WST-1 **58** (Scheme 3.1).¹⁴⁴ Heparin exhibited potent heparanase activity, and 100% inhibition was achieved with ~20 nM (Figure 3.7). However, our pseudo-hexasaccharides did not exhibit significant heparanase inhibitory activity (Figure 3.8). Compound **50a** and **50f** were added up to 1 and 10 μ M, respectively, and the absorbance did not decrease dramatically.



Scheme 3.1. Heparanase colorimetric assay.

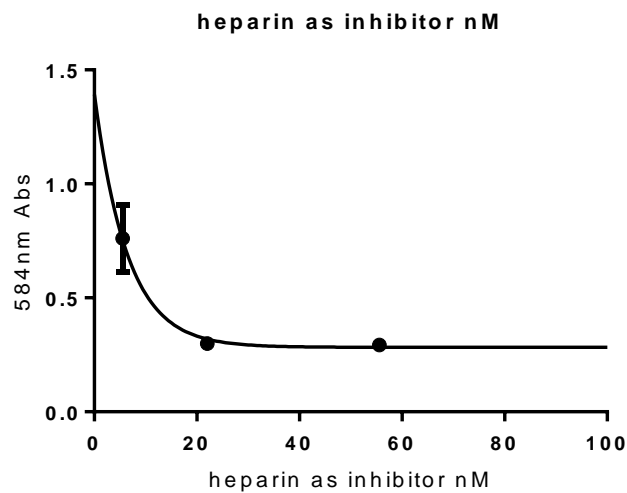


Figure 3.7. Inhibition of heparanase by heparin

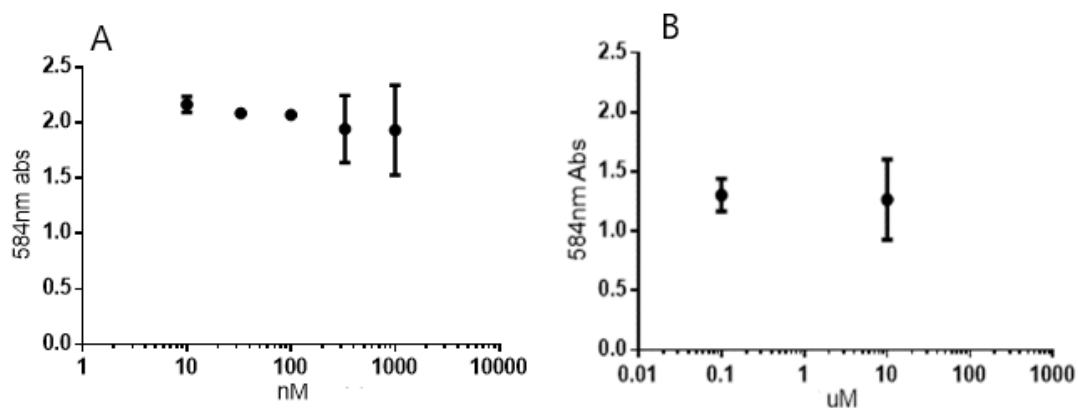


Figure 3.8. Inhibition of heparanase by A: compound **50a** (10, 50, 100, 1000, and 1000 nM). B: compound **50f** (0.1, and 10 uM).

3.4. Experimental Section

3.4.1. Bio-Layer Interferometry (BLI).

Samples or buffers were dispensed into 96-well microtiter plates (Millipore, Billerica,

MA) at a volume of 200 uL per well. The operating temperature was maintained at 25 °C. Streptavidin-coated biosensor tips (FortéBio, Inc., Molecular Devices) were pre-wetted with PBS buffer for 10 min, and biotinylated heparin (27.5 nM) was loaded for 5 min. Various concentrations of analytes were then immobilized on the biosensor tips while agitating for 10 min at 1000 rpm, and biosensors was dipped into PBS buffer for 10 min for dissociation. NaCl solution (2.0 M) was employed for regeneration to achieve baseline status. All measurements were performed using 0.05% surfactant P-20 PBS buffer.

3.4.2. Surface Plasmon Resonance (SPR).

FGF-2 was immobilized on sensor chip by primary amine coupling reaction. The surface of a CDH sensor chip (FortéBio, Inc., Molecular Devices, USA) was activated using freshly mixed N-hydroxysuccinimide (NHS; 0.05 M) and 1-(3-(dimethylamino)propyl)-ethylcarbodiimide (EDC; 0.2 M) (1/1,v/v) in water, followed by the injection of FGF-2 (50 ug/ml) in PBS buffer. The remaining active esters were quenched by ethanolamine (1.0 M). All measurements were performed using 0.01% Tween 20 PBS buffer. Aqueous NaCl (2.0 M) was employed for regeneration to achieve baseline status.

3.4.3. Heparanase Colorimetric Assays.

Fondaparinux colorimetric heparanase assays were carried out in 96 well microplates (NEST Scientific 96 Well Cell Culture Plate, 701002) pre-treated with a solution of 4% BSA in phosphate-buffered saline containing 0.05% Tween 20 (PBST) for 2 h at 37 °C. Assay solutions (100 ul) contained sodium acetate buffer (40 mM, pH 5.0) and fondaparinux (100 mM,

MedChemExpress), heparanase (5 nM) and varying concentrations of compounds of interests or heparin. The mixture was kept at 37 °C for 20 h, which was followed by the addition of a solution of WST-1 (1.69 mM WST-1 in 0.1 M NaOH, 100 uL) and incubation at 60 °C for 1 h after which the absorbance at 584 nm was measured (Fluostar Optima platereader, BMG Labtech).

REFERENCES

REFERENCES

1. Linhardt, R. J.; Liu, J., Synthetic heparin. *Curr. Opin. Pharmacol.* **2012**, *12*, 217-219.
2. Cifonelli, J. A.; Dorfman, A., The uronic acid of heparin. *Biochem. Biophys. Res. Commun.* **1962**, *7*, 41-45.
3. Wardrop, D.; Keeling, D., The story of the discovery of heparin and warfarin. *Br. J. Haematol.* **2008**, *141*, 757-763.
4. Barrowcliffe, T. W., History of heparin. *Handb. Exp. Pharmacol.* **2012**, *207*, 3-22.
5. Marcum, J. A., The origin of the dispute over the discovery of heparin. *J. Hist. Med. Allied Sci.* **2000**, *55*, 37-66.
6. Thunberg, L.; Bäckström, G.; Lindahl, U., Further characterization of the antithrombin-binding sequence in heparin. *Carbohydr. Res.* **1982**, *100*, 393-410.
7. Alquwaizani, M.; Buckley, L.; Adams, C.; Fanikos, J., Anticoagulants: a review of the pharmacology, dosing, and complications. *Curr. Emerg. Hosp. Med. Rep.* **2013**, *1*, 83-97.
8. Oduah, E. I.; Linhardt, R., J.; Sharfstein, S. T., Heparin: past, present, and future. *Pharmaceuticals* **2016**, *9*, 38-49.
9. Blossom, D. B.; Kallen, A. J.; Patel, P. R.; Elward, A.; Robinson, L.; Gao, G.; Langer, R.; Perkins, K. M.; Jaeger, J. L.; Kurkjian, K. M.; Jones, M.; Schillie, S. F.; Shehab, N.; Ketterer, D.; Venkataraman, G.; Kishimoto, T. K.; Shriver, Z.; McMahon, A. W.; Austen, K. F.; Kozlowski, S.; Srinivasan, A.; Turabelidze, G.; Gould, C. V.; Arduino, M. J.; Sasisekharan, R., Outbreak of adverse reactions associated with contaminated heparin. *N. Engl. J. Med.* **2008**, *359*, 2674-2684.
10. Chess, E. K.; Bairstow, S.; Donovan, S.; Havel, K.; Hu, P.; Johnson, R. J.; Lee, S.; McKee, J.; Miller, R.; Moore, E.; Nordhaus, M.; Ray, J.; Szabo, C.; Wielgos, T., Case study: contamination of heparin with oversulfated chondroitin sulfate. *Handb. Exp. Pharmacol.* **2012**, *207*, 99-125.
11. Martínez-González, J.; Rodríguez, C., New challenges for a second-generation low-molecular-weight heparin: focus on bemiparin. *Expert Rev. Cardiovasc. Ther.* **2010**, *8*, 625-634.
12. Rostoker, G.; Durand-Zaleski, I.; Petit-Phar, M.; Ben Maadi, A.; Jazaerli, N.; Radier, C.; Rahmouni, A.; Mathieu, D.; Vasile, N.; Rosso, J.; Meignan, M.; Remy, P.; Lang, P.; weil, B., Prevention of thrombotic complications of the nephrotic syndrome by the low-molecular-weight heparin enoxaparin. *Nephron* **1995**, *69*, 20-28.
13. Joannidis, M.; Kountchev, J.; Rauchenzauner, M.; Schusterschitz, N.; Ulmer, H.;

Mayr, A.; Bellmann, R., Enoxaparin vs. unfractionated heparin for anticoagulation during continuous veno-venous hemofiltration: a randomized controlled crossover study. *Intensive Care Med.* **2007**, *33*, 1571-1579.

14. Sinaÿ, P.; Jacquinet, J. C.; Petitou, M.; Duchaussoy, P.; Lederman, I.; Choay, J., Total synthesis of a heparin pentasaccharide fragment having high affinity for antithrombin III. *Carbohydr. Res.* **1984**, *132*, C5-C9.

15. Li, T.; Ye, H.; Cao, X.; Wang, J.; Liu, Y.; Zhou, L.; Liu, Q.; Wang, W.; Shen, J.; Zhao, W.; Wang, P., Total synthesis of anticoagulant pentasaccharide fondaparinux. *ChemMedChem* **2014**, *9*, 1071-1080.

16. Bishop, J. R.; Schuksz, M.; Esko, J. D., Heparan sulphate proteoglycans fine-tune mammalian physiology. *Nature* **2007**, *446*, 1030-1037.

17. Vlodaysky, I.; Ilan, N.; Naggi, A.; Casu, B., Heparanase: structure, biological functions, and inhibition by heparin-derived mimetics of heparan sulfate. *Curr. Pharm. Des.* **2007**, *13*, 2057-2073.

18. Miao, H. Q.; Liu, H.; Navarro, E.; Kussie, P.; Zhu, Z., Development of heparanase inhibitors for anti-cancer therapy. *Curr. Med. Chem.* **2006**, *13*, 2101-2111.

19. Kilarski, W. W.; Bikfalvi, A., Recent developments in tumor angiogenesis. *Curr. Pharm. Biotechnol.* **2007**, *8*, 3-9.

20. Zong, C.; Venot, A.; Li, X.; Lu, W.; Xiao, W.; Wilkes, J. L.; Salanga, C. L.; Handel, T. M.; Wang, L.; Wolfert, M. A., Heparan sulfate microarray reveals that heparan sulfate-protein binding exhibits different ligand requirements. *J. Am. Chem. Soc.* **2017**, *139*, 9534-9543.

21. Miller, G. J.; Hansen, S. U.; Avizienyte, E.; Rushton, G.; Cole, C.; Jayson, G. C.; Gardiner, J. M., Efficient chemical synthesis of heparin-like octa-, deca- and dodecasaccharides and inhibition of FGF2- and VEGF₁₆₅-mediated endothelial cell functions. *Chem. Sci.* **2013**, *4*, 3218-3222.

22. Hansen, S. U.; Miller, G. J.; Jayson, G. C.; Gardiner, J. M., First gram-scale synthesis of a heparin-related dodecasaccharide. *Org. Lett.* **2012**, *15*, 88-91.

23. Hansen, S. U.; Miller, G. J.; Cliff, M. J.; Jayson, G. C.; Gardiner, J. M., Making the longest sugars: a chemical synthesis of heparin-related [4]_n oligosaccharides from 16-mer to 40-mer. *Chem. Sci.* **2015**, *6*, 6158-6164.

24. Hu, Y. P.; Zhong, Y. Q.; Chen, Z. G.; Chen, C. Y.; Shi, Z.; Zulueta, M. M.; Ku, C. C.; Lee, P. Y.; Wang, C. C.; Hung, S. C., Divergent synthesis of 48 heparan sulfate-based disaccharides and probing the specific sugar-fibroblast growth factor-1 interaction. *J. Am. Chem. Soc.* **2012**, *134*, 20722-20727.

25. Noti, C.; de Paz, J. L.; Polito, L.; Seeberger, P. H., Preparation and use of microarrays containing synthetic heparin oligosaccharides for the rapid analysis of heparin–protein interactions. *Chem. Eur. J.* **2006**, *12*, 8664-8686.
26. Kreuger, J.; Kjellén, L., Heparan sulfate biosynthesis: regulation and variability. *J. Histochem. Cytochem.* **2012**, *60*, 898–907.
27. Xu, Y.; Masuko, S.; Takiyeddin, M.; Xu, H.; Liu, R.; Jing, J.; Mousa, S. A.; Linhardt, R., J.; Liu, J., Chemoenzymatic synthesis of homogeneous ultralow molecular weight heparins. *Science* **2011**, *334*, 498-501.
28. Oosta, G. M.; Gardner, W. T.; Beeler, D. L.; Rosenberg, R. D., Multiple functional domains of the heparin molecule. *Proc. Natl. Acad. Sci. U.S.A.* **1981**, *78*, 829-833.
29. Xu, Y.; Pempe, E. H.; Liu, J., Chemoenzymatic synthesis of heparin oligosaccharides with both anti-factor Xa and anti-factor IIa activities. *J. Biol. Chem.* **2012**, *287*, 29054-29061.
30. Chandarajoti, K.; Xu, Y.; Sparkenbaugh, E.; Key, N. S.; Pawlinski, R.; Liu, J., De novo synthesis of a narrow size distribution low-molecular-weight heparin. *Glycobiology* **2014**, *24*, 476-486.
31. Xu, Y.; Cai, C.; Chandarajoti, K.; Hsieh, P. H.; Li, L.; Pham, T. Q.; Sparkenbaugh, E. M.; Sheng, J.; Key, N. S.; Pawlinski, R.; Harris, E. N.; Linhardt, R., J.; Liu, J., Homogeneous low-molecular-weight heparins with reversible anticoagulant activity. *Nat. Chem. Biol.* **2014**, *10*, 248-250.
32. Liu, J.; Linhardt, R., J., Chemoenzymatic synthesis of heparan sulfate and heparin. *Nat. Prod. Rep.* **2014**, *31*, 1676-1685.
33. Wang, T.; Liu, L.; Voglmeir, J., Chemoenzymatic synthesis of ultralow and low-molecular weight heparins. *BBA - Proteins and Proteomics* **2020**, *1868*, 140301.
34. Mohamed, S.; Coombe, D. R., Heparin mimetics: their therapeutic potential. *Pharmaceuticals* **2017**, *10*, 78.
35. Mende, M.; Bednarek, C.; Wawryszyn, M.; Sauter, P.; Biskup, M. B.; Schepers, U.; Brase, S., Chemical synthesis of glycosaminoglycans. *Chem. Rev.* **2016**, *116*, 8193-8255.
36. Dulaney, S. B.; Huang, X., Chapter 3 - strategies in synthesis of heparin/heparan sulfate oligosaccharides: 2000–present. *Adv. Carbohydr. Chem. Biochem.* **2012**, *67*, 95-136.
37. Gustafsson, D.; Bylund, R.; Antonsson, T.; Nilsson, I.; Nyström, J. E.; Eriksson, U.; Bredberg, U.; Teger-Nilsson, A. C., A new oral anticoagulant: the 50-year challenge. *Nat. Rev. Drug Discovery* **2004**, *3*, 649-659.
38. Furie, B.; Furie, B. C., Mechanisms of thrombus formation. *N. Engl. J. Med.* **2008**, *359*,

938-949.

39. Raskob, G. E.; Angchaisuksiri, P.; Blanco, A. N.; Buller, H.; Gallus, A.; Hunt, B. J.; Hylek, E. M.; Kakkar, A.; Konstantinides, S. V.; McCumber, M.; Ozaki, Y.; Wendelboe, A.; Weitz, J. I., Thrombosis: a major contributor to global disease burden. *Arterioscler., Thromb., Vasc. Biol.* **2014**, *34*, 2363-2371.
40. Rabenstein, D. L., Heparin and heparan sulfate: structure and function. *Nat. Prod. Rep.* **2002**, *19*, 312-331.
41. Warkentin, T. E.; Chong, B. H.; Greinacher, A., Heparin-induced thrombocytopenia: towards consensus. *J. Thromb. Haemostasis* **1998**, *79*, 1-7.
42. Thomas, D. P., Does low molecular weight heparin cause less bleeding? *J. Thromb. Haemostasis* **1997**, *78*, 1422-1425.
43. Shen, J. I.; Winkelmayr, W. C., Use and safety of unfractionated heparin for anticoagulation during maintenance hemodialysis. *Am. J. Kidney Dis.* **2012**, *60*, 473-486.
44. Arepally, G. M.; Ortel, T. L., Clinical practice. Heparin-induced thrombocytopenia. *N. Engl. J. Med.* **2006**, *355*, 809-817.
45. Diuguid, D. L., Choosing a parenteral anticoagulant agent *N. Engl. J. Med.* **2001**, *345*, 1340-1342.
46. Pineo, G. F.; Hull, R. D., Low-molecular-weight heparin: prophylaxis and treatment of venous thromboembolism. *Annu. Rev. Med.* **1997**, *48*, 79-91.
47. Melnikova, I., The anticoagulants market. *Nat. Rev. Drug Discovery* **2009**, *8*, 353-354.
48. Basten, J.; Jaurand, G.; Olde-Hanter, B.; Duchaussoy, P.; Petitou, M.; van Boeckel, C. A. A., Biologically active heparin-like fragments with a “non-glycosamino” glycan structure. Part 3 : o-alkylated-o-sulphated pentasaccharides. *Bioorg. Med. Chem. Lett.* **1992**, *2*, 905-910.
49. Bousser, M. G.; Bouthier, J.; Büller, H. R.; Cohen, A. T.; Crijns, H.; Davidson, B. L.; Halperin, J.; Hankey, G.; Levy, S.; Pengo, V.; Prandoni, P.; Prins, M. H.; Tomkowski, W.; Torp-Pedersen, C.; Wyse, D. G., Comparison of idraparinux with vitamin K antagonists for prevention of thromboembolism in patients with atrial fibrillation: a randomised, open-label, non-inferiority trial. *Lancet* **2008**, *371*, 315-321.
50. Buller, H. R.; Cohen, A. T.; Davidson, B.; Decousus, H.; Gallus, A. S.; Gent, M.; Pillion, G.; Piovella, F.; Prins, M. H.; Raskob, G. E., Idraparinux versus standard therapy for venous thromboembolic disease. *N. Engl. J. Med.* **2007**, *357*, 1094-1104.
51. Herbert, J. M.; Héroult, J. P.; Bernat, A.; van Amsterdam, R. G. M.; Lormeau, J. C.; Petitou, M.; van Boeckel, C.; Hoffmann, P.; Meuleman, D. G., Biochemical and

pharmacological properties of SANORG 34006, a potent and long-acting synthetic pentasaccharide. *Blood* **1998**, *91*, 4197-4205.

52. Investigators, A novel long-acting synthetic factor Xa inhibitor (SanOrg34006) to replace warfarin for secondary prevention in deep vein thrombosis. A Phase II evaluation. *J. Thromb. Haemostasis* **2004**, *2*, 47-53.

53. Savi, P.; Héroult, J. P.; Duchaussoy, P.; Millet, L.; Schaeffer, P.; Petitou, M.; Bono, F.; Herbert, J. M., Reversible biotinylated oligosaccharides: a new approach for a better management of anticoagulant therapy. *J. Thromb. Haemostasis* **2008**, *6*, 1697-1706.

54. Paty, I.; Trelu, M.; Destors, J. M.; Cortez, P.; Boëlle, E.; Sanderink, G., Reversibility of the anti-FXa activity of idrabiotaparinux (biotinylated idraparinux) by intravenous avidin infusion. *J. Thromb. Haemostasis* **2010**, *8*, 722-729.

55. Song, Y.; Li, X.; Pavithra, S.; Li, D., Idraparinux or idrabiotaparinux for long-term venous thromboembolism treatment: a systematic review and meta-analysis of randomized controlled trials. *PLoS One* **2013**, *8*, e78972.

56. Petitou, M.; Héroult, J. P.; Bernat, A.; Driguez, P. A.; Duchaussoy, P.; Lormeau, J. C.; Herbert, J. M., Synthesis of thrombin-inhibiting heparin mimetics without side effects. *Nature* **1999**, *398*, 417-422.

57. Maccarana, M.; Lindahl, U., Mode of interaction between platelet factor 4 and heparin. *Glycobiology* **1993**, *3*, 271-277.

58. Herbert, J. M.; Héroult, J. P.; Bernat, A.; Savi, P.; Schaeffer, P.; Driguez, P. A.; Duchaussoy, P.; Petitou, M., SR123781A, a synthetic heparin mimetic. *J. Thromb. Haemostasis* **2001**, *85*, 852-860.

59. Hoppensteadt, D. A.; Cunanan, J.; Geniaux, E.; Lorenz, M.; Viskov, C.; Ythier-Moury, P.; Brin, J. F.; Jeske, W. P., AVE5026: a novel, extractive heparinoid with enriched anti-Xa activity and enhanced antithrombotic activity. *Blood* **2007**, *110*, 1881.

60. Westerduin, P.; Basten, J. E. M.; Broekhoven, M. A.; de Kimpe, V.; Will, I.; Kuijpers, H. A.; van Boeckel, C. A. A., Synthesis of tailor-made glycoconjugates showing AT III-mediated inhibition of blood coagulation factors Xa and thrombin. *Angew. Chem. Int. Ed.* **1996**, *35*, 331-333.

61. Kitazawa, S.; Okumura, M.; Kinomura, K.; Sakakibara, T., Syntheses and properties of novel vinyl monomers bearing a glycoside residue. *Chem. Lett.* **1990**, *19*, 1733-1736.

62. Fukudome, N.; Suzuki, K.; Yashima, E.; Akashi, M., Synthesis of nonionic and anionic hydrogels bearing a monosaccharide residue and their properties. *J. Appl. Polym. Sci.* **1994**, *52*, 1759-1763.

63. Nakamae, K.; Miyata, T.; Jikihara, A.; Hoffman, A. S., Formation of poly(glucosyloxyethyl methacrylate)-concanavalin A complex and its glucose-sensitivity. *J. Biomater. Sci., Polym. Ed.* **1994**, *6*, 79-90.
64. Akashi, M.; Sakamoto, N.; Suzuki, K.; Kishida, A., Synthesis and anticoagulant activity of sulfated glucoside-bearing polymer. *Bioconjugate Chem.* **1996**, *7*, 393-395.
65. Oh, Y. I.; Sheng, G. J.; Chang, S. K.; Hsieh-Wilson, L. C., Tailored glycopolymers as anticoagulant heparin mimetics. *Angew. Chem., Int. Ed. Engl.* **2013**, *52*, 11796-11799.
66. Harder, S.; Parisius, J.; Picard-Willems, B., Monitoring direct FXa-inhibitors and fondaparinux by Prothrombinase-induced Clotting Time (PiCT): relation to FXa-activity and influence of assay modifications. *Thromb. Res.* **2008**, *123*, 396-403.
67. Yun, Y. R.; Won, J. E.; Jeon, E.; Lee, S.; Kang, W.; Jo, H.; Jang, J. H.; Shin, U. S.; Kim, H. W., Fibroblast growth factors: biology, function, and application for tissue regeneration. *J. Tissue Eng.* **2010**, 218142.
68. Freeman, C.; Liu, L.; Banwell, M. G.; Brown, K. J.; Bezos, A.; Ferro, V.; Parish, C. R., Use of sulfated linked cyclitols as heparan sulfate mimetics to probe the heparin/heparan sulfate binding specificity of proteins. *J. Biol. Chem.* **2005**, *280*, 8842-8849.
69. Liu, L.; Li, C. P.; Cochran, S.; Ferro, V., Application of the four-component Ugi condensation for the preparation of sulfated glycoconjugate libraries. *Bioorg. Med. Chem. Lett.* **2004**, *14*, 2221-2226.
70. Liu, L.; Li, C.; Cochran, S.; Jimmink, S.; Ferro, V., Synthesis of a heparan sulfate mimetic library targeting FGF and VEGF via click chemistry on a monosaccharide template. *ChemMedChem* **2012**, *7*, 1267-1275.
71. Liu, L.; Li, C.; Cochran, S.; Feder, D.; Guddat, L. W.; Ferro, V., A focused sulfated glycoconjugate Ugi library for probing heparan sulfate-binding angiogenic growth factors. *Bioorg. Med. Chem. Lett.* **2012**, *22*, 6190-6194.
72. Miao, H. Q.; Ornitz, D. M.; Aingorn, E.; Ben-Sasson, S. A.; Vlodaysky, I., Modulation of fibroblast growth factor-2 receptor binding, dimerization, signaling, and angiogenic activity by a synthetic heparin-mimicking polyanionic compound. *J. Clin. Invest.* **1997**, *99*, 1565-1575.
73. Schlessinger, J.; Plotnikov, A. N.; Ibrahimi, O. A.; Eliseenkova, A. V.; Yeh, B. K.; Yayon, A.; Linhardt, R., J.; Mohammadi, M., Crystal structure of a ternary FGF-FGFR-heparin complex reveals a dual role for heparin in FGFR binding and dimerization. *Mol. Cell.* **2000**, *6*, 743-750.
74. Vázquez-Campos, S.; St. Hilaire, P. M.; Damgaard, D.; Meldal, M., GAG mimetic libraries: sulphated peptide as heparin-like glycosaminoglycan mimics in their interaction with FGF-1. *QSAR Comb. Sci.* **2005**, *24*, 923-942.

75. de Paz, J. L.; Noti, C.; Böhm, F.; Werner, S.; Seeberger, P. H., Potentiation of fibroblast growth factor activity by synthetic heparin oligosaccharide glycodendrimers. *Chem. Biol.* **2007**, *14*, 879-887.
76. Huang, M. L.; Smith, R. A.; Triegeer, G. W.; Godula, K., Glycocalyx remodeling with proteoglycan mimetics promotes neural specification in embryonic stem cells. *J. Am. Chem. Soc.* **2014**, *136*, 10565-10568.
77. Ying, Q. L.; Stavridis, M.; Griffiths, D.; Li, M.; Smith, A., Conversion of embryonic stem cells into neuroectodermal precursors in adherent monoculture. *Nat. Biotechnol.* **2003**, *21*, 183-186.
78. Jiménez Blanco, J. L.; Ortega-Caballero, F.; Ortiz Mellet, C.; García Fernández, J. M., (Pseudo)amide-linked oligosaccharide mimetics: molecular recognition and supramolecular properties. *Beilstein J. Org. Chem.* **2010**, *6*, 20.
79. Revuelta, J.; Fuentes, R.; Lagartera, L.; José Hernáiz, M.; Bastida, A.; García-Junceda, E.; Fernández-Mayoralas, A., Assembly of glycoamino acid building blocks: a new strategy for the straightforward synthesis of heparan sulfate mimics. *Chem. Commun.* **2018**, *54*, 13455-13458.
80. Xu, D.; Esko, J. D., Demystifying heparan sulfate-protein interactions. *Annu. Rev. Biochem.* **2014**, *83*, 129-157.
81. Reiland, J.; Sanderson, R. D.; Waguespack, M.; Barker, S. A.; Long, R.; Carson, D. D.; Marchetti, D., Heparanase degrades syndecan-1 and perlecan heparan sulfate: functional implications for tumor cell invasion. *J. Biol. Chem.* **2004**, *279*, 8047-8055.
82. Karoli, T.; Liu, L.; Fairweather, J. K.; Hammond, E.; Li, C. P.; Cochran, S.; Bergefall, K.; Trybala, E.; Addison, R. S.; Ferro, V., Synthesis, biological activity, and preliminary pharmacokinetic evaluation of analogues of a phosphosulfomannan angiogenesis inhibitor (PI-88). *J. Med. Chem.* **2005**, *48*, 8229-8236.
83. Parish, C. R.; Freeman, C.; Brown, K. J.; Francis, D. J.; Cowden, W. B., Identification of sulfated oligosaccharide-based inhibitors of tumor growth and metastasis using novel in vitro assays for angiogenesis and heparanase activity. *Cancer Res.* **1999**, *59*, 3433-3441.
84. Cochran, S.; Li, C.; Fairweather, J. K.; Kett, W. C.; Coombe, D. R.; Ferro, V., Probing the interactions of phosphosulfomannans with angiogenic growth factors by surface plasmon resonance. *J. Med. Chem.* **2003**, *46*, 4601-4608.
85. Liang, X. J.; Yuan, L.; Hu, J.; Yu, H. H.; Li, T.; Lin, S. F.; Tang, S. B., Phosphomannopentaose sulfate (PI-88) suppresses angiogenesis by downregulating heparanase and vascular endothelial growth factor in an oxygen-induced retinal neovascularization animal model. *Mol. Vision* **2012**, *18*, 1649-1657.
86. Iversen, P. O.; Sorensen, D. R.; Benestad, H. B., Inhibitors of angiogenesis selectively

reduce the malignant cell load in rodent models of human myeloid leukemias. *Leukemia* **2002**, *16*, 376-381.

87. Hossain, M. M.; Hosono-Fukao, T.; Tang, R.; Sugaya, N.; van Kuppevelt, T. H.; Jenniskens, G. J.; Kimata, K.; Rosen, S. D.; Uchimura, K., Direct detection of HSulf-1 and HSulf-2 activities on extracellular heparan sulfate and their inhibition by PI-88. *Glycobiology* **2010**, *20*, 175-186.

88. Dredge, K.; Hammond, E.; Davis, K.; Li, C. P.; Liu, L.; Johnstone, K.; Handley, P.; Wimmer, N.; Gonda, T. J.; Gautam, A.; Ferro, V.; Bytheway, I., The PG500 series: novel heparan sulfate mimetics as potent angiogenesis and heparanase inhibitors for cancer therapy. *Invest. New Drugs* **2010**, *28*, 276-283.

89. Ferro, V.; Liu, L.; Johnstone, K. D.; Wimmer, N.; Karoli, T.; Handley, P.; Rowley, J.; Dredge, K.; Li, C. P.; Hammond, E.; Davis, K.; Sarimaa, L.; Harenberg, J.; Bytheway, I., Discovery of PG545: a highly potent and simultaneous inhibitor of angiogenesis, tumor growth, and metastasis. *J. Med. Chem.* **2012**, *55*, 3804-3813.

90. Katz, A.; Barash, U.; Boyango, I.; Feld, S.; Zohar, Y.; Hammond, E.; Ilan, N.; Kremer, R.; Vlodaysky, I., Patient derived xenografts (PDX) predict an effective heparanase-based therapy for lung cancer. *Oncotarget*. **2018**, *9*, 19294-19306.

91. Dredge, K.; Brennan, T. V.; Hammond, E.; Lickliter, J. D.; Lin, L.; Bampton, D.; Handley, P.; Lankesheer, F.; Morrish, G.; Yang, Y.; Brown, M. P.; Millward, M., A Phase I study of the novel immunomodulatory agent PG545 (pixatimod) in subjects with advanced solid tumours. *Br. J. Cancer* **2018**, *118*, 1035-1041.

92. Zhao, H.; Liu, H.; Chen, Y.; Xin, X.; Li, J.; Hou, Y.; Zhang, Z.; Zhang, X.; Xie, C.; Geng, M.; Ding, J., Oligomannururate sulfate, a novel heparanase inhibitor simultaneously targeting basic fibroblast growth factor, combats tumor angiogenesis and metastasis. *Cancer Res.* **2006**, *66*, 8779-8787.

93. Zhang, J.; Xin, X.; Chen, Q.; Xie, Z.; Gui, M.; Chen, Y.; Lin, L.; Feng, J.; Li, Q.; Ding, J.; Geng, M., Oligomannururate sulfate sensitizes cancer cells to doxorubicin by inhibiting atypical activation of NF- κ B via targeting of Mre11. *Int. J. Cancer* **2012**, *130*, 467-477.

94. Nakajima, M.; DeChavigny, A.; Johnson, C. E.; Hamada, J.; Stein, C. A.; Nicolson, G. L., Suramin. A potent inhibitor of melanoma heparanase and invasion. *J. Biol. Chem.* **1991**, *266*, 9661-9666.

95. Li, H.; Li, H.; Qu, H.; Zhao, M.; Yuan, B.; Cao, M.; Cui, J., Suramin inhibits cell proliferation in ovarian and cervical cancer by downregulating heparanase expression. *Cancer Cell Int.* **2015**, *15*, 52.

96. Kobayashi, K.; Weiss, R. E.; Vogelzang, N. J.; Vokes, E. E.; Janisch, L.; Ratain, M. J., Mineralocorticoid insufficiency due to suramin therapy. *Cancer.* **1996**, *78*, 2411-2420.

97. La Rocca, R. V.; Meer, J.; Gilliatt, R. W.; Stein, C. A.; Cassidy, J.; Myers, S. E.; Dalakas, M. C., Suramin-induced polyneuropathy. *Neurology* **1990**, *40*, 954-960.
98. Figg, W. D.; Cooper, M. R.; Thibault, A.; Headlee, D.; Humphrey, J.; Bergan, R. C.; Reed, E.; Sartor, O., Acute renal toxicity associated with suramin in the treatment of prostate cancer. *Cancer*. **1994**, *74*, 1612-1614.
99. Firsching, A.; Nickel, P.; Mora, P.; Allolio, B., Antiproliferative and angiostatic activity of suramin analogues. *Cancer Res.* **1995**, *55*, 4957-4961.
100. Marchetti, D.; Reiland, J.; Erwin, B.; Roy, M., Inhibition of heparanase activity and heparanase-induced angiogenesis by suramin analogues. *Int. J. Cancer* **2003**, *104*, 167-174.
101. Loka, R. S.; Yu, F.; Sletten, E. T.; Nguyen, H. M., Design, synthesis, and evaluation of heparan sulfate mimicking glycopolymers for inhibiting heparanase activity. *Chem. Commun.* **2017**, *53*, 9163-9166.
102. Roy, S.; El Hadri, A.; Richard, S.; Denis, F.; Holte, K.; Duffner, J.; Yu, F.; Galcheva-Gargova, Z.; Capila, I.; Schultes, B.; Petitou, M.; Kaundinya, G. V., Synthesis and biological evaluation of a unique heparin mimetic hexasaccharide for structure-activity relationship studies. *J. Med. Chem.* **2014**, *57*, 4511-4520.
103. Sletten, E. T.; Loka, R. S.; Yu, F.; Nguyen, H. M., Glycosidase inhibition by multivalent presentation of heparan sulfate saccharides on bottlebrush polymers. *Biomacromolecules* **2017**, *18*, 3387-3399.
104. Loka, R. S.; Sletten, E. T.; Barash, U.; Vlodaysky, I.; Nguyen, H. M., Specific inhibition of heparanase by a glycopolymer with well-defined sulfation pattern prevents breast cancer metastasis in mice. *ACS Appl. Mater. Interfaces* **2019**, *11*, 244-254.
105. Zubkova, O. V.; Ahmed, Y. A.; Guimond, S. E.; Noble, S. L.; Miller, J. H.; Smith, R. A. A.; Nurcombe, V.; Tyler, P. C.; Weissmann, M.; Vlodaysky, I.; Turnbull, J. E., Dendrimer heparan sulfate glycomimetics: potent heparanase inhibitors for anticancer therapy. *ACS Chem. Biol.* **2018**, *13*, 3236-3242.
106. Casu, B.; Lindahl, U., Structure and biological interactions of heparin and heparan sulfate. *Adv. Carbohydr. Chem. Biochem.* **2001**, *57*, 159-206.
107. Capila, I.; Linhardt, R., J., Heparin-protein interactions. *Angew. Chem., Int. Ed. Engl.* **2002**, *41*, 391-412.
108. Brinkhous, K. M.; Smith, H. P.; Warner, E. D.; Seegers, W. H., The inhibition of blood clotting: an unidentified substance which acts in conjunction with heparin to prevent the conversion of prothrombin into thrombin. *Am. J. Physiol.* **1939**, *125*, 683-687.
109. Lindahl, U.; Bäckström, G.; Höök, M.; Thunberg, L.; Fransson, L. A.; Linker, A.,

Structure of the antithrombin-binding site in heparin. *Proc. Natl. Acad. Sci. U. S. A.* **1979**, *76*, 3198-3202.

110. Lane, D. A.; Denton, J.; Flynn, A. M.; Thunberg, L.; Lindahl, U., Anticoagulant activities of heparin oligosaccharides and their neutralization by platelet factor 4. *Biochem. J.* **1984**, *218*, 725-732.

111. Oosta, G. M.; Gardner, W. T.; Beeler, D. L.; Rosenberg, R. D., Multiple functional domains of the heparin molecule. *Proc. Natl. Acad. Sci. U. S. A.* **1981**, *78*, 829-833.

112. Sugahara, K.; Kitagawa, H., Heparin and heparan sulfate biosynthesis. *IUBMB Life* **2002**, *54*, 163-175.

113. Li, Y. C.; Ho, I. H.; Ku, C. C.; Zhong, Y. Q.; Hu, Y. P.; Chen, Z. G.; Chen, C. Y.; Lin, W. C.; Zulueta, M. M.; Hung, S. C.; Lin, M. G.; Wang, C. C.; Hsiao, C. D., Interactions that influence the binding of synthetic heparan sulfate based disaccharides to fibroblast growth factor-2. *ACS Chem. Biol.* **2014**, *9*, 1712-1717.

114. Faham, S.; Hileman, R. E.; Fromm, J. R.; Linhardt, R., J.; Rees, D. C., Heparin structure and interactions with basic fibroblast growth factor. *Science.* **1996**, *271*, 1116-1120.

115. Raman, R.; Sasisekharan, V.; Sasisekharan, R., Structural insights into biological roles of protein-glycosaminoglycan interactions. *Chem. Biol.* **2005**, *12*, 267-277.

116. Beenken, A.; Mohammadi, M., The FGF family: biology, pathophysiology and therapy. *Nat. Rev. Drug Discovery* **2009**, *8*, 235-253.

117. Ago, H.; Kitagawa, Y.; Fujishima, A.; Matsuura, Y.; Katsube, Y., Crystal structure of basic fibroblast growth factor at 1.6 Å resolution. *J. Biochem.* **1991**, *110*, 360-363.

118. Plotnikov, A. N.; Hubbard, S. R.; Schlessinger, J.; Mohammadi, M., Crystal structures of two FGF-FGFR complexes reveal the determinants of ligand-receptor specificity. *Cell.* **2000**, *101*, 413-424.

119. Thompson, L. D.; Pantoliano, M. W.; Springer, B. A., Energetic characterization of the basic fibroblast growth factor-heparin interaction: identification of the heparin binding domain. *Biochemistry* **1994**, *33*, 3831-3840.

120. Ulrich, S.; Boturyn, D.; Marra, A.; Renaudet, O.; Dumy, P., Oxime ligation: a chemoselective click-type reaction for accessing multifunctional biomolecular constructs. *Chem. - Eur. J.* **2013**, *20*, 34-41.

121. Sun, B.; Srinivasan, B.; Huang, X., Pre-activation based one-pot synthesis of an α -(2,3)-sialylated core-fucosylated complex type bi-antennary N-glycan dodecasaccharide. *Chem. Eur. J.* **2008**, *14*, 7072-7081.

122. Miermont, A.; Zeng, Y.; Jing, Y.; Ye, X. S.; Huang, X., Syntheses of lewis^X and dimeric lewis^X construction of branched oligosaccharides by a combination of preactivation and reactivity based chemoselective one-pot glycosylations. *J. Org. Chem.* **2007**, *72*, 8958-8961.
123. Huang, L.; Wang, Z.; Li, X.; Ye, X. S.; Huang, X., Iterative one-pot syntheses of chitotetroses. *Carbohydr. Res.* **2006**, *341*, 1669-1679.
124. Wang, Z.; Xu, Y.; Yang, B.; Tiruchinapally, G.; Sun, B.; Liu, R.; Dulaney, S.; Liu, J.; Huang, X., Preactivation-based, one-pot combinatorial synthesis of heparin-like hexasaccharides for the analysis of heparin–protein interactions. *Chem. Eur. J.* **2010**, *16*, 8365-8375.
125. Mohr, J.; Oestreich, M., B(C₆F₅)₃-catalyzed hydrogenation of oxime ethers without cleavage of the N-O bond. *Angew. Chem., Int. Ed. Engl.* **2014**, *53*, 13278-13281.
126. Takenaka, Y.; Kiyosu, T.; Choi, J. C.; Sakakura, T.; Yasuda, H., Selective synthesis of N-aryl hydroxylamines by the hydrogenation of nitroaromatics using supported platinum catalysts. *Green Chem.* **2009**, *11*, 1385–1390.
127. Gomez, S.; Peter, J. A.; Maschmeyer, T., The reductive amination of aldehydes and ketones and the hydrogenation of nitriles: mechanistic aspects and selectivity control. *Adv. Synth. Catal.* **2002**, *344*, 1037-1057.
128. Abdel-Magid, A. F.; Carson, K. G.; Harris, B. D.; Maryanoff, C. A.; Shah, R. D., Reductive amination of aldehydes and ketones with sodium triacetoxyborohydride. Studies on direct and indirect reductive amination procedures. *J. Org. Chem.* **1996**, *61*, 3849-3862.
129. Jiang, Y.; Han, J.; Yu, C.; Vass, S. O.; Searle, P. F.; Browne, P.; Knox, R. J.; Hu, L., Design, synthesis, and biological evaluation of cyclic and acyclic nitrobenzylphosphoramidate mustards for *E. coli* nitroreductase activation. *J. Med. Chem.* **2006**, *49*, 4333-4343.
130. Obkircher, M.; Stähelin, C.; Dick, F., Formation of Fmoc-β-alanine during Fmoc-protections with Fmoc–OSu. *J. Pept. Sci.* **2008**, *14*, 763-766.
131. Akl, M. R.; Nagpal, P.; Ayoub, N. M.; Tai, B.; Prabhu, S. A.; Capac, C. M.; Gliksman, M.; Goy, A.; Suh, K. S., Molecular and clinical significance of fibroblast growth factor 2 (FGF2 /bFGF) in malignancies of solid and hematological cancers for personalized therapies. *Oncotarget* **2016**, *7*, 44735-44762.
132. Florkiewicz, R. Z.; Sommer, A., Human basic fibroblast growth factor gene encodes four polypeptides: three initiate translation from non-AUG codons. *Proc. Natl. Acad. Sci. U. S. A.* **1989**, *86*, 3978-3981.
133. Ibrahimi, O. A.; Zhang, F.; Hrstka, S. C.; Mohammadi, M.; Linhardt, R., J., Kinetic model for FGF, FGFR, and proteoglycan signal transduction complex assembly. *Biochemistry* **2004**, *43*, 4724-4730.

134. Dunham-Ems, S. M.; Lee, Y. M.; K., S. E.; Pudavar, H.; Claus, P.; Prasad, P. N.; Stachowiak, M. K., Fibroblast growth factor receptor-1 (FGFR1) nuclear dynamics reveal a novel mechanism in transcription control. *Mol. Biol. Cell* **2009**, *20*, 2401-2412.
135. Korc, M.; Friesel, R. E., The role of fibroblast growth factors in tumor growth. *Curr. Cancer Drug Targets* **2009**, *9*, 639-651.
136. Ornitz, D. M.; Itoh, N., The fibroblast growth factor signaling pathway. *Wiley Interdiscip. Rev.: Dev. Biol.* **2015**, *4*, 215-266.
137. Powers, C. J.; McLeskey, S. W.; Wellstein, A., Fibroblast growth factors, their receptors and signaling. *Endocr.-Relat. Cancer* **2000**, *7*, 165-97.
138. Vlodaysky, I.; Gross-Cohen, M.; Weissmann, M.; Ilan, N.; Sanderson, R. D., Opposing functions of heparanase-1 and heparanase-2 in cancer progression. *Trends Biochem. Sci.* **2018**, *43*, 18-31.
139. Fux, L.; Ilan, N.; Sanderson, R. D.; Vlodaysky, I., Heparanase: busy at the cell surface. *Trends Biochem. Sci.* **2009**, *34*, 511-519.
140. He, Y. Q.; Sutcliffe, E. L.; Bunting, K. L.; Li, J.; Goodall, K. J.; Poon, I. K.; Hulett, M. D.; Freeman, C.; Zafar, A.; McInnes, R. L.; Taya, T.; Parish, C. R.; Rao, S., The endoglycosidase heparanase enters the nucleus of T lymphocytes and modulates H3 methylation at actively transcribed genes via the interplay with key chromatin modifying enzymes. *Transcription* **2012**, *3*, 130-145.
141. Heyman, B.; Yang, Y., Mechanisms of heparanase inhibitors in cancer therapy. *Exp. Hematol.* **2016**, *44*, 1002-1012.
142. Mohan, C. D.; Hari, S.; Preetham, H. D.; Rangappa, S.; Barash, U.; Ilan, N.; Nayak, S. C.; Gupta, V. K.; Basappa; Vlodaysky, I.; Rangappa, K. S., Targeting heparanase in cancer: inhibition by synthetic, chemically modified, and natural compounds. *iScience* **2019**, *15*, 360-390.
143. Rivara, S.; Milazzo, F. M.; Giannini, G., Heparanase: a rainbow pharmacological target associated to multiple pathologies including rare diseases. *Future Med. Chem.* **2016**, *8*, 647-680.
144. Hammond, E.; Li, C. P.; Ferro, V., Development of a colorimetric assay for heparanase activity suitable for kinetic analysis and inhibitor screening. *Anal. Biochem.* **2010**, *396*, 112-116.